Co-funded by the European Union

Grant agreement no.:
101060634

Project acronym:
PURPEST

Project full title:
Plant pest prevention through technology-guided monitoring and site-specific control

Collaborative Project (RIA Research and Innovation action)

HORIZON EUROPE CALL – HORIZON-CL6-2021-FARM2FORK-01

Start date of project: 2023-01-01
Duration: 4 years

D 5.2
Report on the regional distribution of damage costs by farm type

Due delivery date: 31-12-2024
Actual delivery date: 31-01-2025

Organization name of lead contractor for this deliverable:
Wageningen University

Project co-funded by the European Commission within HORIZON 2020 (2016-2020)		
Dissemination Level		
PU	Public, fully open, e.g. web	X
CO	Confidential, restricted under conditions set out in Model Grant Agreement	
CI	Classified, information as referred to in Commission Decision 2001/844/EC.	

Deliverable number:	D 5.2

Deliverable name:	Report on the regional distribution of damage costs by farm type
Work package:	5 – Analyze the impact and implementation of PurPest
Lead contractor:	Prof. Dr. Justus Wesseler

Author(s)		
Name	**Organisation**	**E-mail**
Stelios Kartakis	WU	stelios.kartakis@wur.nl
Kutay Cingiz	WU	kutay.cingiz@wur.nl
Justus Wesseler	WU	justus.wesseler@wur.nl

Abstract

This report (D5.2) presents the results of the potential direct economic damage impact assessment for five invasive alien species (*Halyomorpha halys*, *Helicoverpa armigera*, *Spodoptera frugiperda*, *Bursaphelenchus xylophilus*, and *Phytophthora ramorum*) under a "no-control" scenario in Europe.

Public introduction[1]

Invasive alien species are a growing threat to ecosystems, biodiversity, agriculture, and forestry, often causing severe ecological and economic harm as they establish in new environments. The increasing globalization of trade and travel, coupled with the effects of climate change, has accelerated the introduction and spread of these species, making biological invasions a pressing issue for Europe. Understanding the economic impact of invasive species is crucial for guiding effective management strategies, as early prevention and control are far more cost-effective than addressing established infestations. Quantitative impact assessments provide essential insights by estimating the potential damage these species can cause, helping to prioritize resources and evaluate the feasibility of mitigation efforts. This report examines four invasive species of concern in Europe — *Halyomorpha halys*, *Helicoverpa armigera*, *Spodoptera frugiperda*, *Bursaphelenchus xylophilus,* and *Phytophthora ramorum* — and by examining their potential distribution, spread, and direct economic damage impact under a "no-control" scenario.

[1] According to Deliverables list in Annex I, all restricted (RE) deliverables will contain an introduction that will be made public through the project WEBSITE

TABLE OF CONTENTS

Page

TABLE OF FIGURES

Page

TABLE OF TABLES

Page

1 THE POTENTIAL DIRECT ECONOMIC IMPACT OF *HALYOMORPHA HALYS* IN EUROPE

1.1 Background

The brown marmorated stink bug (BMSB), *Halyomorpha halys* (Stål, 1855) (Hemiptera: Pentatomidae), is a major agricultural pest due to its invasive behavior, wide host range, and dispersal capability (Zhu et al., 2017). Native in Asia (China, Japan, Korea, and Taiwan), BMSB was introduced in the USA in 1996, and almost a decade later in the European continent (Switzerland) (Leskey & Nielsen, 2018; Wermelinger et al., 2007). In the latter case, it is suspected that BSBM was accidentally imported with woody plants (EPPO Reporting Service, 2008). Today, the pest has spread to 47 states, 4 Canadian provinces, and most of Europe (**Fig. 1.1**) (StopBMSB, EPPO Global Database, 2024).

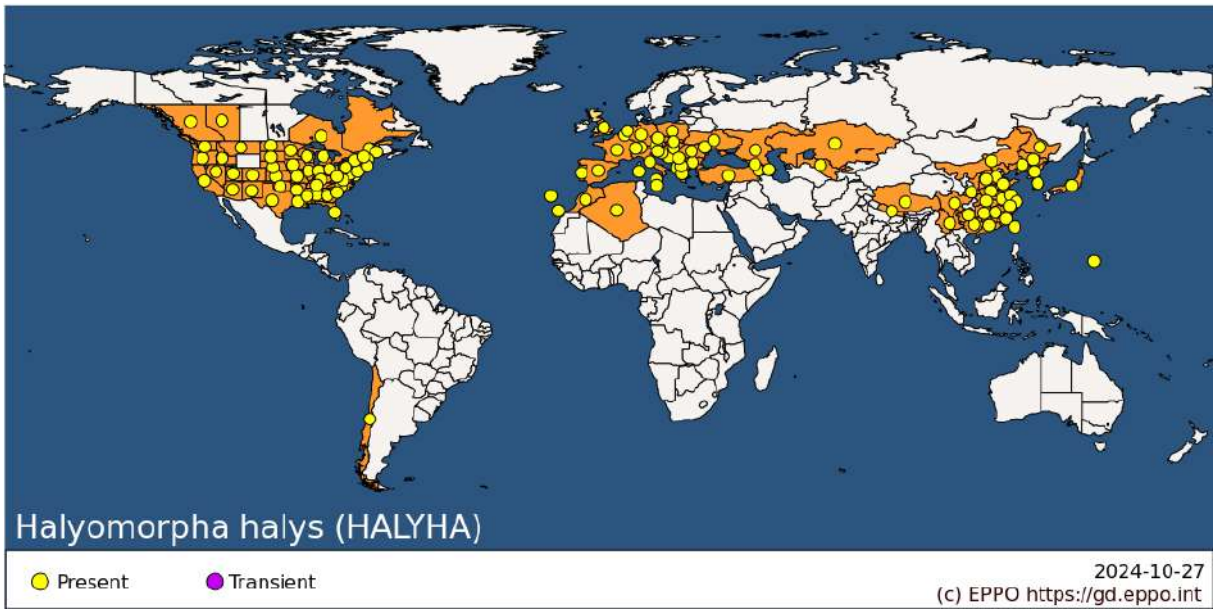

Figure 1.1. The current global distribution of *Halyomorpha halys.* (Source: EPPO Global Database)

BMSB became a major pest in several mid-Atlantic states of the USA, causing substantial losses in annual and perennial crops. For example, (Leskey, Hamilton, et al., 2012) reports US$ 37 million losses in Mid-Atlantic apple production in 2010 and >90% in stone fruit production. To tackle the issue, farmers increased the number of insecticide applications fourfold for the growing season 2010-2011 (Leskey, Short, et al., 2012). A survey revealed that the majority of the sampled growers in the mid-Atlantic region suffered profit losses of up to 33% and/or up to US$ 10,000 due to BMSB in 2012 and 2014 (Dellinger et al., 2016). In New Zealand, the incurred costs due to BMSB are estimated to lead to a GDP drop of $1.8 and $3.6 billion, and total real export volume losses between $312 and $554 million, under a "do nothing scenario[2]" by 2038 (NZIER, 2017). BMSB was *"(...) not considered an economically important pest in Europe (...)"* and no severe economic damage had been reported in field crops, despite the pest's presence for over a decade (Costi et al., 2017; Haye et al., 2014). However, in 2019, BMSB "caused serious damage to the fruit and vegetables production in the affected regions[3], infecting pears, peaches and nectarines,

[2] Assuming that BSBM is left untreated.
[3] Emilia Romagna, Veneto, Trentino, Alto-adige, Lombardia, Piemonte and Friuli Venezia Giulia.

apples, kiwis, cherries and apricots", which prompted the EU to provide financial support to the affected growers; the estimates losses caused by BMSB in those regions were estimated to reach €500 million only for that year (European Commission, 2020).
This report assesses the potential direct economic impact of an uncontrolled BMSB invasion in Europe. To achieve this, we integrated information on the pest's potential distribution in Europe with economic statistics on key host plants, namely apple and pear trees. This analysis delivers a bandwidth of annual damage costs due to BMSB based on different yield loss, spread rate, and revenue level scenarios.

1.2 Data, Methodology, and Results

This study used farm-level data from the Farm Accountancy Data Network (FADN). This database is based on an annual farm survey carried out by the EU Member States and consists of farm accountancy data from approximately 80000 agricultural holdings. It is the only source of micro-economic data that is harmonized and is representative of the commercial European agricultural holdings (above a minimum economic size). The sample covers about 90% of the total utilized agricultural area and accounts for roughly 90% of the total agricultural production of the Union (COMMITTEE FOR THE FARM ACCOUNTANCY DATA NETWORK (FADN), 2020).
Data on the total country area were obtained from Eurostat (**Table 1.2**). Further, we extracted farm-level data for all EU-27 Member States, including the United Kingdom, over the period 2013-2021[4] using the FADN database. The results are aggregated and reported at the NUTS0 (country) level. More specifically, we used information regarding the crop-specific cultivated area, production, and total output of each farm per year. Yields and revenues per hectare were calculated at individual farm level and then aggregated by country and year. Subsequently, averages over 2013-2021 were calculated for each country, summarizing average apple and pear area, production, total output, yield, and revenue per hectare (**Table 1.4**, **Table 1.5**).
It should be noted that to properly extrapolate the FADN data in the sample to all holdings in the EU covered by the survey, a special weighting system needs to be applied. This system is based on the "free expansion" principle, where an extrapolation factor (weight) is assigned to each farm in the sample. The weight corresponds to the ratio between the number of agricultural holdings in the population and the number of holdings in the sample for the same classification cell (region x type of farming x economic size class). Thus, weighted averages are then calculated to represent the broader population while accounting for sampling differences.

1.2.1 Potential Distribution and Spread in Europe

1.2.1.1 State of invasion / Infested area

Data on the current distribution of BMSB in Europe were sourced from the EPPO Global Database and relevant literature (**Table 1.1**). This included the year of the pest's first detection in each country and its current "pest status", as evaluated by the EPPO Secretariat. Using this information, we approximated the currently infested area (as of 2024) by considering both the qualitative status of the invasion and the time since BMSB was first detected in each country. For example, countries where BMSB is classified as "widespread" were assumed to have higher infestation rates compared to those with a "restricted distribution" status. **Table 1.1** provides a summary of pest status and corresponding infestation estimates.

[4] Data for the United Kingdom were available up to 2020.

In the case of BMSB, the pest status categories and their associated infestation ranges are as follows[5]:

i. **Absent, *intercepted only / pest eradicated / unreliable record***: The infested area is set at 0%. Similarly, countries labeled 'Absent/Not detected' (as of 11 November 2024) have a 0% infested area.
ii. **Present, *few occurrences***: 10–20% of the susceptible area is infested.
iii. **Present**, ***restricted distribution***: 20–40% of the susceptible area is infested.
iv. **Present, *widespread***: 60–80% of the susceptible area is infested.
v. **Present, *no details***: In this case, the uncertainty around the current degree of BMSB infestation is greater compared to the precedented categories. Therefore, we consider the year of first detection as the defining factor and any additional information we could obtain from EPPO and the literature. The range of infested areas extends from 10 to 80% of the susceptible area following the assumed ranges above.

Time since the first detection was incorporated to refine these estimates. Countries with detections within the past five years (2019 or later) were placed at the lower end of the assigned range, reflecting the early invasion stage. For detections between five and ten years ago, estimates were placed in the middle of the range. Detections older than ten years were placed at the higher end, indicating more advanced invasion stages. For "present, no details" status, the broad range was narrowed using information from National Plant Protection Organizations and the literature.

Table 1.1. Distribution details of *Halyomorpha halys* in Europe and estimated (%) infested area for each country.

Country	Year of First Detection	Pest status	EPPO Link	Infested Area (as % of susceptible area)	Additional reasoning
Belgium	2011	Present, no details	Distribution details in Belgium	60	BMSB is reported in 337 of 581 municipalities **(Fig. A1.2)**
Bulgaria	2016	Present, no details	Distribution details in Bulgaria	45	
Cyprus	-[6]	Absent / Not detected	-	0	
Czech Republic	2018	Present, restricted distribution	Distribution details in the Czech Republic	30	
Denmark	-	Absent / Not detected	-	0	

[5] It has to be highlighted that, even though the assigned quantitative percentages provide a "logical" framework to approximate the current state of invasion, they are not trivial. The main purpose of the EPPO's "pest status" classification is to indicate the presence or absence of a specific species in a country that was developed in a plant quarantine context (personal communication with EPPO).
[6] Not listed / Pest has not been reported.

Germany	2011	Present, few occurrences	Distribution details in Germany	20	
Greece	2011	Present, no details	Distribution details in Greece	50	Reported records in northern Greece, Lesbos, Attica and Crete. Neighbor countries[7] have reported low BMSB infestation levels.
Spain	2016	Present, restricted distribution	Distribution details in Spain	30	
Estonia	-	Absent / Not detected	-	0	
France	2012	Present, widespread	Distribution details in France	80	Rapid geographical expansion **(Fig. A1.3)** and the absence of official control measures in the country (EPPO, 2024b)
Croatia	2017	Present, restricted distribution	Distribution details in Croatia	30	**Fig. A1.4**
Hungary	2013	Present, restricted distribution	Distribution details in Hungary	40	
Ireland	-	Absent / Not detected	-	0	
Italy	2007	Present, widespread	Distribution details in Italy	80	
Lithuania	-	Absent / Not detected	-	0	
Luxembourg	-	Absent / Not detected	-	0	
Latvia	-	Absent / Not detected	-	0	
Malta	2018	Present, restricted distribution	Distribution details in Malta	30	

[7] Albania (present, few occurrences), Bulgaria (present, no details), North Macedonia (present, restricted distribution), and Turkey (present, restricted distribution).

Netherlands	2018	Present, no details	Distribution details in the Netherlands	40	**Fig. A1.5**
Austria	2015	Present, restricted distribution	Distribution details in Austria	30	
Poland	2018	Present, few occurrences	Distribution details in Poland	15	
Portugal	2018	Present, widespread	Distribution details in Portugal	70	
Romania	2014	Present, restricted distribution	Distribution details in Romania	40	
Finland	-	Absent / Not detected	-	0	
Sweden	2016	Absent, intercepted only	Distribution details in Sweden	0	
Slovakia	2016	Present, widespread	Distribution details in Slovakia	70	No official phytosanitary measure applied (EPPO, 2024c)
Slovenia	2017	Present, restricted distribution	Distribution details in Slovenia	30	
United Kingdom	2019	Present, restricted distribution	Distribution details in the United Kingdom	20	

1.2.1.2 The area under risk / Susceptible area

The first step of the analysis is to identify the areas where the climatic conditions are favorable for BMSB establishment. It is well known that the ultimate limits of the geographical distribution of a species are determined by climate (Andrewartha & Birch, 1954; Woodward, 1996). Climate is not the sole factor limiting species' geographical distribution, but it is tractable and can provide an initial estimate of the potential distribution of a species (D. Kriticos et al., 2015). We used the CLIMEX climate-based niche model to project the potential distribution of BMSB in Europe, applying the parameter values proposed by Kriticos et al. (2017) **(Fig. 1.2)**. The exact parameter values are included in the Appendix **(Table A1.1)**. CLIMEX is a process-based bioclimatic modeling package that estimates suitable areas for population growth and long-term survival for a species. The model utilizes a set of fitted growth and stress functions along with meteorological data to compute an annual index of climate suitability, the so-called Ecoclimatic Index (EI) (D. Kriticos et al., 2015). The EI is scaled from 0 (unsuitable) to a theoretical 100 (climatically optimal all year round). For visualization purposes, the EI is classified into four arbitrary classes to display potential geographic distribution for mapping in QGIS: marginal ($1< EI \leq 5$), moderate ($5 < EI \leq 15$), suitable ($15 < EI \leq 30$), and optimal ($EI > 30$) **(Fig. 1.2)**.

Kriticos et al. (2017) used the CliMond CM10 World (1975H V1.1) climate dataset for their BMSB CLIMEX model. This global dataset is interpolated at a 10-arc-minute gridded resolution and consists of 30-year averages centered on 1975 (1961–1990) for daily minimum and maximum temperature (°C), monthly precipitation (mm), and relative humidity (%) recorded at 9:00 and 15:00 h. Our analysis employed a more recent climatology: the CliMond CM_TC10 World dataset, centered on 1995 (1981–2010) (*unpublished,* provided after personal communication with Darren J. Kriticos). The updated dataset uses more locations (808020 locations compared to 565801 in the original) and better reflects current climatic conditions. This improved climatology enhances the accuracy and detail of the projections, providing more realistic results, particularly in the context of ongoing climate change.

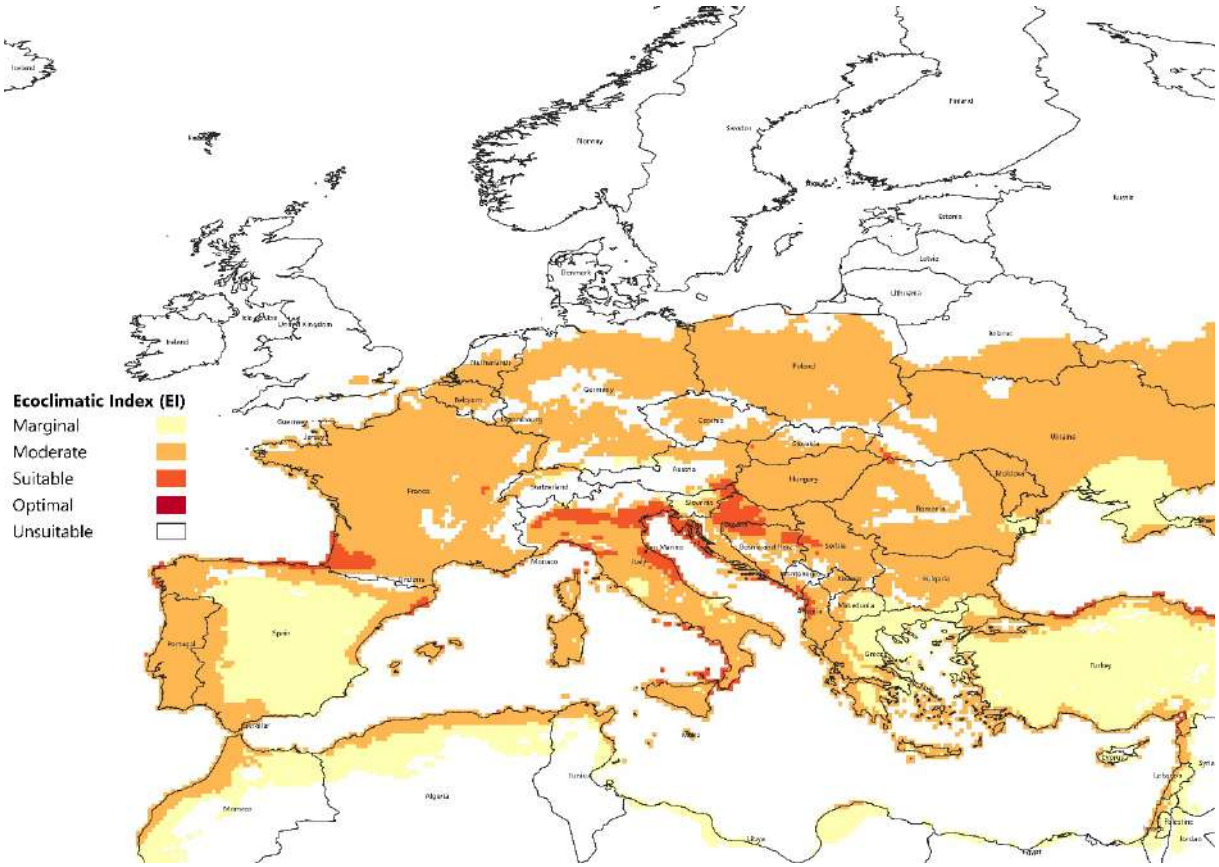

Figure 1.2. Modeled climate suitability (CLIMEX Ecoclimatic Index) for *Halyomorpha halys* under current climatic conditions in Europe. The figure was created with QGIS Desktop version 3.38.1 (https://www.qgis.org/).

Fig. 1.2 illustrates the climatically suitable areas of BMSB in Europe under the current climatic conditions. To determine the susceptible area for each country, we treated the Ecoclimatic Index (EI) as a binary variable, without further differentiation between suitability classes. The climatic suitability layer was reclassified into a binary map, identifying areas as either suitable (EI = 1) or unsuitable (EI = 0) for BMSB persistence. This reclassified map was then overlaid with country boundaries, and the susceptible area within each country was calculated as a percentage of its total land area **(Table 1.2)**.

Table 1.2. Country size, area susceptible, and area not yet infested but susceptible to Halyomorpha halys infestation in Europe.

Country	Total area[8]	Susceptible area		Infested area	Area not yet infested but susceptible	
	km²	km²	%	km²	km²	%[9]
Belgium	30667	21919	71	13151	8767	40
Bulgaria	110996	100612	91	45276	55337	55
Cyprus	9253	7918	86	0	7918	100
Czech Republic	78871	41658	53	12497	29161	70
Denmark	42925	0	0	0	0	0
Germany	357569	217587	61	43517	174070	80
Greece	131694	130322	99	78193	52129	40
Spain	505983	483827	96	145148	338679	70
Estonia	45336	0	0	0	0	0
France	638475	556056	87	444845	111211	20
Croatia	56594	51967	92	15590	36377	70
Hungary	93012	93012	100	37205	55807	60
Ireland	69947	0	0	0	0	0
Italy	302079	258826	86	207061	51765	20
Lithuania	65284	0	0	0	0	0
Luxembourg	2595	1543	59	0	1543	100
Latvia	64586	0	0	0	0	0
Malta	316	315	100	94	220	70
Netherlands	37378	21741	58	8696	13045	60
Austria	83878	32186	38	9656	22530	70
Poland	311928	246781	79	37017	209764	85
Portugal	92227	92227	100	64559	27668	30
Romania	238398	191903	80	76761	115142	60
Finland	338411	0	0	0	0	0
Sweden	447424	0	0	0	0	0
Slovakia	49035	31194	64	21836	9358	30
Slovenia	20273	16218	80	4865	11352	70
United Kingdom	243610	2945	1	589	2356	80
Total	4468744	2600756	58.2[10]	1266557	1334200	29.9

The results show that the sum of the total area of the countries considered is approximately 4.4 million km², of which 58.2% is identified as prone to BMSB establishment based on the CLIMEX model output. This corresponds to 2.6 million km² of susceptible area. Notably, countries such as Bulgaria, Cyprus, Greece, Spain, France, Croatia, Hungary, Italy, Malta, Portugal, Romania, and

[8] Source: EUROSTAT (2024) Area by NUTS 3 region
[9] In percentage of the total susceptible area.
[10] In percentage of the sum of total area. The same applies to the total percentage of the area not yet infested but susceptible.

Slovenia have over 80% of their total land area classified as susceptible. In contrast, Denmark, Estonia, Ireland, Lithuania, Latvia, Finland, and Sweden appear unsuitable for BMSB establishment under current climatic conditions and face no immediate risk of damage. Nevertheless, evidence suggests climate change could expand BMSB's potential range northward (Kistner, 2017). The area not yet infested but susceptible to BMSB infestation is estimated at 1.33 million km², representing 29.9% of the total land area or 51% of the climatically suitable area.

1.2.2 Spread

The spread rate is an important factor influencing the damage costs associated with BMSB which are closely related to the extent of the infested area. BMSB possesses a huge invasion and establishment capacity in non-native regions, due to its high reproductive and dispersal capabilities. On average, females lay 240 eggs per season, and BMSB adults can fly up to 72 km per day (Lee et al., 2013; Nielsen et al., 2008). Wiman et al. (2015) suggested a clear distinction between short- and long-distance BMSB fliers, with adults covering either less or more than 5 km per day, respectively, based on samples from Oregon. In the same study, the maximum distances recorded were 67 km for males and 75 km for females (Wiman et al., 2015). Another study reports BMSB maximum flight distance of 117 km (Lee & Leskey, 2015).
Following the framework of Wesseler & Fall (2010), we compute the annual infested area per country and per year by using a radial range expansion model:

$$IA_{i,t} = \begin{cases} (rr \cdot t)^2 \cdot \pi & if IA_{i,t} < SA_i \\ SA_i & if\ IA_{i,t} \geq SA_i \end{cases} \quad (1)$$

where $i = 1, 2, \ldots, n$.
In this model, $IA_{i,t}$ is the infested area in the country i and year t, rr is the rate of spread (km^2/yr), π is the mathematical constant (3.14), n is the number of countries considered, and SA_i is the susceptible area to BMSB infestation in the country i. The total infested area TIA_t^A (km^2) at year t is the sum of the annual infested areas:

$$TIA_t^A = \sum_{i=1}^{n} IA_{i,t} \quad (2)$$

If we assume that BMSB is introduced in all countries considered simultaneously, and define the total susceptible area as $SA = \sum_{i=1}^{n} SA_i$, then the total infested area TIA_t^B at time t is computed as:

$$TIA_t^B = \begin{cases} n \cdot (rr \cdot t)^2 \cdot \pi & if\ n \cdot (rr \cdot t)^2 \cdot \pi < SA \\ SA & if\ n \cdot (rr \cdot t)^2 \cdot \pi \geq SA \end{cases} \quad (3)$$

Table 1.3 presents the number of years required for BMSB to infest the entire SA_i, under different annual spread rate scenarios ranging from 10 to 120 km²/year. As expected, the results highlight that smaller countries such as Luxembourg and Malta require fewer years to be totally infested, while larger countries such as France and Spain take longer, even at higher spread rates. For example, at a 50 km²/year spread rate, the susceptible area of France would be completely infested in approximately 9 years, whereas for smaller countries such as Belgium or Cyprus would take just 2 years. The calculations for "Total A" consider the country-specific SA_i, while "Total B" assumes BMSB is introduced simultaneously across all countries, thereby including transboundary spread effects.

Table 1.3. Number of years until the country area is infested for different annual spread rates. Total A represents the results considering the sum of the susceptible area of each country, and Total B presents the results considering the area not yet infested but susceptible, as reported in **Table 1.2** and BMSB disperses beyond country borders.

Country	Susceptible area (km²)	Number of years until total infestation					
		Annual speed of spread (km²/year)					
		10	30	50	70	90	120
Belgium	21919	9	3	2	2	1	1
Bulgaria	100612	18	6	4	3	2	2
Cyprus	7918	6	2	2	1	1	1
Czech Republic	41658	12	4	3	2	2	1
Denmark	0	0	0	0	0	0	0
Germany	217587	27	9	6	4	3	3
Greece	130322	21	7	5	3	3	2
Spain	483827	40	14	8	6	5	4
Estonia	0	0	0	0	0	0	0
France	556056	43	15	9	7	5	4
Croatia	51967	13	5	3	2	2	2
Hungary	93012	18	6	4	3	2	2
Ireland	0	0	0	0	0	0	0
Italy	258826	29	10	6	5	4	3
Lithuania	0	0	0	0	0	0	0
Luxembourg	1543	3	1	1	1	1	1
Latvia	0	0	0	0	0	0	0
Malta	315	2	1	1	1	1	1
Netherlands	21741	9	3	2	2	1	1
Austria	32186	11	4	3	2	2	1
Poland	246781	29	10	6	5	4	3
Portugal	92227	18	6	4	3	2	2
Romania	191903	25	9	5	4	3	3
Finland	0	0	0	0	0	0	0
Sweden	0	0	0	0	0	0	0
Slovakia	31194	10	4	2	2	2	1
Slovenia	16218	8	3	2	2	1	1
United Kingdom	2945	4	2	1	1	1	1
Total A	2600757	91	31	19	13	11	8
Total B	1334200	66	22	14	10	8	6

As noted by Wesseler & Fall (2010), these country-specific results may underestimate the time required for total infestation in large countries (e.g., Germany, France), as the model does not account for encroachment from neighboring countries. Conversely, for elongated countries such as Portugal, the results may be overestimated due to the radial spread modeling approach, which assumes a circular expansion based on the country's total area.

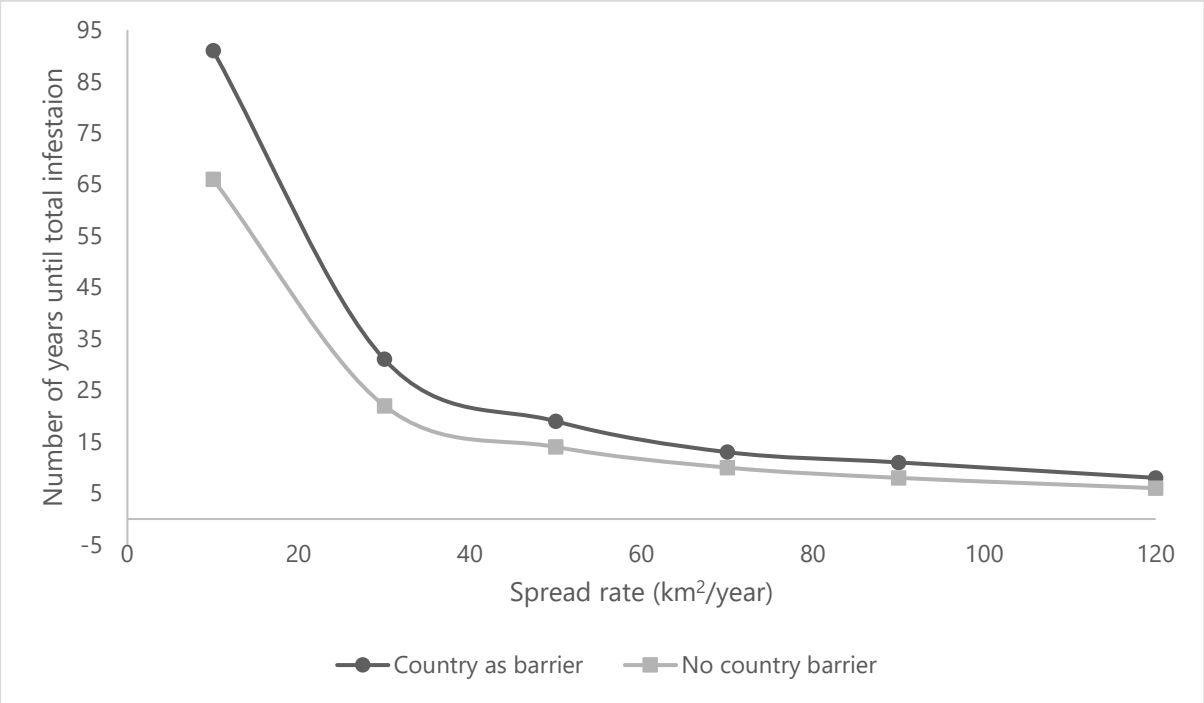

Figure 1.3. Rate of spread and number of years until total infestation, based on the results of **Table 1.3**.

Fig. 1.3 illustrates the relationship between the rate of spread and the time until total infestation under two scenarios: 'Total A,' representing the presence of country barriers, and 'Total B,' assuming no country barriers. The results show that the time required for total infestation decreases exponentially as the rate of spread increases. This effect is particularly pronounced at lower spread rates, where reducing the spread from 30 km²/year to 10 km²/year could triple the infestation time. Conversely, at higher spread rates, the increase in infestation time is modest. This pattern underscores the importance of early detection and rapid eradication during the initial stages of an invasion, during which intervention efforts are most effective and cost-efficient.

1.2.3 Host range and determination of impacts

BMSB is a polyphagous pest known to feed on over a hundred host plants in 45 families, including several economically important annual and perennial crops. Those crops include cotton, soybean, peach, apple, pear, grapes, kiwi, and hazelnut. BMSB causes injury to plants by inserting its feeding stylets into plant fruiting bodies, which are often the marketable part of them (Haye et al., 2015). During feeding, BMSB deposits saliva within the plant tissues, which may lead to discolored flesh on the internal part of the fruit, faded sunken spots, deformed fruits, seeds, or pods, white spongy patches on the surface, and scarring (Kuhar et al., 2018; Leskey et al., 2009; Nielsen & Hamilton, 2009; Rice et al., 2014). While feeding may occur on leaves, shoots, stems, and even bark, both nymphs and adults exhibit a preference for growing and ripened fruits and seeds of host plants (Martinson et al., 2015; Rice et al., 2014).
This analysis focuses on **two key host plants**: apples and pears.

1.2.3.1 Apples

J.-M. Zhang et al. (2007) report 28.8% ± 4.1%, 23.4% ± 4.6%, and 30.8% ± 3.6%, damage rates for early, mid-, and late varieties, respectively. In New Zealand, NZIER (2017) assumed yield losses of 47% under a “do nothing” and 40% under a “do minimum” scenario, 10 years after

BMSB full population establishment. In untreated (control) apple orchards in West Virginia, Short et al. (2017) reported fruit damage of approximately 45% in 2013, and 70% in 2014, while Leskey et al., (2020) recorded apple losses of 25.95% ± 2.28% and 31.82% ± 2.22% in 2015 and 2016, respectively. A more recent study in northwest Italy documented 7.4% ± 1.7% fruit damage in 2016 (Candian et al., 2018). Notably, infestations in apple orchards in the eastern United States in 2010 resulted in up to 100% crop loss (Leskey, Short, et al., 2012), while (Akotsen-Mensah et al., 2018) reported apple fruit injury ranging from 19% ± 2.7% to 93% ± 3.8% in 2016.

Table 1.4 summarizes the average apple tree area, production, total output, yield, and revenue across the EU-27 and the UK for the period 2013–2021. Poland, Italy, and France appear to be the leading apple producers in Europe, with average productions of 3245, 1907, and 1068 thousand tonnes, respectively, collectively contributing approximately 60% of the Union's total apple production. Conversely, countries like Ireland, Luxembourg, and Malta do not report any land allocated to apple tree cultivation, based on FADN data. The total apple tree area across the EU-27 and the UK amounts to roughly 400000 hectares (4000 km^2), yielding an annual apple production of approximately 10.3 million tonnes.

Table 1.4. Average apple tree area, production, total output, yield, and revenue per hectare for EU-27 and the UK (2013-2021).

Country	Apple area (ha)	Apple area on total land (%)	Production (1000 t)	Total Output (million €)	Yield (t/ha)	Revenue (€/ha)
Belgium	6041	0.20	275	106	43.2	17128
Bulgaria	4060	0.04	49	15	10.4	3255
Cyprus	430	0.05	3	3	9.3	7956
Czech Republic	9121	0.12	168	55	10.6	3638
Denmark	NA	NA	NA[11]	NA	NA	NA
Germany	28213	0.08	848	374	22.5	9996
Greece	9798	0.07	238	106	21.8	10938
Spain	15740	0.03	530	171	26.5	7709
Estonia	553	0.01	1	0.3	2.0	1049
France	32140	0.05	1068	558	25.6	13950
Croatia	4475	0.08	100	22	14.3	3762
Hungary	19311	0.21	421	77	19.2	3628
Ireland	NA	NA	NA	NA	NA	NA
Italy	50227	0.17	1907	789	32.4	13819
Lithuania	1537	0.02	13	3	5.1	1771
Luxembourg	NA	NA	NA	NA	NA	NA
Latvia	1747	0.03	9	5	4.1	1539
Malta	NA	NA	NA	NA	NA	NA
Netherlands	8402	0.22	365	192	38.3	18907
Austria	6964	0.08	189	71	19.7	7823
Poland	137257	0.44	3245	540	20.4	3211
Portugal	8773	0.10	136	45	10.8	4105
Romania	28232	0.12	326	101	10.8	3455
Finland	20	0.0001	0	0.05	1.1	1456
Sweden[12]	1112	0.0025	28	27	24.7	23709
Slovakia	1134	0.02	13	3	3.9	967
Slovenia	3381	0.17	68	25	12.2	4706
United Kingdom	15456	0.20	381	163	15.7	6743

[11]Denmark did not report any apple production for the selected years (CAPL_PRQ FADN variable), unlike apple tree area and total output. We made no assumptions on the apple production in Denmark since it does not affect the analysis (Country area susceptible = 0 ha) and was excluded from the analysis.
[12] The sample for Sweden is unbalanced thus the considered period is 2016-2019. The apple tree area is reported as zero for the years 2013-2015 and was extremely low for the years 2020 and 2021 (not a representative sample).

Average		0.121[13]			16.9	7301
Total	395161		10381			

The average apple revenue across all countries is 7301 €/ha. Despite having the lowest production volume, Sweden reports the highest average revenue per hectare. The Netherlands and Belgium follow with average revenues of 18.9 and 17 thousand €/ha, respectively, while France and Italy both average 10 thousand €/ha.
Countries were grouped into Low, Medium, and High revenue categories using income terciles[14], which divide the distribution into three equal parts. The Low revenue group includes countries in the bottom third of the revenue distribution, the Medium revenue group represents those in the middle third, and the High revenue group encompasses those in the top third. The calculated average revenues for each group were: Low – 2088 €/ha, Medium – 4899 €/ha, and High – 13803 €/ha. Additionally, we considered three yield loss scenarios: 10%, 20%, and 30%, based on the most frequently reported damages in Italian apple orchards between 2016 and 2023 (**Table A1.3**) (Maistrello, 2024). Lastly, an average of 0.121% of apple tree area on total land has been considered.

1.2.3.2 Pears

The susceptibility of pear trees to BMSB damage varies throughout the growing season; fruits injured in July developed external symptoms, while those damaged a month later showed no external signs but suffered internal quality degradation (Lee et al., 2013; Qin, 1990). In China's Shandong Province, BMSB damage affected 10-35% of pears (Ming et al., 2001; Yang et al., 2009). In Hebei Province, 40-60% of pear production was reported to be harmed, while in Beijing, the damage ranged from 50-70% (Qin, 1990; C. Zhang et al., 1993). In Italy, a BMSB monitoring program observed over 50% of deformed fruits during 2014-2016, with yield losses exceeding 40% on most monitored farms. Farms near the borders reported almost complete crop failure (Maistrello et al., 2017). Similarly, Bariselli et al., (2016) documented over 50% damage in early-maturing pear cultivars during the 2015 harvest. Yang et al. (2009) summarized yield losses in pears from various studies, with the reported damage ranging between 10% and 70%.
Table 1.5 shows the average values for pear tree area, production, total output, yield, and revenue across the EU-27 and the UK for the period 2013-2021. Italy, Spain, and the Netherlands are the major European pear producers, averaging 344, 342, and 327 thousand tonnes, respectively, and together accounting for approximately 55% of the Union's total pear production. Conversely, countries such as Ireland, Luxembourg, Finland, and Sweden report no area allocated to pear tree cultivation according to FADN data. The total pear tree area in the EU-27 and the UK is approximately 90281 hectares (903 km^2), yielding an estimated total production of 1.8 million tonnes of pears annually.

[13] Countries without apple tree production and countries not susceptible to BMSB were excluded from the computation of the average. The countries excluded are Denmark, Estonia, Ireland, Lithuania, Luxembourg, Latvia, Malta, Finland, and Sweden.
[14] For more information: Glossary: Income terciles

Table 1.5. Average pear tree area, production, total output, yield, and revenue per hectare for EU-27 and the UK (2013-2021).

Country	Pear area (ha)	Pear area on total land (%)	Production (1000 t)	Total Output (million €)	Yield (t/ha)	Revenue (€/ha)
Belgium	7468	0.24	275	149	35.4	19418
Bulgaria	816	0.01	4	2	4.7	2349
Cyprus	69	0.01	0.4	0.5	8.5	9972
Czech Republic	602	0.01	5	2	7.3	3178
Denmark[15]	NA		NA	NA	NA	NA
Germany	4846	0.01	103	70	15.8	9170
Greece	2371	0.02	42	25	14.2	10438
Spain	20491	0.04	342	142	19.0	7442
Estonia	1		0.001	0.001	0.4	360
France	3856	0.01	78	62	17.8	15155
Croatia	169	0.003	1	0.2	4.6	2120
Hungary	1398	0.02	11	4	8.0	3473
Ireland	NA		NA	NA	NA	NA
Italy	18827	0.06	344	202	17.7	10036
Lithuania	19		0.3	0.1	4.0	1721
Luxembourg	NA		NA	NA	NA	NA
Latvia	72		0.4	0.2	5.4	2514
Malta	5	0.01	0.01	0.01	3.0	2016
Netherlands	8210	0.22	327	175	38.4	20442
Austria	547	0.01	4	3	7.7	5350
Poland	4700	0.02	49	21	10.9	5123
Portugal	12953	0.14	259	88	17.6	6221
Romania	1377	0.01	11	5	8.4	4009
Finland	NA		NA	NA	NA	NA
Sweden	NA		NA	NA	NA	NA
Slovakia	6	0.0001	0.002	0.0003	0.5	56
Slovenia	143	0.01	4	2	10.3	8196
United Kingdom	1175	0.005	10	11	7.5	6620
Average		0.0419[16]			11.6	6755
Total	90121		1869			

[15] Denmark does not report any pear production for the selected years (CPEAR_PRQ FADN variable), unlike pear tree area and total output. We made no assumptions on the pear production in Denmark since it does not affect the analysis (Country area susceptible = 0 ha). Thus, was excluded.

[16] Countries without pear tree production and countries not susceptible to BMSB were excluded from the computation of the average. The countries excluded are Denmark, Estonia, Ireland, Lithuania, Luxembourg, Latvia, Finland, and Sweden.

The average pear revenue among all countries is 6755 €/ha. The Netherlands and Belgium have the highest average pear revenue per hectare with 20442 €/ha, and 19418 €/ha, respectively.
Similar to the analysis for apples, countries were categorized into Low, Medium, and High revenue levels using terciles. The Low revenue group comprises countries in the bottom 33.3% of revenue per hectare, the Medium revenue group represents those between the 33rd and 67th percentiles, and the High revenue group includes countries above the 67th percentile. The average revenue for each group was calculated as follows: Low – 1789 €/ha, Medium – 5133 €/ha, and High – 12252 €/ha. Additionally, we considered three yield loss scenarios: 30%, 50%, and 70%, reflecting the most frequently reported damages observed in several Italian regions during 2016-2023 (**Table A1.4**) (Maistrello, 2024). Lastly, an average of 0.0419% of pear tree area in the country has been considered.

1.2.4 Direct economic impact

To estimate the direct economic impact in Europe incurred by BMSB, we employed a partial budgeting approach under a "no-control" scenario, assuming that no additional regulatory or control measures were in place after the invasion and thus no change in the operating costs. In the case of BMSB, direct impacts involve solely negative effects, namely yield losses and additional operating costs. The direct economic impact is calculated in terms of present value as:

$$PVD = \sum_{i=1}^{\infty} TIA_t^B \cdot \bar{R} \cdot D_t \cdot q^{-t} \quad (4)$$

Where $\bar{R}$ is the average annual revenue in €/ha, TIA_t^B as described in **Eq. 3**, D_t the annual percentage loss in revenue, and q^{-t} the discount factor $(1+r)^{-t}$ where r is the discount rate. **Eq. 4** assumes an infinite planning horizon and applies the transversality condition to ensure that the present value of future losses converges to a finite amount. The transversality condition acts as a boundary condition, ensuring that the discounted impact of the pest diminishes over time as the horizon extends to infinity. This guarantees the economic feasibility of the analysis and reflects the practical assumption that distant future impacts have a negligible contribution.
Observations in Italy two years after BMSB's first report revealed significant injury to fruit orchards and crops, with injury levels consistently higher in the second year of infestation (Maistrello et al., 2016). Thus, the annual values for D_t are computed as:

$$D_t = \begin{cases} D & if\ t \geq 2 \\ D \cdot \frac{t}{2} & if\ t < 2 \end{cases} \quad (5)$$

Where D is the maximum damage potential.
Lastly, the average annual damage AAD has been calculated as:

$$AAD = PVD \cdot i \quad (6)$$

Where i is the 4.49%[17] discount rate in decimal form, representing the conversion factor for transforming present value into an infinite annuity.

[17] We use 4.49% as it is the average discount rate for the majority of Member States (Austria, Belgium, Cyprus, Germany, Estonia, Greece, Spain, Finland, France, Croatia, Ireland, Italy, Lithuania, Luxembourg, Latvia, Malta, the Netherlands, Portugal, Slovenia, and Slovakia) over the period 2023-2024. Source: Reference and discount rates (in %) since 01.08.1997

1.3 Results

1.3.1.1 Apples

Table 1.6 presents the results of an example scenario, which assumes an average apple tree area of 0.121% of the total country area, a BMSB spread rate of 30 km²/year, and an average apple revenue of 7301 €/ha. **Table 1.7** expands on this analysis by exploring various scenarios based on different revenue groups (Low, Medium, and High, as previously described), yield loss intensities (10%, 20%, and 30%), and spread rates (10, 30, 50, 70, 90, and 120 km²/year). The visual representation of these scenarios is depicted in **Fig. 1.4**, illustrating the interplay of spread rates, revenue levels, and yield loss intensities.

Table 1.6. Damage of *Halyomorpha halys* spreading further in the EU assuming a spread rate of 30 km²/year, 20% yield loss, 7301 €/ha revenue, and 0.121% of apple tree area on total land area.

Year	Infested area (km²)	Apple area infested (km²)	Incremental apple area infested (km²)	Annual incremental damage costs per additional apple area infested (million €)					Value of yield loss (million €)	Discount factor	Present value of yield loss (million €)
				Additional apple area (km²)							
				65	195	325	455	574			
1	53721	65	65	4.7					4.7	0.957	4.54
2	214885	260	195	9.5	14.2				23.7	0.916	21.72
3	483491	585	325	9.5	28.5	23.7			61.7	0.877	54.06
4	859540	1040	455	9.5	28.5	47.4	33.2		118.6	0.839	99.49
5	1332436	1612	572	9.5	28.5	47.4	66.4	41.8	193.6	0.803	155.40
6	1332436	1612	0	9.5	28.5	47.4	66.4	83.5	235.3	0.768	180.81
7	1332436	1612	0	9.5	28.5	47.4	66.4	83.5	235.3	0.735	173.04
8	1332436	1612	0	9.5	28.5	47.4	66.4	83.5	235.3	0.704	165.60
9	1332436	1612	0	9.5	28.5	47.4	66.4	83.5	235.3	0.673	158.49
10…∞	1332436	1612	0	9.5	28.5	47.4	66.4	83.5	235.3		3527[18]
Total											4541

The total infested area increases annually, stabilizing at an additional 1612 km² of infested apple tree area by the fifth year. Incremental damage costs associated with these newly infested areas peak at €83.5 million per year. Over the entire simulation period, the total discounted value of yield losses for this specific example amounts to €4.5 billion.

[18] Discounted sum from year 10 until infinity in present value.

Table 1.7. Average annual damage costs due to *Halyomorpha halys* in European apple tree cultivation in million € under different revenue groups yield loss and spread rate scenarios.

Scenario	Revenue group (€/ha)	Yield loss (%)	Average annual damage costs (million €) for different spread rates (km²/year)					
			10	30	50	70	90	120
1	2088	10	154	292	309	316	320	324
2	2088	20	308	583	618	633	640	648
3	2088	30	462	875	927	949	960	972
4	4899	10	361	684	725	742	751	760
5	4899	20	723	1368	1450	1485	1502	1521
6	4899	30	1084	2052	2176	2227	2253	2281
7	13803	10	1018	1927	2043	2092	2116	2143
8	13803	20	2036	3854	4087	4184	4232	4285
9	13803	30	3054	5782	6130	6275	6348	6428

The results reveal that even under the best-case scenario, the average annual damage costs are projected to reach approximately €154 million. Conversely, in the worst-case scenario, these costs of apple production could exceed €6.4 billion per year. The most likely scenario falls between these extremes. As illustrated in **Table 1.7** and **Fig. 1.4**, economic losses increase disproportionately with higher spread rates, especially under scenarios with high yield loss and revenue.

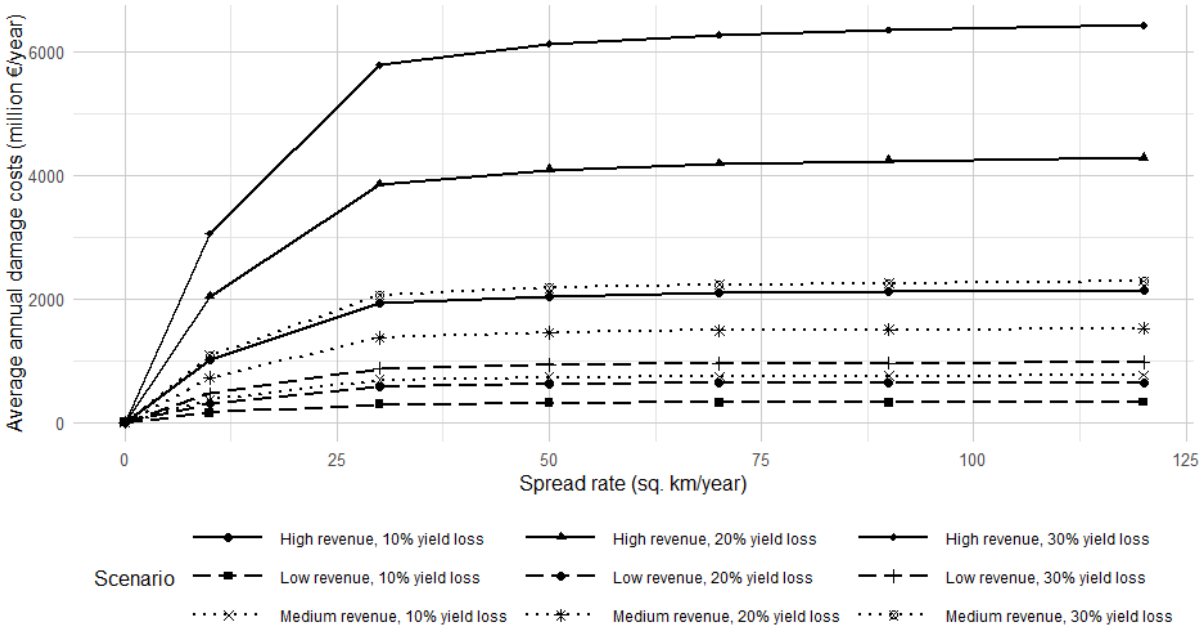

Figure 1.4. Average annual damage costs of *Halyomorpha halys* on European apple production.

Table 1.8 presents the average annual damage costs by country, assuming a spread rate of 30 km² per year and a 20% yield loss. The results reveal substantial differences among countries. Estonia, Denmark, Lithuania, Ireland, Latvia, Finland, Sweden, and Norway[19] are unlikely to experience any apple production losses from BMSB due to unfavorable climatic conditions for the pest's establishment under current average climatic conditions. Conversely, while countries such as Malta and Luxembourg are climatically suitable for BMSB, they report no apple production in the FADN dataset, resulting in no economic losses in this context.

[19] Not considered in the analysis.

Table 1.8. Average annual damage costs of *Halyomorpha halys* on European apple production by country for a spread rate of 30 km^2/year and 20% yield loss.

Country	Revenue (€/ha)	Apple area on total land (%)	Average annual damage costs (million €)
Belgium	17128	0.20	187.88
Bulgaria	3255	0.04	22.04
Cyprus	7956	0.05	6.48
Czech Republic	3638	0.12	56.92
Denmark	10679	NA	
Germany	9996	0.08	408.46
Greece	10938	0.07	175.95
Spain	7709	0.03	138.55
Estonia	1049	0.01	
France	13950	0.05	405.69
Croatia	3762	0.08	29.54
Hungary	3628	0.21	118.64
Ireland	NA	NA	
Italy	13819	0.17	1031.18
Lithuania	1771	0.02	
Luxembourg	NA	NA	
Latvia	1539	0.03	
Malta	NA	NA	
Netherlands	18907	0.22	285.60
Austria	7823	0.08	92.98
Poland	3211	0.44	652
Portugal	4105	0.10	61.02
Romania	3455	0.12	149.77
Finland	1456	0.0001	
Sweden	23709	0.0025	
Slovakia	967	0.02	1.94
Slovenia	4706	0.17	29.41
United Kingdom	6743	0.20	159.53
Total			4013.25

Countries with low average revenue per hectare, such as Slovakia and Bulgaria, and those with higher revenues but limited apple production, like Cyprus, Croatia, and Slovenia, experience annual damage costs ranging from approximately €2 to €30 million. However, control efforts in these countries generate positive externalities for neighboring countries by limiting BMSB's spread. On the contrary, countries with high average revenue per hectare, such as the Netherlands and Belgium, and those with significant apple production, including Italy, France, Germany, and Poland, are likely to face the highest annual economic losses. These losses range from roughly €188 million in Belgium to over 1 billion € in Italy. Italy's substantial damage costs can be attributed to its combination of high apple revenue per hectare and large-scale apple production.

1.3.1.2 Pears

Table 1.9 illustrates a sample scenario using an average of 0.0419% pear tree area on the total country area, a BMSB spread rate of 30 km²/year, and an average pear revenue of 6755 €/ha. **Table 1.10** expands on this by presenting various scenarios with different revenue groups (Low, Medium, High), yield loss intensities (30%, 50%, 70%), and spread rates (10, 30, 50, 70, 90, 120 km²/year). The results of these scenarios are visually represented in **Fig. 1.5** highlighting the relationship between spread rates and potential economic losses.

Table 1.9. Damage of Halyomorpha halys spreading further in the EU assuming a spread rate of 30 km2/year, 50% yield loss, 6755 €/ha revenue, and 0.0419% of apple tree area on total land area.

Year	Infested area (km²)	Pear area infested (km²)	Incremental pear area infested (km²)	Annual incremental damage costs per additional pear area infested (million €)					Value of yield loss (million €)	Discount factor	Present value of yield loss (million €)
				Additional pear area (km²)							
				24	71	119	166	180			
1	56549	24	24	4.0					4.0	0.957	3.83
2	226195	95	71	8.0	12.0				20.0	0.916	18.34
3	508938	213	119	8.0	24.0	20.0			52.1	0.877	45.63
4	904779	379	166	8.0	24.0	40.0	28.0		100.1	0.839	83.98
5	1332656	559	179	8.0	24.0	40.0	56.1	30.3	158.4	0.803	127.19
6	1332656	559	0	8.0	24.0	40.0	56.1	60.6	188.7	0.768	145.01
7	1332656	559	0	8.0	24.0	40.0	56.1	60.6	188.7	0.735	138.78
8	1332656	559	0	8.0	24.0	40.0	56.1	60.6	188.7	0.704	132.81
9	1332656	559	0	8.0	24.0	40.0	56.1	60.6	188.7	0.673	127.11
10…∞	1332656	559	0	8.0	24.0	40.0	56.1	60.6	188.7		2829[20]
Total											3652

The total infested area increases over time, stabilizing at 559 km² of additional infested pear tree area by the 5th year. Incremental damage costs associated with these newly infested pear areas reach a maximum of €60 million per year. Over the entire simulation period, the total discounted value of yield losses amounts to €3.6 billion. It should be noted that the yield loss assumptions for pear are higher than those used for apple, based on the frequency of the reported damage proportion in Italy (**Table A1.3**, **Table A1.4**) (Maistrello, 2024).

[20] Discounted sum from year 10 until infinity in present value.

Table 1.10. Average annual damage costs due to *Halyomorpha halys* in European pear tree cultivation in million € under different revenue groups yield loss and spread rate scenarios.

Scenario	Revenue group (€/ha)	Yield loss (%)	Average annual damage costs (million €) for different spread rates (km²/year)					
			10	30	50	70	90	120
1	1789	30	144	261	276	283	286	289
2	1789	50	241	434	460	471	476	482
3	1789	70	337	608	644	660	666	675
4	5133	30	414	748	791	811	819	830
5	5133	50	691	1246	1319	1352	1365	1383
6	5133	70	967	1744	1846	1893	1911	1937
7	12252	30	989	1784	1889	1936	1955	1981
8	12252	50	1649	2974	3148	3227	3259	3302
9	12252	70	2308	4163	4407	4517	4563	4622

The results indicate that even in the best-case scenario, the average annual damage costs are estimated at approximately €144 million. Conversely, in the worst-case scenario, these costs on pear production could exceed €4.6 billion per year. The most probable scenario lies between these extremes. Again, as shown in **Table 1.10** and **Fig. 1.5** economic losses increase disproportionately with rising spread rates, particularly under scenarios involving high yield loss and revenue. It is important to note that the assumed yield loss range for pears is higher than the one considered for apples.

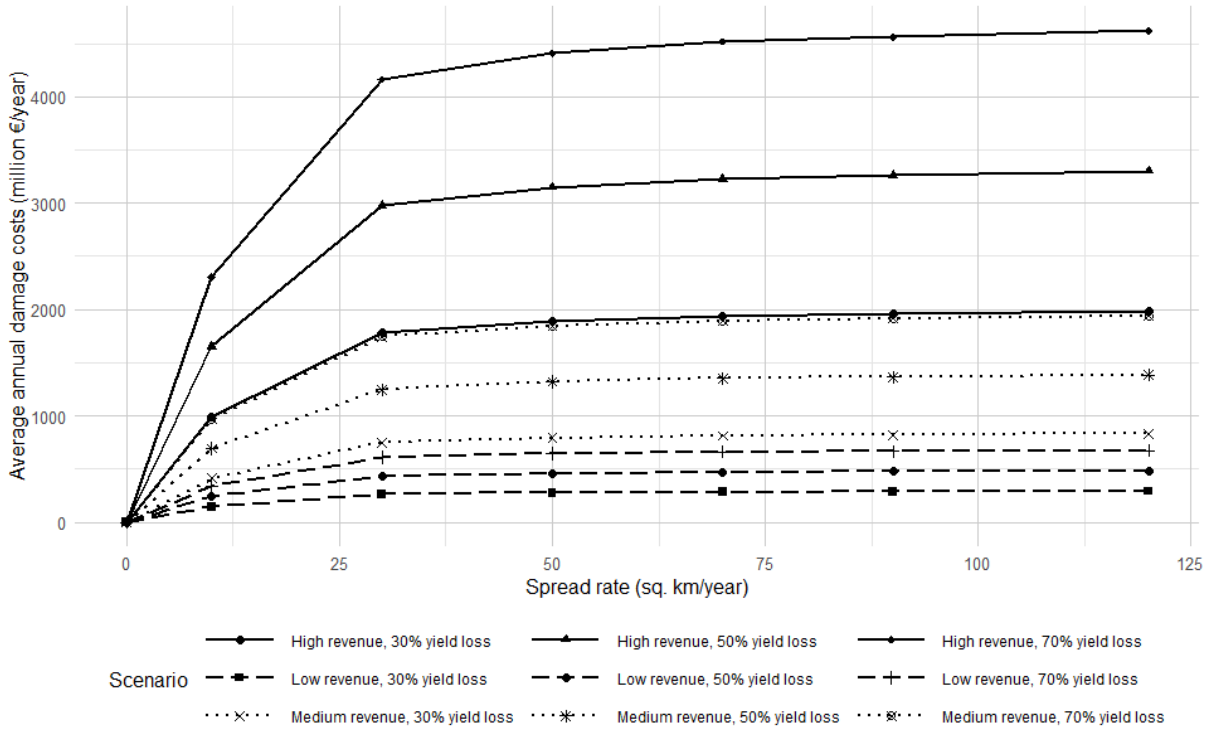

Figure 1.5. Average annual damage costs of *Halyomorpha halys* on European pear production.

Table 1.11 presents the average annual damage costs by country for a spread rate of 30 km² per year and 50% yield loss. Estonia, Denmark, Lithuania, Ireland, Latvia, Finland, Sweden, and Norway are unlikely to experience pear production losses due to unfavorable climatic conditions for BMSB establishment under current climatic averages. Similarly, while Luxembourg is climatically suitable for BMSB, it does not report pear production in the FADN dataset, resulting in no economic losses.

Table 1.11. Average annual damage costs of *Halyomorpha halys* on European pear production by country for a spread rate of 30 km2/year and 50% yield loss.

Country	Revenue (€/ha)	Pear area on total land (%)	Average annual damage costs (million €)
Belgium	19418	0.24	658.31
Bulgaria	2349	0.01	7.99
Cyprus	9972	0.01	3.27
Czech Republic	3178	0.01	8.20
Denmark	NA		
Germany	9170	0.01	160.90
Greece	10438	0.02	101.59
Spain	7442	0.04	435.26
Estonia	360		
France	15155	0.01	132.19
Croatia	2120	0.003	1.57
Hungary	3473	0.02	20.55
Ireland	NA		
Italy	10036	0.06	701.76
Lithuania	1721		
Luxembourg	NA		
Latvia	2514		
Malta	2016	0.01	0.05
Netherlands	20442	0.22	754.26
Austria	5350	0.01	12.49
Poland	5123	0.02	89
Portugal	6221	0.14	341.33
Romania	4009	0.01	21.19
Finland	NA		
Sweden	NA		
Slovakia	56	0.0001	0.002
Slovenia	8196	0.01	5.42
United Kingdom	6620	0.005	29.77
Total			3485

Countries with low average revenue per hectare, such as Slovakia, Malta, and several countries with higher revenues but a small apple production, such as Bulgaria, Cyprus, Czech Republic, Croatia, Hungary, Austria, and Romania, exhibit annual damage costs ranging from roughly 0.002 to €21 million. On the contrary, countries with high average revenue per hectare, such as the Netherlands and Belgium, as well as countries with large apple production, such as Spain, Italy, and Portugal may suffer the greatest annual economic losses, ranging roughly from €340 million in Portugal up to a €754 million in the Netherlands.

1.4 References

[1] Akotsen-Mensah, C., Kaser, J. M., Leskey, T. C., & Nielsen, A. L. (2018). Halyomorpha halys (Hemiptera: Pentatomidae) Responses to Traps Baited With Pheromones in Peach and Apple Orchards. Journal of Economic Entomology, 111(5), 2153–2162. https://doi.org/10.1093/JEE/TOY200

[2] Andrewartha, H. G. ., & Birch, Charles. (1954). The distribution and abundance of animals. 782. https://books.google.com/books/about/The_Distribution_and_Abundance_of_Animal.html?id=3uzaAAAAMAAJ

[3] Aukema, B., den Bieman, C. F. M., Lommen, G., van de Maat, G., Troisfontaine, L., & Vossen, P. (2019). Nieuwe en interessante Nederlandse wantsen IX (Hemiptera: Heteroptera). Nederlandse Faunistische Mededelingen, 52, 25–41.

[4] Bariselli, M., Bugiani, R., & Maistrello, L. (2016). Distribution and damage caused by Halyomorpha halys in Italy. EPPO Bulletin, 46(2), 332–334. https://doi.org/10.1111/EPP.12289

[5] Candian, V., Pansa, M., Briano, R., Peano, C., Tedeschi, R., & Tavella, L. (2018). Exclusion nets: a promising tool to prevent Halyomorpha halys from damaging nectarines and apples in NW Italy. Bulletin of Insectology.

[6] Chartois, M., Streito, J. C., Pierre, É., Armand, J. M., Gaudin, J., & Rossi, J. P. (2021). A crowdsourcing approach to track the expansion of the brown marmorated stinkbug Halyomorpha halys (Stål, 1855) in France. Biodiversity Data Journal 9: E66335, 9, e66335-. https://doi.org/10.3897/BDJ.9.E66335

[7] COMMITTEE FOR THE FARM ACCOUNTANCY DATA NETWORK (FADN). (2020). Definitions of Variables used in FADN standard results. EUROPEAN COMMISSION.

[8] Costi, E., Haye, T., & Maistrello, L. (2017). Biological parameters of the invasive brown marmorated stink bug, Halyomorpha halys, in southern Europe. Journal of Pest Science, 90(4), 1059–1067. https://doi.org/10.1007/S10340-017-0899-Z/TABLES/4

[9] Dellinger, T. A., Day, E. R., & Pfeiffer, D. G. (2016). Brown Marmorated Stink Bug in the Mid-Atlantic States: Assessing Grower Perceptions, Economic Impact, and Progress. U.S. Cooperative Extension System. http://hdl.handle.net/10919/73745

[10] EPPO. (2024a). Halyomorpha halys (HALYHA) [France]| . EPPO Global Database. https://gd.eppo.int/taxon/HALYHA/distribution/FR

[11] EPPO. (2024b). Halyomorpha halys (HALYHA)[Slovakia]|. EPPO Global Database. https://gd.eppo.int/taxon/HALYHA/distribution/SK

[12] EPPO Global Database. (2024). Halyomorpha halys (HALYHA). https://gd.eppo.int/taxon/HALYHA

[13] EPPO Reporting Service. (2008). First record of Halyomorpha halys in Switzerland: addition to the EPPO Alert List. EPPO Global Database. https://gd.eppo.int/reporting/article-823?utm_source=chatgpt.com

[14] European Commission. (2020). COMMISSION IMPLEMENTING REGULATION (EU) 2020/465 of 30 March 2020 on emergency measures in support of fruit and vegetables producer organisations in the Italian regions of Emilia Romagna, Veneto, Trentino Alto-Adige, Lombardia, Piemonte and Friuli Venezia Giulia in view of the damage caused to their production by the Asian brown marmorated stink bug (Halyomorpha halys). In Official Journal of the European Union.

[15] Haye, T., Abdallah, S., Gariepy, T., & Wyniger, D. (2014). Phenology, life table analysis and temperature requirements of the invasive brown marmorated stink bug, Halyomorpha halys, in Europe. Journal of Pest Science, 87(3), 407–418. https://doi.org/10.1007/S10340-014-0560-Z/FIGURES/5

[16] Haye, T., Gariepy, T., Hoelmer, K., Rossi, J. P., Streito, J. C., Tassus, X., & Desneux, N. (2015). Range expansion of the invasive brown marmorated stinkbug, Halyomorpha halys: an increasing

threat to field, fruit and vegetable crops worldwide. Journal of Pest Science, 88(4), 665–673. https://doi.org/10.1007/S10340-015-0670-2/FIGURES/1

[17] Kistner, E. J. (2017). Climate Change Impacts on the Potential Distribution and Abundance of the Brown Marmorated Stink Bug (Hemiptera: Pentatomidae) With Special Reference to North America and Europe. Environmental Entomology, 46(6), 1212–1224. https://doi.org/10.1093/EE/NVX157

[18] Kriticos, D., Kean, J. M., Phillips, C. B., Senay, S. D., Acosta, H., & Haye, T. (2017). The potential global distribution of the brown marmorated stink bug, Halyomorpha halys, a critical threat to plant biosecurity. Journal of Pest Science, 90(4), 1033–1043. https://doi.org/10.1007/S10340-017-0869-5/FIGURES/5

[19] Kriticos, D., Maywald, G., Yonow, T., Zurcher, E., Herrmann, N., & Sutherst, R. (2015). CLIMEX. Version 4. Exploring the Effects of Climate on Plants, Animals and Diseases.

[20] Kuhar, T. P., Kamminga, K. L., Whalen, J., Dively, G. P., Brust, G., Hooks, C. R. R., Hamilton, G., & Herbert, D. A. (2018). The Pest Potential of Brown Marmorated Stink Bug on Vegetable Crops. Https://Doi.Org/10.1094/PHP-2012-0523-01-BR, 13(1). https://doi.org/10.1094/PHP-2012-0523-01-BR

[21] Lee, D. H., & Leskey, T. C. (2015). Flight behavior of foraging and overwintering brown marmorated stink bug, Halyomorpha halys (Hemiptera: Pentatomidae). Bulletin of Entomological Research, 105(5), 566–573. https://doi.org/10.1017/S0007485315000462

[22] Lee, D. H., Short, B. D., Joseph, S. V., Bergh, J. C., & Leskey, T. C. (2013). Review of the Biology, Ecology, and Management of Halyomorpha halys (Hemiptera: Pentatomidae) in China, Japan, and the Republic of Korea. Environmental Entomology, 42(4), 627–641. https://doi.org/10.1603/EN13006

[23] Leskey, T. C., Hamilton, G. C., Nielsen, A. L., Polk, D. F., Rodriguez-Saona, C., Christopher Bergh, J., Ames Herbert, D., Kuhar, T. P., Pfeiffer, D., Dively, G. P., Hooks, C. R. R., Raupp, M. J., Shrewsbury, P. M., Krawczyk, G., Shearer, P. W., Whalen, J., Koplinka-Loehr, C., Myers, E., Inkley, D., … Wright, S. E. (2012). Pest Status of the Brown Marmorated Stink Bug, Halyomorpha Halys in the USA. Outlooks on Pest Management, 23(5), 218–226. https://doi.org/10.1564/23OCT07

[24] Leskey, T. C., & Nielsen, A. L. (2018). Impact of the Invasive Brown Marmorated Stink Bug in North America and Europe: History, Biology, Ecology, and Management. Annual Review of Entomology, 63(Volume 63, 2018), 599–618. https://doi.org/10.1146/ANNUREV-ENTO-020117-043226/CITE/REFWORKS

[25] Leskey, T. C., Short, B. D., Butler, B. R., & Wright, S. E. (2012). Impact of the Invasive Brown Marmorated Stink Bug, Halyomorpha halys (Stål), in Mid-Atlantic Tree Fruit Orchards in the United States: Case Studies of Commercial Management. Psyche: A Journal of Entomology, 2012(1), 535062. https://doi.org/10.1155/2012/535062

[26] Leskey, T. C., Short, B. D., & Ludwick, D. (2020). Comparison and Refinement of Integrated Pest Management Tactics for Halyomorpha halys (Hemiptera: Pentatomidae) Management in Apple Orchards. Journal of Economic Entomology, 113(4), 1725–1734. https://doi.org/10.1093/JEE/TOAA067

[27] Leskey, T. C., Short, B. D., Wright, S. E., & Brown, M. W. (2009). Diagnosis and Variation in Appearance of Brown Stink Bug (Hemiptera: Pentatomidae) Injury on Apple. Journal of Entomological Science, 44(4), 314–322. https://doi.org/10.18474/0749-8004-44.4.314

[28] Maistrello, L. (2024). Case Study 2: Halyomorpha halys (Stål) in Europe. 271–359. https://doi.org/10.1007/978-3-031-69742-5_15

[29] Maistrello, L., Costi, E., Caruso, S., Vaccari, G., Bortolotti, P., Nannini, R., Casoli, L., Montermini, A., Bariselli, M., & Guidetti, R. (2016). Halyomorpha halys in Italy: first results of field monitoring in fruit orchards. 112, 1–5.

[30] Martinson, H. M., Venugopal, P. D., Bergmann, E. J., Shrewsbury, P. M., & Raupp, M. J. (2015). Fruit availability influences the seasonal abundance of invasive stink bugs in ornamental tree

nurseries. Journal of Pest Science, 88(3), 461–468. https://doi.org/10.1007/S10340-015-0677-8/FIGURES/4

[31] Ming, G.-Z., Zhao, X.-B., Wang, P., & Zhao, X. Z. (2001). he damage of Halyomorpha halys to pear and its control techniques. Plant Protection Technology and Extension, 21.

[32] Nielsen, A. L., & Hamilton, G. C. (2009). Seasonal Occurrence and Impact of Halyomorpha halys (Hemiptera: Pentatomidae) in Tree Fruit. Journal of Economic Entomology, 102(3), 1133–1140. https://doi.org/10.1603/029.102.0335

[33] Nielsen, A. L., Hamilton, G. C., & Matadha, D. (2008). Developmental Rate Estimation and Life Table Analysis for Halyomorpha halys (Hemiptera: Pentatomidae). Environmental Entomology, 37(2), 348–355. https://doi.org/10.1093/EE/37.2.348

[34] NZIER. (2017). Quantifying the economic impacts of a Brown Marmorated Stink Bug incursion in New Zealand. https://www.nzier.org.nz/publications/quantifying-the-economic-impacts-of-a-brown-marmorated-stink-bug-incursion-in-new-zealand

[35] Pajač Živković, I., Čirjak, D., Miklečić, I., Pintar, M., Duralija, B., & Lemic, D. (2023). First evidence of the brown marmorated stink bug and its population size in perennial crops in Croatia. Journal of Central European Agriculture, 24(4), 908–915. https://doi.org/10.5513/JCEA01/24.4.4092

[36] Qin, W. (1990). Occurrence rule and control techniques of Halyomorpha picus. Plant Protection, 22(16).

[37] Rice, K. B., Bergh, C. J., Bergmann, E. J., Biddinger, D. J., Dieckhoff, C., Dively, G., Fraser, H., Gariepy, T., Hamilton, G., Haye, T., Herbert, A., Hoelmer, K., Hooks, C. R., Jones, A., Krawczyk, G., Kuhar, T., Martinson, H., Mitchell, W., Nielsen, A. L., … Tooker, J. F. (2014). Biology, Ecology, and Management of Brown Marmorated Stink Bug (Hemiptera: Pentatomidae). Journal of Integrated Pest Management, 5(3), A1–A13. https://doi.org/10.1603/IPM14002

[38] Short, B. D., Khrimian, A., & Leskey, T. C. (2017). Pheromone-based decision support tools for management of Halyomorpha halys in apple orchards: development of a trap-based treatment threshold. Journal of Pest Science, 90(4), 1191–1204. https://doi.org/10.1007/S10340-016-0812-1/FIGURES/9

[39] Wermelinger, B., Wyniger, D., & Forster, B. (2007). First records of an invasive bug in Europe: Halyomorpha halys Stål (Heteroptera: Pentatomidae), a new pest on woody ornamentals and fruit trees?

[40] Wesseler, J., & Fall, E. H. (2010). Potential damage costs of Diabrotica virgifera virgifera infestation in Europe – the 'no control' scenario. Journal of Applied Entomology, 134(5), 385–394. https://doi.org/10.1111/j.1439-0418.2010.01510.x

[41] Wiman, N. G., Walton, V. M., Shearer, P. W., Rondon, S. I., & Lee, J. C. (2015). Factors affecting flight capacity of brown marmorated stink bug, Halyomorpha halys (Hemiptera: Pentatomidae). Journal of Pest Science, 88(1), 37–47. https://doi.org/10.1007/S10340-014-0582-6/FIGURES/7

[42] Woodward, F. I. . (1996). Climate and plant distribution. 174.

[43] Yang, Z. Q., Yao, Y. X., Qiu, L. F., & Li, Z. X. (2009). A New Species of Trissolcus (Hymenoptera: Scelionidae) Parasitizing Eggs of Halyomorpha Halys (Heteroptera: Pentatomidae) in China with Comments on its Biology. Annals of the Entomological Society of America, 102(1), 39–47. https://doi.org/10.1603/008.102.0104

[44] Zhang, C., Li, D., Su, H., & Xu, G. (1993). A study on the biological characteristics of Halyomorpha picus and Erthesina fullo. Forest Research.

[45] Zhang, J.-M., Wang, H., Zhao, L.-X., Zhang, F., & Yu, G.-Y. (2007). Damage to an organic apple orchard by the brown marmorated stink bug, Halyomorpha halys and its control strategy. Chinese Bulletin of Entomology, 44, 898–901.

[46] Zhu, G., Gariepy, T. D., Haye, T., & Bu, W. (2017). Patterns of niche filling and expansion across the invaded ranges of Halyomorpha halys in North America and Europe. Journal of Pest Science, 90(4), 1045–1057. https://doi.org/10.1007/S10340-016-0786-Z/FIGURES/4

1.5 Acknowledgments

We thank DG AGRI for providing access to the EU-FADN data (agreement IFD 2024_09). We also thank Darren J. Kriticos for kindly providing us with the CliMond CM_TC10 World dataset, centered on 1995.

1.6 Appendix

Table A1.1. CLIMEX model parameters for *Halyomorpha halys* adopted from (D. Kriticos et al., 2017). Parameter values without units are dimensionless indices of plant available soil moisture.

Parameters	Description	Unit	Current study
DV0	Lower temperature threshold	°C	**12**
DV1	Lower optimal for growth	°C	**27**
DV2	Upper optimal for growth	°C	**30**
DV3	Upper temperature threshold	°C	**33**
SM0	Lower soil moisture threshold		**0.1**
SM1	Lower optimal soil moisture		**0.5**
SM2	Upper optimal soil moisture		**1**
SM3	Upper soil moisture threshold		**1.5**
TTCS	Cold stress temperature threshold	°C	**-18**
THCS	Cold stress accumulation rate	$week^{-1}$	**-0.01**
TTHS	Heat stress temperature threshold	°C	**33**
THHS	Heat stress accumulation rate	$week^{-1}$	**0.01**
SMDS	Soil moisture dry stress threshold		**0.1**
HDS	Dry stress accumulation rate	$week^{-1}$	**-0.01**
SMWS	Soil moisture wet stress threshold		**1.5**
HWS	Wet stress accumulation rate	$week^{-1}$	**0.002**
DPD0	Diapause induction day length	h light	**12**
DPT0	Diapause induction temperature	°C	**5**
DPT1	Diapause termination temperature	°C	**5**
DPD	Diapause development days	days	**0**
DPSW	Diapause summer (1) or winter (0)		**0**

TTHW	Threshold soil moisture (Hot-Wet Stress)		**28**
MTHW	Threshold temperature (Hot-Wet Stress)	°C	**1.5**
PHW	Stress accumulation rate (Hot-Wet Stress)	week^{-1}	**0.007**

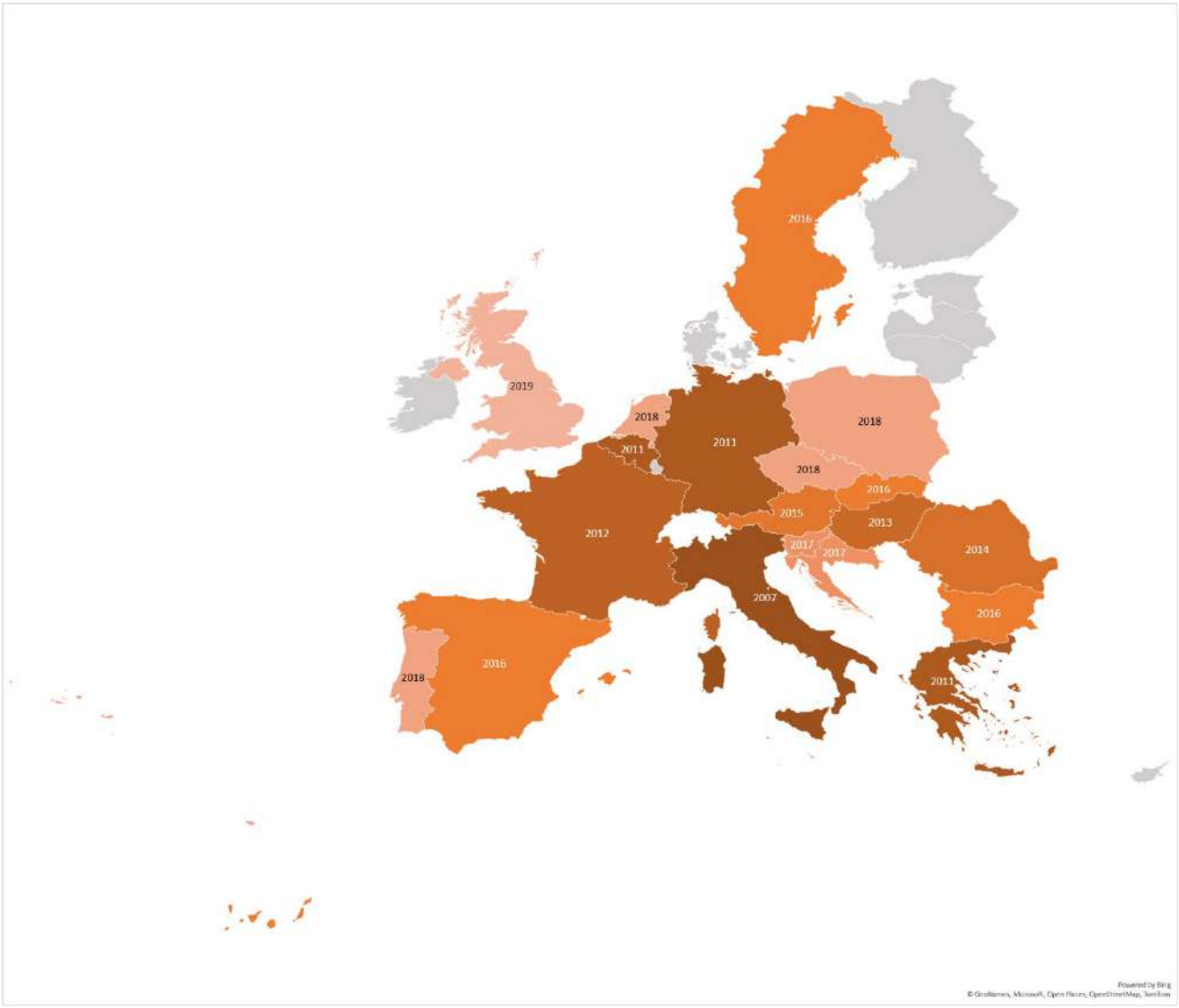

Figure A1.1. Geographical expansion of *Halyomorpha halys* in Europe by year of first detection. (Source: https://gd.eppo.int/taxon/HALYHA/distribution)

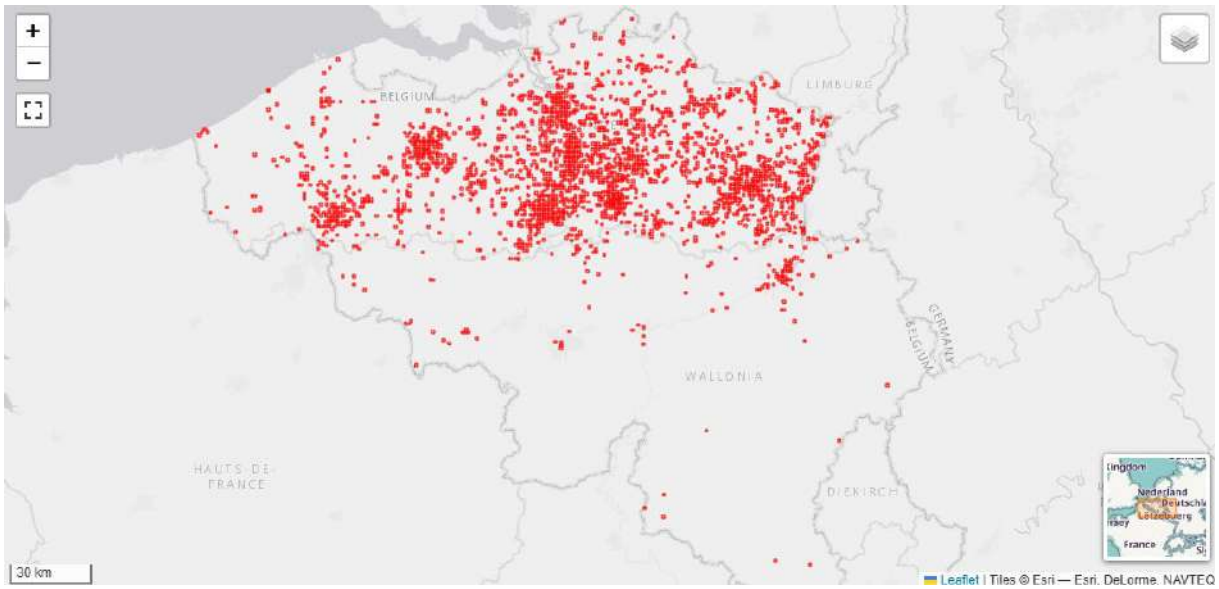

Figure A1.2. Occurrence map of Halyomorpha halys in Belgium. Each red grid cell represents a 1km^2 area. (Source: Waarnemingen.be)

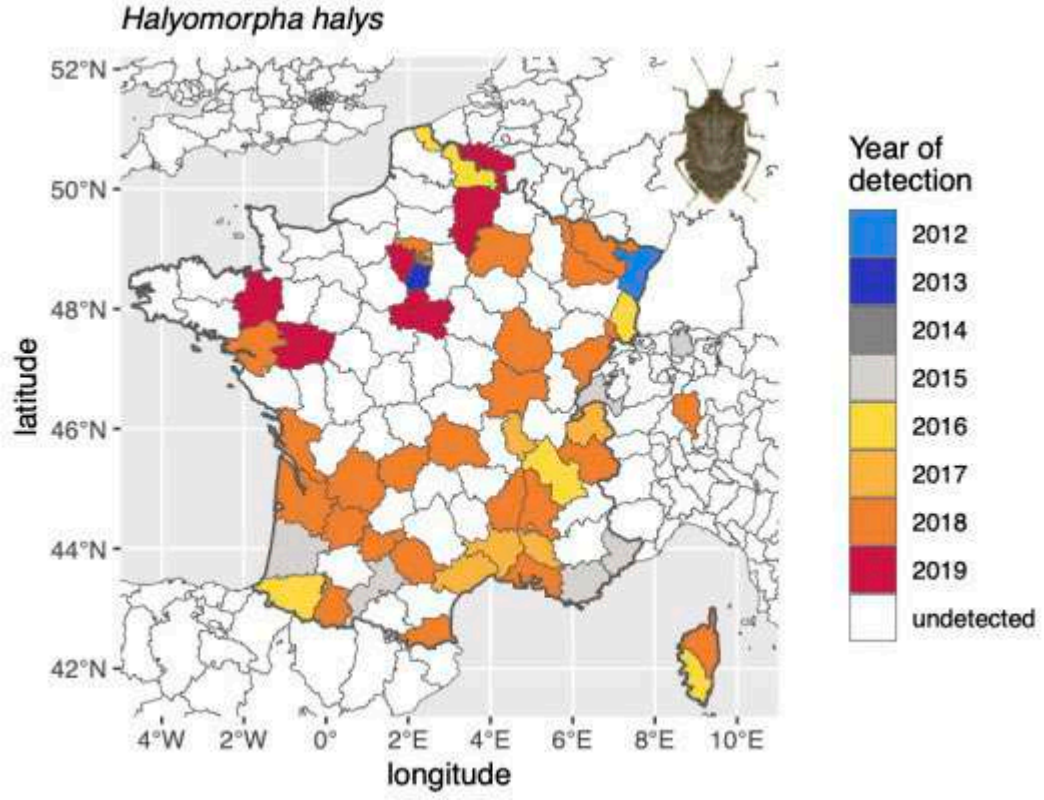

Figure A1.3. The geographical expansion of *Halyomorpha halys* from 2012 to 2019. This figure was produced by (Chartois et al., 2021).

Figure A1.4. Population size of *Halyomorpha halys* during the vegetation season in Croatia. This figure was produced by (Pajač Živković et al., 2023)

Figure A1.5. Occurrence records of *Halyomorpha halys* in the Netherlands. This figure was produced by (Aukema et al., 2019)

Table A1.2. List of FADN variables used in this study.

Variable	Common name	Unit	Description
COUNTRY	COUNTRY	NA	
YEAR	YEAR	Accounting year	
CAPL_A	Apples area	Hectares	Farm size
CAPL_PRQ	Apples production quantity	Tonnes	
CAPL_TO	Apples total output value	Euros	= Sales + farm use + farmhouse consumption + (closing valuation – opening valuation)
CPEAR_A	Pears area	Hectares	Farm size
CPEAR_PRQ	Pears production quantity	Tonnes	
CPEAR_TO	Pears total output value	Euros	= Sales + farm use + farmhouse consumption + (closing valuation – opening valuation)
WEIGHT (SYS02)		Number	Sum of weighting coefficients of individual holdings in the sample (=sample farm's weight for individual farms)

Table A1.3. Damage reported on apple tree cultivation caused by *Halyomorpha halys* in Italian regions over eight years. Evaluations from researchers and managers of the Italian regional plant health services. (The numbers indicate the yield loss intensity detected, as (1): <10%, (2): 10-30%, (3): 30-70%, and (4): >70%). Source: (Maistrello, 2024)

Region	2016	2017	2018	2019	2020	2021	2022	2023
Emilia Romagna	2	2	3	3	2	3	2	2
Veneto	3	3	2	3	2	2	2	2
Piedmont	2	2	3	3	2	2	2-3	3
Lombardy	2	3	2	3	2	2	3	2
Trentino	1	1	1	3	2	2	1	1
Alto Adige	1	1	1	2	2	2	2	1
Val d'Aosta	-	-	-	-	1	1	1	1
Friuli Venezia Giulia	3	3	3	3	2	1-2	1	1-2
Umbria	-	-	-	3	2	2	2	2
Campania	-	-	-	-	2	2	2	2

Table A1.4. Damage reported on pear tree cultivation caused by *Halyomorpha halys* in Italian regions over eight years. Evaluations from researchers and managers of the Italian regional plant health services. (The numbers indicate the yield loss intensity detected, as (1): <10%, (2): 10-30%, (3): 30-70%, and (4): >70%). Source: (Maistrello, 2024)

Region	2016	2017	2018	2019	2020	2021	2022	2023
Emilia Romagna	3	2	3	4	2-3	3	2	2-3
Veneto	3	3	3	4	2-3	-	2	2-3
Piedmont	3	3	3	4	2	2-3	3	3
Lombardy	3	3	3	4	2-3	3	3	3

2 THE POTENTIAL DIRECT ECONOMIC IMPACT OF *HELICOVERPA ARMIGERA* IN EUROPE

2.1 Background

The cotton bollworm (CBW), *Helicoverpa armigera* (Hübner) – also known as the Old World bollworm, African cotton bollworm, or corn earworm – is a polyphagous pest, causing severe economic losses to the "Old World" (Asia, Europe, Africa) and Australasia (Tay et al., 2013). The pest is listed as an EPPO A2 quarantine pest, and its presence is confirmed in most countries across the EPPO region (**Fig. 2.1**) (CABI, 2021; EPPO, 2024). Hardwick (1965) suggested the CBW's native range is between the latitudes of 40°N and 40°S. Evidently, CBW is considered a global pest with a rapidly expanding distribution, high dispersal capacity, and wide feeding range (EPPO, 2024d). Noteworthy, the pest has not been detected in the USA, although it has been recognized as an important biosecurity threat; a big chunk of North America has favorable climatic conditions for CBW permanent population establishment (**Fig. A2.1**).

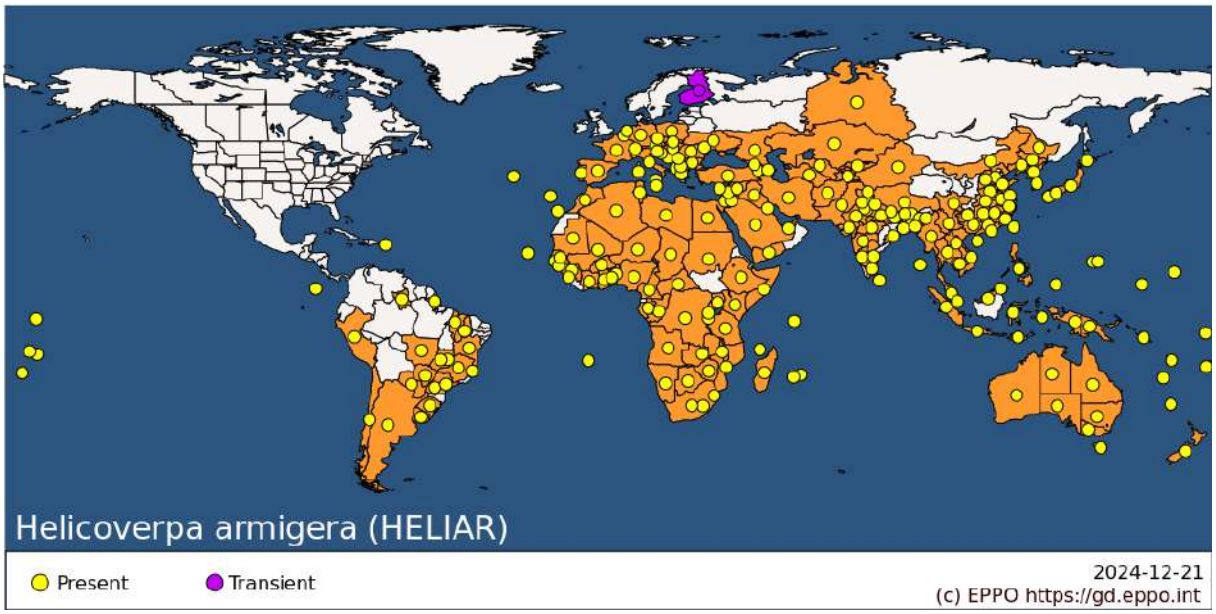

Figure 2.1. The current global distribution of *Helicoverpa armigera.* (Source: EPPO Global Database)

CBW feeds on a broad range of host plants (>180), including field crops, such as cotton, sunflower, chickpeas, and soybeans; horticultural crops, such as tomato, lettuce, and peppers; and flowers, such as roses and chrysanthemums (Haile et al., 2021; D. J. Kriticos, Ota, et al., 2015; Lammers & MacLeod, 2007). The larvae are the most destructive stage of CBW's lifecycle, feeding primarily on the reproductive structures of the host plants, especially from the third instar onward (Riaz et al., 2021). Feeding stunts plant growth, delays flowering and fruit production, and leads to direct infestation and spoilage of certain fruits, such as tomatoes (Riaz et al., 2021; Tripathy et al., 1999).

The economic impact of CBW was estimated to exceed US$2 billion annually even before its introduction to Latin America and without accounting for the additional costs of control measures (Tay et al., 2013). Upon its arrival in Brazil, the pest caused an estimated US$800 million in damage during the first crop season (2012/2013) (Haile et al., 2021; Pomari-Fernandes et al., 2015). During the same crop season, another study reports that the economic losses reached US$1 billion only in western Bahia of Brazil, and yield losses on major crops were up to 35%

(Mastrangelo et al., 2014). Since then, its annual economic impact has been projected to reach several billion USD and is expected to rise further as the pest continues to establish itself in new regions (Leite et al., 2014). In India, in the late 1980s, losses of both pulses and cotton were estimated to exceed US$500 million, with annual additional spending on control of $US127 million (CABI, 2021).

2.2 Data, Methodology, and Results

This report utilized individual farm-level data from the Farm Accountancy Data Network (FADN), an annual farm survey conducted by EU Member States. The FADN database includes accountancy data from approximately 80000 agricultural holdings, making it the only harmonized and representative source of microeconomic data for commercial agricultural holdings in Europe (above a minimum economic size). The database covers roughly 90% of the total utilized agricultural area and accounts for approximately 90% of the Union's total agricultural production (COMMITTEE FOR THE FARM ACCOUNTANCY DATA NETWORK (FADN), 2020).
Data on the total country area were sourced from Eurostat. Farm-level data for all EU-27 Member States, including the United Kingdom, were extracted from the FADN database for the period 2013–2021. The results were aggregated and reported at the NUTS0 (country) level. Specifically, the analysis focused on crop-specific cultivated area, production, and total output for each farm per year (**Table A2.3**). Yields and revenues per hectare were calculated at the farm level and subsequently aggregated by country and year. Finally, averages over the 2013–2021 period were computed for each country, summarizing the average tomato and sunflower area, production, total output, yield, and revenue per hectare (**Table 2.4**, **Table 2.5**).
To extrapolate FADN data to represent all agricultural holdings in the EU, a specialized weighting system has to be applied. This system, based on the "free expansion" principle, assigns an extrapolation factor (weight) to each farm in the sample. The weight corresponds to the ratio between the number of agricultural holdings in the population and the number of holdings in the sample for the same classification cell (region x type of farming x economic size class). These weights ensure that the weighted averages calculated accurately represent the broader population, accounting for sampling differences.

2.2.1 Potential Distribution and Spread in Europe

2.2.1.1 State of invasion / Infested area

Information on the current distribution of CBW in Europe[21] was determined using information from the EPPO Global Database (EPPO Global Database, 2024) which includes information on the year of first detection and the pest's current "pest status" as evaluated by the EPPO Secretariat. To estimate the infested area, we incorporated this qualitative information on pest status and the time elapsed since its first detection in each country. For example, higher infestation rates were assumed in countries where CBW is categorized as "widespread" compared to those with "restricted distribution". **Table 2.1** provides a summary of this information and presents an estimated percentage of CBW's current state of invasion in each country.
We approximated the infested area by linking EPPO pest status categories to specific ranges of infestation within the susceptible area. These assumptions are detailed below[22]:

[21] As of 2024.
[22] It is important to emphasize that, while the assigned quantitative percentages offer a "logical" framework for approximating the current state of invasion, they remain inherently non-trivial. The primary purpose of EPPO's "pest status" classification is to indicate the presence or absence of a specific species within a country—a system originally

vi. **Absent, *intercepted only / pest eradicated / pest no longer present***: For countries categorized as "Absent" and CBW has been eradicated or intercepted or is no longer present, the infested area is assumed to be 0%. Similarly, countries where CBW has not been reported (as of December 2024) are assigned an infested area of 0%.

vii. **Present**, ***few occurrences***: In countries with a limited presence of CBW, 10–20% of the susceptible area is assumed to be infested.

viii. **Present**, ***restricted distribution***: For countries reporting CBW with a restricted distribution, the estimated infested area ranges from 20–40% of the susceptible area.

ix. **Present**, ***widespread***: Countries where CBW is classified as "widespread" are assumed to have an infested area of 60–80% of their susceptible area.

x. **Present**, ***no details***: In cases where CBW is reported as present but without specific distribution details, there is greater uncertainty regarding infestation levels. The infested area is estimated based on the year of first detection and ranges from 10–80% of the susceptible area. Additional data from EPPO or relevant literature were incorporated where available.

xi. **Transient**: No assumptions were made regarding the percentage of transient populations currently infested. The uncertainty of assigning a percentage of annual infestation level for transient populations is extremely high, so these countries were excluded from the economic analysis. This includes Finland and Sweden, where CBW can only form transient populations[23] (**Fig. A2.3**). Estonia and Denmark may also host transient CBW populations that may occur but were excluded due to limited data availability.

In addition to pest status categories, the time since the first CBW detection was used as a secondary factor to refine estimates of the infested area. Countries with more recent CBW detections (within the past five years, after 2019) were assigned infestation estimates at the lower end of the corresponding range, reflecting an early invasion stage. Countries with detections between five and ten years ago were assigned mid-range values, while those with detections over ten years ago were assigned estimates at the higher end of the range. For the "present, no details" category, the broad range was further narrowed using additional information from National Plant Protection Organizations and relevant literature.

developed for use in a plant quarantine context and not in a biological invasion one (personal communication with EPPO)

[23] In the case of Sweden, the area that may support permanent population establishment is negligible (**Fig. A2.2**).

Table 2.1. Distribution details of *Helicoverpa armigera* in Europe and estimated (%) infested area for each country.

Country	Year of First Detection	Status	EPPO Link	Infested Area (as % of susceptible area)	Additional reasoning
Belgium	2006	Present, few occurrences	Distribution details in Belgium	20	
Bulgaria	1993	Present, widespread	Distribution details in Bulgaria	80	
Cyprus	1993	Present, widespread	Distribution details in Cyprus	80	
Czech Republic	1994	Present, few occurrences	Distribution details in Czech Republic	20	
Denmark	-	Absent, intercepted only	Distribution details in Denmark	0	
Germany	1993	Present, few occurrences	Distribution details in Germany	20	
Greece	1941[24]	Present, widespread	Distribution details in Greece	80	
Spain	1993	Present, widespread	Distribution details in Spain	80	
Estonia	1993	Absent, pest no longer present	Distribution details in Estonia	0	
France	1987[25]	Present, restricted distribution	Distribution details in France	40	**Fig. A2.4**
Croatia	1993	Present, no details	Distribution details in Croatia	80	

[24] A resurgence of CBW was observed in 2010 in Greece, although the first records of its presence and damage records date back many decades (Isaakides, 1941; Mironidis et al., 2013).
[25] *Helicoverpa armigera* samples were collected from tomato plants in southern France in 1987. (Nibouche et al., 1998b)

Hungary	1951	Present, restricted distribution	Distribution details in Hungary	80	The pest was found in most Hungarian counties. The authors estimated that CBW occupied 94% of Hungary within 8 years (Keszthelyi et al., 2013). (**Fig. A2.5**)
Ireland	-	Absent / Not detected	-	0	
Italy	1993	Present, restricted distribution	Distribution details in Italy	40	
Lithuania	-	Absent / Not detected	-	0	
Luxembourg	-	Absent / Not detected	-	0	
Latvia	1993	Absent, pest no longer present	Distribution details in Latvia	0	
Malta	1993	Present, restricted distribution	Distribution details in Malta	80	
Netherlands	1999	Present, few occurrences	Distribution details in the Netherlands	20	
Austria	2003	Present, few occurrences	Distribution details in Austria	20	
Poland	2003[26]	Present, few occurrences	Distribution details in Poland	20	
Portugal	1992[27]	Present, widespread	Distribution details in Portugal	80	
Romania	1993	Present, widespread	Distribution details in Romania	80	
Finland	1997	Transient	Distribution details in Finland	-	CBW occurs seasonally in southern coastal areas (EPPO,

[26] The first reports of CBW in Poland come from 2003 on maize cultivations (Bereś, 2008).
[27] *Helicoverpa armigera* samples were collected from tomato plants in Portugal in 1992 (Nibouche et al., 1998b).

					2024d). **Fig. A2.6** shows the location of the observations.
Sweden	-	Absent / Not detected	-	0	
Slovakia	1996	Present, restricted distribution	Distribution details in Slovakia	40	
Slovenia	2000[28]	Present restricted distribution	Distribution details in Slovenia	40	
United Kingdom	1992	Absent, pest eradicated	Distribution details in the United Kingdom	0	

2.2.1.2 The area under risk / Susceptible area

The starting point of this analysis was to identify areas where climatic conditions allow the CBW permanent population establishment. While several factors influence a species' geographical distribution, climate is a key determinant (Andrewartha & Birch, 1954; Woodward, 1996). Although not the sole limiting factor, climate is quantifiable and provides a practical starting point for estimating a species' potential geographical distribution (D. Kriticos et al., 2015).

To project CBW's potential distribution in the EU, we used the CLIMEX climate-based niche model with parameter values tailored to CBW's growth and development requirements, as proposed by (D. J. Kriticos, Ota, et al., 2015). The exact parameter values are provided in the **Appendix** (**Table A2.1**). CLIMEX is a process-based bioclimatic modeling tool that integrates species-specific climatic responses with meteorological data to predict potential distribution and relative abundance (D. Kriticos et al., 2015). The model assumes that a specie's population experiences two seasons: a favorable season for growth, represented by the annual growth index (GI_A), which integrates temperature (TI) and moisture indices (MI), and an unfavorable season, defined by stress indices (cold, dry, hot, wet) and their interactions. An annual index of climatic suitability was obtained with the weekly integration of the growth (favorable season) and stress (unfavorable season) indices. This integrated index describes the level of climatic suitability and is known as the ecoclimatic index (EI). Both EI and GI_A range from 0 to 100, where 0 represents unsuitable conditions for species persistence or growth, respectively, and a theoretical maximum of 100 (optimal conditions). More specifically, an area with $GI_A > 0$ and $EI = 0$ may support transient CBW population establishment, and an area with $EI > 0$ can support permanent CBW populations. For visualization in QGIS, the EI was classified into four categories: unsuitable ($EI = 0$), marginal ($1 < EI \leq 5$), moderate ($5 < EI \leq 15$), and optimal ($EI > 15$) (**Fig. 2.2**).

As stated above, we did not consider countries or areas that only support transient CBW population establishment. However, a map with both GI_A and EI indices is provided in the Appendix (**Fig. A2.3**) along with the modified values of **Table 2.2**[29] (**Table A2.2**).

(D. J. Kriticos, Ota, et al., 2015) originally used the CliMond CM10 World (1975H V1.1) climate dataset in their CBW CLIMEX model, which includes 30-year averages centered on 1975 (1961–

[28] The EPPO Secretariat had previously no data on the occurrence of *Helicoverpa armigera* in Slovenia.
[29] In the scenario we would not differentiate between the two climatic suitability indices and treat them as a composite index.

1990). The dataset consists of daily minimum and maximum temperatures (°C), monthly precipitation (mm), and relative humidity (%) recorded at 9:00 and 15:00 h, interpolated at a 10-arc-minute gridded resolution. For our analysis, we updated this to a more recent climatology: the CliMond CM_TC10 World dataset (1981–2010), centered on 1995) (*unpublished,* provided after personal communication with Darren J. Kriticos). The updated dataset offers a greater number of locations (808020 locations compared to 565801 in the original), which better reflects current climatic conditions. This updated climatology enhances the accuracy and detail of the projections, providing more realistic results, particularly in the context of ongoing climate change.

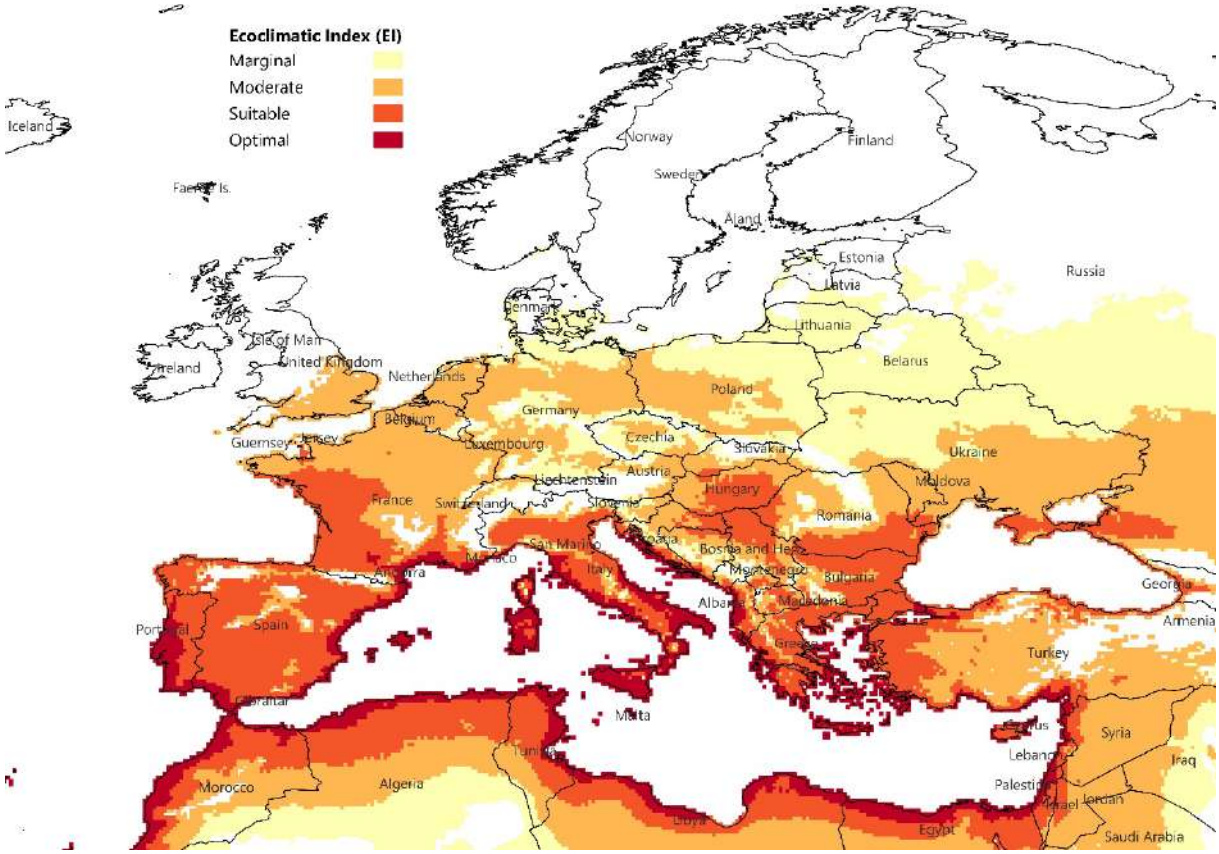

Figure 2.2. Modeled climate suitability (CLIMEX Ecoclimatic Index) for *Helicoverpa armigera* under current climatic conditions in Europe. The figure was created with QGIS Desktop version 3.38.1 (https://www.qgis.org/).

Fig. 2.2 shows the areas in Europe that are climatically suitable for the establishment of CBW permanent populations. To simplify the analysis, the EI values were converted into a binary variable, disregarding distinctions between different suitability levels. Thus, the resulting binary layer classified regions are suitable (EI = 1) or unsuitable (EI = 0) for CBW persistence. Subsequently, it intersected with country boundaries, and the susceptible area in each country was computed as a percentage of its total land area (**Table 2.2**).

Table 2.2. Country size, area susceptible, and area not yet infested but susceptible to *Helicoverpa armigera* infestation in Europe.

Country	Total area[30]	Susceptible area		Infested area	Area not yet infested but susceptible	
	km²	km²	%	km²	km²	%[31]
Belgium	30667	27152	89	5430	21722	80
Bulgaria	110996	103296	93	82637	20659	20
Cyprus	9253	9253	100	7402	1851	20
Czech Republic	78871	59838	76	11968	47871	80
Denmark	42925	15502	36	0	15502	100
Germany	357569	318110	89	63622	254488	80
Greece	131694	128947	98	103158	25789	20
Spain	505983	464792	92	371833	92958	20
Estonia	45336	1819	4	0	1819	100
France	638475	588623	92	235449	353174	60
Croatia	56594	55214	98	44171	11043	20
Hungary	93012	93012	100	74410	18602	20
Ireland	69947	0	0	0	0	100
Italy	302079	266961	88	106784	160176	60
Lithuania	65284	56721	87	0	56721	100
Luxembourg	2595	2524	97	0	2524	100
Latvia	64586	20372	32	0	20372	100
Malta	316	316	100	253	63	20
Netherlands	37378	37378	100	7476	29902	80
Austria	83878	35620	42	7124	28496	80
Poland	311928	294962	95	58992	235970	80
Portugal	92227	92220	100	73776	18444	20
Romania	238398	201377	84	161102	40275	20
Finland	338411	0	0	0	0	-
Sweden	447424	925	0.9	0.2	925	100
Slovakia	49035	33353	68	13341	20012	60
Slovenia	20273	17411	86	6964	10446	60
United Kingdom	243610	60998	25	0	60998	100
Total	4468744	2986696	67	1435893	1550803	

The results indicate that the total area of the countries considered is approximately 4.4 million km², with 67% of this area – equivalent to 2.9 million km² - being susceptible to CBW infestation. The % of susceptible areas is based on the CLIMEX output and represents the percentage of each country that has favorable climatic conditions that allow CBW year-round persistence. Most of the countries considered appear to be largely suitable for permanent CBW establishment to a large extent. More specifically, countries such as Belgium, Bulgaria, Germany, Greece, Spain, France,

[30] Source: EUROSTAT (2024) Area by NUTS 3 region
[31] In percentage of the total susceptible area.

Croatia, Italy, Lithuania, Luxembourg, and Poland have over 85% of their total area classified as suitable. Notably, countries such as Cyprus, Hungary, Malta, the Netherlands, and Portugal appear suitable to their total extent. On the other hand, Ireland, Lithuania, Luxembourg, Latvia, Finland, and Sweden are classified as unsuitable for permanent CBW population establishment under current climatic conditions.

2.2.2 Spread

The spread rate is a critical factor impacting the damage costs associated with CBW, as these costs are directly linked to the extent of the infested area. CBW adults are capable of long-distance migration when environmental conditions become unfavorable or when they seek available host plants (C. M. Jones et al., 2019). Assisted by wind currents, CBW adults can travel distances exceeding 250 km in a single day (Feng et al., 2009; Haile et al., 2021). Jones et al., (2015) report flying distances of up to 40.6 km in a single night. In contrast, there is evidence that CBW adults are able to migrate across distances beyond 2000 km (e.g., from the northern frontier of the Sahara to the sub-Saharan zone) (Nibouche et al., 1998a; Riaz et al., 2021).

Most of the European continent is suitable for CBW overwintering populations, especially the Mediterranean and southern regions, whereas northern areas host transient populations during spring and early summer (Lammers & MacLeod, 2007). Southern Europe and North Africa are source locations for CBW northward migration, with adults found in the UK from March to November, Northern Ireland from July to October, and a few records in Sweden, Finland, and Estonia (Baker et al., 2014; Heath & Emmet, 1991; Pedgley, 1985; Thompson & Nelson, 2003).

Following the framework of Wesseler & Fall (2010), we compute the annual infested area per country and per year by using a radial range expansion model:

$$IA_{i,t} = \begin{cases} (rr \cdot t)^2 \cdot \pi & if IA_{i,t} < SA_i \\ SA_i & if\ IA_{i,t} \geq SA_i \end{cases} \quad (1)$$

where $i = 1, 2, \ldots, n$.

In this model, $IA_{i,t}$ is the infested area in the country i and year t, rr is the rate of spread (km^2/yr), π is the mathematical constant, n is the number of countries considered, and SA_i is the susceptible area to BMSB infestation in the country i. The total infested area TIA_t^A (km^2) at year t is the sum of the annual infested areas:

$$TIA_t^A = \sum_{i=1}^{n} IA_{i,t} \quad (2)$$

If we assume that BMSB is introduced in all countries considered simultaneously and define the total susceptible area as $SA = \sum_{i=1}^{n} SA_i$, then the total infested area TIA_t^B at time t is computed as:

$$TIA_t^B = \begin{cases} n \cdot (rr \cdot t)^2 \cdot \pi & if\ n \cdot (rr \cdot t)^2 \cdot \pi < SA \\ SA & if\ n \cdot (rr \cdot t)^2 \cdot \pi \geq SA \end{cases} \quad (3)$$

Table 2.3 presents the estimated number of years required for CBW to infest the susceptible area of each country (SA_i), under various annual spread rate scenarios ranging from 10 to 120 km^2/year. As expected, smaller countries like Luxembourg and Malta, as well as countries with limited suitable area for CBW establishment, such as Sweden and Estonia, require fewer years to reach complete infestation. Conversely, larger countries like France and Spain take rather long, even at higher spread rates. For instance, at a spread rate of 50 km²/year, the susceptible area of France would be fully infested in approximately 9 years, whereas smaller countries like Belgium or Cyprus would require only 2 years. The calculations for "Total A" consider the country-specific

SA_i, while "Total B" assumes simultaneous CBW introduction across all countries, accounting for transboundary spread effects.

Table 2.3. Number of years until the country area is infested for different annual spread rates. Total A represents the results considering the sum of the susceptible area of each country, and Total B presents the results considering the area not yet infested but susceptible, as reported in **Table 2.2** and *Helicoverpa armigera* disperses beyond country borders.

Country	Susceptible area (km^2)	Number of years until total infestation					
		Annual speed of spread (km^2/year)					
		10	30	50	70	90	120
Belgium	27152	10	4	2	2	2	1
Bulgaria	103296	19	7	4	3	3	2
Cyprus	9253	6	2	2	1	1	1
Czech Republic	59838	14	5	3	2	2	2
Denmark	15502	8	3	2	2	1	1
Germany	318110	32	11	7	5	4	3
Greece	128947	21	7	5	3	3	2
Spain	464792	39	13	8	6	5	4
Estonia	1819	3	1	1	1	1	1
France	588623	44	15	9	7	5	4
Croatia	55214	14	5	3	2	2	2
Hungary	93012	18	6	4	3	2	2
Ireland	0	0	0	0	0	0	0
Italy	266961	30	10	6	5	4	3
Lithuania	56721	14	5	3	2	2	2
Luxembourg	2524	3	1	1	1	1	1
Latvia	20372	9	3	2	2	1	1
Malta	316	2	1	1	1	1	1
Netherlands	37378	11	4	3	2	2	1
Austria	35620	11	4	3	2	2	1
Poland	294962	31	11	7	5	4	3
Portugal	92220	18	6	4	3	2	2
Romania	201377	26	9	6	4	3	3
Finland	0	0	0	0	0	0	0
Sweden	925	2	1	1	1	1	1
Slovakia	33353	11	4	3	2	2	1
Slovenia	17411	8	3	2	2	1	1
United Kingdom	60998	14	5	3	2	2	2
Total A	2986696	98	33	20	14	11	9
Total B	1550803	71	24	15	11	8	6

These country-specific estimates may underestimate the time required for total infestation in large countries such as Germany and France, as the model does not incorporate encroachment from neighboring countries (Wesseler & Fall, 2010). On the other hand, for elongated countries like

Portugal, the results might overestimate infestation timelines due to the radial spread modeling approach, which assumes a uniform circular expansion based solely on the country's total area.

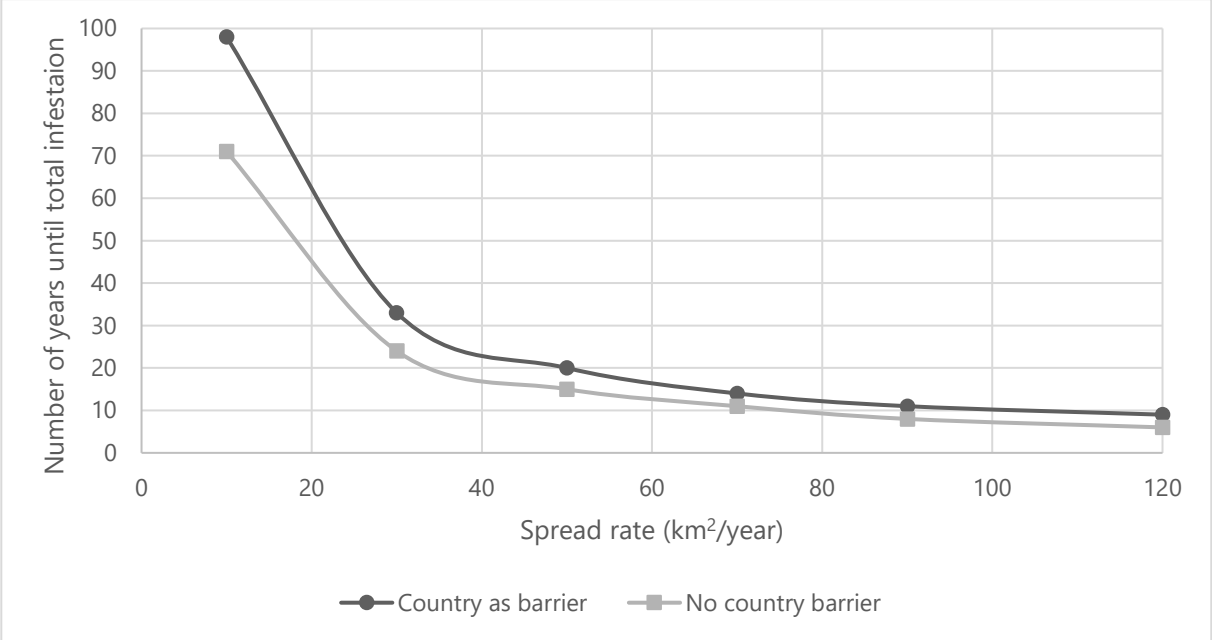

Figure 2.3. Rate of spread and number of years until total infestation, based on the results of **Table 2.3**.

Fig. 2.3 illustrates the relationship between the spread rate and the time required for total infestation under two scenarios: "Total A" which accounts for country barriers, and "Total B" which assumes no country barriers. The results indicate an exponential decrease in infestation time as the spread rate increases. This effect is particularly noticeable at lower spread rates; for example, reducing the spread rate from 30 km²/year to 10 km²/year could result in a threefold increase in infestation time. In contrast, at higher spread rates, the decrease in infestation time becomes less apparent. These findings highlight the critical importance of early detection and rapid eradication during the initial stages of an invasion, when intervention efforts are most effective and cost-efficient.

2.2.3 Determination of impacts – Yield losses

Four key traits responsible for the notoriety of CBW are its polyphagy (wide host range), high fecundity, facultative diapause, and exceptional mobility rates (Rahman et al., 2016). Additional factors are the pest's direct feeding on reproductive structures of the host plant, multivoltine lifecycle, nocturnal behavior, and the presence of overlapping generations (Meena & Raju, 2014). This analysis focuses on **two important host plants of CBW**, namely tomato and sunflower seeds.

2.2.3.1 Tomato

CBW is primarily a pest of outdoor tomato cultivations in southern Europe (Lammers & MacLeod, 2007). Young tomato fruits often drop prematurely due to CBW larvae. Larger larvae may bore into older fruits, creating entry points for secondary infection by other organisms (CABI, 2021). Almost 40 years ago, CBW was reported to inflict 5-55% yield losses in tomato-growing areas in India (Kashyap & Verma, 1987). Another study reports that yield losses may reach 60% (Montmany, 1993). Similarly, field trials in eight different tomato varieties in India revealed that

the damage percentage varied from 15.5% up to 45.3% in the absence of control methods (Thakur et al., 2017). (Torres-Vila et al., 2003) measured yield loss at different CBW larval intensities, resulting in observed losses from 0-62%. Tomato plots without any control measure exhibited losses of up to 87.5%, whereas, to those where insecticides were applied, yield losses reached 42.5% (Hanafy & El-Sayed, 2013).

Table 2.4 presents the average tomato area, production, total output, yield, and revenue across the EU-27 and the UK for the period 2013–2021. Spain, the Netherlands, and France are the major tomato producers of the EU, with average annual production of 2087, 910, and 682 thousand tonnes, respectively. These three countries account for approximately 70% of the total tomato production in the Union. In contrast, countries such as Denmark, Luxembourg, Germany, Latvia, Malta, Austria, and Poland report no land allocated to tomato production, according to FADN data. Overall, the total area used for tomato cultivation is roughly 44200 hectares in the EU-27 and the UK, yielding an annual production of 5300 thousand tonnes.

Table 2.4. Average tomato area, production, total output, yield, and revenue per hectare for EU-27 and the UK (2013-2021).

Country	Tomato area (ha)	Tomato area on total land (%)	Production (1000 t)	Total Output (million €)	Yield (t/ha)	Revenue (€/ha)
Belgium	480	0.02	256	202	493	373502
Bulgaria	2239	0.02	109	42	49	20847
Cyprus	182	0.02	8	5	38	22701
Czech Republic	8	0.0001	0.3	0.2	30	20959
Denmark	NA		NA	NA	NA	NA
Germany	NA		NA	NA	NA	NA
Greece	2443	0.02	286	184	92	63628
Spain	22305	0.04	2087	1047	103	62373
Estonia	2	0.00004	0.1	0.1	28	42205
France	2750	0.004	682	822	178	224118
Croatia	76	0.001	10	4	116	51165
Hungary	1219	0.01	254	182	140	110767
Ireland	NA		NA	NA	NA	NA
Italy	7567	0.03	506	385	49	41383
Lithuania	4	0.0001	0.3	0.2	90	47847
Luxembourg	NA		NA	NA	NA	NA
Latvia	NA		NA	NA	NA	NA
Malta	NA		NA	NA	NA	NA
Netherlands	1719	0.05	910	835	529	476695
Austria	NA		NA	NA	NA	NA
Poland	NA		NA	NA	NA	NA
Portugal	1234	0.01	42	22	30	24624
Romania	1593	0.01	43	17	27	13627
Finland	122		12	118	61	NA
Sweden	94		39	62	344	NA
Slovakia	110	0.002	46	73	209	299852
Slovenia	22	0.001	1	1	43	33168
United Kingdom	253	0.001	3	116	45	334491
Average		0.0129[32]			127	125775
Total	44206		5294			

The average tomato revenue per unit area across the considered countries is 125775 €/ha. The Netherlands, followed by Belgium, report the highest revenues per hectare, with 476695 €/ha and

[32] Countries without tomato tree production and countries not susceptible to CBW were excluded from the computation of the average. The countries excluded are Denmark, Germany, Ireland, Lithuania, Luxembourg, Latvia, Malta, Austria, Poland, Finland, and Sweden.

373502 €/ha, respectively. On the other hand, Romania and Bulgaria are at the bottom of the list with 13627 €/ha and 20847 €/ha, respectively.
To analyze revenue variability, countries were grouped into Low, Medium, and High revenue categories based on income terciles[33], dividing the revenue distribution into three equal parts. The Low revenue group includes countries in the bottom third of the distribution, the Medium group represents those in the middle third, and the High group consists of those in the top third. The resulting revenue groups were: Low – 22654 €/ha, Medium – 51433 €/ha, and High – 341732 €/ha. Furthermore, three yield loss scenarios—10%, 20%, and 30%—were considered to evaluate potential impacts on revenues under varying levels of damage. An average of 0.0129% of tomato area on total land has been considered.

2.2.3.2 Sunflower

CBW larvae primarily feed on sunflower plant stems, leaf blades, and reproductive structures. Defoliated plants may exhibit 72-85% reduction in production (Truzi et al., 2017). In 2003, Hungary experienced a severe CBW infestation of sunflowers, with approximately 65% of the sunflower heads affected (Horváth et al., 2004). In the so-called "Sunflower State" of Karnataka in India, CBW damage nearly resulted in a complete loss of harvest (Jagadish et al., 2016). In another region of India – the Krasnodar region – where again sunflower is the primary oil crop, annual yield losses due to CBW reach up to 35% (Semerenko & Bushneva, 2020). Another study reports yield losses of up to 60% (Lewin et al., 1973; Shankar & Mukhtar, 2023).
Table 2.5 presents the average values for the sunflower area, production, total output, yield, and revenue across the EU-27 and the UK during the period 2013–2021. Romania, Bulgaria, and Hungary emerge as the leading sunflower producers in the Union, with average annual productions of 2500, 2082, and 1435 thousand tonnes, respectively, These three countries contribute roughly 72% of the Union's total sunflower production. On the other hand, countries like Belgium, Cyprus, and the Netherlands, do not report any area allocated for sunflower production in the country, according to FADN data. Overall, the total sunflower area in the EU-27 and the UK is approximately 3.6 million km², yielding to an average sunflower production of 8350 thousand tonnes per year.

[33] For more information: Glossary: Income terciles

Table 2.5. Average sunflower area, production, total output, yield, and revenue per hectare for EU-27 and the UK (2013-2021).

Country	Sunflower seed area (ha)	Sunflower seed area on total land (%)	Production (1000 t)	Total Output (million €)	Yield (t/ha)	Revenue (€/ha)
Belgium	NA		NA	NA	NA	NA
Bulgaria	881211	7.94	2082	682	2.2	696
Cyprus	NA		NA	NA	NA	NA
Czech Republic	13952	0.18	36	12	2.5	826
Denmark	NA		NA	NA	NA	NA
Germany	7059	0.02	16	7	2.3	861
Greece	35161	0.27	94	35	2.8	1057
Spain	515078	1.02	674	221	1.5	496
Estonia	NA		NA	NA	NA	NA
France	468734	0.73	1035	389	2.2	841
Croatia	30823	0.54	87	23	2.9	761
Hungary	513704	5.52	1435	491	2.7	915
Ireland	NA		NA	NA	NA	NA
Italy	80139	0.27	198	63	2.5	794
Lithuania	NA		NA	NA	NA	NA
Luxembourg	NA		NA	NA	NA	NA
Latvia	NA		NA	NA	NA	NA
Malta	NA		NA	NA	NA	NA
Netherlands	NA		NA	NA	NA	NA
Austria	13165	0.16	29	10	2.1	740
Poland	1363	0.00	3	1	3.0	1074
Portugal	8246	0.09	12	4	1.5	540
Romania	991403	4.16	2500	730	2.5	712
Finland	92	0.0003	0.01	0.002	0.2	40
Sweden	NA		NA	NA	NA	NA
Slovakia	54317	1.11	145	49	2.6	864
Slovenia	87	0.004	0.1	0.05	0.5	323
United Kingdom	NA		NA	NA	NA	NA
Average		1.38[34]			2.1	721
Total	3614532		8345			

The average sunflower seed revenue across the countries considered is 721 €/ha. Poland, Greece, and Hungary exhibit the highest average revenues per hectare, at 1074 €/ha, 1057 €/ha, and 915 €/ha, respectively.

[34] Countries without sunflower seed production and countries not susceptible to CBW were excluded from the computation of the average. The countries excluded are Belgium, Cyprus, Denmark, Estonia, Ireland, Lithuania, Luxembourg, Latvia, Malta, the Netherlands, Sweden, and the United Kingdom.

Following an identical approach to the one in the case of tomato, countries were grouped into Low, Medium, and High revenue categories using terciles. The Low revenue group includes countries in the bottom third of the revenue distribution, the Medium group represents those between the 33rd and 67th percentiles, and the High group consists of countries in the top third. The resulting revenue groups were: Low – 468 €/ha, Medium – 780 €/ha, and High – 935 €/ha. Again, the same yield loss scenarios—10%, 20%, and 30%—and an average of 1.38% of sunflower seed area on total land have been considered.

2.2.4 Direct economic impact

To estimate the direct economic impact of BMSB in Europe, we applied a partial budgeting approach under a "no-control" scenario. This assumes that no additional regulatory or control measures are implemented following the invasion, resulting in no changes to operating costs. In the case of CBW, the direct impacts of the invasion consist solely of negative effects, such as yield losses and additional farm operating costs.
The direct economic impact is expressed in terms of present value as:

$$PVD = \sum_{i=1}^{\infty} TIA_t^B \cdot \bar{R} \cdot D \cdot q^{-t} \quad (4)$$

Where $\bar{R}$ is the average annual revenue in €/ha, TIA_t^B as described in **Eq. 3**, D_t the annual percentage loss in revenue, and q^{-t} the discount factor $(1+r)^{-t}$ where r is the discount rate. **Eq. 4** assumes an infinite planning horizon and incorporates the transversality condition to ensure the present value of future losses converges to a finite amount. By acting as a boundary condition, the transversality condition ensures that the discounted impact of the pest diminishes over time as the horizon extends to infinity. This guarantees the economic feasibility of the analysis and reflects the practical assumption that distant future impacts contribute negligibly.
We assume that CBW can reach its maximum damage potential within the first year of population establishment in a previously uninvaded area. This assumption is based on its impact in Brazil, where it caused an estimated loss of US$ 800 million in the same year it was first detected (Haile et al., 2021; Pomari-Fernandes et al., 2015).
Finally, the average annual damage (AAD) is calculated using the following formula:

$$AAD = PVD \cdot i \quad (5)$$

Where i represents the discount rate, set at 4.49%[35], which serves as the conversion factor for transforming PVD into an infinite annuity.

2.3 Results

2.3.1 Tomato

Table 2.6 shows the results of an example scenario, assuming that the average tomato area constitutes a 0.0129% average of the total country area (Total B), 20% yield loss, with CBW spread at a rate of 30 km^2/year and an average tomato revenue of 125775 €/ha. **Table 2.7** illustrate the average annual damage costs by exploring a range of scenarios that incorporate different

[35] We use 4.49% as it is the average discount rate for the majority of Member States (Austria, Belgium, Cyprus, Germany, Estonia, Greece, Spain, Finland, France, Croatia, Ireland, Italy, Lithuania, Luxembourg, Latvia, Malta, the Netherlands, Portugal, Slovenia, and Slovakia) over the period 2023-2024. Source: Reference and discount rates (in %) since 01.08.1997

revenue categories (as defined above), varying yield loss intensities (10%, 20%, and 30%), and a range of spread rates (10, 30, 50, 70, 90, and 120 km^2/year).

Table 2.6. Damage of *Helicoverpa armigera* spreading further in the EU assuming a spread rate of 30 km^2/year, 20% yield loss, 125775 €/ha revenue, and 0.0129% of tomato area on total land area.

Year	Infested area (km^2)	Tomato area infested (km^2)	Incremental tomato area infested (km^2)	Annual incremental damage costs per additional tomato area infested (million €)					Value of yield loss (million €)	Discount factor	Present value of yield loss (million €)
				Additional tomato area (km^2)							
				7	20	33	46	23			
1	50894	7	7	16.5					16.5	0.957	15.83
2	203575	26	20	16.5	49.6				66.2	0.916	60.59
3	458044	59	33	16.5	49.6	82.7			148.9	0.877	130.48
4	814301	105	46	16.5	49.6	82.7	115.8		264.6	0.839	221.99
5	992464	128	23	16.5	49.6	82.7	115.8	57.9	322.5	0.803	258.94
6	992464	128	0	16.5	49.6	82.7	115.8	57.9	322.5	0.768	247.81
7	992464	128	0	16.5	49.6	82.7	115.8	57.9	322.5	0.735	237.16
8	992464	128	0	16.5	49.6	82.7	115.8	57.9	322.5	0.704	226.97
9	992464	128	0	16.5	49.6	82.7	115.8	57.9	322.5	0.673	217.22
10…∞	992464	128	0	16.5	49.6	82.7	115.8	57.9	322.5		4834[36]
Total											6452

The total infested area expands annually, stabilizing at an additional 128 km^2 of infested tomato area by the 5th year. The associated incremental damage costs for these newly infested areas peak at €57.9 million per year. Over the entire simulation period (infinite time horizon, until total infestation of susceptible area). The total discounted value of damage costs for this scenario is approximately €6.5 billion.

[36] Discounted sum from year 10 until infinity in present value.

Table 2.7. Average annual damage costs due to CBW in European tomato production in a million €.

Scenario	Revenue category (€/ha)	Yield loss (%)	Average annual damage costs (million €) for different spread rates (km²/year)					
			10	30	50	70	90	120
1	22654	10	173	261	274	281	284	288
2	22654	20	346	522	549	563	567	576
3	22654	30	518	783	823	844	851	864
4	51433	10	392	592	623	639	644	654
5	51433	20	785	1185	1246	1277	1288	1308
6	51433	30	1177	1777	1870	1916	1932	1962
7	341732	10	2607	3935	4141	4244	4278	4346
8	341732	20	5213	7871	8281	8488	8557	8692
9	341732	30	7820	11806	12422	12732	12835	13038

The results indicate that even in the best-case scenario (10 km^2/year spread rate, 10% mortality rate), the average annual damage costs are estimated at approximately €173 million. In contrast, under the worst-case scenario (120 km^2/year spread rate, 30% mortality rate), these costs could surpass €13 billion per year. The most likely scenario is expected to fall within these two extremes, highlighting the potential variability in outcomes depending on the spread rate, yield loss intensity, and regional susceptibility. Economic losses escalate disproportionately as spread rates increase, particularly in scenarios characterized by increased yield losses in countries with high revenues per hectare.

Table 2.8 provides the average annual damage costs by country, based on a CBW spread rate of 30 km² per year and a 20% yield loss scenario. The results highlight significant variability among countries. Ireland, Finland, Sweden, and Norway are unlikely to incur any tomato production losses, as current climatic conditions are unsuitable, at least for permanent CBW population establishment. Similarly, while parts of Malta, Luxembourg, Germany, and Latvia are climatically suitable for CBW, they report no tomato production according to the FADN dataset or that is a case of missing data, resulting in no economic losses in this context.

Table 2.8. Average annual damage costs of *Helicoverpa armigera* on European tomato production by country for a spread rate of 30 km^2/year and 20% yield loss.

Country	Revenue (€/ha)	Tomato area on total land (%)	Average annual damage costs (million €)
Belgium	373502	0.02	332.37
Bulgaria	20847	0.02	79.55
Cyprus	22701	0.02	8.01
Czech Republic	20959	0.0001	0.29
Denmark	NA		
Germany	NA		
Greece	63628	0.02	260.86
Spain	62373	0.04	1623.38
Estonia	42205	0.00004	0.15
France	224118	0.004	569.98
Croatia	51165	0.001	6.98
Hungary	110767	0.01	233.69
Ireland	NA		
Italy	41383	0.03	475.49
Lithuania	47847	0.0001	0.37
Luxembourg	NA		
Latvia	NA		
Malta	NA		
Netherlands	476695	0.05	1505.17
Austria	NA		
Poland	NA		
Portugal	24624	0.01	52.60
Romania	13627	0.01	34.06
Finland	NA		
Sweden	NA		
Slovakia	299852	0.002	59.646
Slovenia	33168	0.001	1.38
United Kingdom	334491	0.001	132.25
Total			5376

Countries with low average tomato revenue per hectare, such as Romania, Czech Republic, Slovenia, and Cyprus, and those with higher revenues but limited tomato production, such as Estonia, Croatia, and Lithuania, experience annual damage costs ranging from approximately €0.15 million to €35 million. Notably, control efforts in these countries provide positive externalities by limiting the spread of BMSB to neighboring regions. On the other hand, countries with high average tomato revenue per hectare, such as the Netherlands and Belgium, and those with large tomato production, including Spain, France, and Italy, may undergo the highest annual economic losses. These losses range from approximately €475 million in Italy to over €1.6 billion in Spain. The high damage costs in Spain are primarily due to its combination of high tomato revenues per hectare and extensive production.

2.3.2 Sunflower

Table 2.9 presents an example scenario of potential direct damage costs due to CBW on sunflower seed production, assuming an average sunflower area of 1.38% of total land (Total B), a 40 km^2/year spread rate, 20% yield loss, and an average sunflower seed revenue of 721 €/ha. As above, **Table 2.10** shows additional insights by exploring various scenarios, such as different yield loss intensities (10%, 20%, and 30%), revenue categories, and spread rates (10, 20, 30, 50, 70, 90, 120 km^2/year).

Table 2.9. Damage of *Helicoverpa armigera* spreading further in the EU assuming a spread rate of 40 km^2/year, 20% yield loss, 721 €/ha revenue, and 1.38% of sunflower area on total land area.

Year	Infested area (km^2)	Sunflower seed area infested (km^2)	Incremental sunflower seed area infested (km^2)	Annual incremental damage costs per additional sunflower area infested (million €)					Value of yield loss (million €)	Discount factor	Present value of yield loss (million €)
				Additional sunflower area (km^2)							
				1106	3319	5532	7744	710			
1	80425	1106	1106	16					16.0	0.957	15.27
2	321699	4425	3319	16	47.9				63.8	0.916	58.47
3	723823	9957	5532	16	47.9	79.8			143.6	0.877	125.89
4	1286796	17701	7744	16	47.9	79.8	111.7		255.3	0.839	214.20
5	1338404	18411	710	16	47.9	79.8	111.7	10.2	265.6	0.803	213.21
6	1338404	18411	0	16	47.9	79.8	111.7	10.2	265.6	0.768	204.05
7	1338404	18411	0	16	47.9	79.8	111.7	10.2	265.6	0.735	195.28
8	1338404	18411	0	16	47.9	79.8	111.7	10.2	265.6	0.704	186.89
9	1338404	18411	0	16	47.9	79.8	111.7	10.2	265.6	0.673	178.86
10…∞	1338404	18411	0	16	47.9	79.8	111.7	10.2	265.6		3979[37]
Total											5371

The total infested area expands annually, stabilizing at 18411 km² of infested sunflower area per year by the 5th year. After that year, no additional area is newly infested, and the annual damage costs stabilize at €265.6 million. Over the entire simulation period, the total discounted value of yield losses is estimated at €5.37 billion. It should be noted that the spread rate in this example scenario is higher (40 km²/year) compared to the example for tomato (30 km²/year)[38].

[37] Discounted sum from year 10 until infinity in present value.
[38] The total present value loss from sunflower production assuming a 30 km²/year CBW spread rate and keeping all the other parameters the same is €5157 million.

Table 2.10. Average annual damage costs due to *Helicoverpa armigera* in European sunflower seed production in million €.

Scenario	Revenue category (€/ha)	Yield loss (%)	Average annual damage costs (million €) for different spread rates (km²/year)					
			10	30	50	70	90	120
1	468	10	338	752	800	822	836	844
2	468	20	676	1503	1601	1643	1671	1689
3	468	30	1014	2255	2401	2465	2507	2533
4	780	10	563	1253	1334	1370	1393	1407
5	780	20	1126	2505	2668	2739	2785	2814
6	780	30	1689	3758	4002	4109	4178	4221
7	935	10	675	1501	1599	1642	1669	1687
8	935	20	1350	3003	3198	3283	3338	3373
9	935	30	2025	4504	4797	4925	5008	5060

The results reveal that damage costs escalate significantly with higher yield loss intensities, higher revenue levels, and faster spread rates. For example, at a spread rate of 30 km²/year, the damage costs range from €1 billion in a low-revenue and high-yield loss scenario (Scenario 3) to €4.5 billion in a high-revenue, high-yield loss scenario (Scenario 9). The impact of increased spread rates is particularly pronounced in high-revenue scenarios, with damage costs reaching over €5 billion annually at a spread rate of 120 km²/year. Conversely, in low-revenue, low-yield loss scenarios, the annual damage costs are more moderate, ranging from €338 million at 10 km²/year to €844 million at 120 km²/year.

Table 2.11 presents the potential average annual damage costs to sunflower seed production due to CBW by country, assuming a spread rate of 30 km² per year and 20% yield loss. First of all, as mentioned above, Ireland, Finland, Sweden, and Norway are unlikely to incur any tomato production losses, as current climatic conditions are unsuitable, at least for permanent CBW population establishment. Further, countries such as Belgium, Cyprus, Denmark, Estonia, Lithuania, Luxembourg, Latvia, Malta, and the UK either do not have any sunflower seed production or data is missing based on FADN. Thus, for these countries, there are no results.

Table 2.11. Average annual damage costs of *Helicoverpa armigera* on European sunflower seed production by country for a spread rate of 30 km^2/year and 20% yield loss.

Country	Revenue (€/ha)	Sunflower area on total land (%)	Average annual damage costs (million €)
Belgium	NA		
Bulgaria	696	0.07939	1045.14
Cyprus	NA		
Czech Republic	826	0.00177	20.21
Denmark	NA		
Germany	861	0.00020	9.00
Greece	1057	0.00267	62.35
Spain	496	0.01018	298.08
Estonia	NA		
France	841	0.00734	364.33
Croatia	761	0.00545	42.04
Hungary	915	0.05523	813.27
Ireland	NA		
Italy	794	0.00265	96.63
Lithuania	NA		
Luxembourg	NA		
Latvia	NA		
Malta	NA		
Netherlands	NA		
Austria	740	0.00157	16.98
Poland	1074	0.00004	2
Portugal	540	0.00089	7.72
Romania	712	0.04159	1107.88
Finland	40		
Sweden	NA		
Slovakia	864	0.01108	84.96
Slovenia	323	0.00004	0.05
United Kingdom	NA		
Total			3970.85

Based on the results, countries with limited sunflower production and those with lower average revenues per hectare, such as Poland, Slovenia, Portugal, Czech Republic, Germany, and Austria, face annual damage costs ranging from €0.05 million up to roughly €20 million. Conversely, countries with extensive sunflower production, such as Romania and Bulgaria, experience the highest annual damage costs incurred by CBW, reaching over €1 billion, despite their relatively low revenue per hectare.

2.4 References

[1] Andrewartha, H. G. ., & Birch, Charles. (1954). The distribution and abundance of animals. 782. https://books.google.com/books/about/The_Distribution_and_Abundance_of_Animal.html?id=3uzaAAAAMAAJ

[2] Baker, R., Bragard, C., Candresse, T., Gilioli, G., Grégoire, J.-C., Holb, I., John Jeger, M., Evtimova Karadjova, O., Magnusson, C., Makowski, D., Manceau, C., Navajas, M., Rafoss, T., Rossi, V., Schans, J., Schrader, G., Urek, G., Vloutoglou, I., & van der Werf, W. (2014). Scientific Opinion on the pest categorisation of Helicoverpa armigera (Hübner). EFSA Journal, 12(10), 3833. https://doi.org/10.2903/J.EFSA.2014.3833

[3] Bereś, P. K. (2008). COTTON BOLLWORM (HELICOVERPA ARMIGERA HÜB.) – QUARANTINE MAIZE PEST. Progress in Plant Protection, 48(1).

[4] CABI. (2021). Helicoverpa armigera (cotton bollworm). CABI Compendium. https://doi.org/10.1079/CABICOMPENDIUM.26757

[5] EPPO. (2024). Helicoverpa armigera (HELIAR). EPPO Global Database. https://gd.eppo.int/taxon/HELIAR/datasheet

[6] EPPO Global Database. (2024). Halyomorpha halys (HALYHA). https://gd.eppo.int/taxon/HALYHA

[7] Feng, H., Wu, X., Wu, B. O., & Wu, K. (2009). Seasonal Migration of Helicoverpa armigera (Lepidoptera: Noctuidae) Over the Bohai Sea. Journal of Economic Entomology, 102(1), 95–104. https://doi.org/10.1603/029.102.0114

[8] Haile, F., Nowatzki, T., & Storer, N. (2021). Overview of Pest Status, Potential Risk, and Management Considerations of Helicoverpa armigera (Lepidoptera: Noctuidae) for U.S. Soybean Production. Journal of Integrated Pest Management, 12(1), 1–10. https://doi.org/10.1093/JIPM/PMAA030

[9] Hanafy, H. E., & El-Sayed, W. (2013). Efficacy of bio-and chemical insecticides in the control of Tuta absoluta (Meyrick) and Helicoverpa armigera (Hubner) infesting tomato plants. Australian Journal of Basic and Applied Sciences, 7(2). https://www.researchgate.net/publication/283604790_Efficacy_of_bio-and_chemical_insecticides_in_the_control_of_Tuta_absoluta_Meyrick_and_Helicoverpa_armigera_Hubner_infesting_tomato_plants

[10] Hardwick, D. F. (1965). The Corn Earworm Complex. The Memoirs of the Entomological Society of Canada, 97(S40), 5–247. https://doi.org/10.4039/ENTM9740FV

[11] Heath, J., & Emmet, A. M. (1991). The Moths and butterflies of Great Britain and Ireland. In (No Title). Brill. https://cir.nii.ac.jp/crid/1130000798271839488

[12] Horváth, Z., Boros, J., & Škorić, F. D. (2004). Damage of Sunflower Caused by the Cotton Bollworm (Helicoverpa Armigera, Hübner) in the Region of Kecskemét and Bácsalmás in 2003/Los Daños Causados Por La Oruga Del Algodón (Helicoverpa Armigera) En El AñO 2003 En La Zona De Bácsalmás Y Kecskemét/Dommages Causés Au Tournesol Par La Noctuelle Du Coton (Helicoverpa Armigera, Hübner) Dans Les Régions De Kecskemét Et Bácsalmás En 2003. Helia, 27(41), 173–180. https://doi.org/10.2298/HEL0441173H/MACHINEREADABLECITATION/RIS

[13] Isaakides, C. (1941). Insects interesting the Greek agriculture with some observations on them (in Greek). Proceeding of Academy of Athens, 16, 238–263.

[14] Jagadish, K., Babu, C., Dharshini, G., & Basavaraj, K. (2016). Pest management trends in sunflower in Karnataka. Mysore Journal of Agricultural Sciences, 50(1), 1–18. https://www.cabidigitallibrary.org/doi/full/10.5555/20163364390

[15] Jones, C. M., Papanicolaou, A., Mironidis, G. K., Vontas, J., Yang, Y., Lim, K. S., Oakeshott, J. G., Bass, C., & Chapman, J. W. (2015). Genomewide transcriptional signatures of migratory flight activity in a globally invasive insect pest. Molecular Ecology, 24(19), 4901–4911. https://doi.org/10.1111/MEC.13362

[16] Jones, C. M., Parry, H., Tay, W. T., Reynolds, D. R., & Chapman, J. W. (2019). Movement Ecology of pest helicoverpa: Implications for ongoing spread. Annual Review of Entomology, 64(Volume 64, 2019), 277–295. https://doi.org/10.1146/ANNUREV-ENTO-011118-111959/CITE/REFWORKS

[17] Kashyap, R. K., & Verma, A. N. (1987). Factors imparting resistance to fruit damage by Heliothis armigera (Hubner) in some tomato phenotypes. International Journal of Tropical Insect Science, 8(01), 111–114. https://doi.org/10.1017/S1742758400007086/METRICS

[18] Keszthelyi, S., Nowinszky, L., & Puskás, J. (2013). The growing abundance of Helicoverpa armigera in Hungary and its areal shift estimation. Central European Journal of Biology, 8(8), 756–764. https://doi.org/10.2478/S11535-013-0195-0/METRICS

[19] Kriticos, D. J., Ota, N., Hutchison, W. D., Beddow, J., Walsh, T., Tay, W. T., Borchert, D. M., Paula-Moreas, S. V., Czepak, C., & Zalucki, M. P. (2015). The Potential Distribution of Invading Helicoverpa armigera in North America: Is It Just a Matter of Time? PLOS ONE, 10(3), e0119618. https://doi.org/10.1371/JOURNAL.PONE.0119618

[20] Kriticos, D., Maywald, G., Yonow, T., Zurcher, E., Herrmann, N., & Sutherst, R. (2015). CLIMEX. Version 4. Exploring the Effects of Climate on Plants, Animals and Diseases.

[21] Lammers, J. W., & MacLeod, A. (2007). Report of a Pest Risk Analysis - Helicoverpa armigera (Hübner, 1808) .

[22] Leite, N. A., Alves-Pereira, A., Corrêa, A. S., Zucchi, M. I., & Omoto, C. (2014). Demographics and Genetic Variability of the New World Bollworm (Helicoverpa zea) and the Old World Bollworm (Helicoverpa armigera) in Brazil. PLOS ONE, 9(11), e113286. https://doi.org/10.1371/JOURNAL.PONE.0113286

[23] LEWIN, H., K, T., S, K., & D, S. (1973). STUDIES ON THE COMMON AND DESTRUCTIVE PESTS OF SUNFLOWER (HELIANTHUS ANNUUS LIN.). STUDIES ON THE COMMON AND DESTRUCTIVE PESTS OF SUNFLOWER (HELIANTHUS ANNUUS LIN.).

[24] Mastrangelo, T., Paulo, D. F., Bergamo, L. W., Morais, E. G. F., Silva, M., Bezerra-Silva, G., & Azeredo-Espin, A. M. L. (2014). Detection and Genetic Diversity of a Heliothine Invader (Lepidoptera: Noctuidae) From North and Northeast of Brazil. Journal of Economic Entomology, 107(3), 970–980. https://doi.org/10.1603/EC13403

[25] Meena, L. K., & Raju, S. V. S. (2014). Bioefficacy of newer insecticides against tomtato fruit borer, Helicoverpa armigera (Hübner) on tomato, Lycopersicon esculentum mill under field conditions. The Bioscan, 9(Supplement 1), 347–350. https://thebioscan.com/index.php/pub/article/view/1901

[26] Mironidis, G. K., Kapantaidaki, D., Bentila, M., Morou, E., Savopoulou-Soultani, M., & Vontas, J. (2013). Resurgence of the cotton bollworm Helicoverpa armigera in northern Greece associated with insecticide resistance. Insect Science, 20(4), 505–512. https://doi.org/10.1111/J.1744-7917.2012.01528.X

[27] MNHN & OFB. (2024). Sheet of Helicoverpa armigera (Hübner, 1808). Inventaire National Du Patrimoine Naturel (INPN). https://inpn.mnhn.fr/espece/cd_nom/249325

[28] Montmany, F. M. (1993). Nivel de daños de Heliothis Armigera, en tomate exterior, para el consumo en fresco: Ensayos sobre la eficacia y persistencia en laboratorio de productos insecticidas. Valoraciones económicas de la protección insecticida, sobre un cultivo exterior de tomateras. Treball fi de carrera-Universitat Politècnica de Catalunya. Escola Superior d'Agricultura de Barcelona. Especialitat Hortofructicultura i Jardineria. https://books.google.gr/books/about/Nivel_de_da%C3%B1os_de_Heliothis_Armigera_en.html?id=tMKYMwEACAAJ&redir_esc=y

[29] Nibouche, S., Buès, R., Toubon, J. F., & Poitout, S. (1998a). Allozyme polymorphism in the cotton bollworm Helicoverpa armigera (Lepidoptera: Noctuidae): comparison of African and

European populations. Heredity 1998 80:4, 80(4), 438–445. https://doi.org/10.1046/j.1365-2540.1998.00273.x

[30] Nibouche, S., Buès, R., Toubon, J. F., & Poitout, S. (1998b). Allozyme polymorphism in the cotton bollworm Helicoverpa armigera (Lepidoptera: Noctuidae): comparison of African and European populations. Heredity 1998 80:4, 80(4), 438–445. https://doi.org/10.1046/j.1365-2540.1998.00273.x

[31] Pedgley, D. E. (1985). Windborne migration of Heliothis armigera (Hübner) (Lepidoptera: Noctuidae) to the British Isles. Entomologist's Gazette, 36(1), 15–20. https://www.cabidigitallibrary.org/doi/full/10.5555/19860533574

[32] Pomari-Fernandes, A., Adeney De Freitas Bueno, ;, Daniel, ;, Sosa-Gómez, R., & Bueno, A. F. (2015). Helicoverpa armigera: current status and future perspectives in Brazil. Current Agricultural Science and Technology, 21(1), 1–7. https://doi.org/10.18539/cast.v21i1.4234

[33] Rahman, A. K. M. Z., Haque, M. A., Alam, S. N., Begum, K., & Sarker, A. D. (2016). Development of integrated pest management approaches against Helicoverpa armigera (Hubner) in tomato. Bangladesh Journal of Agricultural Research, 41(2), 287–296. https://doi.org/10.3329/BJAR.V41I2.28231

[34] Riaz, S., Johnson, J. B., Ahmad, M., Fitt, G. P., & Naiker, M. (2021). A review on biological interactions and management of the cotton bollworm, Helicoverpa armigera (Lepidoptera: Noctuidae). Journal of Applied Entomology, 145(6), 467–498. https://doi.org/10.1111/JEN.12880

[35] Semerenko, S., & Bushneva, N. (2020). The efficiency of control of the number of Helicoverpa armigera Hbn. in sunflower sowings. E3S Web of Conferences, 222, 02035. https://doi.org/10.1051/E3SCONF/202022202035

[36] Shankar, U., & Mukhtar, Y. (2023). Pest management practices impact Helicoverpa armigera infestation and foraging behaviour of pollinators in sunflower. International Journal of Pest Management. https://doi.org/10.1080/09670874.2023.2216667

[37] Tay, W. T., Soria, M. F., Walsh, T., Thomazoni, D., Silvie, P., Behere, G. T., Anderson, C., & Downes, S. (2013). A Brave New World for an Old World Pest: Helicoverpa armigera (Lepidoptera: Noctuidae) in Brazil. PLOS ONE, 8(11), e80134. https://doi.org/10.1371/JOURNAL.PONE.0080134

[38] Thakur, P., Rana, R., Sharma, A., Priyanka Thakur, C., & Kumar, A. (2017). Biophysical characters of tomato varieties in relation to resistance against tomato fruit borer, Helicoverpa armigera (Hubner). ~ 108 ~ Journal of Entomology and Zoology Studies, 5(6), 108–112.

[39] Thompson, R., & Nelson, B. (2003). Scarce Bordered Straw - Butterflies and Moths of Northern Ireland. https://www.habitas.org.uk/moths/species.asp?item=6506

[40] Torres-Vila, L. M., Rodríguez-Molina, M. C., & Lacasa-Plasencia, A. (2003). Impact of Helicoverpa armigera larval density and crop phenology on yield and quality losses in processing tomato: developing fruit count-based damage thresholds for IPM decision-making. Crop Protection, 22(3), 521–532. https://doi.org/10.1016/S0261-2194(02)00205-3

[41] Tripathy, M., Kumar, R., & Singh, H. (1999). Host range and population dynamics of Helicoverpa armigera Hubn. in Eastern Uttar Pradesh. Journal of Applied Zoological Research, 10, 22–24.

[42] Truzi, C. C., Vieira, N. F., de Laurentis, V. L., Vacari, A. M., & De Bortoli, S. A. (2017). Development and feeding behavior of Helicoverpa armigera (Hübner) (Lepidoptera: Noctuidae) on different sunflower genotypes under laboratory conditions. Arthropod-Plant Interactions, 11(6), 797–805. https://doi.org/10.1007/S11829-017-9534-4/TABLES/11

[43] Wesseler, J., & Fall, E. H. (2010). Potential damage costs of Diabrotica virgifera virgifera infestation in Europe – the 'no control' scenario. Journal of Applied Entomology, 134(5), 385–394. https://doi.org/10.1111/j.1439-0418.2010.01510.x

[44] Woodward, F. I. . (1996). Climate and plant distribution. 174.

2.5 Acknowledgments

We thank DG AGRI for providing access to the EU-FADN data (agreement IFD 2024_09). We also thank Darren J. Kriticos for kindly providing us with the CliMond CM_TC10 World dataset, centered on 1995.

2.6 Appendix

Table A2.1. CLIMEX model parameters for *Helicoverpa armigera* from (D. J. Kriticos, Ota, et al., 2015). Parameter values without units are dimensionless indices of plant available soil moisture.

Parameters	Description	Unit	Current study
DV0	Lower temperature threshold	°C	**11**
DV1	Lower optimal for growth	°C	**20**
DV2	Upper optimal for growth	°C	**31**
DV3	Upper temperature threshold	°C	**37**
SM0	Lower soil moisture threshold		**0.1**
SM1	Lower optimal soil moisture		**0.7**
SM2	Upper optimal soil moisture		**1**
SM3	Upper soil moisture threshold		**2**
TTCS	Cold stress temperature threshold	°C	**-**
THCS	Cold stress accumulation rate	$week^{-1}$	**-**
TTHS	Heat stress temperature threshold	°C	**37**
THHS	Heat stress accumulation rate	$week^{-1}$	**0.001**
SMDS	Soil moisture dry stress threshold		**0.1**
HDS	Dry stress accumulation rate	$week^{-1}$	**-0.004**
SMWS	Soil moisture wet stress threshold		**2**
HWS	Wet stress accumulation rate	$week^{-1}$	**0.005**
DPD0	Diapause induction day length	h light	**11**
DPT0	Diapause induction temperature	°C	**10**
DPT1	Diapause termination temperature	°C	**10**
DPD	Diapause development days	days	**0**
DPSW	Diapause summer (1) or winter (0)		**0**
DTCS	Cold-Stress Degree-day Threshold	°C days	**28**

DHCS	Cold-Stress accumulation rate	week^{-1}	**-0.0005**

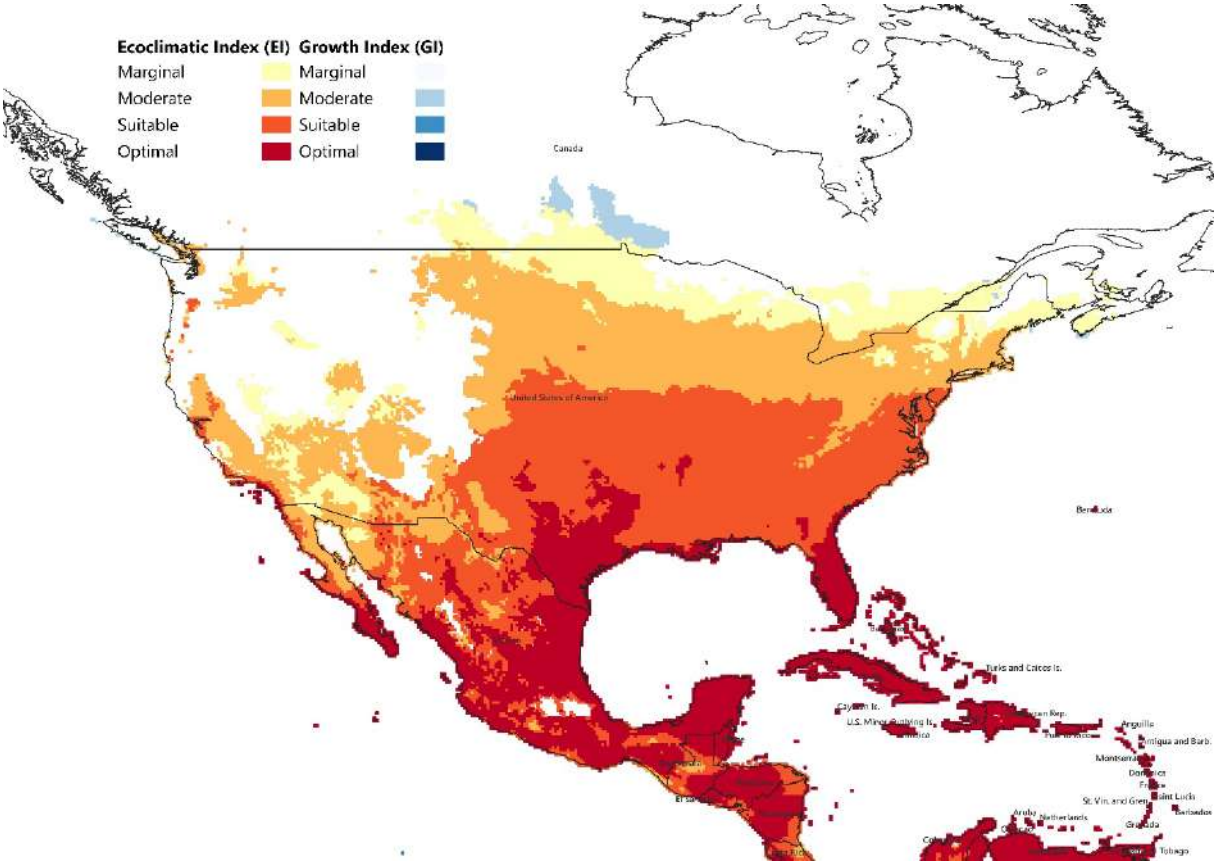

Figure A2.1. Modeled climate suitability (CLIMEX Ecoclimatic Index and Growth Index) for *Helicoverpa armigera* under current climatic conditions in North America. The figure was created with QGIS Desktop version 3.38.1 (https://www.qgis.org/).

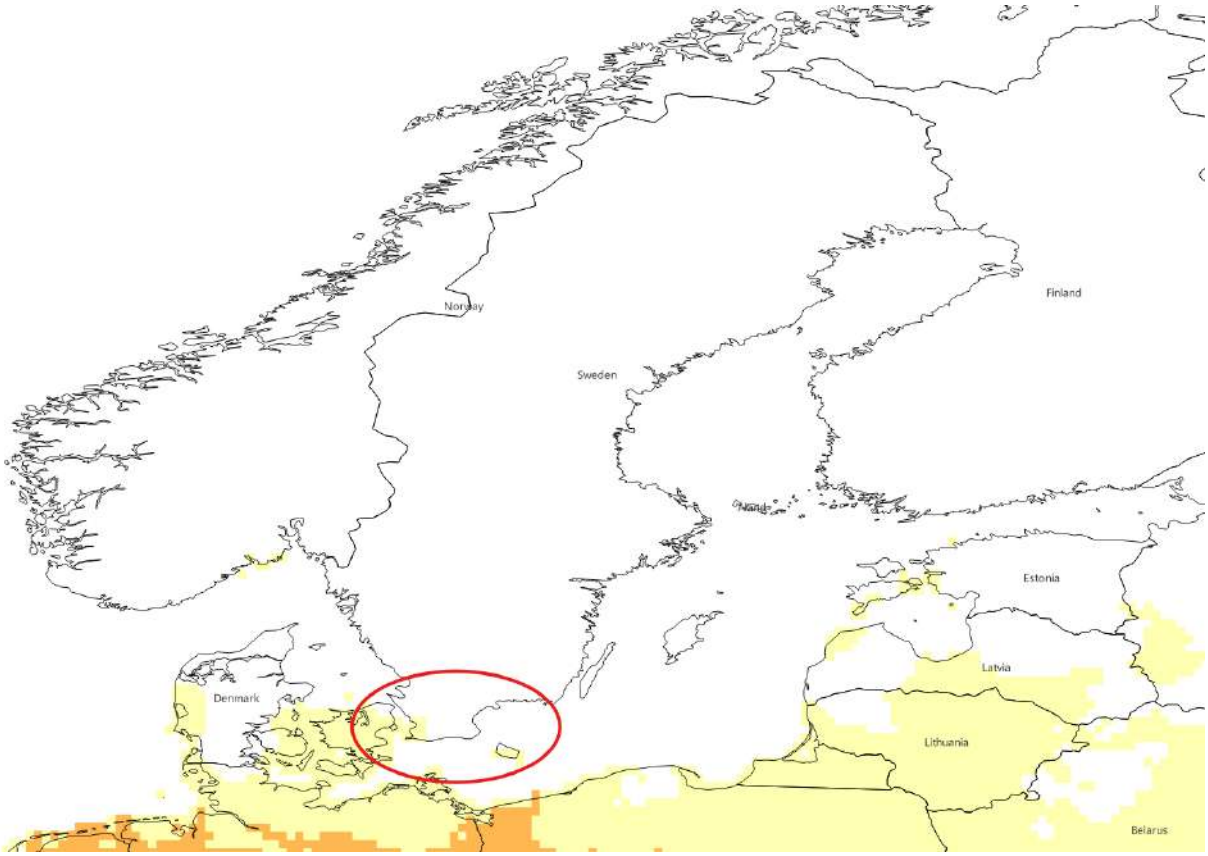

Figure A2.2. Modeled climate suitability (CLIMEX Ecoclimatic Index) for *Helicoverpa armigera* under current climatic conditions zoomed in on Sweden. The figure was created with QGIS Desktop version 3.38.1 (https://www.qgis.org/).

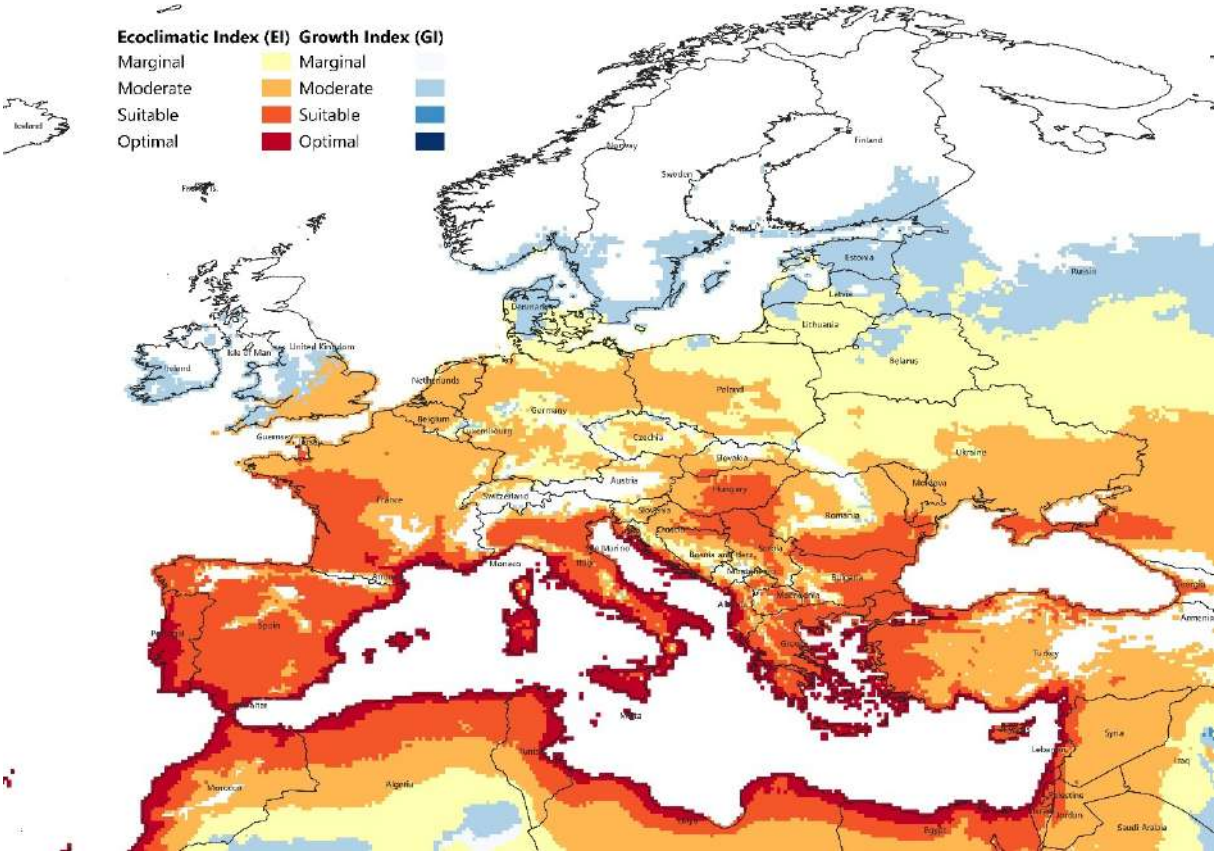

Figure A2.3. Modeled climate suitability (CLIMEX Ecoclimatic Index and Growth Index) for *Helicoverpa armigera* under current climatic conditions in Europe. The figure was created with QGIS Desktop version 3.38.1 (https://www.qgis.org/).

Table A2.2. Country size, area susceptible, and area not yet infested but susceptible to *Helicoverpa armigera* infestation in Europe. The results of the susceptible area were derived by combining regions with both EI>0 and GI>0 values. The resulting layer, representing areas suitable for CBW establishment, was treated as a composite susceptible area layer. This approach incorporated GI>0 regions—where CBW transient populations can establish—by treating them equivalently to EI>0 regions, effectively expanding the definition of susceptibility to include areas capable of supporting transient populations[39].

Country	Total area[40]	Susceptible area		Infested area	Area not yet infested but susceptible	
	km²	km²	%	km²	km²	%[41]
Belgium	30667	28392	93	5678	22714	80
Bulgaria	110996	103311	93	82649	20662	20
Cyprus	9253	9253	100	7402	1851	20
Czechia	78871	61811	78	12362	49449	80
Denmark	42925	42925	100	0	42925	100
Germany	357569	327623	92	65525	262099	80
Greece	131694	128961	98	103168	25792	20
Spain	505983	464863	92	371891	92973	20
Estonia	45336	43665	96	0	43665	100
France	638475	586588	92	234635	351953	60
Croatia	56594	55717	98	44574	11143	20
Hungary	93012	93012	100	74410	18602	20
Ireland	69947	27385	39	0	27385	100
Italy	302079	270938	90	108375	162563	60
Lithuania	65284	65284	100	0	65284	100
Luxembourg	2595	2595	100	0	2595	100
Latvia	64586	61666	95	0	61666	100
Malta	316	316	100	253	63	20
Netherlands	37378	37378	100	7476	29902	80
Austria	83878	35621	42	7124	28497	80
Poland	311928	301243	97	60249	240994	80
Portugal	92227	92227	100	73782	18445	20
Romania	238398	205002	86	164002	41000	20
Finland	338411	37898	11	0	18949	100
Sweden	447424	71312	16	0	71312	100
Slovakia	49035	33355	68	13342	20013	60
Slovenia	20273	17655	87	7062	10593	60
United Kingdom	243610	111572	46	0	111572	100

[39] As mentioned earlier, these results were not included in the main analysis because it is not possible to reliably estimate the percentage of the susceptible area in regions where only transient populations can establish for some time within a given year.
[40] Source: EUROSTAT (2024)
https://ec.europa.eu/eurostat/databrowser/view/reg_area3__custom_13538495/default/table?lang=en
[41] In percentage of the total susceptible area.

Total	4468744	3317568		1443958	1854661	

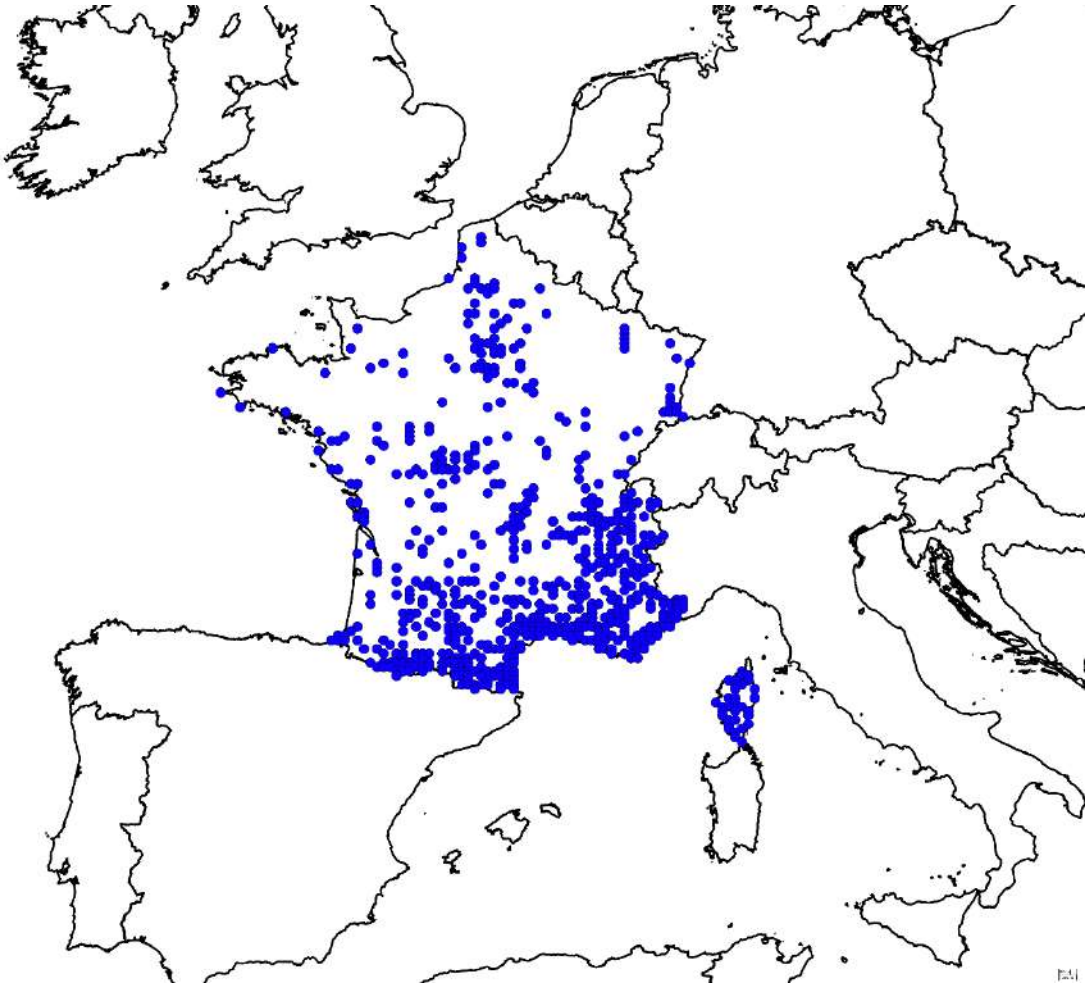

Figure A2.4. Occurrence records of *Helicoverpa armigera* in France. Source: (MNHN & OFB, 2024)

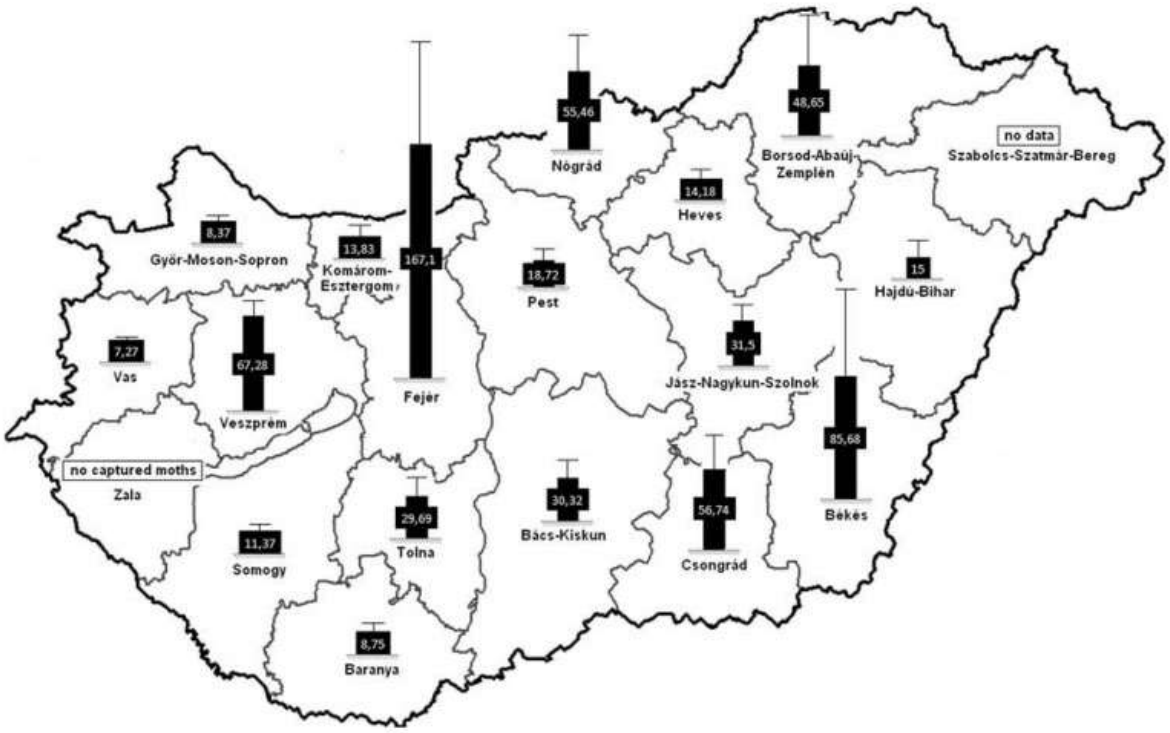

Figure A2.5. The average number of trapped *Helicoverpa armigera* individuals by Hungarian county from 1993 to 2011. Source: (Keszthelyi et al., 2013)

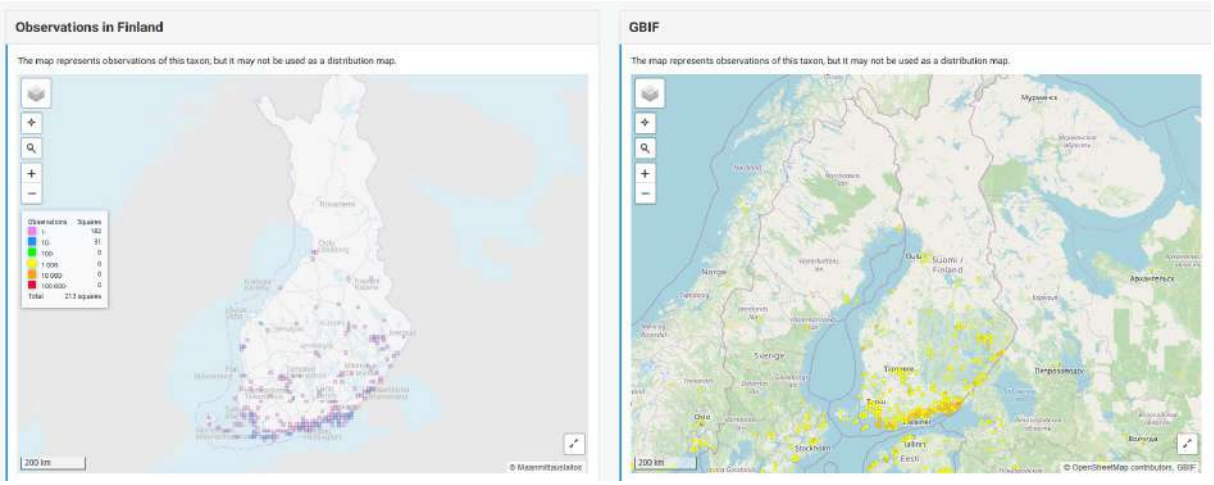

Figure A2.6. Observations of *Helicoverpa armigera* in Finland. Source: [Helicoverpa armigera | Occurence | Finnish Biodiversity Info Facility]

Table A2.3. List of FADN variables used in this study.

Variable	Common name	Unit	Description
COUNTRY	COUNTRY	NA	
YEAR	YEAR	Accounting year	
CTOMAT_A	Tomato area	Hectares	Farm size
CTOMAT_PRQ	Tomato production quantity	Tonnes	
CTOMAT_TO	Tomato total output value	Euros	= Sales + farm use + farmhouse consumption + (closing valuation – opening valuation)
CPSNFL_A	Sunflower area	Hectares	Farm size
CSNFL_PRQ	Sunflower production quantity	Tonnes	
CSNFL_TO	Sunflower total output value	Euros	= Sales + farm use + farmhouse consumption + (closing valuation – opening valuation)
WEIGHT (SYS02)		Number	Sum of weighting coefficients of individual holdings in the sample (=sample farm's weight for individual farms)

3 THE POTENTIAL DIRECT ECONOMIC IMPACT OF *SPODOPTERA FRUGIPERDA* IN EUROPE

3.1 Background

The fall armyworm (FAW), *Spodoptera frugiperda* (J.E. Smith, 1979) (Lepidoptera: Noctuidae), is a highly polyphagous herbivorous moth that feeds on over 350 different host plants from 76 botanical families (Kenis et al., 2023; Montezano et al., 2018). Its larvae feed upon the aerial parts of these plants, causing severe yield losses in a wide range of economically important crops (Kenis et al., 2023). These include cereals, forage crops, and grasses, with maize, rice, and sorghum being particularly affected. Other crops impacted by FAW infestations include soybean, cotton, grapes, citrus, and berries (Barros et al., 2010; Oliveira et al., 2014; Prasanna et al., 2021; Wu et al., 2021). A wide host range, high reproductive capacity, and strong migratory potential enable its rapid expansion into new regions (Johnson, 1987; Z. Zhao et al., 2023). Its first detection outside its native range – the Americas – occurred in West and Central Africa in 2016 (Goergen et al., 2016). Within two years, it spread rapidly across sub-Saharan Africa (Kenis et al., 2023). By 2018, it was reported in parts of Asia, including India, Yemen, Bangladesh, Myanmar, Sri Lanka, and Thailand. In 2019, FAW reached China, South Korea, and Japan (EPPO, 2024). Currently, its presence has been documented in over 50 African countries and much of Southeast Asia and Oceania (**Fig. 3.1**).

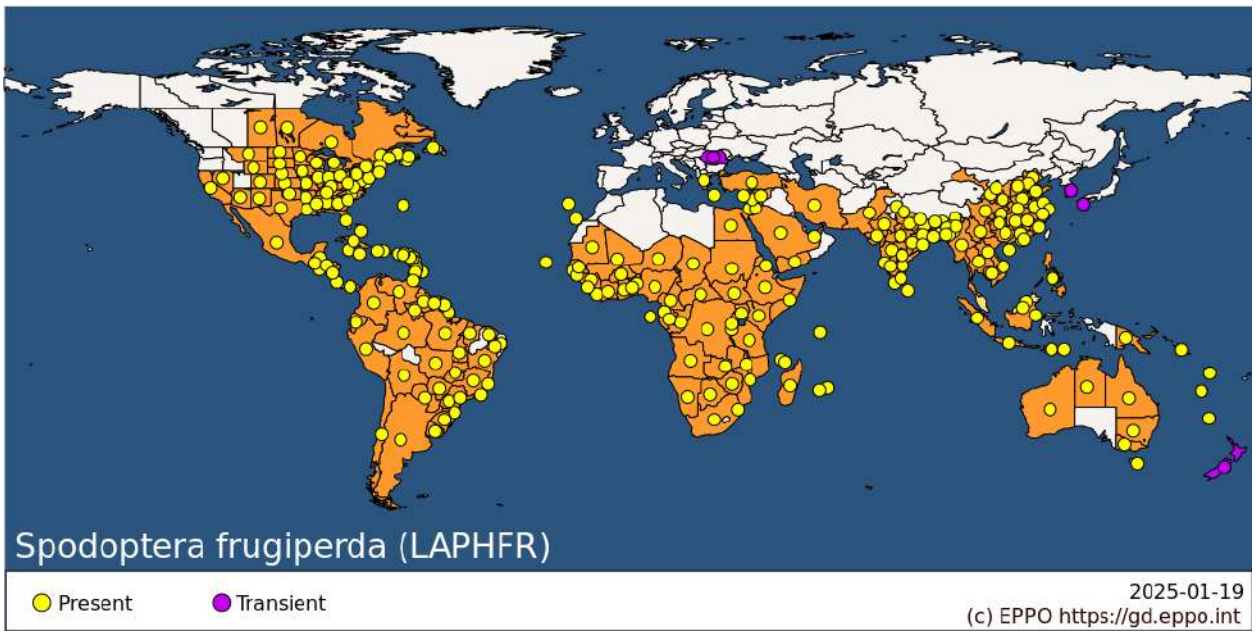

Figure 3.1. The global geographical distribution of *Spodoptera frugiperda*. (Source: EPPO Global Database)

The rapid global spread of FAW poses a significant threat to food security (Farias et al., 2014; Harte et al., 2024; Rajashekhar et al., 2024). Furthermore, its resistance to synthetic insecticides and transgenic *Bacillus thuringiensis* (Bt) crops exacerbates its ability to inflict widespread yield losses (Bolzan et al., 2019; Farias et al., 2016; Gutirrez-Moreno et al., 2019; Storer et al., 2010). Reported yield losses caused by FAW infestations vary across crops and management practices. For maize, FAW-induced losses can reach up to 73% when infestation rates are between 50% and 100% (Hruska & Gould, 1997). In its native range, economic losses were estimated at $60 million annually in the southeastern USA between 1975 and 1983 (Sparks, 1986). In Brazil, a more recent analysis revealed a 34% reduction in grain maize yields, corresponding to US$ 400 million in

yield losses and US$ 600 million in annual control costs (De et al., 2005; Lima et al., 2010). In invaded regions, FAW's impacts are equally severe. For instance, surveys in Ethiopia and Kenya in 2017 recorded average maize crop damage of 32% and 47.3%, respectively (Kumela et al., 2019). Day et al., (2017) estimated that annual FAW-related maize production losses in 12 African countries range from 21% to 53%, while total annual losses are projected at US$ 2.2 to US$ 5.5 billion for 10 major maize-producing African countries (CABI, 2017), and US$ 9.4 billion for the whole continent (Eschen et al., 2021). Additionally, FAW's migratory behavior and the establishment of transient populations significantly amplify its destructive potential (Overton et al., 2021).

FAW was added to the European and Mediterranean Plant Protection Organization (EPPO) A1 List of pests recommended for regulation as a quarantine pest in 2016. The A1 List targets pests absent in EPPO member countries, requiring regulatory measures to prevent their introduction. Following detections in EPPO member countries, FAW was reclassified to the A2 List, which includes pests present but subject to official control (EPPO, 2024). Under EU law, FAW is listed in Part A of Annex II to Commission Implementing Regulation (EU) 2019/2072 as a pest not known to occur in the Union territory. It is prohibited to introduce, move, hold, multiply, or release FAW within EU borders. Moreover, FAW is one of the top 10 priority quarantine pests in the EU due to its significant economic, environmental, and social threats (European Commission, 2019b). It has been designated as a priority pest under Commission Delegated Regulation (EU) 2019/1702, underscoring its critical importance for Union biosecurity measures (European Commission, 2019a).

3.2 Data and Methodology

3.2.1 State of invasion

In Europe, the fall armyworm was first identified in Madeira (Portugal) in September 2023 (EPPO, 2023b). Shortly after, FAW adults were detected in mainland Greece, specifically in Laconia and Eastern Attica, with subsequent detections reported in Evvoia and eastern Crete (EPPO, 2023a). The pest's presence was later confirmed in southern Romania (EPPO, 2024h), and more recently, Malta reported a possible incursion of FAW on the island (EPPO, 2024i). These findings mark the early stages of FAW's invasion into Europe. The suitability of climatic conditions in countries like Greece and Malta may facilitate the permanent establishment of FAW populations.

3.2.2 Fall armyworm occurrence records

FAW occurrence records were compiled from multiple sources, including the Global Biodiversity Information Facility (*GBIF.Org*, 2024) (GBIF), Butterflies and Moths of North America (BAMONA), the European and Mediterranean Plant Protection Organization (EPPO), and the Center for Agriculture and Biosciences International (CABI). Additional records were derived from published datasets (Early et al., 2018; Paudel Timilsena et al., 2022) and literature searches using the keywords "Spodoptera frugiperda [country name]" in Google Scholar for countries with confirmed FAW presence as reported by EPPO (last update for all sources: February 2024). GBIF records were retrieved using the "rgbif" R package (Chamberlain et al., 2024), and filtered using the taxon ID 5109855 for FAW.

We conducted a data cleaning process for the GBIF occurrence dataset by using the "CoordinateCleaner"(Zizka et al., 2019) (version 3.0.1) and "dplyr"(Wickham et al., 2023) R packages. Records with missing coordinates, those classified as "Absent," "Fossil," or "Living" specimens, and records dated prior to 1950 were excluded. Additionally, erroneous data points such as country centroids, zoo locations, or records with high uncertainty, were removed. Entries

lacking precise coordinates but containing descriptive locations were georeferenced. After integrating data from all sources and eliminating duplicates, the final dataset comprised 6851 unique records. The occurrence records used in this study are depicted in **Fig. 3.2.**

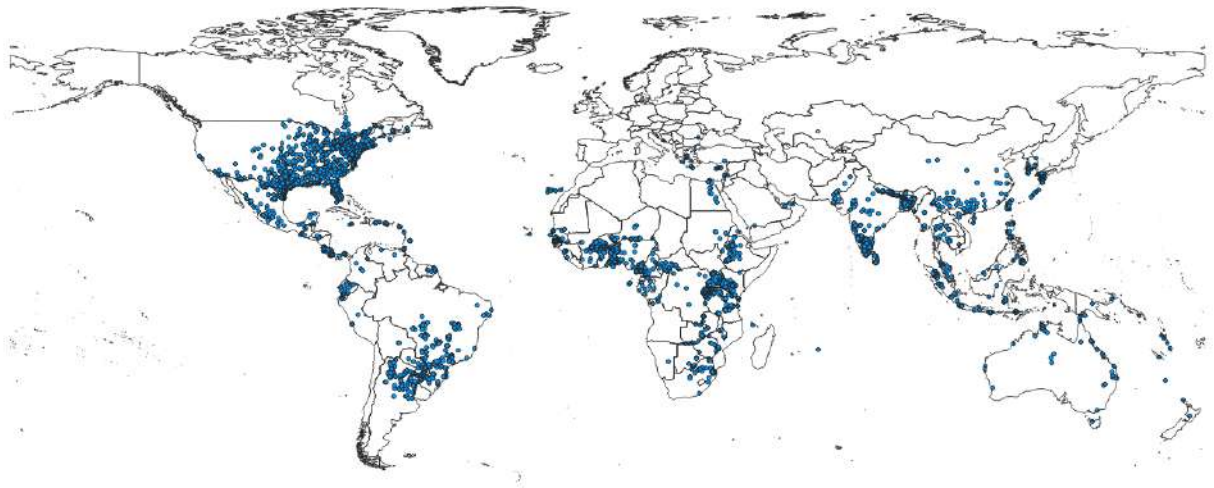

Figure 3.2. Confirmed presence records of *Spodoptera frugiperda* around the globe.

3.2.3 Climate data

We used the "CliMond CM_TC10: World" climatology (*unpublished, provided after personal communication with Darren J. Kriticos*) to fit the current climatic suitability of FAW under both rainfed and irrigation scenarios. This dataset provides a 10-arc-minute spatial resolution and consists of 30-year climatic averages centered on 1995 (1981–2010), covering daily minimum and maximum temperatures (°C), monthly precipitation (mm), and relative humidity (%) at 9:00 and 15:00 h. To assess the robustness of our model outputs, we compared the CLIMEX results derived from the 1995-centered dataset with those from an equivalent dataset centered on 1975 (1961–1990), which is frequently employed in CLIMEX studies (du Plessis et al., 2018; Paudel Timilsena et al., 2022; Ramirez-Cabral et al., 2017; Senay et al., 2022; Wang et al., 2023). An advantage of the more recent climatology is the greater number of locations used (808020 compared to 565801), resulting in more detailed outputs. In addition, given the ongoing impacts of climate change and global warming, an updated climate dataset that reflects better the current climatic conditions is likely to improve the accuracy and relevance of model projections.

3.2.4 The CLIMEX model

CLIMEX is a process-based niche model that allows the estimation of the potential distribution of species as a response to the current or future climate. Several suitability indicators are calculated for each pixel/unit area by combining occurrence records, climatic data, and species-specific ecophysiological growth parameters, offering a comprehensive understanding of the pest's ecological niche. The model is based on the assumption that a species' population experiences one or more (un)favorable periods for growth in a given year (D. J. Kriticos, Maywald, et al., 2015;

Sutherst & Maywald, 1985). The favorable season, defined by the annual Growth Index (GI_A), reflects periods where weekly temperature and soil moisture thresholds support population growth. Conversely, unfavorable conditions, characterized by stress indices—cold, hot, dry, wet—and their interactions, predict population decline. These parameters are synthesized into the Ecoclimatic Index (EI), a composite indicator that ranges from 0 (unsuitable for population establishment) to 100 (optimal suitability). This study classified EI and GI_A values into five categories: unsuitable (EI = 0), marginal ($0 < EI \leq 5$), moderate ($5 < EI \leq 15$), suitable ($15 < EI \leq 30$), and optimal (EI > 30), ensuring comparability with prior studies on FAW using CLIMEX. Detailed information on the reasoning behind choosing specific parameter values is provided in the Appendix.

3.2.5 Predicted migration distances in Europe

FAW regularly migrates long distances during the summer, with transient populations causing significant seasonal damage in North America, including the USA and southern Canada (EPPO, 2024g; Westbrook et al., 2016). To analyze this migratory behavior, we used a subset of the distribution dataset (n = 1831) containing transient occurrence records in the USA and Canada. These records, characterized by EI = 0 and $GI_A > 0$, based on our CLIMEX model, represent areas where FAW populations cannot persist year-round but allow seasonal growth potential. The minimum distance between each transient occurrence point and the nearest permanent establishment area (EI > 0; southern USA coast) was calculated using the QGIS "Distance to nearest hub (line to hub)" algorithm **(Fig. 3.3)**. A similar methodology was applied by Weinberg et al., (2022) to study the dispersal of the southern armyworm (*Spodoptera eridania*).
To reduce overestimation bias, 115 occurrence records from Bermuda Island (EI > 0) were excluded, as their inclusion would imply FAW flying over 1000 km across open ocean in a single event. The resulting dataset provided a distribution of minimum distances between transient records and permanent establishment hubs. From this distribution, we created dispersal frequency zones in the form of buffer zones around modeled EI > 0 areas. These zones illustrate areas accessible to FAW transient populations, with migration risk decreasing as the distance from the EI > 0 region increases. Two buffer zones were defined: the 50^{th} percentile (median migration extent) and the 100^{th} percentile (maximum migration extent). $GI_A > 0$ areas adjacent to or within these zones are considered vulnerable to FAW migration, while areas beyond the maximum buffer zone are presumed inaccessible by natural flight under average climatic conditions.

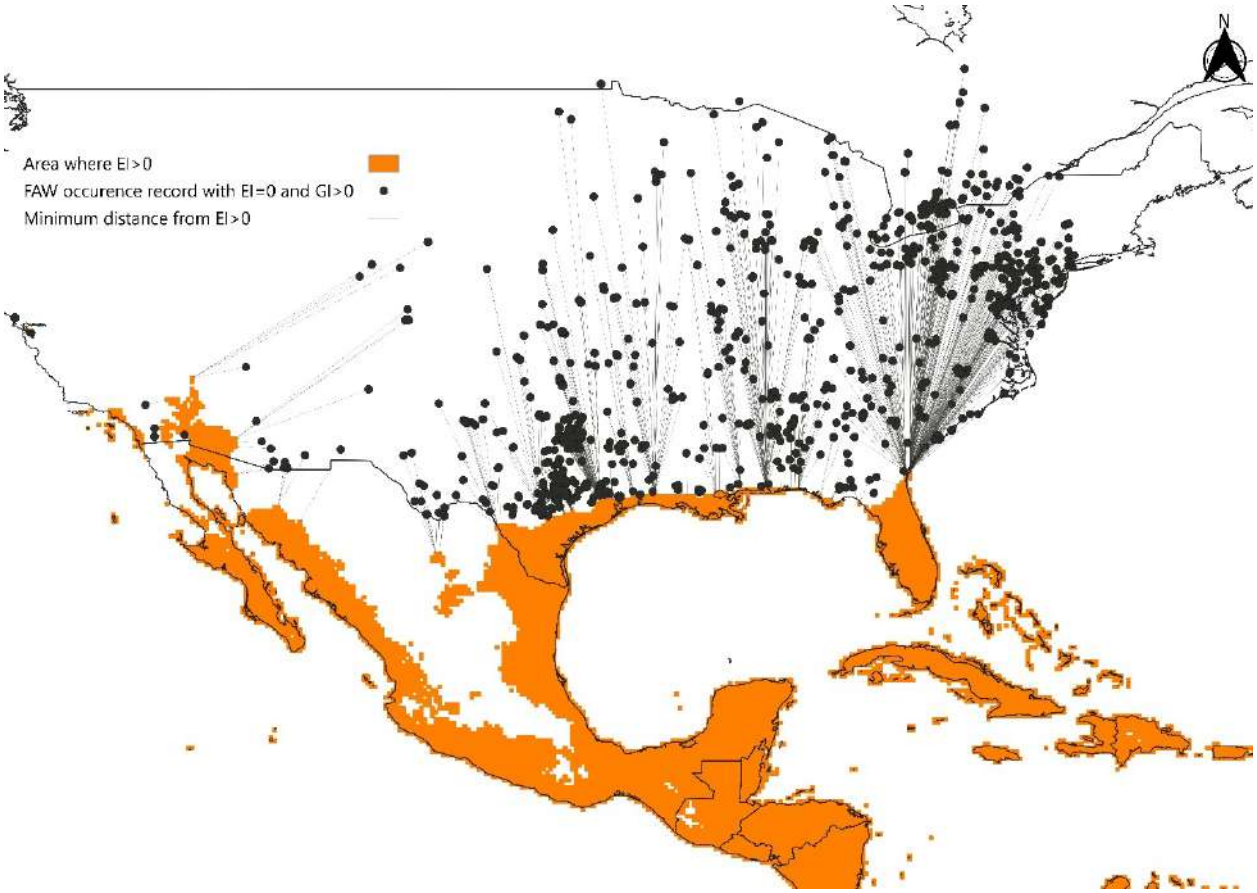

Figure 3.3. Occurrence records of *Spodoptera frugiperda* representing ephemeral populations in the USA and Canada. These occurrence records were used for the "distance to nearest hub (line to hub)" analysis.

To assess potential FAW migration in Europe, we extrapolated these dispersal frequency zones across the continent, assuming FAW migratory behavior in Europe mirrors that observed in its native range. These zones were evaluated alongside CLIMEX model predictions, which identify climatically suitable areas for seasonal FAW populations ($GI_A > 0$) in Europe, providing insights into regions at risk of transient population establishment.

3.2.6 Direct economic impact

3.2.6.1 Economic data

National average values of **grain maize** revenues and operating costs from 2010 to 2020 were obtained from the EU Cereal Farms database of the Farm Accountancy Data Network (FADN) for 13 EU MSs: Austria, Bulgaria, Croatia, France, Germany, Greece, Hungary, Italy, Poland, Portugal, Slovakia, Slovenia, and Spain. We also used EUROSTAT to obtain information on the grain maize cultivated area for each MS. These MSs contributed to the total grain maize production in the EU-27 by more than 80% for the years 2022 and 2023, respectively (own calculation based on EUROSTAT data). Moreover, the European Food Safety Authority (EFSA) provides expert-elicited estimates on grain maize yield losses due to FAW, based on formal EKE methodology (Baker, Gilioli, Behring, Candiani, Gogin, Kaluski, Kinkar, Mosbach-Schulz, et al., 2019; EFSA et al., 2019; European Food Safety Authority, 2014). In the case of grain maize, losses are the consequences of plant decline and rejected and unharvested cobs. A key assumption

of the EKE data is that similar levels of yield loss occur in both permanent and transient FAW population areas.

3.2.6.2 Economic model

To estimate the direct economic impact of FAW invasion on European grain maize production, we used a partial budgeting approach, a method widely used to evaluate the economic consequences of a shock, such as a pest invasion, by accounting for the potential economic benefits and losses (Soliman et al., 2015). In the case of FAW, direct impacts include solely negative effects, namely, yield losses and additional operating costs. The direct economic impact was estimated over the study area where the CLIMEX model projected the permanent establishment of FAW (Mediterranean coast) but was limited to where the migratory capacity analysis suggested the likelihood of seasonal populations. However, this encapsulated all of the 13 EU MSs included in the FADN dataset. We performed the analysis under the irrigation scenario since it better reflects FAW's ecological niche. Furthermore, baseline grain maize gross margins were computed and compared with gross margins under FAW presence.

The analysis relied on several key assumptions. First, it was conducted under a post-invasion no-control scenario (Wesseler & Fall, 2010), reflecting a worst-case benchmark where no additional regulatory or control measures mitigate FAW's spread. Second, it assumed complete occupation of climatically suitable areas (EI > 0), with these zones serving as the source for annual migration. The migratory capacity of FAW was modeled to align with observed patterns in its native range, and the probability of pest impact was assumed to diminish with distance from the permanent establishment zones. Lastly, the analysis only accounted for natural dispersal via flight, excluding other pathways such as trade or human activity.

3.2.6.3 Baseline gross margins

We used the gross margin per hectare (€/ha) as a baseline indicator of the current economic performance of grain maize production in EU Member States. Gross margins are particularly suitable for assessing farm-level profitability as they account for the difference between revenues and operating costs, offering a more precise measure of economic health than revenue figures alone.

The gross margin is calculated as follows:

$$GM_i^{baseline} = \frac{1}{n}\sum_{t=1}^{n}(R_{i,t} - OC_{i,t}) \quad (1)$$

$GM_i^{baseline}$ is the average grain maize gross margin per hectare (€/ha) which is determined by the difference between annual revenues per hectare $R_{i,t}$ and operating costs per hectare $OC_{i,t}$ in each MS i and for each year t over the period 2010-2020. The $OC_{i,t}$ component takes into account several cost categories, such as specific costs (€/ha) (seeds, fertilizers, crop protection, water, other specific costs) and non-specific costs (€/ha) (motor fuels and lubricants, machines, buildings, contract work, energy (electricity, heating fuels) and other direct costs).

3.2.6.4 Gross margins with FAW

We calculated the gross margins under FAW presence to represent the post-invasion economic state of grain maize production in each EU MS, as:

$$GM_i^{FAW} = \bar{R}_i\left(1 - PP_i\frac{YL_{i,s}}{100}\right) - \overline{OC}_i \quad (2)$$

GM_i^{FAW} is the grain maize gross margin with FAW presence in MS i (€/ha), $\bar{R}_i$ and $\overline{OC_i}$ are the average revenue and operating costs (€/ha) in MS i, respectively, $YL_{i,s}$ is the EKE yield loss for MS i and yield loss scenario s, and PP_i is the probability of FAW presence for MS i.
The PP_i parameter accounts for each MS's annual risk of FAW invasion, factoring in geographical proximity to areas of permanent FAW establishment (EI>0). Proximity corresponds to higher invasion risks, with southern MSs at greater risk due to their closeness to Mediterranean regions identified as permanent FAW hubs. More specifically, PP_i captures the probability of FAW presence in a MS, considering the pest's migratory capacity (flight distance), whereas $YL_{i,s}$ incorporates the expert-elicited yield losses (EFSA et al., 2019) that may be affected by several factors, including FAW population abundance and short generation time (**Table 3.1**).
To estimate the PP_i for each MS i, we used an empirical cumulative distribution function (ECDF) derived from the migration distance distribution of transient FAW populations in North America. An ECDF value represents the proportion of all observed migration distances that are less than or equal to a specific distance away from the projected area of permanent FAW establishment. The PP_i parameter is calculated as:

$$PP_i = 1 - F(D_i) \quad (3)$$

where D_i denotes the distance from the centroid of MS i to the nearest area with EI>0 along the Mediterranean coast and $F(D_i) \in [0,1]$ is the ECDF value at that distance. This approach assumes the inverse relation between distance and invasion risk with proximity to EI>0 corresponding to higher risks of FAW invasion.
To scale the direct economic impacts to national levels, we multiplied per-hectare gross margins by the total grain maize cultivation area in each MS, using EUROSTAT data (2013–2023).
Lastly, the direct economic impact $DEI_{i,s}$ is calculated by comparing the baseline gross margins to those under FAW presence:

$$DEI_{i,s} = GM_i^{baseline} - GM_{i,s}^{FAW} \quad (4)$$

Three scenarios were considered to capture the bandwidth of the potential impact of FAW on European grain maize production: a best-case, moderate-case, and worst-case scenario that assume a yield loss percentage equal to the 2.25th, 50th, and 97.5th percentiles of the MS-specific yield loss distribution, respectively. These yield loss scenarios are based on the EFSA EKE data (Baker, Gilioli, Behring, Candiani, Gogin, Kaluski, Kinkar, Mosbach-Schulz, et al., 2019; EFSA et al., 2019; European Food Safety Authority, 2014), derived from different assumptions, including the effectiveness of control measures against FAW, climate, and damage type. The reasoning behind each scenario is provided in **Table A3.2** and the exact values are included in **Table 3.1**.

Table 3.1. Expert elicited parameter for potential yield impacts by *Spodoptera frugiperda* on grain maize per EU Member State. Source: Spodoptera frugiperda−Pest Report and Datasheet to support ranking of EU candidate priority pests

Member State	Yield loss (%) distribution percentile				
	2.25th	25th	50th	75th	97.5th
Austria	0.22	1.40	2.88	5.06	11.02
Bulgaria	0.406	2.57	5.27	9.27	20.16
Germany	0.20	1.27	2.61	4.59	9.98
Greece	0.53	3.40	6.99	12.28	26.71
Spain	0.50	3.17	6.52	11.45	24.92
France	0.29	1.89	3.88	6.81	14.82
Croatia	0.41	2.61	5.36	9.41	20.48
Hungary	0.30	1.93	3.96	6.96	15.139
Italy	0.45	2.87	5.90	10.37	22.56
Poland	0.20	1.26	2.60	4.57	9.94
Portugal	0.46	2.93	6.01	10.56	22.98
Slovenia	0.36	2.28	4.68	8.22	17.88
Slovakia	0.24	1.52	3.12	5.48	11.92

3.3 Results

3.3.1 Potential Distribution in Europe

The modeled global climatic suitability for FAW aligns with the pest's known distribution and migratory behavior (**Fig. A3.1)**. Based on the Köppen-Geiger climate classification system (Beck et al., 2018), tropical, subtropical, and select Mediterranean climates are suitable for permanent FAW establishment. Optimal conditions for year-round populations are observed in tropical climates (rainforest, monsoon, savanna) and subtropical climates (humid subtropical, subtropical highland) with EI values exceeding 30. Irrigation significantly expands suitability, allowing FAW establishment in otherwise arid regions, including pockets of hot semi-arid, hot-summer Mediterranean, and even hot desert climates. Additionally, areas with humid continental, Mediterranean (hot-summer, cold-summer, warm-summer), and humid subtropical climates support transient FAW populations, as indicated by GI_A values (GI_A >15, EI = 0). Desert climates (hot, cold, semi-arid) show only marginal to moderate suitability for permanent populations under irrigation scenarios.

In Europe, the Mediterranean coast emerges as a key area for permanent FAW establishment under both rainfed and irrigation scenarios. Notable hotspots include southern Portugal, Spain, Greece, Italy, Cyprus, Turkey, and the Balearic Islands. Northern parts of the Mediterranean basin, including Egypt, Tunisia, Libya, Morocco, and Algeria, also exhibit favorable conditions for year-round populations. Beyond permanent establishment zones, vast regions of Europe, particularly the western Balkans, southern France, and northern Italy, are vulnerable to seasonal FAW populations, as reflected in moderate to high GIA values. Under irrigation, southern, western, and eastern EU Member States become highly suitable for migrating FAW populations (GI_A >15). Detected FAW presence in mainland Greece (Laconia and Eastern Attica) aligns with areas predicted as suitable for population persistence. However, the occurrence record in Romania lies outside areas of projected year-round establishment, suggesting migratory dynamics.

3.3.2 Spread / Migration extent

The analysis of FAW migration dynamics in North America reveals a broad dispersal range, as shown in **Fig. A3.2**. Assuming that historical FAW occurrence records represent transient populations migrating by flight, the distribution of migration distances is multimodal and right-skewed, with multiple peaks and most occurrences concentrated at shorter distances from areas of permanent population establishment (EI>0) **(Fig. A3.3)**. The migration distances span from 30 km (2.5th percentile) to 1624 km (97.5th percentile), with a median of 465 km. Notably, FAW's migration range may extend beyond 2000 km, as demonstrated by the farthest observed occurrence in Ontario, Canada.

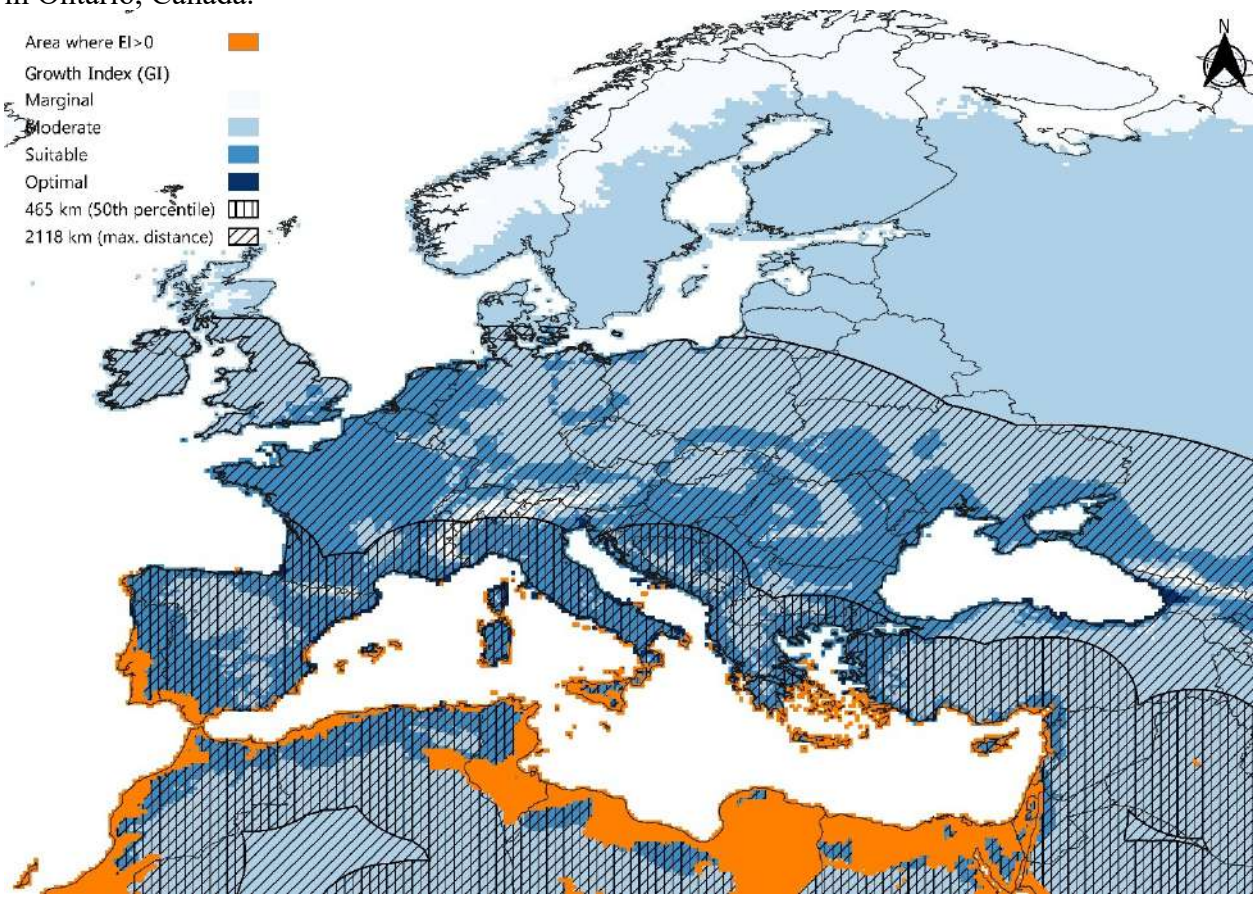

Figure 3.4. Projected climatic suitability of *Spodoptera frugiperda* in Europe modeled using the Compare Locations module in CLIMEX v4.1.1.0 ran with 30-year average climatic data centered on 1995 (CM_TC10_1995_v1). FAW dispersal frequency zones are depicted using cross-hatching buffer zones and are based on FAW's migratory patterns in the USA and Canada. The vertical hatching buffer zone extends to a 465 km distance from the area of permanent establishment (50th percentile) and the diagonal hatching buffer zone to a 2118 km distance.

In Europe, Mediterranean MSs are at the highest risk of experiencing seasonal FAW populations. Countries such as Portugal, Spain, Malta, Italy, Greece, southern France, and the southwestern Balkans are located within the median migration range of 465 km from areas with positive EI values **(Fig. 3.4).** Further north, countries like Austria, Switzerland, Hungary, Serbia, and substantial parts of France, Germany, and Romania fall within the 75th percentile range of 1079 km from EI>0 areas. While northern European nations, including Poland, northern Germany, the

Netherlands, Ireland, and the UK (excluding Scotland), are within the maximum migration distance of 2118 km, these areas are less likely to sustain seasonal FAW populations compared to regions closer to the EI>0 zones.

3.3.3 Direct economic impact

Table 3.2 the average annual economic impact of FAW invasion on grain maize production across 13 European MSs, providing insights into both gross margin losses per hectare (€/ha) and the total economic impact per hectare (€/ha). The baseline gross margins for grain maize production vary significantly among these countries. Among the MSs analyzed, Slovenia, Slovakia, and Croatia recorded the lowest baseline gross margins, at 81 €/ha, 189 €/ha, and 196 €/ha, respectively. In contrast, Spain, Greece, and Portugal exhibit the highest baseline gross margins at 985 €/ha, 766 €/ha, and 760 €/ha, respectively. These countries, while having more profitable grain maize sectors, are also at higher risk due to their proximity to areas with positive EI values and their climatic suitability for FAW establishment.

Table 3.2. Average annual grain maize gross margins and direct economic impact (€/ha) of *Spodoptera frugiperda* in Europe under different yield loss scenarios.

	Gross margin (€/ha)				Direct economic impact (€/ha)		
Member State	**Baseline**	**Best Case**	**Moderate Case**	**Worst Case**	**Best Case**	**Moderate Case**	**Worst Case**
Austria	373	372	354	300	1	19	73
Bulgaria	446	444	420	346	2	26	100
Croatia	196	194	166	80	2	30	116
France	375	373	346	264	2	29	111
Germany	343	342	330	293	1	13	51
Greece	766	755	623	220	11	143	546
Hungary	417	415	396	337	2	21	80
Italy	756	748	652	357	8	104	398
Poland	408	408	400	377	1	8	31
Portugal	760	752	645	321	9	115	440
Slovakia	189	188	175	137	1	14	52
Slovenia	81	78	50	-37	2	31	118
Spain	985	979	905	679	6	80	306
Average	469	465	420	283	4	49	186

Under the best-case scenario (spread and mortality rates at 2.5th percentile), annual grain maize gross margins exhibit minimal differences across most EU MSs. Relative losses range from 0.15% in Poland to 3% in Slovenia, with Greece experiencing the highest absolute loss of 11 €/ha. In the moderate-case scenario (spread and mortality rate at 50th percentile - median), gross margin losses intensify, ranging from 2% in Poland to 62% in Slovenia. Greece remains the most affected, with losses of 143 €/ha, followed by Portugal (115 €/ha) and Italy (104 €/ha). In the worst-case scenario (spread and mortality rate at 97.5th percentile), Mediterranean MSs bear the greatest consequences with gross margin losses peaking at 546 €/ha in Greece, 440 €/ha in Portugal, 398 €/ha in Italy, and 306 €/ha in Spain. Notably, Slovenia reports unprofitable grain maize cultivation under this scenario, with negative gross margins of -37 €/ha.

At the national level, **Table 3.3** highlights scaled gross margins and direct economic impacts in € million. Baseline gross margins vary significantly, from 7 million € in Slovakia to 585 million € in France. France, Italy, Hungary, and Spain emerge as the leading grain maize-producing MSs, with annual averages of 496 million €, 423 million €, and 349 million €, respectively. These results underline the regional disparities in economic vulnerability to FAW invasion across Europe.

Table 3.3. Average annual gross margins and direct economic impact (in million €) of *Spodoptera frugiperda* on grain maize production in Europe under different yield loss scenarios.

	Gross margin (million €)				Direct economic impact (million €)		
Member State	**Baseline**	**Best Case**	**Moderate Case**	**Worst Case**	**Best Case**	**Moderate Case**	**Worst Case**
Austria	78	78	74	63	0.3	4.0	15.2
Bulgaria	217	216	204	168	1.0	12.8	48.7
Croatia	52	51	44	21	0.6	8.0	30.7
France	585	582	540	412	3.5	45.3	172.9
Germany	152	152	146	130	0.5	5.9	22.6
Greece	102	101	83	29	1.5	19.1	72.8
Hungary	423	421	402	342	1.6	21.2	81.1
Italy	496	490	427	234	5.3	68.4	261.3
Poland	328	327	321	303	0.5	6.6	25.0
Portugal	65	65	55	28	0.8	9.9	37.8
Slovakia	7	7	7	5	0.0	0.5	2.1
Slovenia	15	15	9	-7	0.4	5.8	22.2
Spain	349	347	321	241	2.2	28.4	108.6
Sum	2870	2852	2634	1969	18.1	235.9	901.1

Our findings show a substantial variation in annual gross margin losses across EU MSs, with Slovakia experiencing the lowest losses at 0.04 million € under the best-case scenario, and Italy the highest at 5.3 million €. These results underscore the disparities between countries, particularly when compared on a per-hectare basis. Under the moderate and worst-case scenarios, Slovakia consistently shows the lowest economic impact in million €, while Italy, France, and Spain face the greatest risk. Specifically, these three MSs experience direct economic losses ranging from 28 to 68 million € annually under the moderate scenario, and from 109 to 261 million € under the worst-case scenario.

When aggregated across all 13 MSs analyzed, the total annual direct economic losses are estimated at 18 million € for the best-case scenario, 236 million € for the moderate-case scenario, and 901 million € under the worst-case scenario. These findings highlight the potential direct economic impact of FAW invasion in Europe, with substantial risks concentrated in Mediterranean MSs and leading maize producers like France, Italy, and Spain.

3.4 References

[1] Baker, R., Gilioli, G., Behring, C., Candiani, D., Gogin, A., Kaluski, T., Kinkar, M., Mosbach-Schulz, O., Neri, F. M., Siligato, R., Stancanelli, G., & Tramontini, S. (2019). Report on the methodology applied by EFSA to provide a quantitative assessment of pest-related criteria required to rank candidate priority pests as defined by Regulation (EU) 2016/2031. EFSA Journal, 17(6), e05731. https://doi.org/10.2903/j.efsa.2019.5731

[2] Barros, E. M., Torres, J. B., Ruberson, J. R., & Oliveira, M. D. (2010). Development of Spodoptera frugiperda on different hosts and damage to reproductive structures in cotton. Entomologia Experimentalis et Applicata, 137(3), 237–245. https://doi.org/10.1111/J.1570-7458.2010.01058.X

[3] Beck, H. E., Zimmermann, N. E., McVicar, T. R., Vergopolan, N., Berg, A., & Wood, E. F. (2018). Present and future Köppen-Geiger climate classification maps at 1-km resolution. Scientific Data 2018 5:1, 5(1), 1–12. https://doi.org/10.1038/sdata.2018.214

[4] Bolzan, A., Padovez, F. E. O., Nascimento, A. R. B., Kaiser, I. S., Lira, E. C., Amaral, F. S. A., Kanno, R. H., Malaquias, J. B., & Omoto, C. (2019). Selection and characterization of the inheritance of resistance of Spodoptera frugiperda (Lepidoptera: Noctuidae) to chlorantraniliprole and cross-resistance to other diamide insecticides. Pest Management Science, 75(10), 2682–2689. https://doi.org/10.1002/PS.5376

[5] CABI. (2017, September 13). Africa faces permanent $2bn+ maize deficit if Fall Armyworm poorly managed. CABI News. https://www.cabi.org/news-article/africa-faces-permanent-2bnplus-maize-deficit-if-fall-armyworm-poorly-managed/

[6] Chamberlain, S., Oldoni, D., Barve, V., Desmet, P., Geffert, L., & Ram, K. (2024). rgbif: Interface to the Global Biodiversity Information Facility API. R package version 3.7.9. https://cran.r-project.org/package=rgbif

[7] Day, R., Abrahams, P., Bateman, M., Beale, T., Clottey, V., Cock, M., Colmenarez, Y., Corniani, N., Early, R., Godwin, J., Gomez, J., Moreno, P. G., Murphy, S. T., Oppong-Mensah, B., Phiri, N., Pratt, C., Silvestri, S., & Witt, A. (2017). Fall Armyworm: Impacts and Implications for Africa. Outlooks on Pest Management, 28(5), 196–201. https://doi.org/10.1564/V28_OCT_02

[8] De, M., Figueiredo, L. C., Penteado-Dias, A. M., Cruz, I., & Agr, E. (2005). Danos provocados por Spodoptera frugiperda na produção de matéria seca e nos rendimentos de grãos, na cultura do milho. http://www.infoteca.cnptia.embrapa.br/handle/doc/489728

[9] Du Plessis, H., Schlemmer, M. L., & Van den Berg, J. (2020). The Effect of Temperature on the Development of Spodoptera frugiperda (Lepidoptera: Noctuidae). Insects 2020, Vol. 11, Page 228, 11(4), 228. https://doi.org/10.3390/INSECTS11040228

[10] du Plessis, H., van den Berg, J., Ota, N., & Kriticos, D. J. (2018). Spodoptera frugiperda (Fall Armyworm). Pest Geography.

[11] Early, R., González-Moreno, P., Murphy, S. T., & Day, R. (2018). Forecasting the global extent of invasion of the cereal pest Spodoptera frugiperda, the fall armyworm. NeoBiota 40: 25-50, 40(40), 25–50. https://doi.org/10.3897/NEOBIOTA.40.28165

[12] EFSA, Baker, R., Gilioli, G., Behring, C., Candiani, D., Gogin, A., Kaluski, T., Kinkar, M., Mosbach-Schulz, O., Neri Franco, M., Preti, S., Rosace, M. C., Siligato, R., Stancanelli, G., & Tramontini, S. (2019). Spodoptera frugiperda−Pest Report and Datasheet to support ranking of EU candidate priority pests [Data set]. In Zenodo. https://doi.org/https://doi.org/10.5281/zenodo.2789779

[13] EPPO. (2023a). First report of Spodoptera frugiperda in Greece. EPPO Reporting Service. https://gd.eppo.int/reporting/article-7707

[14] EPPO. (2023b, September). First report of Spodoptera frugiperda in Portugal (Madeira). EPPO Global Database. https://gd.eppo.int/reporting/article-7708

[15] EPPO. (2024a). Spodoptera frugiperda. EPPO datasheets on pests recommended for regulation. https://gd.eppo.int/
[16] EPPO. (2024b, January). First report of Spodoptera frugiperda in Romania. EPPO Reporting Service. https://gd.eppo.int/reporting/article-7753
[17] EPPO. (2024c, May). Possible incursion of Spodoptera frugiperda in Malta. EPPO Reporting Service. https://gd.eppo.int/reporting/article-7851
[18] Eschen, R., Beale, T., Bonnin, J. M., Constantine, K. L., Duah, S., Finch, E. A., Makale, F., Nunda, W., Ogunmodede, A., Pratt, C. F., Thompson, E., Williams, F., Witt, A., & Taylor, B. (2021). Towards estimating the economic cost of invasive alien species to African crop and livestock production. CABI Agriculture and Bioscience, 2(1), 1–18. https://doi.org/10.1186/S43170-021-00038-7/FIGURES/2
[19] European Commission. (2019a). COMMISSION DELEGATED REGULATION (EU) 2019/1702 of 1 August 2019 supplementing Regulation (EU) 2016/2031 of the European Parliament and of the Council by establishing the list of priority pests. In Official Journal of the European Union. Official Journal of the European Union. https://eur-lex.europa.eu/eli/reg_del/2019/1702/oj
[20] European Commission. (2019b). COMMISSION IMPLEMENTING REGULATION (EU) 2019/2072 of 28 November 2019 establishing uniform conditions for the implementation of Regulation (EU) 2016/2031 of the European Parliament and the Council, as regards protective measures against pests of plants, and repealing Commission Regulation (EC) No 690/2008 and amending Commission Implementing Regulation (EU) 2018/2019. In Official Journal of the European Union. Official Journal of the European Union. http://data.europa.eu/eli/reg_impl/2019/2072/oj
[21] European Food Safety Authority. (2014). Guidance on Expert Knowledge Elicitation in Food and Feed Safety Risk Assessment. EFSA Journal, 12(6), 3734. https://doi.org/10.2903/j.efsa.2014.3734
[22] Farias, J. R., Andow, D. A., Horikoshi, R. J., Bernardi, D., Ribeiro, R. da S., do Nascimento, A. R. B., dos Santos, A. C., & Omoto, C. (2016). Frequency of Cry1F resistance alleles in Spodoptera frugiperda (Lepidoptera: Noctuidae) in Brazil. Pest Management Science, 72(12), 2295–2302. https://doi.org/10.1002/PS.4274
[23] Farias, J. R., Andow, D. A., Horikoshi, R. J., Sorgatto, R. J., Fresia, P., dos Santos, A. C., & Omoto, C. (2014). Field-evolved resistance to Cry1F maize by Spodoptera frugiperda (Lepidoptera: Noctuidae) in Brazil. Crop Protection, 64, 150–158. https://doi.org/10.1016/J.CROPRO.2014.06.019
[24] GBIF.org. (2024, February 13). GBIF Occurrence Download.
[25] Goergen, G., Kumar, P. L., Sankung, S. B., Togola, A., & Tamò, M. (2016). First Report of Outbreaks of the Fall Armyworm Spodoptera frugiperda (J E Smith) (Lepidoptera, Noctuidae), a New Alien Invasive Pest in West and Central Africa. PLOS ONE, 11(10), e0165632. https://doi.org/10.1371/JOURNAL.PONE.0165632
[26] Gutirrez-Moreno, R., Mota-Sanchez, D., Blanco, C. A., Whalon, M. E., Terán-Santofimio, H., Rodriguez-Maciel, J. C., & Difonzo, C. (2019). Field-Evolved Resistance of the Fall Armyworm (Lepidoptera: Noctuidae) to Synthetic Insecticides in Puerto Rico and Mexico. Journal of Economic Entomology, 112(2), 792–802. https://doi.org/10.1093/JEE/TOY372
[27] Harte, S. J., Bray, D. P., Nash-Woolley, V., Stevenson, P. C., & Fernández-Grandon, G. M. (2024). Antagonistic and additive effect when combining biopesticides against the fall armyworm, Spodoptera frugiperda. Scientific Reports 2024 14:1, 14(1), 1–11. https://doi.org/10.1038/s41598-024-56599-w
[28] Hruska, A. J., & Gould, F. (1997). Fall Armyworm (Lepidoptera: Noctuidae) and Diatraea lineolata (Lepidoptera: Pyralidae): Impact of Larval Population Level and Temporal Occurrence on Maize Yield in Nicaragua. Journal of Economic Entomology, 90(2), 611–622. https://doi.org/10.1093/jee/90.2.611

[29] Huang, L. L., Xue, F. Sen, Chen, C., Guo, X., Tang, J. J., Zhong, L., & He, H. M. (2021). Effects of temperature on life-history traits of the newly invasive fall armyworm, Spodoptera frugiperda in Southeast China. Ecology and Evolution, 11(10), 5255–5264. https://doi.org/10.1002/ECE3.7413

[30] Huang, Y., Lv, H., Dong, Y., Huang, W., Hu, G., Liu, Y., Chen, H., Geng, Y., Bai, J., Guo, P., & Cui, Y. (2022). Mapping the Spatio-Temporal Distribution of Fall Armyworm in China by Coupling Multi-Factors. Remote Sensing, 14(17), 4415. https://doi.org/10.3390/RS14174415/S1

[31] Johnson, S. J. (1987). Migration and the life history strategy of the fall armyworm, Spodoptera frugiperda in the western hemisphere*. International Journal of Tropical Insect Science, 8(4-5–6), 543–549. https://doi.org/10.1017/S1742758400022591

[32] Kenis, M., Benelli, G., Biondi, A., Calatayud, P.-A., Day, R., Desneux, N., Harrison, R. D., Kriticos, D., Rwomushana, I., van den Berg, J., Verheggen, F., Zhang, Y.-J., Agboyi, L. K., Ahissou, R. B., Ba, M. N., & Wu, K. (2023). Invasiveness, biology, ecology, and management of the fall armyworm, Spodoptera frugiperda. Entomologia Generalis, 43(2), 187–241. https://doi.org/10.1127/entomologia/2022/1659

[33] Kriticos, D. J., Maywald, G. F., Yonow, T., Zurcher, E. J., Herrmann, N. I., & Sutherst, R. (2015). Exploring the effects of climate on plants, animals and diseases. CLIMEX Version, 4.

[34] Kumela, T., Simiyu, J., Sisay, B., Likhayo, P., Mendesil, E., Gohole, L., & Tefera, T. (2019). Farmers' knowledge, perceptions, and management practices of the new invasive pest, fall armyworm (Spodoptera frugiperda) in Ethiopia and Kenya. International Journal of Pest Management, 65(1), 1–9. https://doi.org/10.1080/09670874.2017.1423129

[35] Lima, M. S., Silva, P. S. L., Oliveira, O. F., Silva, K. M. B., & Freitas, F. C. L. (2010). Corn yield response to weed and fall armyworm controls. Planta Daninha, 28(1), 103–111. https://doi.org/10.1590/S0100-83582010000100013

[36] Malekera, M. J., Acharya, R., Hwang, H. S., & Lee, K. Y. (2022). Effect of cold acclimation and rapid cold-hardening on the survival of Spodoptera frugiperda (J.E. Smith) (Lepidoptera: Noctuidae) under cold stress. Journal of Asia-Pacific Entomology, 25(1), 101862. https://doi.org/10.1016/J.ASPEN.2021.101862

[37] Malekera, M. J., Acharya, R., Mostafiz, M. M., Hwang, H. S., Bhusal, N., & Lee, K. Y. (2022). Temperature-Dependent Development Models Describing the Effects of Temperature on the Development of the Fall Armyworm Spodoptera frugiperda (J. E. Smith) (Lepidoptera: Noctuidae). Insects 2022, Vol. 13, Page 1084, 13(12), 1084. https://doi.org/10.3390/INSECTS13121084

[38] Montezano, D. G., Specht, A., Sosa-Gómez, D. R., Roque-Specht, V. F., Sousa-Silva, J. C., Paula-Moraes, S. V., Peterson, J. A., & Hunt, T. E. (2018). Host Plants of Spodoptera frugiperda (Lepidoptera: Noctuidae) in the Americas. Https://Doi.Org/10.4001/003.026.0286, 26(2), 286–300. https://doi.org/10.4001/003.026.0286

[39] Oliveira, C. M., Auad, A. M., Mendes, S. M., & Frizzas, M. R. (2014). Crop losses and the economic impact of insect pests on Brazilian agriculture. Crop Protection, 56, 50–54. https://doi.org/10.1016/J.CROPRO.2013.10.022

[40] Overton, K., Maino, J. L., Day, R., Umina, P. A., Bett, B., Carnovale, D., Ekesi, S., Meagher, R., & Reynolds, O. L. (2021). Global crop impacts, yield losses and action thresholds for fall armyworm (Spodoptera frugiperda): A review. Crop Protection, 145, 105641. https://doi.org/10.1016/J.CROPRO.2021.105641

[41] Paudel Timilsena, B., Niassy, S., Kimathi, E., Abdel-Rahman, E. M., Seidl-Adams, I., Wamalwa, M., Tonnang, H. E. Z., Ekesi, S., Hughes, D. P., Rajotte, E. G., & Subramanian, S. (2022). Potential distribution of fall armyworm in Africa and beyond, considering climate change and irrigation patterns. Scientific Reports, 12(1), 539. https://doi.org/10.1038/s41598-021-04369-3

[42] Prasanna, B. M., Huesing, J. E., & Peschke, V. M. (2021). Fall armyworm in Asia: a guide for integrated pest management. CIMMYT. https://hdl.handle.net/10883/21658

[43] Rajashekhar, M., Rajashekar, B., Reddy, T. P., Manikyanahalli Chandrashekara, K., Vanisree, K., Ramakrishna, K., Sunitha, V., Shaila, O., Sathyanarayana, E., Shahanaz, Reddy, S. S., Shankar, A., Jahan, A., Kumar, P. V., & Reddy, M. J. M. (2024). Evaluation of farmers friendly IPM modules for the management of fall armyworm, Spodoptera frugiperda (JE Smith) in maize in the hot semiarid region of India. Scientific Reports 2024 14:1, 14(1), 1–13. https://doi.org/10.1038/s41598-024-57860-y

[44] Ramirez-Cabral, N. Y. Z., Kumar, L., & Shabani, F. (2017). Future climate scenarios project a decrease in the risk of fall armyworm outbreaks. The Journal of Agricultural Science, 155(8), 1219–1238. https://doi.org/10.1017/S0021859617000314

[45] Senay, S. D., Pardey, P. G., Chai, Y., Doughty, L., & Day, R. (2022). Fall armyworm from a maize multi-peril pest risk perspective. Frontiers in Insect Science, 2, 971396. https://doi.org/10.3389/FINSC.2022.971396/BIBTEX

[46] Siebert, S., Henrich, V., Frenken, K., & Burke, J. (2013). Update of the digital global map of irrigation areas to version 5. https://doi.org/http://dx.doi.org/10.13140/2.1.2660.6728

[47] Soliman, T., Mourits, M. C. M., Oude Lansink, A. G. J. M., & van der Werf, W. (2015). Quantitative economic impact assessment of invasive plant pests: What does it require and when is it worth the effort? Crop Protection, 69, 9–17. https://doi.org/10.1016/j.cropro.2014.11.011

[48] Sparks, A. N. (1986). Fall Armyworm (Lepidoptera: Noctuidae): Potential for Area-Wide Management. The Florida Entomologist, 69(3), 603. https://doi.org/10.2307/3495397

[49] Storer, N. P., Babcock, J. M., Schlenz, M., Meade, T., Thompson, G. D., Bing, J. W., & Huckaba, R. M. (2010). Discovery and Characterization of Field Resistance to Bt Maize: <I>Spodoptera frugiperda</I> (Lepidoptera: Noctuidae) in Puerto Rico. Journal of Economic Entomology, 103(4), 1031–1038. https://doi.org/10.1603/EC10040

[50] Sutherst, R. W., & Maywald, G. F. (1985). A computerised system for matching climates in ecology. Agriculture, Ecosystems & Environment, 13(3–4), 281–299. https://doi.org/10.1016/0167-8809(85)90016-7

[51] Tanaka, Y., & Matsukura, K. (2023). Quantitative Effects of Temperature and Exposure Duration on the Occurrence and Repair of Indirect Chilling Injury in the Fall Armyworm Spodoptera frugiperda. Insects, 14(4), 356. https://doi.org/10.3390/INSECTS14040356/S1

[52] Tian, T., Ren, Q., Fan, J., Haseeb, M., & Zhang, R. (2022). Too dry or too wet soils have a negative impact on larval pupation of fall armyworm. Journal of Applied Entomology, 146(1–2), 196–202. https://doi.org/10.1111/JEN.12950

[53] Valdez-Torres, J., Soto-Landeros, F., Osuna, T., & Baez, M. (2012). Phenological prediction models for white corn (Zea mays L.) and fall armyworm (Spodoptera frugiperda J.E. Smith). Agrociencia, 46, 399–410. https://www.researchgate.net/publication/287001214_Phenological_prediction_models_for_white_corn_Zea_mays_L_and_fall_armyworm_Spodoptera_frugiperda_JE_Smith

[54] Wang, J., Huang, Y., Huang, L., Dong, Y., Huang, W., Ma, H., Zhang, H., Zhang, X., Chen, X., & Xu, Y. (2023). Migration risk of fall armyworm (Spodoptera frugiperda) from North Africa to Southern Europe. Frontiers in Plant Science, 14, 1141470. https://doi.org/10.3389/FPLS.2023.1141470/BIBTEX

[55] Weinberg, J., Ota, N., Goergen, G., Fagbohoun, J. R., Tepa-Yotto, G. T., & Kriticos, D. J. (2022). Spodoptera eridania: Current and emerging crop threats from another invasive, pesticide-resistant moth. Entomologia Generalis, 42(5), 701–712. https://doi.org/10.1127/ENTOMOLOGIA/2022/1397

[56] Wesseler, J., & Fall, E. H. (2010). Potential damage costs of Diabrotica virgifera virgifera infestation in Europe – the 'no control' scenario. Journal of Applied Entomology, 134(5), 385–394. https://doi.org/10.1111/j.1439-0418.2010.01510.x

[57] Westbrook, J. K., Nagoshi, R. N., Meagher, R. L., Fleischer, S. J., & Jairam, S. (2016). Modeling seasonal migration of fall armyworm moths. International Journal of Biometeorology, 60(2), 255–267. https://doi.org/10.1007/S00484-015-1022-X/FIGURES/6

[58] Wickham, H., François, R., Henry, L., Müller, K., & Vaughan, D. (2023). dplyr: A Grammar of Data Manipulation. R package version 1.1.4. https://dplyr.tidyverse.org/

[59] Wu, P., Wu, F., Fan, J., & Zhang, R. (2021). Potential economic impact of invasive fall armyworm on mainly affected crops in China. Journal of Pest Science, 94(4), 1065–1073. https://doi.org/10.1007/S10340-021-01336-9/FIGURES/1

[60] YANG, X., SONG, Y., SUN, X., SHEN, X., WU, Q., ZHANG, H., ZHANG, D., ZHAO, S., LIANG, G., & WU, K. (2021). Population occurrence of the fall armyworm, Spodoptera frugiperda (Lepidoptera: Noctuidae), in the winter season of China. Journal of Integrative Agriculture, 20(3), 772–782. https://doi.org/10.1016/S2095-3119(20)63292-0

[61] ZHANG, D. dan, ZHAO, S. yuan, WU, Q. lin, LI, Y. yan, & WU, K. ming. (2021). Cold hardiness of the invasive fall armyworm, Spodoptera frugiperda in China. Journal of Integrative Agriculture, 20(3), 764–771. https://doi.org/10.1016/S2095-3119(20)63288-9

[62] Zhao, Z., Hui, C., Peng, S., Yi, S., Li, Z., Reddy, G. V. P., & van Kleunen, M. (2023). The world's 100 worst invasive alien insect species differ in their characteristics from related non-invasive species. Journal of Applied Ecology, 60(9), 1929–1938. https://doi.org/10.1111/1365-2664.14485

[63] Zizka, A., Silvestro, D., Andermann, T., Azevedo, J., Duarte Ritter, C., Edler, D., Farooq, H., Herdean, A., Ariza, M., Scharn, R., Svantesson, S., Wengström, N., Zizka, V., & Antonelli, A. (2019). CoordinateCleaner: Standardized cleaning of occurrence records from biological collection databases. Methods in Ecology and Evolution, 10(5), 744–751. https://doi.org/10.1111/2041-210X.13152

3.5 Acknowledgments

We thank Dušan Drabik, Monique Mourits, and Jacob C. Douma (Wageningen University) for reviewing the draft. We also thank Darren J. Kriticos for kindly providing us with the "CliMond CM_TC10 World" dataset, centered on 1995. Lastly, we largely thank our PurPest partners from Agroscope (WBF), Switzerland (Kiran J, Horrocks, Jana Collatz, and Jörg Romeis) for their contribution.

3.6 Appendix

3.6.1 Model fitting

The climatic suitability of FAW was projected by using the "Compare Location (one species)" module in CLIMEX (version 4.1.1.0) (D. J. Kriticos, Maywald, et al., 2015). We chose the set of CLIMEX parameter values for FAW of the most recently published model (Wang et al., 2023) as a starting point. These parameter values were revised by considering i) recent literature not used in previous CLIMEX models on climatic requirements for the growth and development of FAW, ii) additional FAW global occurrence records, and iii) other published CLIMEX models on FAW (du Plessis et al., 2018; Paudel Timilsena et al., 2022; Ramirez-Cabral et al., 2017; Senay et al., 2022; Wang et al., 2023). The model fitting was an iterative process. The main goal was to fit the model to the occurrence records representing permanent FAW populations in regions where the limits of such populations are known, in the area with positive EI (EI>0). We then confirmed that the occurrence points representing transient populations were within areas where the model predicts positive GI_A (GI_A>0) and EI=0. FAW transient points are in line with the permanent-transient population limits presented by several studies in the Americas (Westbrook et al., 2016) and by Huang et al. in China (Y. Huang et al., 2022). It was not possible to accurately set permanent FAW population limits in southern Africa, Australia, and New Zealand due to insufficient data. The final parameter values used are provided in **Table *4***. Further details on parameter categories are discussed below.

3.6.2 Growth indices

Temperature Index (TI). Senay et al., (2022) chose a lower temperature threshold for development (DV0) of 8.7 °C as the minimum threshold for development averaged across all life stages of FAW, a result based on a second-degree polynomial regression (Valdez-Torres et al., 2012). However, because pupation is required to reach the sexually mature adult life stage and complete a generation, we used 9.4 °C as DV0, corresponding to the minimum temperature threshold for FAW pupal survival (Valdez-Torres et al., 2012). The chosen DV0 value is similar to the field findings YANG et al., (2021), who showed that FAW pupae can overwinter in the northern limit of Kunming in January 2020, where the average temperature was 9.24 °C throughout the month. The temperature range for optimal development was set from 26 °C (lower threshold – DV1) to 30 °C (upper threshold – DV2) following the parameter values selected by du Plessis et al.(Du Plessis et al., 2020) and supported by more recent data on temperature-dependent development and survival rates (L. L. Huang et al., 2021; Malekera, Acharya, Mostafiz, et al., 2022). According to Valdez-Torres et al., (2012), the maximum temperature threshold for FAW is 39.8 °C, thus the upper temperature for development (DV3) was rounded to 39.5 °C.
Moisture Index (MI). Recent experiments indicated that approximately 30% of FAW larvae burrowing in soil with 0% soil moisture were able to successfully pupate (Tian et al., 2022). However, host plants cannot tolerate a complete absence of soil moisture, so we set the lower soil moisture threshold (SM0) at 0.1, the next lowest value after 0. The lower optimal soil moisture (SM1) was adjusted to 0.65, as FAW is highly polyphagous, and many plant species grow well at low moisture levels. The upper optimal soil moisture (SM2) and the upper soil moisture threshold (SM3) remained unchanged from the majority of previous CLIMEX models at 1.5 (du Plessis et al., 2018; Senay et al., 2022; Wang et al., 2023) and 2 (Paudel Timilsena et al., 2022), respectively. This allowed growth in the wettest areas of FAW's distribution.

3.6.3 Stress indices

Cold Stress (CS). FAW potential distribution appears sensitive to the cold stress parameters. The cold stress temperature threshold (TTCS) was set to 9.4 °C, which is the same value as DV0 and commensurate with recent data on cold stress in FAW (Malekera, Acharya, Hwang, et al., 2022; Tanaka & Matsukura, 2023; ZHANG et al., 2021). These studies suggest that FAW survival at different development stages significantly decreases when exposed to temperatures of 9±0.5°C. The cold stress accumulation rate (THCS) was adjusted to -0.003 week^{-1} to allow FAW development in the cooler limits of its permanent populations (Kenis et al., 2023). Specifically, this included records along the Nile River Basin in Egypt, the Mediterranean coast of northern Africa, close to the border of Niger and Nigeria, north Argentina, the Australian state of Queensland, and southern China.
Heat Stress (HS). The heat stress temperature threshold (TTHS) was set to 39.5 °C, which is the value for DV3. The heat stress accumulation rate (THHS) was set to a moderate level of 0.005 week^{-1} following du Plessis et al., (2018) and Senay et al., (2022). This allowed persistence in the hottest areas of FAW's range.
Dry Stress (DS). The soil moisture dry stress threshold (SMDS) was set to 0.1, which is the value for SM0. The dry stress accumulation rate (HDS) was then adjusted to -0.005 week^{-1} to limit the suitability projections to the tropical and subtropical areas where permanent FAW populations occur. This is also in agreement with most published CLIMEX models on FAW (du Plessis et al., 2018; Paudel Timilsena et al., 2022; Senay et al., 2022; Wang et al., 2023).
Wet Stress (WS). The soil moisture wet stress threshold (SMWS) was set to 2 to be consistent with the value of SM3. Then, in accordance with Paudel Timilsena et al., (2022), the wet stress accumulation rate (HWS) was set to 0.01 week^{-1} to restrain FAW suitability to the wetter tropical and subtropical regions where its permanent populations occur.

3.6.4 Minimum degree day sum (PDD)

This parameter describes the minimum required number of growing degree days above DV0 to complete a generation. Based on du Plessis et al., (2020) estimates, FAW needs 391.61 °C days for egg-to-adult development. We rounded this parameter value to the nearest whole number (392 °C days) since CLIMEX is insensitive to such precision.

3.6.5 Irrigation

To account for irrigation, we ran the CLIMEX model with an irrigation scenario applied as an additional 2.5 mm day^{-1} above the default rainfed scenario, throughout the year. The global map of irrigated areas is used to define where the irrigation scenario shall be applied (Siebert et al., 2013). This assumes that no irrigation was added in areas where the rainfall is already equal to or greater than 2.5 mm day^{-1}, under the rainfed scenario. In the case of FAW, dry areas in North Africa, such as the Nile River, in Pakistan and Yemen, where FAW occurs permanently and irrigation is applied, do not appear as climatically suitable under rainfed conditions (Paudel Timilsena et al., 2022).

Table A3.1. CLIMEX parameter values used for modeling the climatic suitability of FAW, in the literature and current study.

Parameters	Description	Unit	Ramirez-Cabral et al. 2017	du Plessis et al. 2018	Timilsena et al. 2022	Senay et al. 2022	Wang et al. 2023	Current study
Temperature Index (TI)								
DV0	Lower temperature threshold	°C	12	12	12	8.7	12	**9.4**
DV1	Lower optimal for growth	°C	22	25	25	24.6	25	**26**
DV2	Upper optimal for growth	°C	27	30	30	32	30	**30**
DV3	Upper temperature threshold	°C	34	39	36	39.5	36	**39.5**
Moisture Index (MI)								
SM0	Lower soil moisture threshold		0.1	0.15	0.15	0.15	0.15	**0.1**
SM1	Lower optimal soil moisture		0.7	0.8	0.8	0.8	0.8	**0.65**
SM2	Upper optimal soil moisture		0.9	1.5	1.5	1.5	1.5	**1.5**
SM3	Upper soil moisture threshold		1.5	2.5	2	2.5	2.5	**2**
Cold Stress (CS)								
TTCS	Cold stress temperature threshold	°C	8	12	8	8.7	8	**9.4**
THCS	Cold stress accumulation rate	week^{-1}	-0.00001	-0.001	-0.005	-0.001	-0.005	**-0.003**
Heat Stress (HS)								
TTHS	Heat stress temperature threshold	°C	38	39	39	39.5	39	**39.5**
THHS	Heat stress accumulation rate	week^{-1}	0.001	0.005	0.0025	0.005	0.0025	**0.005**
Dry Stress (DS)								
SMDS	Soil moisture dry stress threshold		0.1	0.1	0.1	0.1	0.1	**0.1**
HDS	Dry stress accumulation rate	week^{-1}	-0.001	-0.005	-0.005	-0.005	-0.005	**-0.005**
Wet Stress (WS)								
SMWS	Soil moisture wet stress threshold		1.5	2.5	2	2.5	2.5	**2**
HWS	Wet stress accumulation rate	week^{-1}	0.001	0.002	0.01	0.002	0.001	**0.01**
Limiting Conditions								
PDD	Length of growing season / Minimum	°C days	559	600	400	559	391.61	**392**

	degree day sum needed to complete a generation							
Other								
Irrigation		mm day^{-1}	-	2.5	2.5	-	2.5	**2.5**

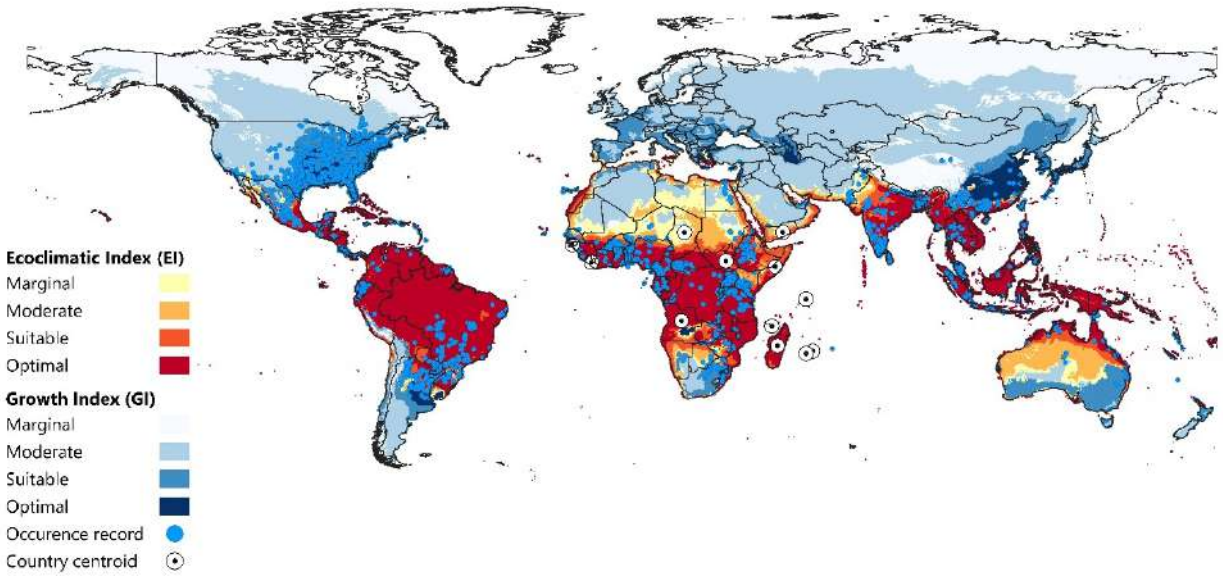

Figure A3.1. Global climatic suitability of *Spodoptera frugiperda* modeled using the Compare Locations module in CLIMEX v4.1.1.0 ran with 30-year average climatic data centered on 1995 (CM_TC10_1995_v1) under a composite irrigation scenario (2.5 mm day^{-1} applied as top-up). The Ecoclimatic Index (EI) and Growth Index (GI_A) are the outputs of the parameters used in **Table A3.1**. The EI gradient (yellow-red) represents areas suitable for all year-round FAW population establishment. The GI_A gradient (light blue-dark blue) depicts areas suitable for seasonal population growth and migration.

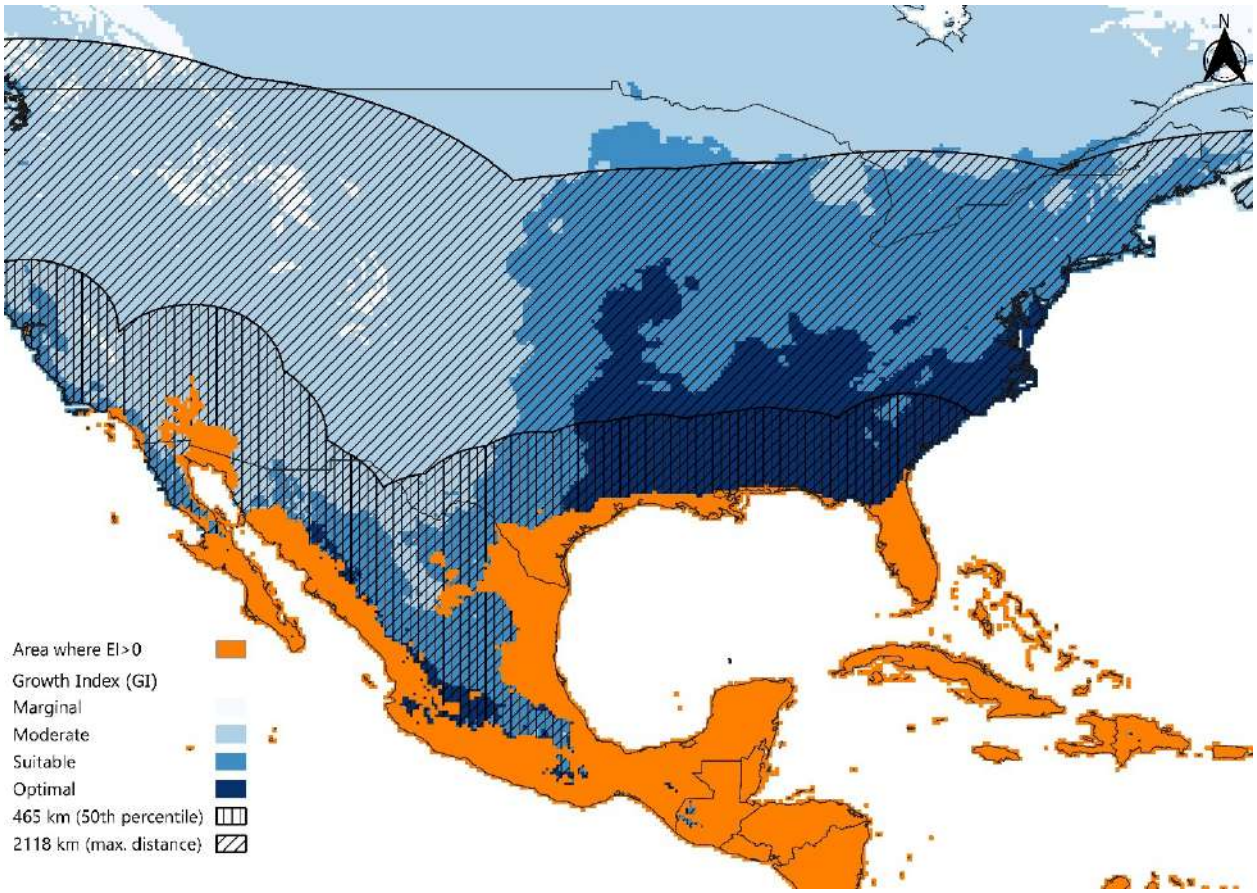

Figure A3.2. Projected climatic suitability modeled using the Compare Locations module in CLIMEX v4.1.1.0 ran with 30-year average climatic data centered on 1995 (CM_TC10_1995_v1). FAW dispersal frequency zones are depicted using cross-hatching buffer zones. The vertical hatching buffer zone extends to a 465 km distance from the area of permanent establishment (50th percentile), and the diagonal hatching buffer zone to a 2118 km distance (maximum recorded distance from EI>0).

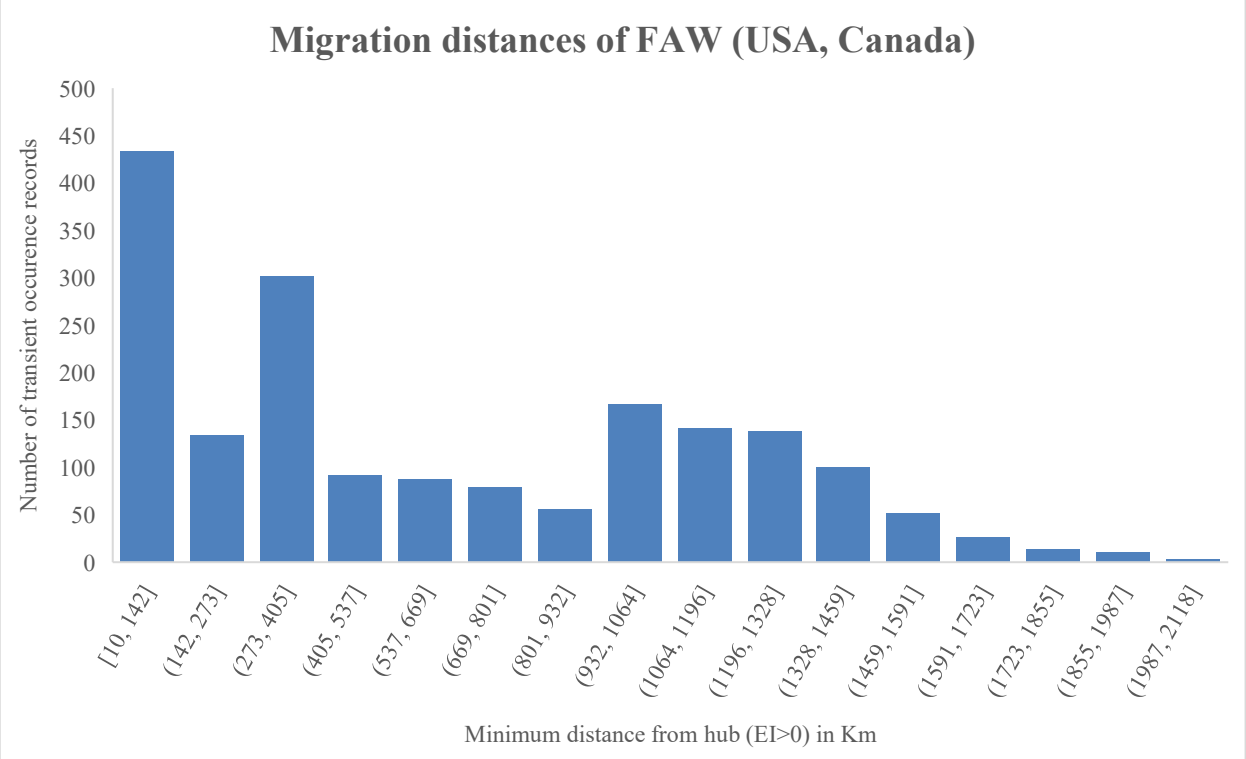

Figure A3.3. Distribution of *Spodoptera frugiperda* migration distances (in km) from the area of permanent establishment (EI>0) in the USA and Canada, using the data subset (n = 1831).

Table A3.2. Justification/Reasoning for each yield loss scenario on grain maize in the EU, based on formal EKE data for *Spodoptera frugiperda.* Source: Spodoptera frugiperda−Pest Report and Datasheet to support ranking of EU candidate priority pests

Yield loss scenario		
Best case (2.5th percentile)	**Moderate case (50th percentile)**	**Worst case (97.5th percentile)**
Current control measures are effective against FAW	Current control methods are effective against FAW	FAW reaches most of the EU's grain maize production area at the most susceptible stage
Treatments are expected to be applied more frequently and with better timing	Some infestation of the cobs may not affect yield substantially (unlike with sweet corn)	High population abundance affects both leaves and cobs
The rejection rate is not as high as other host crops (e.g., sweet corn)	The climate in the EU is not as suitable as in Africa	Only one generation attacks each crop: the following generation flies to the next crop
It is less likely that FAW attacks the cob since infestations begin with the leaves and do not necessarily reach the cob	Infestation is more likely to affect the leaves than the cobs	Treatments that are not targeted at FAW may not be fully effective (e.g., poor timing)

4 THE POTENTIAL DIRECT ECONOMIC IMPACT OF *BURSAPHELENCHUS XYLOPHILUS* IN EUROPE

4.1 Background

The pinewood nematode (PWN), *Bursaphelenchus xylophilus*), is a destructive pest that infects conifers, mainly pine trees (*Pinus* spp.), and is the causal agent of the pine wilt disease (PWD) epidemic. It is considered one of the most significant threats to European forestry, and it belongs among the top 100 most invasive alien species on the continent (Nentwig et al., 2018). It is currently classified as an A2 Quarantine pest (Annex II B) in the EU and by the European Plant Protection Organization (EPPO) (EPPO, 2024a). In particular, PWN poses a high risk, especially in the Mediterranean basin, where extensive forests of susceptible pine tree species are located, potential vectors are present, and current climatic conditions are favorable for the pest's survival and development (Naves et al., 2016; Back et al., 2024).
Losses due to PWD can be significant. In Japan, where PWN was first reported, annual losses of pine wood in m^3 are estimated at 700000, or about 5 million trees, since its introduction (Mamiya & Shoji, 2009). (Kim et al., 2020). indicate more than 55 million m^3 annual loss of pine coverage in Japan between 2004 – 2014. Another study reports that in Japan, the total financial loss was US$ 3700 million, assuming a market price of *P. densiflora* of US$ 100 /m^3 (Taniuchi, 2016; Hirata et al., 2017). In mainland China, the average annual total direct economic loss is estimated at CNY 1.53 billion (approx. €195 million) from 1998 to 2017 (Zhao et al., 2020). On the other hand, another study estimates that China lost US$ 1.11 billion in 2020 due to PWD (Liu et al., 2023). In Europe, the estimated economic impact is €22 billion for the period 2008 – 2030, assuming an uncontrolled invasion (Soliman et al., 2012).

4.1.1 Host range and determination of impacts

The life cycle of PWN can be extremely short, between 4 to 5 days (egg to adult), under favorable climatic conditions (above 20 °C), and the minimum temperature threshold for development is 9.5°C (Naves et al., 2016). Ultimately, PWD leads to the death of the infected trees within a few weeks after infestation (Zhang et al., 2022). More specifically, tree hosts exhibit "drying out" symptoms, reduced oleoresin exudation followed by pine needle yellowing and wilting, and within 30 – 40 days post-infection, they eventually die (Pimentel, 2022).
Pine trees are the major tree hosts of PWN. The European pine species, *Pinus mugo, Pinus nigra, Pinus sylvestris, Pinus radiata,* and *Pinus pinaster* are the most important ones for the continent, due to the high susceptibility (Evans et al., 1996; Zamora et al., 2015). Thus, *Pinus* species differ in their susceptibility to PWN (Hirata et al., 2017). For example, especially under stressful environmental conditions, such as drought, the species *P. pinaster,* and *P. radiata*, are extremely prone to physiological damage and severe symptoms (Estorninho et al., 2022). On the contrary, *P. pinea* has never exhibited symptoms of PWD, since, even in areas with high densities, it has not been found infected with PWN (Naves et al., 2019).

4.1.2 Dispersal mechanisms / Spread

For short-distance dispersal, within the wood tissues of the infected host tree, PWN can actively move and invade an adjoining part (EPPO, 2024a). The nematodes are transmitted from one host tree to another through beetles of the genus *Monochamus* (Evans et al., 1996). The beetle vector oviposits in most coniferous trees, including *Pinus* species. The beetles are essential as they are the exclusive pathway for carrying PWN from a dead tree host to a healthy one within the forest. In Europe, the species *Monochamus galloprovincialis* is the sole insect vector of PWN, being

abundant in Turkey, Greece, Italy, France, Spain, and Portugal (Penas et al., 2006; Koutroumpa et al., 2007; Naves et al., 2016; Sousa et al., 2018) (**Fig. 4.1**). In its native distribution range (North America), the most important vector for the PWN is *M. carolinensis*, while *M. alternatus* and *M. saltuarius* vector the PWN in Japan and China. *Monochamus alternatus* adults have been reported to perform up to 3.3 km long flights (Kobayashi et al., 1984). Another study showed that female *M. carolinensis* beetles could fly up to 10 km with a 2-hour flight duration (Akbulut & Linit, 1999; Akbulut & Stamps, 2012). Lastly, the observed average spread rate of PWN in Portugal is 5.3 km/year, with a maximum of 8.3 km/year (de la Fuente et al., 2018a).

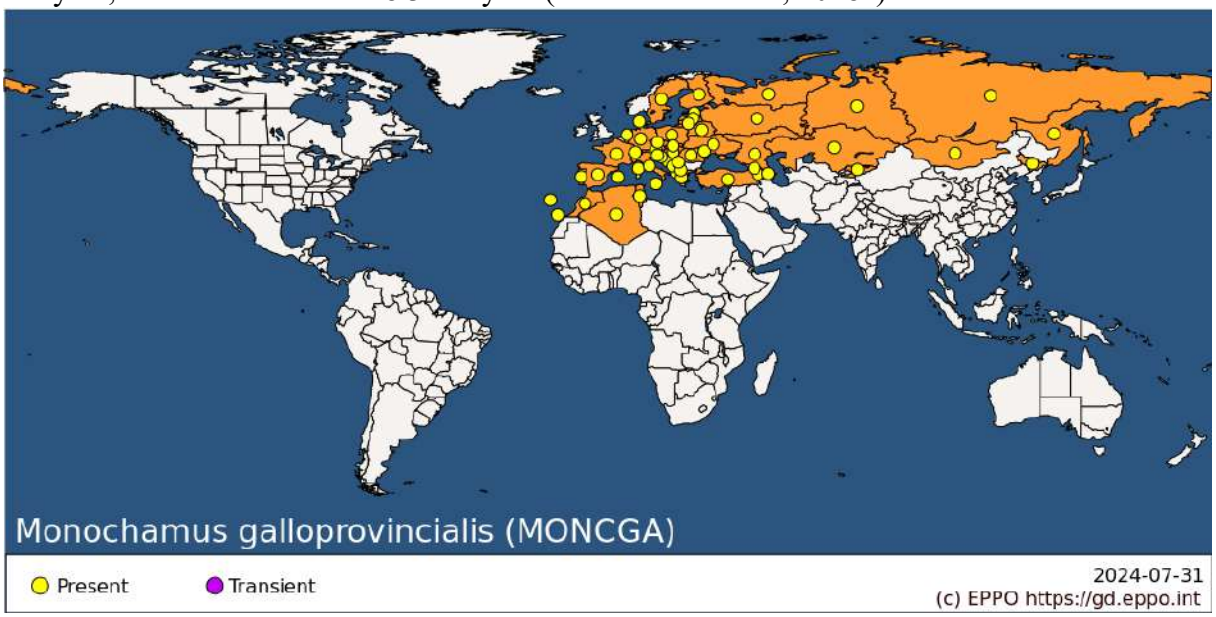

Figure 4.1. Geographical distribution of the PWN beetle vector, *Monochamus galloprovincialis*, in the world. Source: EPPO (2024e)

Human-mediated dispersal is the main factor of PWN long-distance spread. Activities such as logging and the trade of consignments that are transported in wooden packaging material play a key role in further spreading PWN (Robinet et al., 2009). In the latter case, frequently, timber is used to produce such packaging materials (Jones et al., 2008).

4.1.3 History and current distribution

Native to North America, PWN has invaded large parts of the world, including Japan, China, Korea, and more recently, Europe (**Fig. 4.2**). Its first detection in the European continent took place in Portugal in 1999 (Mota et al., 1999). Currently, the entire country of Portugal, including Madeira Island (Fonseca et al., 2012), is considered affected and suffers a severe PWN outbreak, followed by Spain (Abelleira et al., 2011) (**Fig. 4.3**). In these countries, *B. xylophilus* was detected in different *Pinus* species, namely on *P. pinaster* (Mota & Vieira, 2008; Abelleira et al., 2011), *P. nigra* (Inácio et al., 2015), *P. radiata* (Zamora et al., 2015) and *P. sylvestris* (Fonseca et al., 2024).

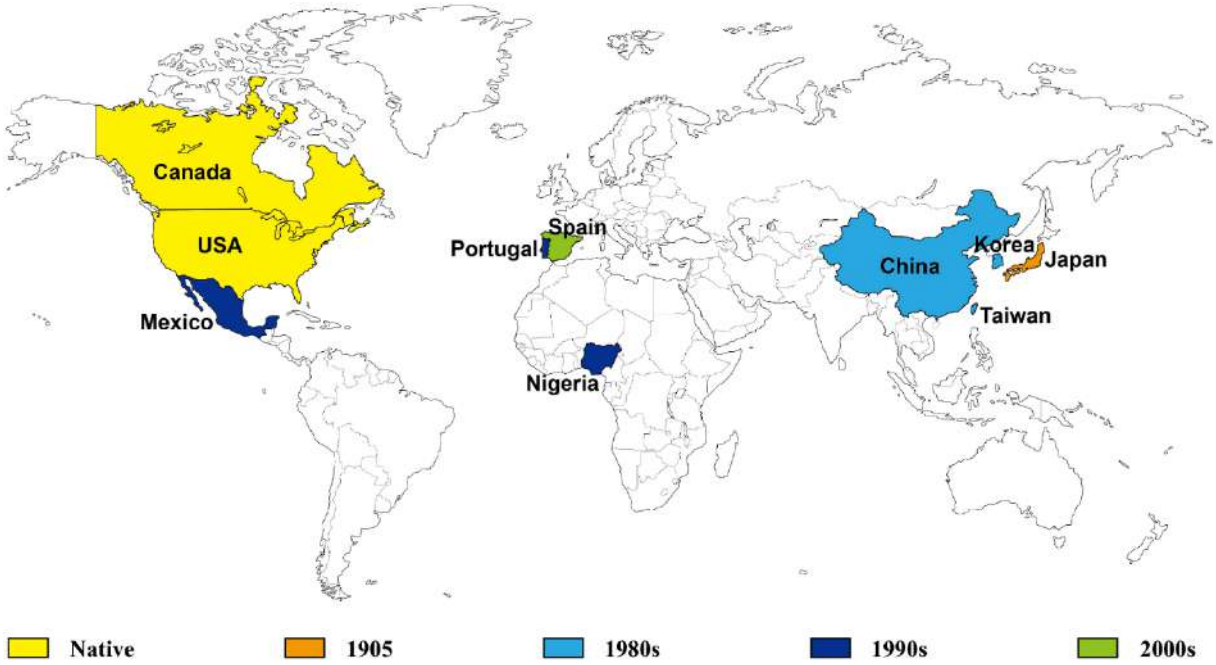

Figure 4.2. History of the invasion of pine wilt disease. Source: Kim et al., (2020)

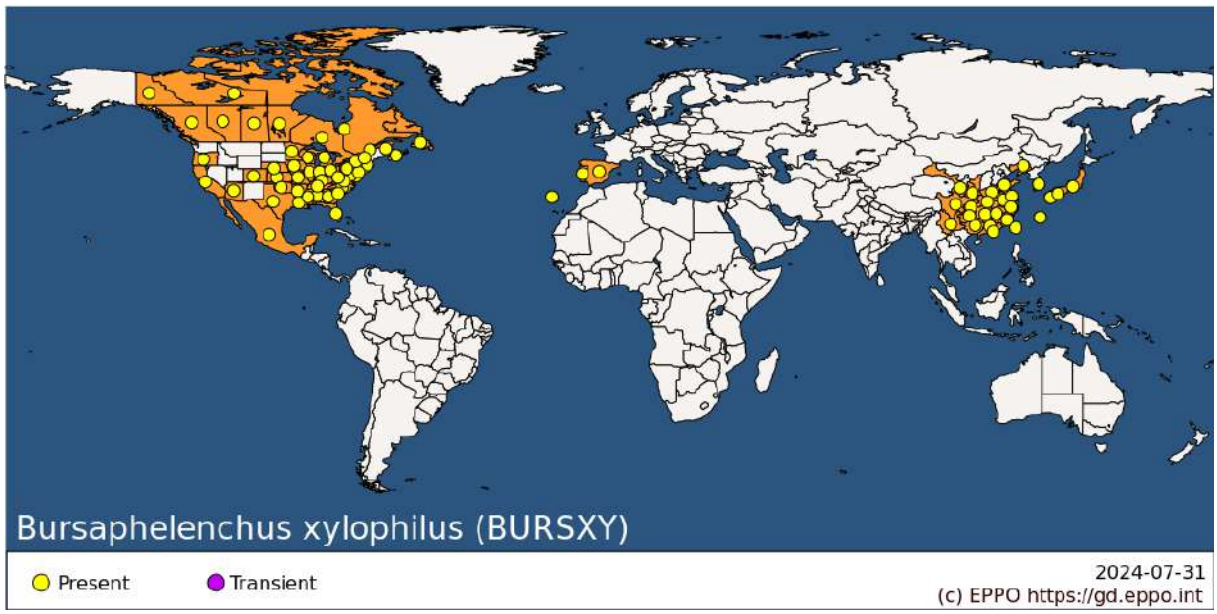

Figure 4.3. Geographical distribution of the Pinewood Nematode in the world. Source: EPPO (2024a)

4.2 Data, Methodology, and Assumptions

The analysis is subject to several assumptions. Firstly, the main vector of PWN in Europe is widespread so it is assumed that the vector availability is not a limiting factor with regard to the spread of the nematode. Further, the direct economic impact assessment assumes the absence of any intervention or management effort to control the spread of PWN, representing the worst-case scenario ("no-control" scenario). Lastly, the market price of round wood remained stable throughout the simulated period, and we assume no change in the structure of the available

standing stock (pine trees). Also, we assume a homogenous distribution of the production volume and tree mortality for each mortality rate scenario.
All the values used for the analysis are presented below in **Table A4.1.**

4.2.1 Climate module

Historical climatic data averaged for the years 1970-2000 were obtained from WorldClim (version 2.1, WorldClim) and extrapolated in 30-second (~1 km^2) resolution (Fick & Hijmans, 2017). The bioclimatic variable "BIO10", representing the mean temperature of the warmest quarter of the year, was used to filter the zone where PWD can be expressed. Based on the Expert Knowledge Elicited (EKE) data(Baker et al., 2019; European Food Safety Authority, 2014), PWD can be expressed and induce significant impacts where the mean summer temperature is ≥19.4 °C. Thus, we applied the 19.4 °C threshold in the BIO10 rasterized data layer and created a binary map. The suitable grid cells for PWD expression (**Fig. 4.4** white zone) were filtered and exported as a new layer, which was overlaid with the host distribution data layer (see below). This allowed us to obtain information on the total susceptible area and the proportion occupied by pine trees in km^2 within that area.

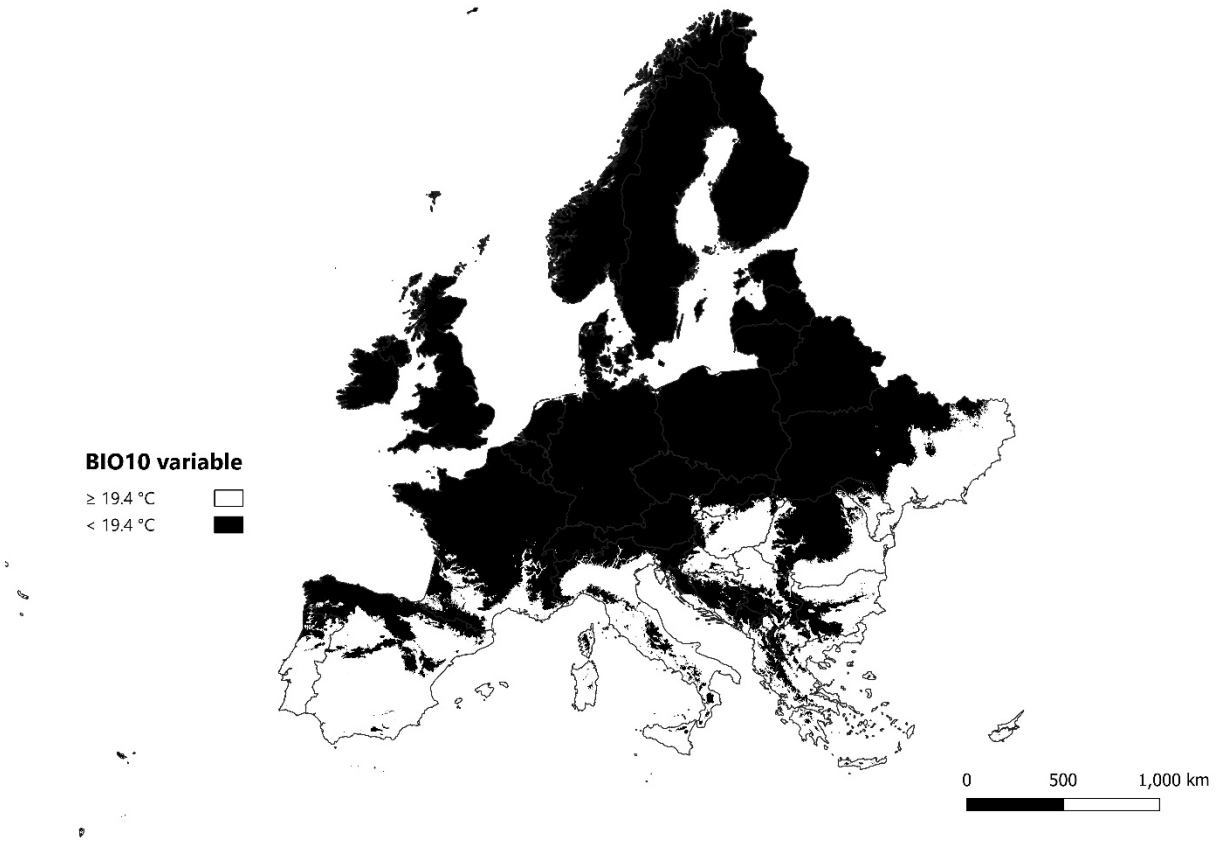

Figure 4.4. The map shows the areas of Europe with mean summer temperatures (BIO10 climatic variable) above ≥ 19.4°C (white) and below <19.4°C (black). Pine Wilt Disease is assumed to be expressed where the mean summer temperature is above the 19.4°C threshold (white zone).

4.2.2 Host trees module

Data on the spatial distribution of pine trees across Europe were obtained from the European Forest Institute (EFI) (Brus et al., 2012). The tree species maps are provided in 1 km^2 resolution, and

each grid cell has a value, ranging from 0 to 100, representing the predicted proportion of the species' presence within the grid cell. **Three raster layers were available for *Pinus* species, namely "Pinus_sylvestris.tif", "Pinus_pinaster.tif", and "Pinus_Misc.tif"; the latter file represents other *Pinus spp.* (miscellaneous).** All data layers used in this analysis were projected in EPSG:3035 – ETRS89-extended / LAEA Europe Coordinate Reference System.
To simplify the analysis, all three layers of *Pinus* species were combined into a single composite layer, representing the proportion of each grid cell covered by pine trees. **The composite *Pinus* layer used in this analysis captures the major European pine species identified as susceptible to PWD, including *Pinus sylvestris* and *Pinus pinaster*, which are explicitly represented in the dataset, as well as other relevant species such as *Pinus nigra*, *Pinus mugo*, and *Pinus radiata*, which are expected to be included within the *Pinus* spp. (miscellaneous) layer**. This aggregation allows for the estimation of total host availability while maintaining coverage of the major host species relevant to the analysis. Consequently, the composite layer is considered to represent the host range required for assessing the potential direct impact of PWD in Europe.

$$Land\ covered\ by\ Pine\ trees\ (km^2) = \sum_{i=1}^{n} \left(\frac{Predicted\ Proportion}{100}\right) \quad (1)$$

Eq. 1 describes the method used to calculate the total land covered by pine trees within the area of interest by summing the proportion values across all relevant n grid cells. Each proportion value was divided by 100 to convert percentages into fractional areas. For example, a cell with a predicted proportion of 45% was calculated as covering 0.45 km².

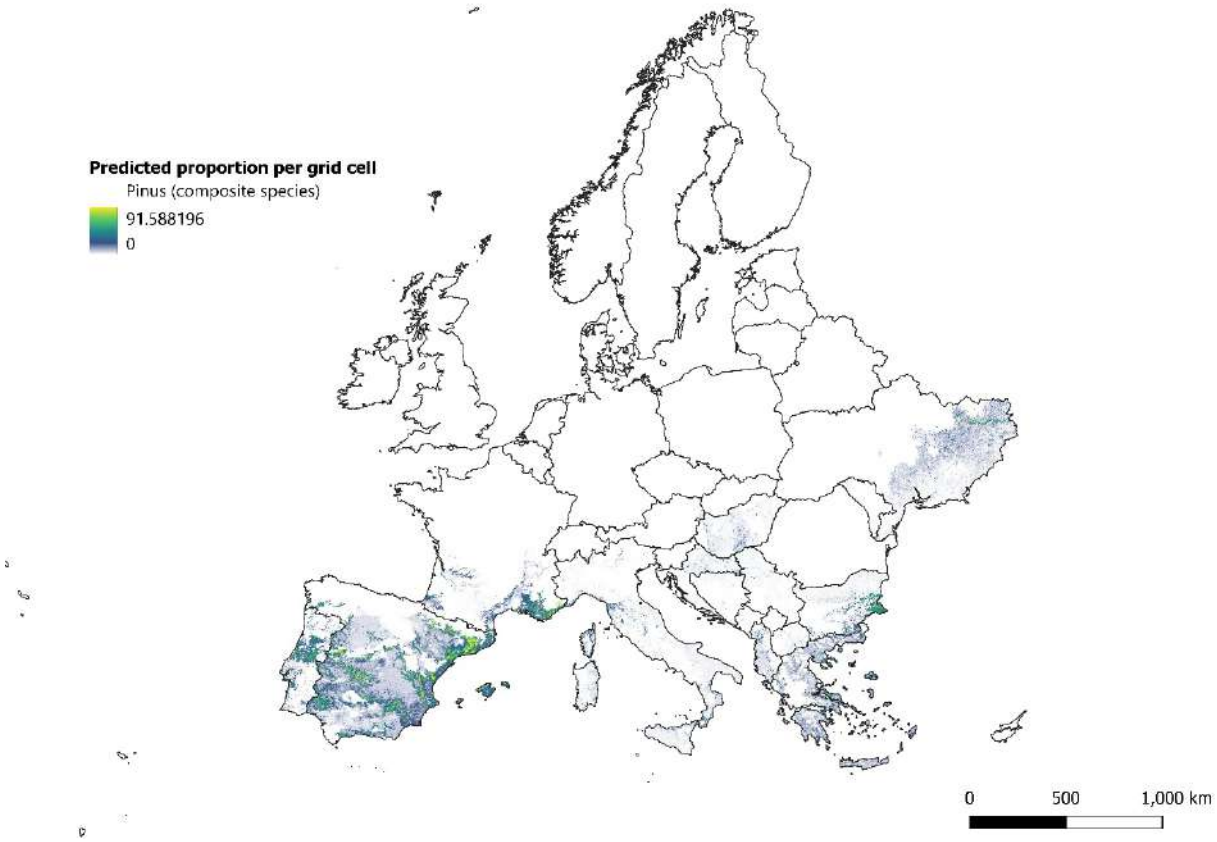

Figure 4.5. Predicted proportion/distribution of *Pinus* (composite) species in zones with mean summer temperature ≥19.4°C across the European continent. Each grid cell has 1 km² resolution.

Fig. 4.5 illustrates the predicted distribution of pine trees within the susceptible area, according to the data by EFI. Notably, the highest concentrations of pine trees within the susceptible area are observed in Portugal, Spain, southern France, Greece, and Ukraine.

4.2.3 Data on mortality and spread rates

The Joint Research Center (JRC) of the European Commission provided us with data from the European Food Safety Authority (EFSA) on mortality and spread rates for PWN. This dataset includes information based on the formal EKE methodology, described in detail by EFSA (European Food Safety Authority, 2014; Baker, et al., 2019; European Commission et al., 2019). In particular, this dataset includes the EKE annual spread rate (km^2/year) and the mortality rates (%) of PWN, presented in different percentiles of a Gaussian distribution. The rate of spread is a single parameter value that encapsulates both population growth and dispersal characteristics (short and long-distance dispersal) and corresponds to a radial range expansion spread model (Robinet et al., 2012; Schneider et al., 2020). Despite its simplicity, this type of spread model seems to perform reasonably well (Hudgins et al., 2017). The mortality rate determines the intensity of pine tree losses.

Table 4.1. Spread and mortality rates for PWN in Europe (averaged), based on formal methods for EKE.

Percentile	Spread rate (km^2/year)	Mortality rate[42] (%) (mean summer temperature ≥19.4 °C)
2.5th	0.339	6
25th	2.24	17
50th	4.432	25
75th	7.591	35
97.5th	16.228	55

Table 1 shows the expert-elicited spread and mortality rates for PWN in the EU. The spread rate ranges from 0.339 km²/year to 16.228 km²/year, while the mortality rates are from 6% to 55% in the best- and worst-case scenarios, respectively.

4.2.4 Extent of PWD outbreak

The first PWN detection in Europe occurred near Setúbal, Portugal (38.5243, -9.0197)[43] in 1999. Despite the establishment of a 30km radius restriction zone, the pest has spread to more than 30% of mainland Portugal, causing large-scale economic damage in the country (Back et al., 2024; de la Fuente et al., 2018b; de la Fuente & Beck, 2018). **Fig. 4.6** presents the initial point of PWN introduction (first detection) in Portugal and the extent of its spread in 2014, as well as in 2024.

[42] The pine species considered when deriving the EKE mortality rate distribution for PWN are *Pinus pinaster, Pinus sylvestris,* and *Pinus radiata.*
[43] Coordinates in decimal form.

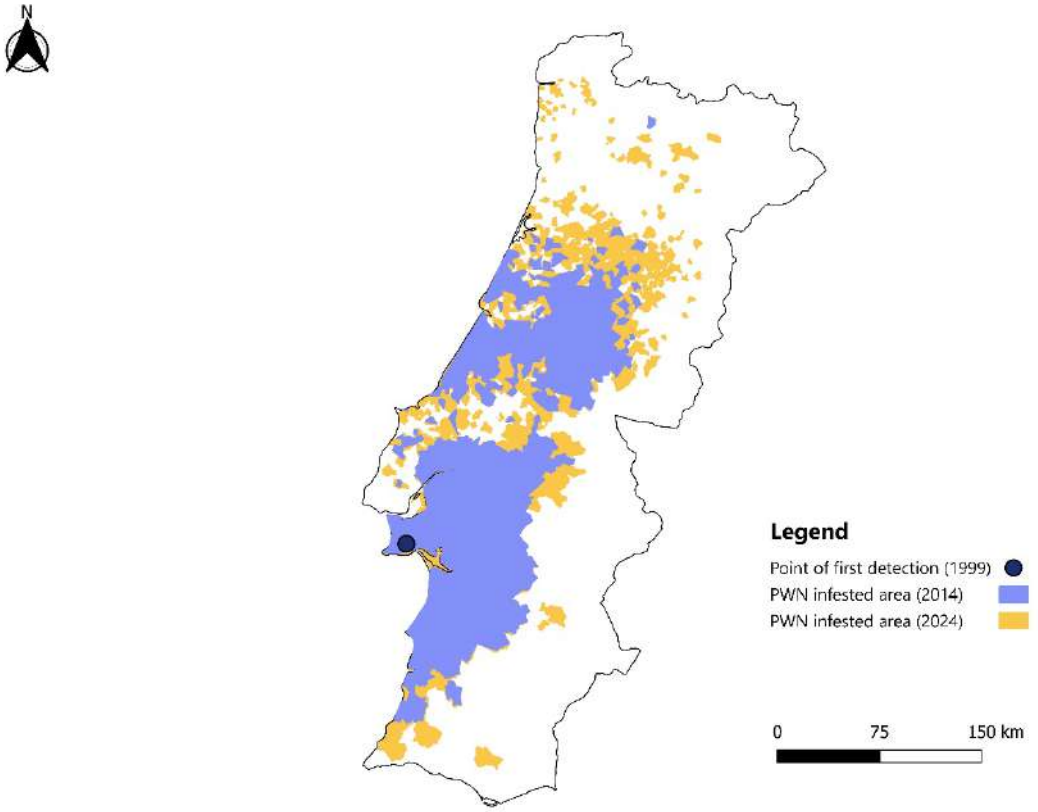

Figure 4.6. The area currently affected by Pine Wilt Disease in continental Portugal. (Petersen-Silva et al., 2014; ICNF, 2024; EPPO, 2024a)

Overlaying the pine composite species data layer by EFI and with information on PWN-infested areas in Portugal by the Instituto da Conservação da Natureza e das Florestas of Portugal (ICNF), the affected pine tree area has reached approximately 9400 km^2 by 2024. This indicates that PWN is reaching the total occupancy of the susceptible pine tree area in the country, which was approximately 10000 km^2 in 2015 (ICNF, 2019).
Beyond Portugal, PWN is also present in Spain. However, information on the current extent of the affected area is limited due to ongoing eradication efforts, which have been partially successful (e.g., the pest was declared absent from País Vasco following a survey, EPPO Reporting Service 2005/050). Given the lack of updates since 2005, no assumptions about the current extent of PWD in Spain are made, and we only utilize the available information for Portugal.

4.2.5 Spread modeling

An important factor that heavily influences the potential direct damage costs of PWN is the spread rate of the pest. In this analysis, we use a spatially implicit radial range expansion model to simulate the spread of PWN. Also, we examine and compare its outcomes with those of a spatially explicit spread model (Appendix). We use the principles of radial range expansion in both cases. For the PWN spread rate parameter value, we used all values of each of the available percentiles of the expert-elicited distribution, representing a best-, best-median, median, and worst-median, worst-case scenario. The spatially implicit spread model is detailed below.

4.2.5.1 Spatially implicit spread model

Initially, we calculated the radius of the current extent of PWN spread in Portugal (in 2024). This step was necessary because the spread originates from an already affected area, expanding outward from the perimeter of that area rather than from a single point. Thus, we converted the irregularly shaped polygon of the initially affected area IA_0[44] into an equivalent radius (circular shape), based on **Eq. 2**:

$$R_0 = \sqrt{\frac{IA_0}{\pi}} \quad (2)$$

Where R_0 is the approximate radius of the IA_0 polygon of **Fig. 4.6**.
Subsequently, the affected area at year *t* was then computed based on **Eq. 3**:

$$IA_{rr,t} = \pi \cdot (R_0 + rr \cdot t)^2 \quad (3)$$

Where $IA_{rr,t}$ is the affected area (km^2) after t years, rr the radial range expansion rate (km^2/year), and π the mathematical constant. As the radius grows over time, the affected area expands quadratically, as per the geometric relation of the area of a circle.
$IA_{rr,t}$ is constraint by the total susceptible area SA, which represents the area where PWD can be expressed. Consequently, $IA_{rr,t}$ cannot exceed SA (km^2). Furthermore, we consider impacts only from 2024 onward. Thus, the incremental infested area IIA_t (km^2) at year *t* (km^2) is expressed as:

$$IIA_t = \max[0, \min(IA_t, SA) - IA_0] \quad (4)$$

Eq. 4 ensures that IA_t does not exceed SA and that IIA_t remains non-negative.

4.2.6 Direct economic impact

The direct economic impact assessment was conducted using a partial budgeting approach under a no-control scenario (Soliman et al., 2015; Wesseler & Fall, 2010). The direct economic impact is expressed in terms of the total loss in production volume, assuming that the standing stock and price remain constant throughout this period of the simulation. The potential direct damage costs are equal to:

$$DD_{m,t} = IA_{rr,t} \cdot VT \cdot \frac{m}{100} \cdot p \quad (5)$$

where,
$DD_{m,t}$: Direct damage costs (€) due to timber loss for each mortality rate scenario m and after t years from the beginning of the simulation.
$IA_{rr,t}$: Affected area (km²) after t elapsed years for spread rate rr.
VT: Average timber volume (m³/km) derived from the EFISCEN Inventory Database (EFISCEN Inventory Database). This represents the average production volume of *Pinus pinaster* in Portugal across age classes, with a resulting value of 9.555 m³/km². We selected *Pinus pinaster*, Portugal's most common commercially exploited species. However, this uniformity might introduce deviations from actual local timber volumes in regions dominated by other *Pinus* species.
$\frac{m}{100}$: Mortality rate (%).

[44] The value of IA_0 was computed at 33823 km^2. This supports the claim that the pest has spread to more than 30% of mainland Portugal (Back et al., 2024; de la Fuente et al., 2018b; de la Fuente & Beck, 2018), as the total country area is 92220 km^2.

p: Market price of timber (€/m³). The market price value is derived from the average price of standing maritime pine timber for 2018-2023 and was provided by Centro Pinus. The exact values are presented in **Table A4.2**.

The total direct economic impact was discounted, in order to account for the future economic losses to their present value. Thus, $DD_{m,t}$ is expressed in terms of present value PVD_t based on the following equation:

$$PVD_{m,t} = \frac{DD_{m,t}}{(1+r)^t} \quad (6)$$

Where $PVD_{m,t}$ stands for the damage costs in present value due to PWN attack/ presence. The denominator is the discount factor, where r is equal to 4.49%[45] and t the time step. **Eq. 6** assumes an infinite time horizon and applies the transversality condition, which ensures that the present value of the state variables converges to zero as the horizon approaches infinity. By serving as a boundary condition, the transversality condition ensures that the discounted economic impact of the pest diminishes over time. This approach guarantees the economic feasibility of the analysis and aligns with the practical assumption that the influence of impacts far into the future is negligible.

The total discounted impact over an infinite time horizon was then used to compute the average annual cost (AAC) as follows:

$$AAC = PVD_{m,t} * r \quad (7)$$

$IA_{rr,t}$ was calculated based on **Eq. 3**, assuming that the spread happens uniformly in all directions until the susceptible area is fully occupied. A fundamental assumption of the "no-control" scenario is that the impact continues perpetually, reflecting a worst-case scenario where PWN spread remains uncontrolled. This way, it provides a metric for average annualized costs.

4.3 Results

4.3.1 Affected Area – spatially implicit spread model

In the case of the spatially implicit spread model, we assume that PWN uniformly disperses throughout the susceptible area in Europe until it reaches an equilibrium (total outbreak) at year *t,* depending on the spread rate.

Table 4.2 presents the progression of PWN, showing the total susceptible area, the corresponding proportion of the total susceptible area infested, and the estimated affected pine tree area. Results are provided for three time horizons (10, 20, and 30 years) and three spread rate scenarios: best-case (2.5th percentile, 0.34 km²/year), moderate-case (50th percentile, 4.43 km²/year), and worst-case (97.5th percentile, 16.23 km²/year), assuming a 6.71% pine tree area on total area.

[45] We use 4.49% as it is the average discount rate for the majority of Member States (Austria, Belgium, Cyprus, Germany, Estonia, Greece, Spain, Finland, France, Croatia, Ireland, Italy, Lithuania, Luxembourg, Latvia, Malta, the Netherlands, Portugal, Slovenia, and Slovakia) over the period 2023-2024. Source: Reference and discount rates (in %) since 01.08.1997

Table 4.2. Example output of total PWN affected area, proportion of affected area to total susceptible area, and affected pine tree area for 6.71% proportion of pine trees on total susceptible area, three different time horizons (10, 20, and 30 years after the beginning of the simulation), and three spread rate scenarios (best-case, 2.5th percentile, 0.339 km^2/year; moderate-case, 50th percentile, 4.432 km^2/year; worst-case, 97.5th percentile, 16.228 km^2/year), using the spatially implicit spread model. We assume a 6.71% proportion of pine trees in the total susceptible area.

Elapsed years	Spread rate (km^2/year)	Total affected area (km^2)	Susceptible area infested (%)	Affected pine tree area (km^2)
10	0.339	36069.9	2.2	2419.9
	4.432	68889.1	4.3	4621.8
	16.228	222355.6	13.8	14918.0
20	0.339	38388.3	2.4	2575.5
	4.432	116296.3	7.2	7802.4
	16.228	576354.0	35.7	38667.9
30	0.339	40779.0	2.5	2735.9
	4.432	176045.4	10.9	11811.0
	16.228	1095818.8	67.9	73519.1

The results indicate that in the best-case scenario, the infection grows slowly over the years, with only 2.5% of the susceptible area being affected after 30 years. This corresponds to an affected pine tree area of 2736 km^2. On the contrary, in the worst-case scenario, the PWD progresses rapidly, covering approximately 68% of the total area within the same period and affecting roughly 73 thousand km^2. The moderate-case scenario shows steady growth within the time horizon considered, with approximately 11% of the total susceptible area affected after 30 years. The rapid expansion of the affected areas, especially under higher spread rates, underscores the importance of controlling pests to limit their spread in an early stage of invasion.

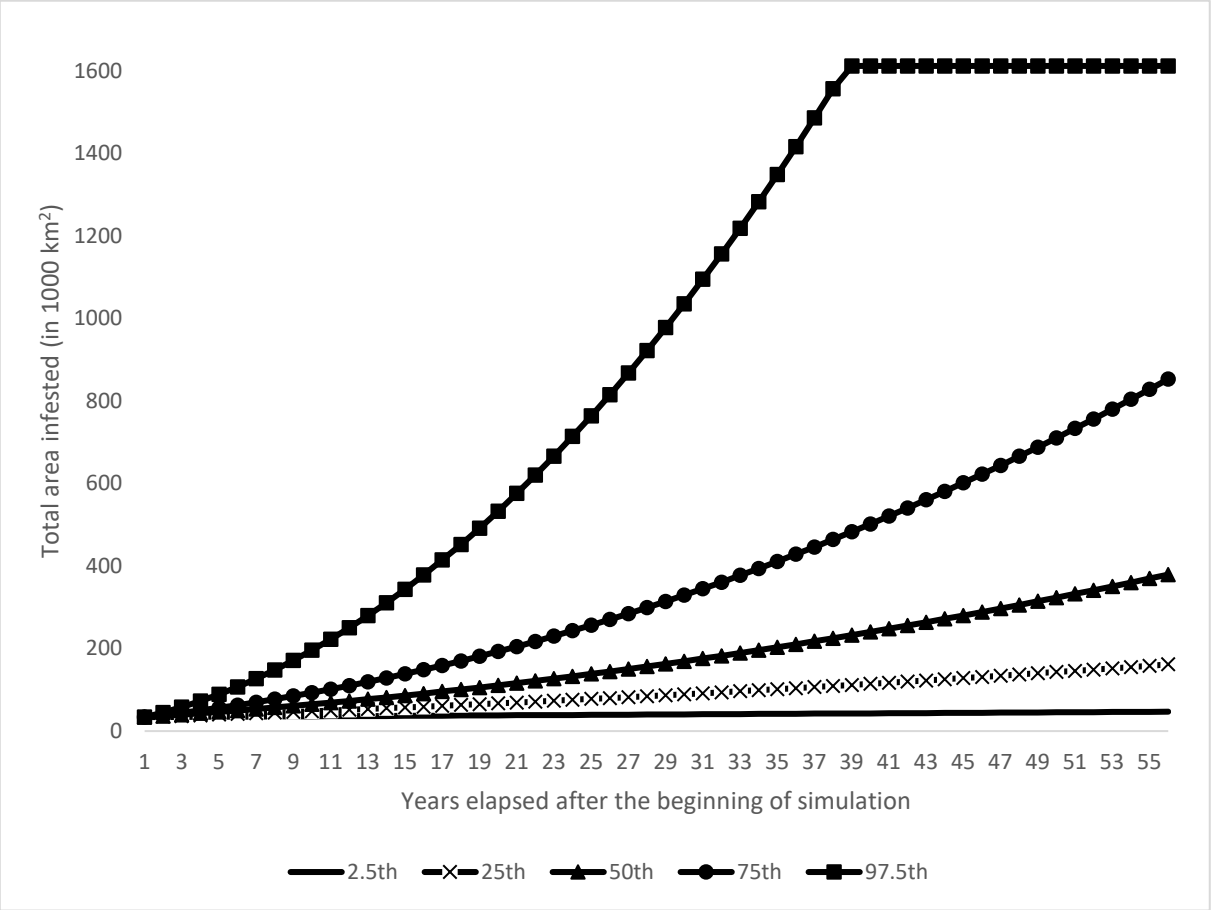

Figure 4.7. Change in the total affected area by the Pinewood Nematode from the spatially implicit spread simulation under the no-control scenario for the first 55 years after the beginning of the simulation. The lines represent trajectories from different spread rates (percentiles), showing the best-case (plain line), worst-case (filled squares), 25th (x-pattern), 50th (filled triangles), and 75th (filled squares) percentiles of the expert-elicited spread rate distribution for PWN.

Fig. 4.7 illustrates the change in the total affected area over time for PWN under different spread rate scenarios, assuming no control measures are in place or implemented. In the best-case spread scenario (2.5th percentile), the affected area expands slowly, reaching approximately 46000 km^2 by year 50. On the other hand, the worst-case spread scenario (97.5th percentile) shows a rapid PWN dispersal that reaches the full occupancy of the susceptible area by year 38. The 50th percentile represents the median annual spread rate scenario, resulting in an affected area of approximately 332570 km^2 after 50 years of spread, while the 25th and 75th percentiles demonstrate intermediate outcomes. Based on our simulation results, the full occupancy of the total susceptible area is reached after 1808, 274, 139, 81, and 38 years of spread for the 2.5th, 25th, 50th, 75th, and 97.5th percentiles of the spread rate distribution, respectively.

4.3.2 Direct economic impact

This section includes an example of the potential direct damage costs due to PWN spread in Europe under a no-control scenario, using the spatially implicit spread model. The calculations are based on parameter values representing a moderate case scenario, illustrating cumulative impacts over time. Further, we include the outcomes for the average annual direct damage costs under varying spread and mortality rate scenarios, which were computed based on **Eq. 7**.

Additional results with different market prices of timber are provided in **Table A4.3**, **Table A4.4**, **Table A4.5**, and **Table A4.6**.

Table 4.3 provides an example calculation of the cumulative direct damage costs over until the full occupancy of the susceptible area, assuming a median spread and mortality rate (50th percentile; 4.432 km^2/year, and 25 %, respectively), 34.5 €/m^3 market price of timber / round wood, 9555 m^3/km^2, and 4.49% discount rate. Further details of other parameter values, such as the initially affected area (km^2), the total susceptible area (km^2), etc., are included in **Table A4.1**.

Table 4.3. Example calculations of potential direct damage costs due to PWN in Europe, using the spatially implicit spread model. The calculations below represent the most likely scenario in terms of mortality and spread rates (50th percentile, representing median values), and an average timber market price for the period 2018-2023 in Portugal.

Elapsed years	Infested area (km^2)	Cumulative infested area (km^2)	Susceptible area infested (%)	Infested pine tree area (km^2)	Timber loss (1000 m^3)	Value of timber loss (€ million)	Discount factor	Present Value of timber loss (€ million)
0	0.0	33823.7	2.1	2269.2	5421	187	1.000	187
1	2951.2	36774.9	2.3	2467.2	5894	203	0.957	195
2	6025.7	39849.4	2.5	2673.5	6386	220	0.916	202
3	9223.7	43047.4	2.7	2888.1	6899	238	0.877	209
4	12545.1	46368.8	2.9	3110.9	7431	256	0.839	215
5	15990.0	49813.7	3.1	3342.0	7983	275	0.803	221
6	19558.2	53381.9	3.3	3581.4	8555	295	0.768	227
7	23249.9	57073.6	3.5	3829.1	9147	316	0.735	232
8	27065.0	60888.7	3.8	4085.1	9758	337	0.704	237
9	31003.5	64827.2	4.0	4349.3	10389	358	0.673	241
10…∞	35065.4	68889.1	4.3	4621.8	11040	381	0.645	18370[46]
Total								20536

The results show that the initially affected area accounts for 2.1% of the total susceptible area. After 10 years of uncontrolled spread, it reaches 4.3% of the total susceptible area, and it fully occupies this area in year 139[47]. The total discounted value of timber loss under the simulated scenario is approximately €20.5 billion.

[46] Discounted sum from year 10 until infinity in present value.
[47] Not shown in the table.

Table 4.4. Average annual direct damage costs due to *Bursaphelenchus xylophilus* in Europe for an average market price of timber of 34.5 €/m^3.

Market price (€/m^3)	Mortality rate (%)	Average annual costs (€ million) for different spread rates (km^2/year)				
		0.339	**2.24**	**4.432**	**7.591**	**16.228**
34.5	6	54	114	221	417	886
	17	154	323	627	1180	2510
	25	226	476	922	1736	3691
	35	316	666	1291	2430	5168
	55	497	1047	2029	3818	8121

Table 4.4 presents the average annual direct economic costs due to PWN for varying spread and mortality rates. Evidently, both play a substantial role in the results. Even in the best-case scenario (0.339 km^2/year spread rate, and 6% mortality rate) the average annual damage costs are estimated at approximately €54 million, whereas under the worst-case scenario (16.228 km^2/year spread rate, and 55% mortality rate), these costs may exceed €8.1 billion per year. The most likely scenario is expected to fall within these two extremes. At a mortality rate of 25%, annual costs range from €226 million under the slowest spread rate (0.339 km²/year) to €3.7 billion under the fastest spread rate (16.228 km²/year).

The annual damage costs escalate sharply, particularly at higher spread rates and mortality rates. The time required for total outbreak decreases exponentially as the spread rate increases, highlighting the critical importance of constraining the speed of spread at early stages of invasion. Reducing the spread rate significantly at early stages can extend the spread timeline, providing more time for effective management and containment efforts. However, at later stages, when the pest reaches higher spread rates, control measures tend to have a more modest effect.

4.4 References

[1] Abelleira, A., Picoaga, A., Mansilla, J. P., & Aguin, O. (2011). Detection of Bursaphelenchus Xylophilus, Causal Agent of Pine Wilt Disease on Pinus pinaster in Northwestern Spain. Https://Doi.Org/10.1094/PDIS-12-10-0902, 95(6), 776–776. https://doi.org/10.1094/PDIS-12-10-0902

[2] Akbulut, S., & Linit, M. J. (1999). Flight Performance of Monochamus carolinensis (Coleoptera: Cerambycidae) with Respect to Nematode Phoresis and Beetle Characteristics. Environmental Entomology, 28(6), 1014–1020. https://doi.org/10.1093/EE/28.6.1014

[3] Akbulut, S., & Stamps, W. T. (2012). Insect vectors of the pinewood nematode: a review of the biology and ecology of Monochamus species. Forest Pathology, 42(2), 89–99. https://doi.org/10.1111/J.1439-0329.2011.00733.X

[4] Back, M. A., Bonifácio, L., Inácio, M. L., Mota, M., & Boa, E. (2024). Pine wilt disease: A global threat to forestry. Plant Pathology, 73(5), 1026–1041. https://doi.org/10.1111/PPA.13875

[5] Baker, R., Gilioli, G., Behring, C., Candiani, D., Gogin, A., Kaluski, T., Kinkar, M., Mosbach-Schulz, O., Neri, F. M., Siligato, R., Stancanelli, G., & Tramontini, S. (2019). Report on the methodology applied by EFSA to provide a quantitative assessment of pest-related criteria required to rank candidate priority pests as defined by Regulation (EU) 2016/2031. EFSA Journal, 17(6), e05731. https://doi.org/10.2903/J.EFSA.2019.5731

[6] Brus, D. J., Hengeveld, G. M., Walvoort, D. J. J., Goedhart, P. W., Heidema, A. H., Nabuurs, G. J., & Gunia, K. (2012). Statistical mapping of tree species over Europe. European Journal of Forest Research, 131(1), 145–157. https://doi.org/10.1007/S10342-011-0513-5/TABLES/6

[7] de la Fuente, B., & Beck, P. S. A. (2018). Invasive Species May Disrupt Protected Area Networks: Insights from the Pine Wood Nematode Spread in Portugal. Forests 2018, Vol. 9, Page 282, 9(5), 282. https://doi.org/10.3390/F9050282

[8] de la Fuente, B., Saura, S., & Beck, P. S. A. (2018a). Predicting the spread of an invasive tree pest: The pine wood nematode in Southern Europe. Journal of Applied Ecology, 55(5), 2374–2385. https://doi.org/10.1111/1365-2664.13177

[9] de la Fuente, B., Saura, S., & Beck, P. S. A. (2018b). Predicting the spread of an invasive tree pest: The pine wood nematode in Southern Europe. Journal of Applied Ecology, 55(5), 2374–2385. https://doi.org/10.1111/1365-2664.13177

[10] EPPO. (2024a). Bursaphelenchus xylophilus. In EPPO datasheets on pests recommended for regulation. https://gd.eppo.int/taxon/BURSXY/datasheet

[11] EPPO. (2024b). Monochamus galloprovincialis. In EPPO Global Database. https://gd.eppo.int/taxon/MONCGA

[12] Estorninho, M., Chozas, S., Mendes, A., Colwell, F., Abrantes, I., Fonseca, L., Fernandes, P., Costa, C., Máguas, C., Correia, O., & Antunes, C. (2022). Differential Impact of the Pinewood Nematode on Pinus Species Under Drought Conditions. Frontiers in Plant Science, 13, 841707. https://doi.org/10.3389/FPLS.2022.841707/BIBTEX

[13] European Commission, Joint Research Centre, Sánchez Berta, Barreiro-Hurle Jesus, Soto Embodas Iria, & Rodriguez-Cerezo Emilio. (2019). The impact Indicator for Priority Pests (I2P2) : a tool for ranking pests according to Regulation (EU) 2016/2031. https://data.europa.eu/doi/10.2760/585182

[14] European Food Safety Authority. (2014). Guidance on Expert Knowledge Elicitation in Food and Feed Safety Risk Assessment. EFSA Journal, 12(6), 3734. https://doi.org/10.2903/j.efsa.2014.3734

[15] Evans, H. F., McNamara, D. G., Braasch, H., Chadoeuf, J., & Magnusson, C. (1996). Pest Risk Analysis (PRA) for the territories of the European Union (as PRA area) on Bursaphelenchus xylophilus and its vectors in the genus Monochamus. EPPO Bulletin, 26(2), 199–249. https://doi.org/10.1111/J.1365-2338.1996.TB00594.X

[16] Fick, S. E., & Hijmans, R. J. (2017). WorldClim 2: new 1-km spatial resolution climate surfaces for global land areas. International Journal of Climatology, 37(12), 4302–4315. https://doi.org/10.1002/JOC.5086

[17] Fonseca, L., Cardoso, J.M.S., Lopes, A., Pestana, M., Abreu, F., Nunes, N., Mota, M., Abrantes, I. (2012). The pinewood nematode, *Bursaphelenchus xylophilus*, in Madeira Island. Helminthologia, 49(2), pp. 96–103.

[18] Fonseca, L., Silva, H., Cardoso, J.M.S., Esteves, I., Maleita, C., Lopes, S., Abrantes, I. (2024). *Bursaphelenchus xylophilus* in Pinus sylvestris—The First Report in Europe. Forests, 15, 1556.

[19] Hirata, A., Nakamura, K., Nakao, K., Kominami, Y., Tanaka, N., Ohashi, H., Takano, K. T., Takeuchi, W., & Matsui, T. (2017). Potential distribution of pine wilt disease under future climate change scenarios. PLOS ONE, 12(8), e0182837. https://doi.org/10.1371/JOURNAL.PONE.0182837

[20] Hudgins, E. J., Liebhold, A. M., & Leung, B. (2017). Predicting the spread of all invasive forest pests in the United States. Ecology Letters, 20(4), 426–435. https://doi.org/10.1111/ELE.12741

[21] ICNF. (2019). IFN6. https://cdn.pefc.org/pefc.pt/media/2020-08/88597cd3-8e82-4bc6-aae6-fb66adb5303f/22eabe74-d55e-5246-bfec-15be43c3c1c9.pdf

[22] ICNF. (2024). BDG/NEMATODO (MapServer). https://sigservices.icnf.pt/server/rest/services/BDG/NEMATODO/MapServer

[23] Inácio, M.L., Nóbrega, F., Vieira, P., Bonifácio, L., Naves, P., Sousa, E., Mota, M. (2015). First detection of Bursaphelenchus xylophilus associated with Pinus nigra in Portugal and in Europe. Forest Pathology, 45(3), pp. 235–238.

[24] Jones, J. T., Moens, M., Mota, M., Li, H., & Kikuchi, T. (2008). Bursaphelenchus xylophilus: opportunities in comparative genomics and molecular host–parasite interactions. Molecular Plant Pathology, 9(3), 357–368. https://doi.org/10.1111/J.1364-3703.2007.00461.X

[25] Kim, B. N., Kim, J. H., Ahn, J. Y., Kim, S., Cho, B. K., Kim, Y. H., & Min, J. (2020). A short review of the pinewood nematode, Bursaphelenchus xylophilus. Toxicology and Environmental Health Sciences, 12(4), 297–304. https://doi.org/10.1007/S13530-020-00068-0/FIGURES/4

[26] Kobayashi, F., Yamane, A., & Ikeda, T. (1984). The Japanese pine sawyer beetle as the vector of pine wilt disease. Annual Review of Entomology. Vol. 29, 29(Volume 29, 1984), 115–135. https://doi.org/10.1146/ANNUREV.EN.29.010184.000555/CITE/REFWORKS

[27] Koutroumpa, F. A., Koutroumpa BIOLOGIE, F. A., & Monochamus Gallo-, P. DE. (2007). BIOLOGIE ET PHYLOGEOGRAPHIE DE MONOCHAMUS GALLOPROVINCIALIS (COLEOPTERA, CERAMBYCIDAE) VECTEUR DU NEMATODE DU PIN EN EUROPE. https://theses.hal.science/tel-00288604

[28] Liu, F., Su, H., Ding, T., Huang, J., Liu, T., Ding, N., & Fang, G. (2023). Refined Assessment of Economic Loss from Pine Wilt Disease at the Subcompartment Scale. Forests 2023, Vol. 14, Page 139, 14(1), 139. https://doi.org/10.3390/F14010139

[29] Mamiya, Y., & Shoji, T. (2009). Pathogenicity of the pinewood nematode, Bursaphelenchus xylophilus, to Japanese larch, Larix kaempferi, seedlings. Journal of Nematology, 41(2), 157. /pmc/articles/PMC3365316/

[30] Mota, M. M., Braasch, H., Bravo, M. A., Penas, A. C., Burgermeister, W., Metge, K., & Sousa, E. (1999). First report of Bursaphelenchus xylophilus in Portugal and in Europe. Nematology, 1(7), 727–734. https://doi.org/10.1163/156854199508757

[31] Mota, M., & Vieira, P. C. (2008). Pine wilt disease in Portugal. In Pine Wilt Disease, B. G. Zhao, K. Futai, J. R. Sutherland, & Y. Takeuchi (Eds.), pp. 33–38. Springer.

[32] Naves, P., Bonifácio, L., & de Sousa, E. (2016). The pine wood nematode and its local vectors in the mediterranean basin. Insects and Diseases of Mediterranean Forest Systems, 329–378. https://doi.org/10.1007/978-3-319-24744-1_12/FIGURES/7

[33] Naves, P., Bonifácio, L., Inácio, M. L., & Sousa, E. (2019). Integrated management of pine wilt disease in Troia. Revista de Ciências Agrárias, 41(spe), 4–7. https://doi.org/10.19084/rca.17060

[34] Nentwig, W., Bacher, S., Kumschick, S., Pyšek, P., & Vilà, M. (2018). More than "100 worst" alien species in Europe. Biological Invasions, 20(6), 1611–1621. https://doi.org/10.1007/S10530-017-1651-6/FIGURES/1

[35] Penas, A. C., Bravo, M. A., Naves, P., Bonifácio, L., Sousa, E., & Mota, M. (2006). Species of Bursaphelenchus Fuchs, 1937 (Nematoda: Parasitaphelenchidae) and other nematode genera associated with insects from Pinus pinaster in Portugal. Annals of Applied Biology, 148(2), 121–131. https://doi.org/10.1111/J.1744-7348.2006.00042.X

[36] Petersen-Silva, R., Naves, P., Godinho-Ferreira, P., Sousa, E., & Pujade-Villar, J. (2014). Distribution, Hosts and Parasitoids of Monochamus galloprovincialis (Coleoptera: Cerambycidae) in Portugal Mainland. INIAV.

[37] Pimentel, C. (2022). Bursaphelenchus xylophilus (pine wilt nematode). CABI Compendium. https://doi.org/10.1079/CABICOMPENDIUM.10448

[38] Robinet, C., Kehlenbeck, H., Kriticos, D. J., Baker, R. H. A., Battisti, A., Brunel, S., Dupin, M., Eyre, D., Faccoli, M., Ilieva, Z., Kenis, M., Knight, J., Reynaud, P., Yart, A., & van der Werf, W. (2012). A Suite of Models to Support the Quantitative Assessment of Spread in Pest Risk Analysis. PLOS ONE, 7(10), e43366. https://doi.org/10.1371/JOURNAL.PONE.0043366

[39] Robinet, C., Roques, A., Pan, H., Fang, G., Ye, J., Zhang, Y., & Sun, J. (2009). Role of Human-Mediated Dispersal in the Spread of the Pinewood Nematode in China. PLOS ONE, 4(2), e4646. https://doi.org/10.1371/JOURNAL.PONE.0004646

[40] Schneider, K., van der Werf, W., Cendoya, M., Mourits, M., Navas-Cortés, J. A., Vicent, A., & Lansink, A. O. (2020). Impact of Xylella fastidiosa subspecies pauca in European olives. Proceedings of the National Academy of Sciences of the United States of America, 117(17), 9250–9259. https://doi.org/10.1073/PNAS.1912206117/-/DCSUPPLEMENTAL

[41] Soliman, T., Mourits, M. C. M., Oude Lansink, A. G. J. M., & van der Werf, W. (2015). Quantitative economic impact assessment of invasive plant pests: What does it require and when is it worth the effort? Crop Protection, 69, 9–17. https://doi.org/10.1016/j.cropro.2014.11.011

[42] Soliman, T., Mourits, M. C. M., van der Werf, W., Hengeveld, G. M., Robinet, C., & Lansink, A. G. J. M. O. (2012). Framework for Modelling Economic Impacts of Invasive Species, Applied to Pine Wood Nematode in Europe. PLoS ONE, 7(9), e45505. https://doi.org/10.1371/journal.pone.0045505

[43] Sousa, E., Bonifacio, L., & Mota, M. (2018). Bursaphelenchus xylophilus (Nematoda; Aphelenchoididae) associated with Monochamus galloprovincialis (Coleoptera; Cerambycidae) in Portugal. https://doi.org/10.1163/156854101300106937

[44] TANIUCHI, H. (2016). Wood flow from logs to products in Iwate prefecture. Wood Preservation, 42(4), 225–228. https://doi.org/10.5990/JWPA.42.225

[45] Wesseler, J., & Fall, E. H. (2010). Potential damage costs of Diabrotica virgifera virgifera infestation in Europe – the 'no control' scenario. Journal of Applied Entomology, 134(5), 385–394. https://doi.org/10.1111/j.1439-0418.2010.01510.x

[46] Zamora, P., Rodríguez, V., Renedo, F., Sanz, A. V., Domínguez, J. C., Pérez-Escolar, G., Miranda, J., Álvarez, B., González-Casas, A., Mayor, E., Dueñas, M., Miravalles, A., Navas, A., Robertson, L., & Martín, A. B. (2015). First Report of *Bursaphelenchus xylophilus* Causing Pine Wilt Disease on Pinus radiata in Spain. https://Doi.Org/10.1094/PDIS-03-15-0252-PDN, 99(10). https://doi.org/10.1094/PDIS-03-15-0252-PDN

[47] Zhang, H., Wei, Z., Liu, X., Zhang, J., & Diao, G. (2022). Growth and decline of arboreal fungi that prey on Bursaphelenchus xylophilus and their predation rate. Journal of Forestry Research, 33(2), 699–709. https://doi.org/10.1007/S11676-021-01334-8/TABLES/7

[48] Zhao, J., Huang, J., Yan, J., & Fang, G. (2020). Economic Loss of Pine Wood Nematode Disease in Mainland China from 1998 to 2017. Forests 2020, Vol. 11, Page 1042, 11(10), 1042. https://doi.org/10.3390/F11101042

4.5 Acknowledgments

We thank Estefanía Vázquez Torres and Kevin Schneider from the Joint Research Centre of the European Commission, Sevilla for providing us with the EKE data by EFSA on PWN mortality rates, spread rates, and the mean summer temperature threshold value for PWD disease expression. We extend our gratitude to our PurPest partners in INIAV and Centro Pinus for helping us obtain the round wood/timber price in Portugal.

4.6 Appendix

Table A4.1. Data sources, parameter values, and key data layers used in this analysis.

Parameters	Notation	Unit	Value	Source
Initially affected area Portugal (2014)	IA_0^{2014}	km^2	23164.5	ICNF
Initially affected area Portugal (2024)	IA_0^{2024}	km^2	33823.6	ICNF
Spread rate (2.5th percentile)	$rr_{2.5}$	km^2/year	0.339	JRC
Spread rate (25th percentile)	rr_{25}	km^2/year	2.24	JRC
Spread rate (50th percentile)	rr_{50}	km^2/year	4.432	JRC
Spread rate (75th percentile)	rr_{75}	km^2/year	7.591	JRC
Spread rate (97.5th percentile)	$rr_{97.5}$	km^2/year	16.228	JRC
Mortality rate (2.5th percentile)	$m_{2.5}$	%	6	JRC
Mortality rate (25th percentile)	m_{25}	%	17	JRC
Mortality rate (50th percentile)	m_{50}	%	25	JRC
Mortality rate (75th percentile)	m_{75}	%	35	JRC
Mortality rate (97.5th percentile)	$m_{97.5}$	%	55	JRC
Average market price of round wood/timber in Portugal	p	$€/m^3$	27.5	Centro Pinus / ICNF
all_pinus.tif	-	km^2	110486.2	EFI / own computation
sylvestris_3035.tif	-	km^2	493503.5	EFI / own computation
bio10_sylvestris.tif	-	km^2	28590.75	EFI / own computation
pinaster_3035.tif	-	km^2	57607.32	EFI / own computation
bio10_pinaster.tif	-	km^2	29496.99	EFI / own computation
misc_3035.tif	-	km^2	77293.35	EFI / own computation
bio10_misc.tif	-	km^2	52398.43	EFI / own computation
Infested_area_overlayed_2024.tif	-	km^2	4629.39	EFI / own computation
spread_10_years_2.5.tif	-	km^2	5459.85	EFI / own computation
spread_20_years_2.5.tif	-	km^2	5788.84	EFI / own computation

spread_30_years_2.5.tif	-	km^2	5947.96	EFI / own computation
sperad_10_years_25.tif	-	km^2	6261.51	EFI / own computation
spread_20_years_25.tif	-	km^2	7874.53	EFI / own computation
spread_30_years_25.tif	-	km^2	10204.86	EFI / own computation
spread_10_years_50.tif	-	km^2	7816.42	EFI / own computation
spread_20_years_50.tif	-	km^2	12723.31	EFI / own computation
spread_30_years_50.tif	-	km^2	16965.4	EFI / own computation
spread_10_years_75.tif	-	km^2	11178	EFI / own computation
spread_20_years_75.tif	-	km^2	18170.2	EFI / own computation
spread_30_years_75.tif	-	km^2	23086.55	EFI / own computation
spread_10_years_97.5.tif	-	km^2	18733.93	EFI / own computation
spread_20_years_97.5.tif	-	km^2	3017012	EFI / own computation
spread_30_years_97.5.tif	-	km^2	3995243	EFI / own computation
Initial point of infection (Portugal, 1999)	-	Decimal coordinate	38.5243, -9.0197	EPPO
Average timber volume by age class in PT	VT	m^3/km^2	9555	EFI; EFISCEN
Discount rate	r	%	4.49	European Commission
Susceptible area (EU)	SA	km^2	1612998.48	Own computation
Initially affected area	R_0	km^2	33823.693	Own computation
Pine tree area within the susceptible area	-	km^2	110486.18	Own computation
Proportion of pine trees within the susceptible area	-	%	6.71	Own computation

Table A4.2. The market price of round wood in Portugal. Source: ICNF; Centro Pinus, *A fileira do pinho*

The (average) market price of round wood/timber in Portugal per year	
Year	**€/m^3**
2018	21
2019	16
2020	24
2021	31
2022	58
2023	57

Table A4.3. Example calculation of potential direct damage costs due to PWN in Europe, using the spatially implicit spread model. The calculations below represent the most likely scenario in terms of mortality and spread rates (50th percentile), and an average timber market price of 16 €/m^3.

Elapsed years	Affected area (km^2)	Cumulative affected area (km^2)	Susceptible area affected (%)	Affected pine tree area (km^2)	Timber loss (1000 m^3)	Value of timber loss (€ million)	Discount factor	PV of timber loss (€ million)
0	0.0	33823.7	2.1	2269.2	5421	87	1.000	87
1	2951.2	36774.9	2.3	2467.2	5894	94	0.957	90
2	6025.7	39849.4	2.5	2673.5	6386	102	0.916	94
3	9223.7	43047.4	2.7	2888.1	6899	110	0.877	97
4	12545.1	46368.8	2.9	3110.9	7431	119	0.839	100
5	15990.0	49813.7	3.1	3342.0	7983	128	0.803	103
6	19558.2	53381.9	3.3	3581.4	8555	137	0.768	105
7	23249.9	57073.6	3.5	3829.1	9147	146	0.735	108
8	27065.0	60888.7	3.8	4085.1	9758	156	0.704	110
9	31003.5	64827.2	4.0	4349.3	10389	166	0.673	112
10…∞	35065.4	68889.1	4.3	4621.8	11040	177	0.645	8519[48]
Total								9523

Table A4.4. Average annual direct damage costs due to *Bursaphelenchus xylophilus* in Europe for an average market price of timber of 16 €/m^3.

Market price (€/m^3)	Mortality rate (%)	Average annual costs (€ million) for different spread rates (km^2/year)				
		0.339	**2.24**	**4.432**	**7.591**	**16.228**
16	6	25	53	103	193	411
	17	71	150	291	547	1164

[48] Discounted sum from year 10 until infinity in present value.

	25	105	221	428	805	1712
	35	147	309	599	1127	2397
	55	231	485	941	1771	3766

Table A4.5. Example calculation of potential direct damage costs due to PWN in Europe, using the spatially implicit spread model. The calculations below represent the most likely scenario in terms of mortality and spread rates (50th percentile) and an average timber market price of 58 €/m^3.

Elapsed years	Affected area (km^2)	Cumulative affected area (km^2)	Susceptible area infested (%)	Affected pine tree area (km^2)	Timber loss (1000 m^3)	Value of timber loss (€ million)	Discount factor	PV of timber loss (€ million)
0	0.0	33823.7	2.1	2269.2	5421	314	1.000	314
1	2951.2	36774.9	2.3	2467.2	5894	327	0.957	327
2	6025.7	39849.4	2.5	2673.5	6386	339	0.916	339
3	9223.7	43047.4	2.7	2888.1	6899	351	0.877	351
4	12545.1	46368.8	2.9	3110.9	7431	362	0.839	362
5	15990.0	49813.7	3.1	3342.0	7983	372	0.803	372
6	19558.2	53381.9	3.3	3581.4	8555	381	0.768	381
7	23249.9	57073.6	3.5	3829.1	9147	390	0.735	390
8	27065.0	60888.7	3.8	4085.1	9758	398	0.704	398
9	31003.5	64827.2	4.0	4349.3	10389	406	0.673	406
10…∞	35065.4	68889.1	4.3	4621.8	11040	413	0.645	30888[49]
Total								34524

Table A4.6. Average annual direct damage costs due to *Bursaphelenchus xylophilus* in Europe for an average market price of timber of 58 €/m^3.

Market price (€/m^3)	Mortality rate (%)	Average annual costs (€ million) for different spread rates (km^2/year)				
		0.339	**2.24**	**4.432**	**7.591**	**16.228**
58	6	91	192	372	700	1489
	17	258	544	1054	1984	4220
	25	380	800	1550	2918	6206
	35	532	1120	2170	4085	8688
	55	836	1759	3410	6419	13652

[49] Discounted sum from year 10 until infinity in present value.

4.6.1 Spatially explicit spread model[50]

The radial range expansion is commonly modeled by designating a single point (source) as the origin of the spread, with the spread progressively expanding based on the specified radial range expansion rate and time step (Robinet et al., 2012; Schneider et al., 2020; Wesseler & Fall, 2010). In this analysis, we created buffer zones around the polygon[51] representing the current extent of PWN distribution in Portugal (as of 2024, **Fig. A4.1**, area in orange). These buffer zones were calculated for each spread rate and time step to simulate the potential future extent of an uncontrolled outbreak.

Grid cells were deemed unsuitable for PWN infestation if they lacked pine trees or had a mean summer temperature (BIO10 variable) value below 19.4°C. In areas without pine trees, we assume that the pest can disperse through these cells, as their resolution is high enough (1 km²) not to restrict PWN movement. Similarly, in regions where climatic conditions are unfavorable for PWD expression, buffer zones may still extend into or overlap with these areas. However, such regions were excluded from the calculation of the affected area because their economic relevance is out of the scope of this analysis. In essence, even if buffer zones encompass climatically unsuitable regions or regions without pine trees, their contribution to the affected pine area remains zero.

The simulations were performed using the geographic information system software QGIS. Three time horizons were considered: 10, 20, and 30 years after 2024. Each simulation began with the current extent of PWN distribution across Portugal. The main advantage of the spatially explicit model lies in its ability to account for local heterogeneities, such as host tree distribution and climatic suitability.

4.6.2 Infested Area – spatially explicit spread model

The spread of PWD was simulated across three different time horizons: 10, 20, and 30 years. The total area of *Pinus spp.* affected by PWD was computed according to **Eq. 1**. The spatially explicit spread model accounts for heterogeneity with regard to the distribution of the pine hosts. The selected results are presented in **Table A4.7**.

[50] The purpose of this section is to provide additional insights on the resulting difference on the outcomes of the affected area, based on the selection of spread modeling approach. It was not used for the economic impact assessment.

[51] We used the polygon that represents the current extent of PWN distribution, instead of the initial point of introduction, as it reflects more accurately the process (personal communication with Kevin Schneider, JRC Sevilla).

Table A4.7. Total affected area with PWN for three different time horizons and three spread rate scenarios (best-case, 2.5th percentile, 0.34 km^2/year; moderate-case, 50th percentile, 4.43 km^2/year; worst-case, 97.5th percentile, 16.228 km^2/year), using the spatially implicit spread model. The value of the affected area represents the km^2 of infected pine tree species and is computed based on **Eq. 1**.

Time Horizon (years)	Spread Rate (km^2/year)	Affected pine area (km^2)
10	0.339	5460
10	4.432	7816
10	16.228	18734
20	0.339	5789
20	4.432	12723
20	16.228	30170
30	0.339	5948
30	4.432	16965
30	16.228	39952

The results above demonstrate a substantial variation in the affected area based on the spread rate and time horizon. After 10 years, the total affected area ranges from 5460 km^2 (best-case scenario; 2.5th percentile) to 18734 km^2 (worst-case scenario; 97.5th percentile). After 20 and 30 years of PWN spread, the affected area remains stable, not exceeding 6000 km^2, under the best-case scenario. However, considering the same time horizons, under the most likely spread scenario (50th percentile) and the worst-case scenario (97.5th percentile), the affected area surpasses 12000 km^2, and 30000 km^2, respectively.

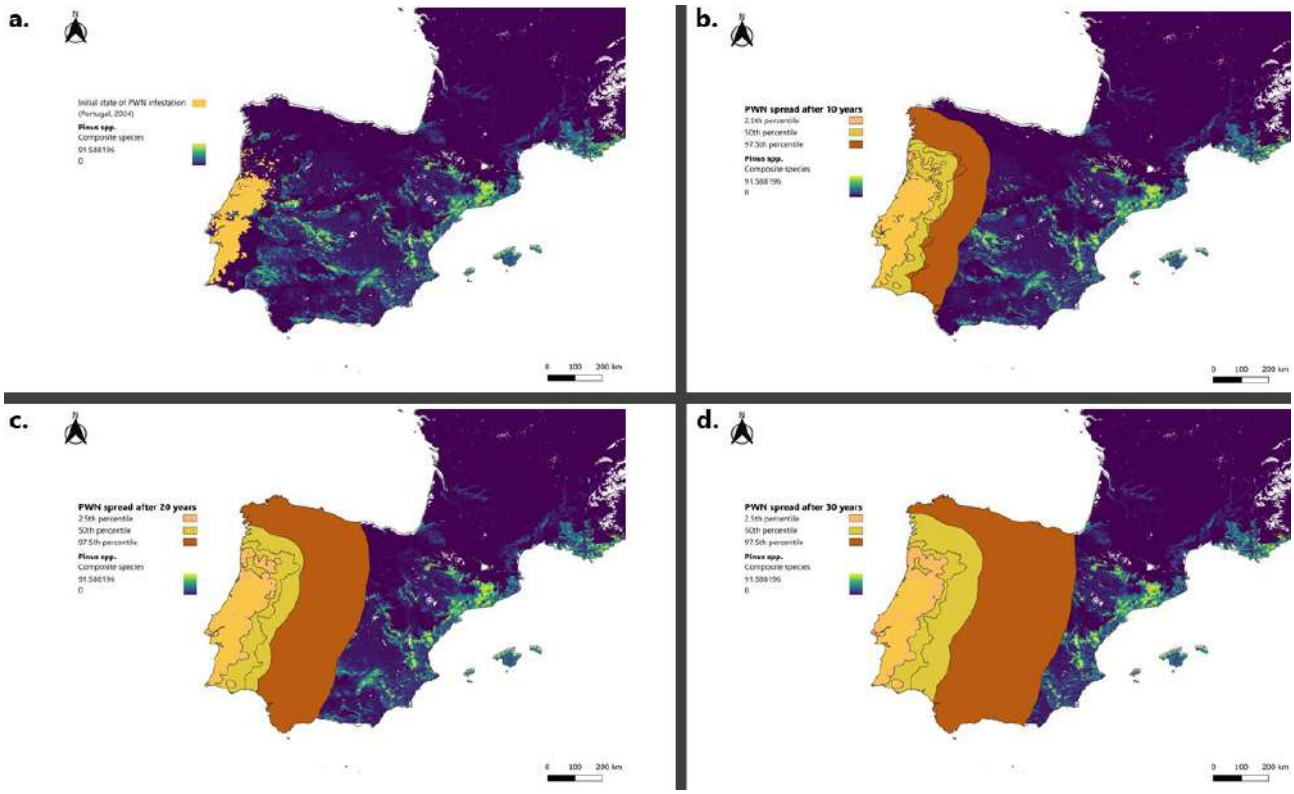

Figure A4.1. Projected PWN spread **(a.)** at the beginning of the simulation (2024) and **(b.)** 10, **(c.)** 20, and **(d.)** 30 years after the beginning of the simulation across the Iberian Peninsula under three spread rate scenarios. The spread starts from the current state of invasion in Portugal (2024). The map includes the *Pinus* spp. distribution within the zone where PWD can be expressed. Each buffer zone corresponds to a spread rate scenario.

Fig. A4.1 provides a visual representation of the projected spread of PWN across the Iberian Peninsula. Under the most likely spread scenario, given the current extent of the outbreak, Portugal will be almost fully affected under a no-control scenario. Also, most of the susceptible to PWD pine trees are located in Portugal and the south of Spain, explaining the disproportionate increase of the affected area: increasing at a decreasing rate when projecting PWN spread in the next 30 years.

4.6.3 Comparison: Affected area

Fig. A4.2 illustrates the differences in the affected area between the spatially implicit and spatially explicit spread models over 10, 20, and 30-year time horizons. The most interesting aspect of this comparison is the progression of the affected area over time. The spatially explicit spread model accounts for the spatial distribution of the hosts; there are more pine trees/unit area in Portugal (where the spread starts) and fewer in neighboring countries (Spain). This is reflected in the results since the affected area increases as the spread progresses but at a decreasing rate. In contrast, the spatially implicit spread model may overpredict the affected area, as a uniform spread and host distribution are assumed. This is evident as the gap between the two models widens, with the spatially implicit spread model indicating almost a twice larger affected area by year 30 compared to the spatially explicit spread model outcomes (97.5th percentile).

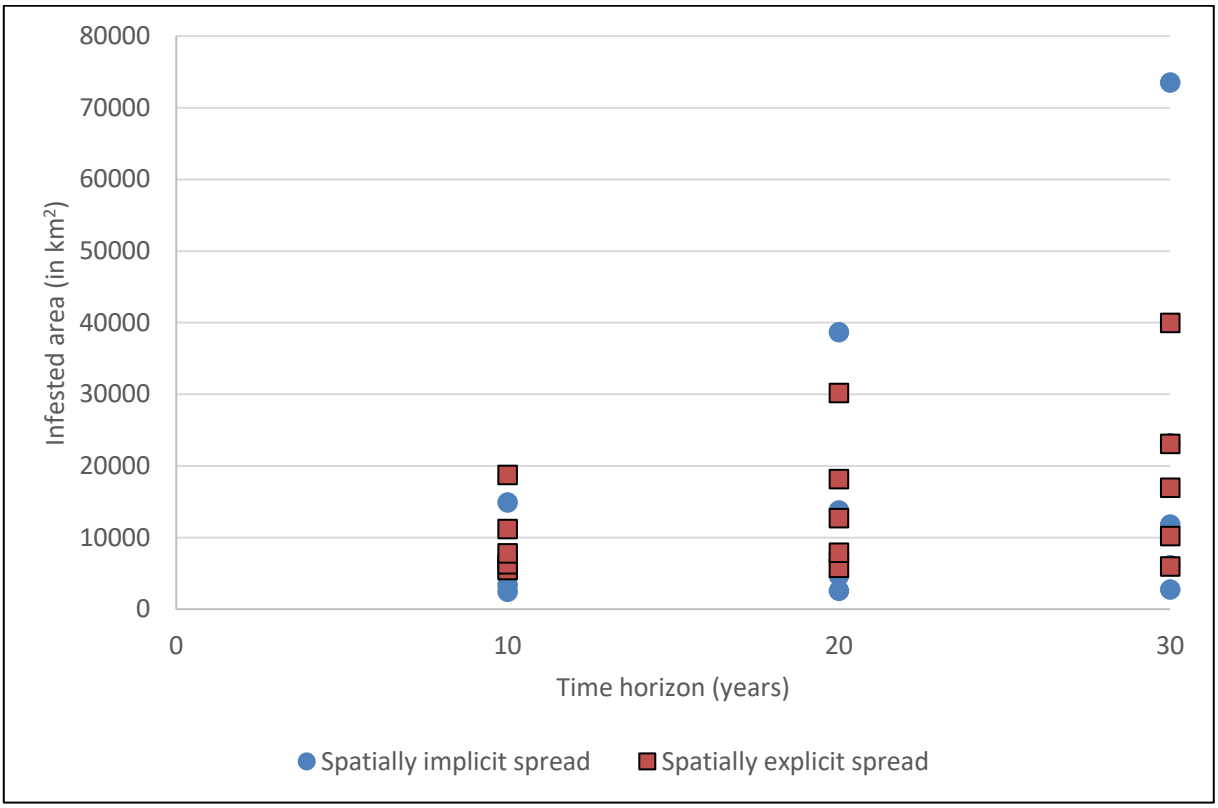

Figure A4.2. Comparative results of the PWN-affected area under the spatially implicit and spatially explicit spread models for the time horizons of 10, 20, and 30 years. The spatially implicit model (blue dots) assumes a uniform spread across the susceptible area, while the spatially explicit model (orange squares) accounts for local host and climatic heterogeneity.

The use of both the spatially explicit and spatially implicit spread models complements our analysis by providing a more comprehensive understanding of the potential spread and economic impact of PWN in Europe. While the spatially explicit model accounts for spatial host distribution, offering region-specific insights, the spatially implicit model provides an overview of the maximum spread and damage potential of PWN. In this report, we solely focused on the output of the spatially implicit model to proceed to the economic analysis, as it is more generic and reproducible.

5 THE POTENTIAL DIRECT ECONOMIC IMPACT OF *PHYTOPHTHORA RAMORUM* IN EUROPE

5.1 Background

The oomycete plant pathogen *Phytophthora ramorum* (PhR) was formally described by Werres et al. (2001) and it is categorized as an A1 Quarantine pest (Annex II A) and regulated non-quarantine pest (RNQP, Annex IV) in the EU and listed in the A2 list of EPPO. PhR is native to Japan, Vietnam, and most likely other East Asian regions (Jung et al., 2020, 2021). It is considered an invasive (alien) species in North America and Europe, and its first formal detection in these regions occurred in the mid-1990s (Rizzo et al., 2005; Webber, 2007; Werres et al., 2001). PhR is the causal agent of a lethal canker disease of oak and tanoak trees in California and Oregon, the so-called Sudden Oak Death (SOD), a lethal canker, needle and shoot blight disease of larch species and hybrids in Brittany, the UK, and Ireland, the so-called Sudden Larch Death (SLD), and twig or ramorum blight of various trees and woody ornamental nursery plant species (Brasier & Webber, 2010; Grünwald et al., 2008; Ivors et al., 2004; Jung et al., 2018; Rizzo et al. 2002). PhR has a self-sterile (heterothallic) mating system with two mating types (A1 and A2) and 12 distinct evolutionary lineages have so far been identified, that have been named after the world region where they were first detected: NA1 and NA2 (= North America), EU1 and EU2 (=Europe), IC1-IC5 (= Vietnam, Indochina) and NP1-NP3 (= Nippon, Japan) (Van Poucke et al., 2012; Jung et al., 2021). The NA1, NA2, IC2, IC3, NP2 and NP3 lineages are of A2 mating type, whereas the EU1, EU2, IC1, IC4 and NP1 lineages are of A1; the IC5 lineage seems to be sterile (Grünwald et al., 2009; Jung et al., 2021; Van Poucke et al., 2012). Moreover, the NA1 lineage is generally detected in native forests and nurseries of North America and has caused the most environmental damage, whereas the NA2 lineage is mostly limited to nurseries (Frankel & Palmieri, 2014; Grünwald et al., 2012a). In contrast, the EU1 lineage is mostly found across Europe, with some exceptions in US nurseries and watercourses, while the EU2 lineage is currently limited to Ireland and a small area in Western Scotland where it is associated with SLD (Grünwald et al., 2012a; King et al., 2015; Van Poucke et al., 2012). The IC1-IC5 and NP1-NP3 lineages occur naturally in the laurosilva forests of Vietnam and Japan, respectively, where they do not cause apparent disease symptoms due to long-term coevolution with the native flora (Jung et al., 2021).
The imminent risk posed by PhR to European plant biosecurity led to the European Commission's decision 2002/757/EC *"on provisional emergency phytosanitary measures to prevent the introduction into and the spread within the Community of Phytophthora ramorum Werres, De Cock & Man in 't Veldsp. nov."* (EC, 2022), followed by subsequent amendments (2004/426/EC, 2007/201/EC, 2013/782/EU, and 2016/1967 EU). This decision mandated annual surveys of nurseries and natural environment to determine the status of PhR in each Member State. Although it is no longer in force (date of end of validity: 10/04/2022), it was repealed by Regulation (EU) 2021/2285 (EC, 2021). This piece of legislation puts in place certain requirements and prohibitions regarding the introduction and movement of plants, plant products, and other objects within the European Union, as well as emergency measures for specific species, including PhR.

5.1.1 Host range and determination of impacts

PhR is a generalist plant pathogen, which is present both in forest ecosystems and the nursery industry (Grünwald et al., 2012b). The pathogen has a wide range of host plants, comprising more than 170 plant species, distributed across forests, urban landscapes (e.g., gardens, parks, etc.), and nurseries (EPPO, 2024; Harris et al., 2021). Infestations of PhR in commercial nurseries and landscaped settings can be managed with conventional control methods (Tjosvold et al., 2005). In contrast, the scale and intensity of outbreaks in natural ecosystems render management efforts

largely unfeasible (Cunniffe et al., 2016). Since its introduction to North America and Europe, PhR is associated with millions of oak (*Quercus spp.*) and tanoak (*Notholithocarpus densiflorus*) deaths in North America, as well as tens of thousands of hectares of larch plantations (*Larix kaempferi, Larix decidua*, *Larix* × *marchinsii*) in the UK, Ireland, and France (Brasier & Webber, 2010; Frankel & Palmieri, 2014; Ministère de l'Agriculture et de la Souveraineté alimentaire, 2017; O'Hanlon et al., 2018; Webber & Brasier, 2018). EPPO categorizes as "Major Host", based on a qualitative evaluation of their importance, the following species: *Kalmia latifolia* (mountain laurel), *L. decidua* (European larch), *L. kaempferi* (Japanese larch), *N. densiflorus* (tanoak), *Quercus agrifolia* (California/Coast live oak), *Rhododendron*, *Syringa vulgaris* (common lilac), *Viburnum* spp., and *Pieris* spp. (EPPO, 2024).

Depending on the host plant, PhR may cause various symptoms and affect different plant parts (Grünwald et al., 2008). On foliar hosts (e.g., California bay laurel, larch and *Rhododendron* species and hybrids, tanoak, etc.), the infection results in a blight of leaves (Ramorum leaf blight, non-lethal) and/or shoots (Ramorum Shoot Dieback) (Pintos et al., 2023). On canker hosts (e.g., oaks, tanoak, European beech, etc.), it leads to bleeding cankers on the stems and decline in sap flow and stem hydraulic conductivity, and eventually to rapid crown decline and tree death (SOD) (Collins et al., 2009). Noteworthy, both tanoak and larch species are unique cases in constituting both leaf and canker hosts (Grünwald et al., 2012a; Harris & Webber, 2016; Jung et al., 2018).

There are challenges in assessing the potential economic impact of PhR in quantitative terms since some hosts (e.g., *Quercus* spp*., N. densiflorus*) do not have a direct commercial value in some regions, especially in non-commercial forests in California, although they have large value due to the ecosystem services they provide (CABI et al., 2020). Direct economic impacts include the loss of resources due to tree mortality, decreased property values, increased fire damage, and expenses associated with the removal of dead trees. Indirect economic costs arise from policies implemented to manage the pathogen (e.g., nursery inspections, phytosanitary and quarantine measures).

Hall & Albers (2009) report for Oregon, within a 20-year time horizon, a range between US$21.3 to US$1238.5 million in expected costs to the forest products industry due to PhR based on assumed spread rates, increases in harvest costs, and the absence of any control program. Also, for Oregon, another report indicates harvest losses of US$100 million per year if eradication is unsuccessful and PhR spreads uncontrolled to the southwest of the state (Kliejunas, 2010). A study in California that included the discounted costs of treatment, removal, and reforestation in response to SOD infestation estimated US$7.5 million and property value losses of $135 million for 2010-2020 (Kovacs et al., 2011). A recent publication shows that the estimated costs in the UK are £4.2 million per year (Eschen et al., 2023). The authors of the same study report approximately £91.5 million in cost estimates due to PhR to the forestry sector in Great Britain, from 2010 to 2017, based on a report by the Forestry Commission; 5% of that amount was lost timber value, 15% management costs, and the remaining 80% indirect costs (Eschen et al., 2023). On the other hand, in Curry County of Oregon, the estimated costs for the nursery industry under a no-control scenario ranged from US$64.93 million to US$652.3 million for the 2009-2028 period (ENTRIX, 2008). Data from 32 nurseries in Washington suggested a mean loss per nursery of US$11,188 and 11,789 in 2004 and 2005, respectively (Dart et al., 2007).

5.1.2 Dispersal mechanisms / Spread

The host plants of PhR can be classified into three general epidemiological categories: hosts that transmit the pathogen but without lethal infection (e.g., California bay laurel *Umbellularia californica*), hosts that transmit and suffer lethal infections (e.g., tanoak *N. densiflorus*), and hosts

that do not transmit the pathogen[52] but undergo lethal infections (e.g., Coast live oak and California black oak, *Q. agrifolia* and *Quercus kelloggii*, respectively) (Cobb et al., 2020).
PhR spreads through four pathways for movement, as categorized by (Grünwald et al., 2012a):

1. Rain and wind
2. Rivers and streams
3. Human activities
4. Animals

More specifically, by releasing zoospores, PhR can colonize neighboring host plants via water splash, but it can also spread to host plants located at greater distances through wind, rain, rivers, and streams (Davidson et al., 2007; Grünwald et al., 2008). In California, rain-splash dispersal is reported to cover 5-10 meters from the inoculum source, while in Oregon, infections across the landscape reached up to 4 km via turbulent air currents (Davidson et al., 2005; Hansen et al., 2008). Stream monitoring using leaf baits reports that PhR dispersed 1-20 km downstream distance, although this pathway is considered a rare event (Grünwald et al., 2012a; Sutton et al., 2009). Human activities, such as human-mediated movement of infected plant material or soil, including national and international trade of plant consignments, contributed significantly to the spreading of the pathogen among natural and nursery environments in Western countries (Cushman & Meentemeyer, 2008). Another factor is the recreational activities in affected areas, which might play a role in the spread of spores via infected soil on vehicles, bike tires, and shoes (Davidson et al., 2007). Lastly, some vertebrates like deer, squirrels, and birds, as well as some invertebrates, such as snails, can serve as vectors, dispersing PhR through infected plant material and soil (Grünwald et al., 2012a).

5.1.3 Current global distribution

Recent research indicates that PhR's native range might be the Laurosilva forests between Indochina (Vietnam) and southwest Japan where 8 new lineages (IC1-IC5 and NP1-NP3) were detected (Jung et al., 2020, 2021). The pest is present in several states of North America and Canada, Argentina, Vietnam, and Japan (**Fig. 5.1**). In Europe[53], PhR is indicated as "present" in Belgium, Croatia, Denmark, France, Germany, Netherlands, Poland, Luxembourg, Ireland, Norway, Slovenia, and the United Kingdom (England, Northern Ireland, Scotland, Wales); "transient" in Finland; "absent" in Austria, Estonia, Portugal, Latvia, and Lithuania and as "absent, pest eradicated" in Czech Republic, Greece, Italy, Serbia, Slovakia, Spain, Sweden, and Switzerland (EPPO, 2024) (**Table A5.1**). However, in Portugal, it was recently reported from a natural stream from which it cannot be eradicated (Horta Jung et al., 2025).

[52] In the case of these "dead-end" host species, PhR infects only the bark—where conditions do not permit sporulation—and fails to induce lesions on the leaves that would support sporangia formation, thereby limiting the pathogen's capacity for further spread.

[53] We did not make any assumptions on the current extent of PhR infestation in Europe since the most available occurrence records are based on observations in *Rhododendron*, a nursery plant. The presence of PhR in nurseries does not provide sufficient information to approximate the % of infested areas, as this report focuses on forestry host species.

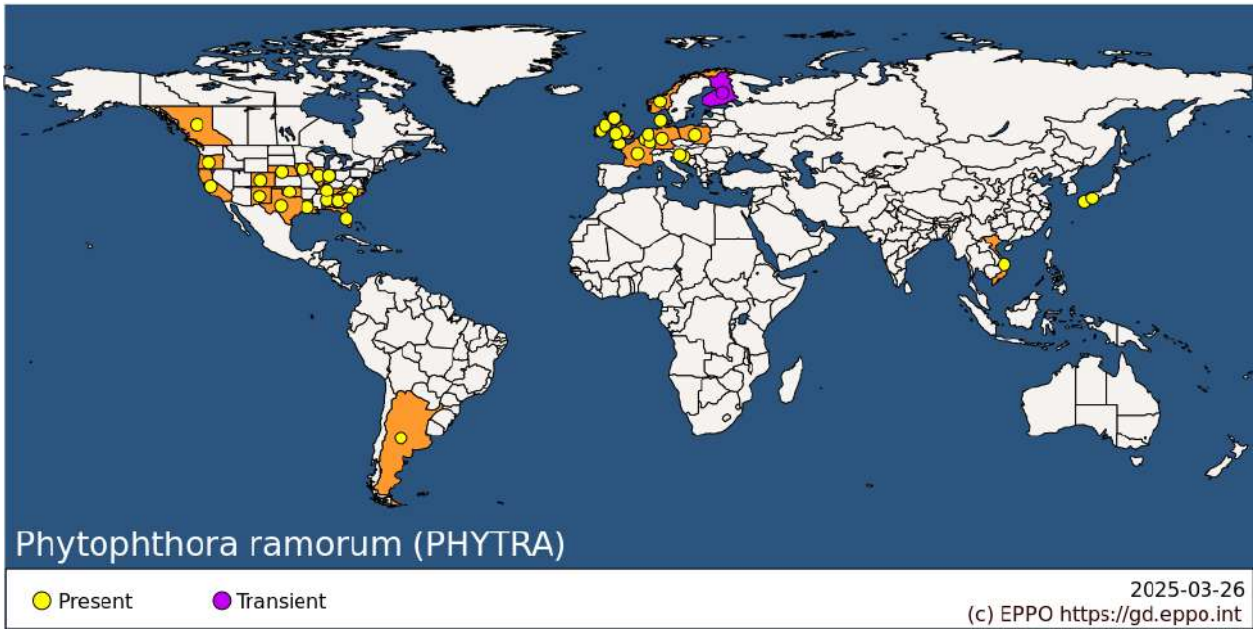

Figure 5.1. Current global distribution of *Phytophthora ramorum*. Source: EPPO Global Database

5.2 Data, Methodology, and Assumptions

5.2.1 Overview

In this analysis, we integrated several types of information. Initially, we utilized the CLIMEX niche model (Kriticos et al., 2015) to identify regions in Europe climatically suitable for the potential distribution of PhR, as well as regions where the climate allows for disease expression. Subsequently, spatial data on primary host species—*Larix* spp. and *Fagus* spp.— and secondary sporulating leaf host species, essential for the infection of *Fagus sylvatica,* namely *Pseudotsuga menziesii*, *Fraxinus excelsior*, *Castanea sativa*, *Larix* spp., and *Rhododendron ponticum,* were combined to create composite maps representing the area under risk. This allowed us to refine the potential area at risk by explicitly accounting for host co-occurrence, a crucial prerequisite for disease development in beech. Finally, these spatial outputs were used as input to quantify the potential direct economic damages caused by PhR under current climatic conditions and varying mortality and spread rate scenarios.

5.2.2 Potential distribution and disease expression in Europe

The starting point of the analysis was to identify the areas where climatic conditions are favorable for the persistent establishment of PhR. While a variety of factors can influence a species' geographic range, climate plays a key role (Andrewartha & Birch, 1954; Woodward, 1987). Although climate is not the only defining factor, it is quantifiable and, hence, serves as a practical starting point for estimating the potential geographical distribution of a species (Kriticos et al., 2015). We used the CLIMEX climate-based niche model to estimate the potential geographical distribution of PhR. CLIMEX integrates a series of growth and stress functions with meteorological data to calculate an annual index of climatic suitability, the Ecoclimatic Index (EI) (Kriticos et al., 2015). The EI ranges from 0, indicating unsuitable conditions, to a theoretical maximum of 100, representing climatically optimal conditions year-round. For visualization purposes, the EI is categorized, after (Ireland et al. (2013), into four classes to map the species'

potential geographic distribution in QGIS: marginal (1 < EI ≤ 5), moderate (5 < EI ≤ 15), suitable (15 < EI ≤ 26), and optimal (EI > 26) **(Fig. 5.2)**.
More specifically, we used the "Compare Locations (1 species)" function in CLIMEX version 4.1.1.0 (Kriticos et al., 2015) and 30-year averaged climatic data centered on 1995 (CliMond CM_TC10 World v1, *unpublished*, provided after personal communication with Darren J. Kriticos). This dataset, interpolated at a 10-arc minute resolution, includes daily minimum and maximum temperatures (°C), monthly precipitation (mm), and relative humidity (%) recorded at 9:00 and 15:00 hours.
In their original study, Ireland et al. (2013) used the CliMond CM10 World (1975H V1.1) climate dataset, which is centered on 1975 (1961–1990) and consists of fewer locations (565801) compared to the updated climatology we used (808020 locations). An updated climate dataset centered closer to the present has increased the accuracy of projections compared to its older counterpart, especially in the context of ongoing climate change.

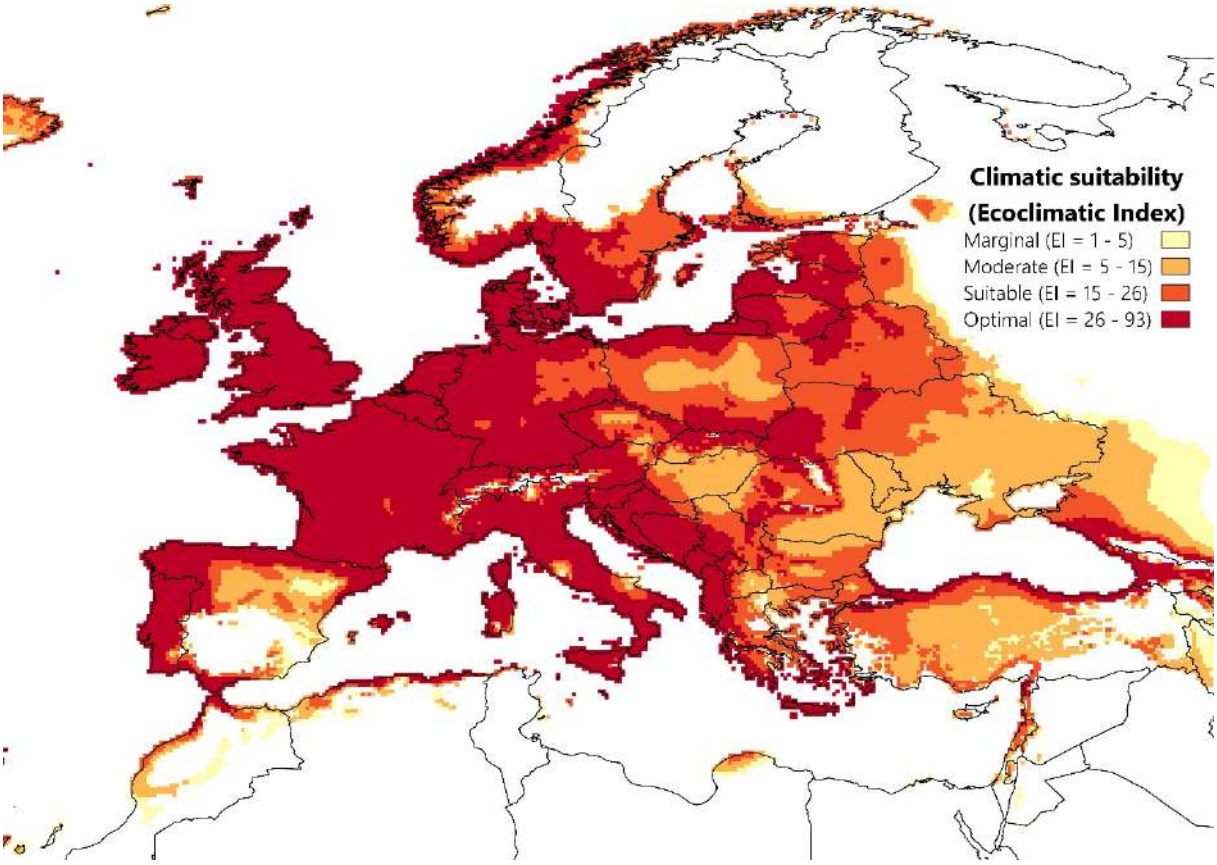

Figure 5.2. Modeled climate suitability (CLIMEX Ecoclimatic Index) for *Phytophthora ramorum* under current climatic conditions in Europe based on original model parameters from Ireland et al. (2013). The areas where EI=0 are white and are classified as unsuitable for PhR establishment. The figure was created with QGIS Desktop version 3.40.2 (https://www.qgis.org/).

Fig. 5.2 illustrates the regions in Europe where climatic conditions are favorable for PhR presence (EI>0). We then calculated the proportion of the climatically suitable area for PhR presence to the total country area.
Table 5.1 shows the suitable area of each country for PhR population persistence based on the CLIMEX model for PhR by Ireland et al. (2013). The total area of the countries considered in the

present analysis is 4.8 million km^{2,} and 78% of that area – equivalent to 3.7 million km^2 – is prone to PhR infestation. According to the results, most countries are largely or entirely suitable for PhR establishment, with over 85% of their total area falling within the EI>0 range, reflecting favorable conditions. Exceptions include the Nordic countries (Finland, Norway, Sweden) and Spain, which have a lower proportion of their total land classified as suitable for PhR population persistence.

Table 5.1. Country total area and proportion of suitable area to *Phytophthora ramorum* infestation in Europe based on Ireland et al. (2013) CLIMEX parameter values.

Country	Country total area[54] (km²)	Country area suitable (%)	Country area suitable (km²)
Austria	83878	89	74651
Belgium	30667	100	30667
Bulgaria	110996	100	110996
Croatia	56594	100	56594
Czech Republic	78871	100	78871
Denmark	42925	100	42925
Estonia	45336	100	45336
Finland	338411	8	27073
France	638475	88	561858
Germany	357569	100	357569
Greece	131694	92	121158
Hungary	93012	100	93012
Ireland	69947	100	69947
Italy	302079	97	293017
Latvia	64586	100	64586
Lithuania	65284	100	65284
Luxembourg	2595	100	2595
Malta	316	100	316
Netherlands	37378	99	37004
Norway	385207	38	146379
Poland	311928	100	311928
Portugal	92227	98	90382
Romania	238398	97	231246
Slovakia	49035	100	49035
Slovenia	20273	100	20273
Spain	505983	71	359248
Switzerland	41285	100	41285
Sweden	447424	38	170021
United Kingdom	243610	100	243610
Total	4885983	78	3796867

As stated above, **Fig. 5.2** represents the potential climatic suitability of Europe for PhR as initially modeled by Ireland et al. (2013), meaning this map illustrates all areas where the pathogen could theoretically persist based solely on climatic conditions (EI > 0). However, pathogen persistence or survival does not necessarily imply disease expression and therefore, considerable economic impact. In the case of PhR, aerial spread of sporangia, infection and symptom expression is

[54] Source: EUROSTAT (2024) Area by NUTS 3 region

influenced by more stringent climatic conditions than those required for basic pathogen persistence. The original model parameters are overly inclusive for our purposes, as they do not specifically address zones where substantial tree mortality and economic damage due to PhR infections might be expected. Hence, we refined the original CLIMEX parameter values proposed by Ireland et al. (2013) to limit the model output to areas with climatic conditions conducive to the aerial spread of sporangia, infection, and disease expression. The original and the refined parameter values are presented in **Table A5.2**. Then, we applied a threshold of EI ≥ 26 to the refined CLIMEX model output. This cut-off point corresponds to EI values classified as optimal by Ireland et al. (2013).

To simplify the analysis, we converted the continuous resulting EI output into a binary layer, with all distinctions between the different climatic suitability classes disregarded. All cells with EI ≥ 26 were assigned a value of 1 (disease expression/tree mortality), and all others were set to 0. The resulting binary suitability layer is shown in **Fig. 5.3**. Compared to **Fig. 5.2**, **Fig. 5.3** is more restrictive and focuses only on zones of expected direct economic relevance.

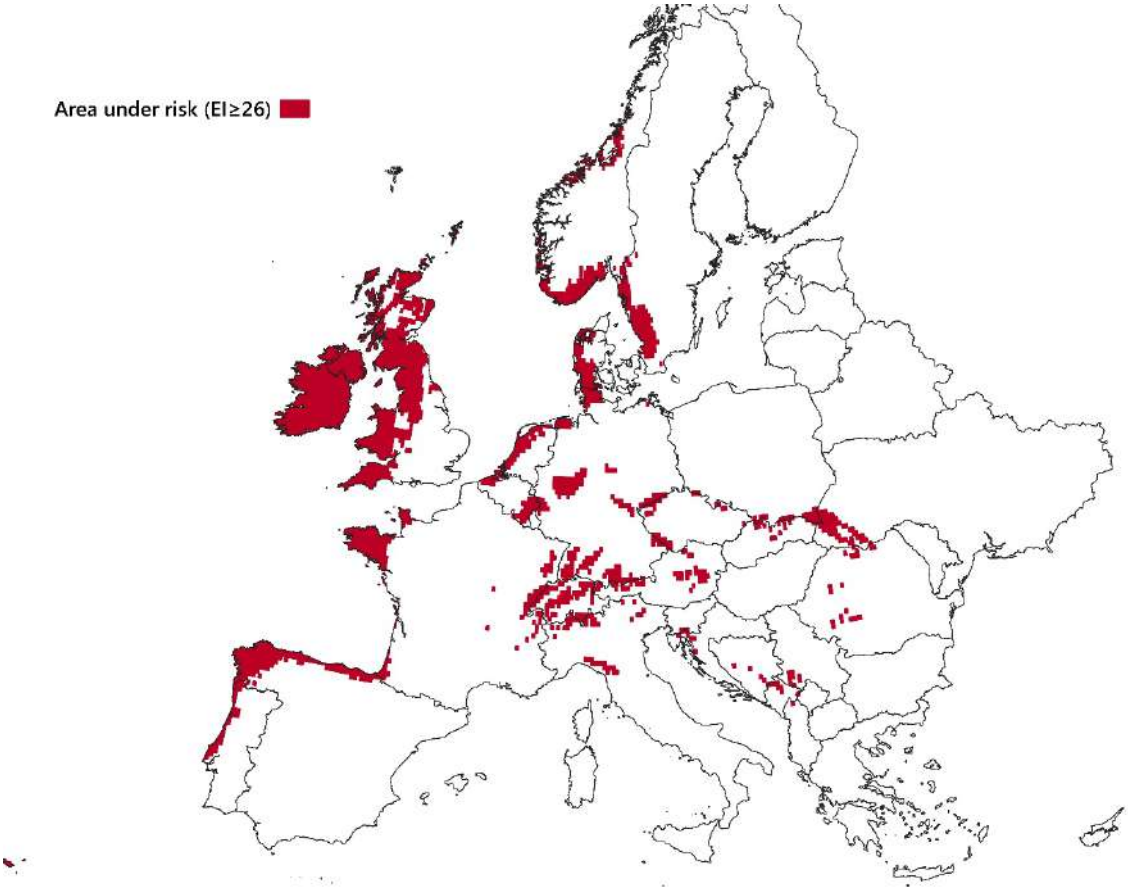

Figure 5.3. Binary climatic suitability map for *Phytophthora ramorum* in Europe based on refined CLIMEX parameter values and an Ecoclimatic Index threshold of EI ≥ 26. This threshold highlights areas with optimal conditions for pathogen spread, infection, and disease expression, where symptomatic infections and tree mortality are expected to occur. The figure was created with QGIS Desktop version 3.40.2 (https://www.qgis.org/).

By excluding marginally suitable areas, the analysis focuses exclusively on regions where PhR is likely to cause mortality, thereby improving the accuracy and relevance of economic impact estimates.

5.2.3 Host availability

The present analysis focuses on the potential direct economic impact of PhR on forestry, specifically targeting larch and beech trees, two ecologically and economically important tree species for Europe.
Larch is a fast-growing conifer known for its adaptability and tannin- and resin-rich, durable wood (Praciak, 2013). Besides other usages, its timber is sought for carpentry, naval construction, traditional wooden houses in mountain areas, furniture, floors, and many weatherproof outdoor objects (da Ronch et al., 2016). Similarly, European beech is recognized as one of the most "successful Central European plant species", sometimes forming pure stands, with approximately 250 documented usages (Houston et al., 2016; Leuschner et al., 2006). It is widely planted and distributed across Central, Western, and Southern Europe, and it is increasingly promoted for reforestation of hilly and mountainous regions (Chalupa, 1996). Beech timber is highly valued for its strength, hardness combined with water-resistance, and flexibility. These properties render it particularly suitable for diverse applications, including boatbuilding, furniture, musical instruments, panels, and plywood (Houston et al., 2016).

5.2.3.1 Data on tree hosts, leaf hosts, and host area estimation

Data on the spatial distribution of larch and beech across Europe were obtained from the European Forest Institute (EFI). The tree species maps are provided in 1 km^2 resolution, and each grid cell has a value, ranging from 0 to 100, representing the predicted proportion of the species' presence within the grid cell. We used two raster layers, entitled "*Larix* spp.*"* and *"Fagus* spp.", as provided by EFI (**Fig. 4**). All the data layers used in this analysis were projected in EPSG:3035 – ETRS89-extended / LAEA Europe Coordinate Reference System.
The genus-level representation of these datasets captures the most relevant host species of PhR in European forests. In the case of beech, *F. sylvatica* is the dominant species across Europe and is fully represented within the *Fagus* spp. layer, while other minor species such as *F. orientalis* may also be included. Similarly, the *Larix* spp. layer encompasses the main European larch species, such as *L. decidua* and *L. kaempferi*.
The total area of each host layer was computed using the following equation:

$$Land\ covered\ by\ host\ trees\ (km^2) = \sum_{i=1}^{n} \left(\frac{Predicted\ Proportion}{100} \right) \quad (1)$$

Eq. 1 describes the method used to calculate the total land covered by host trees within the area of interest by summing the proportion values across all relevant *n* grid cells. Each proportion value was divided by 100 to convert percentages into fractional areas. For example, a cell with a predicted proportion of 45% was calculated as covering 0.45 km². Subsequently, the "Zonal Statistics" function of QGIS was used to assign the area of host trees within each country.

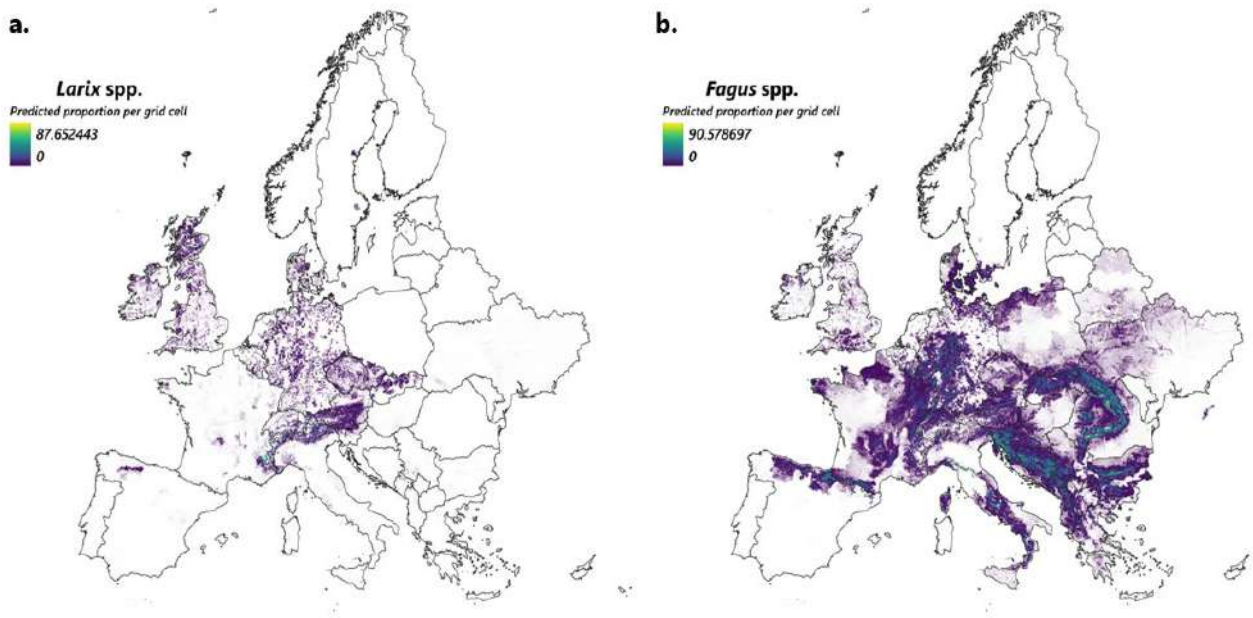

Figure 5.4. Predicted proportion/distribution of **(a.)** *Larix* spp. and **(b.)** *Fagus* spp. across the European continent. Each grid cell has a 1 x 1 km^2 resolution. The figure was created with QGIS Desktop version 3.40.2 (https://www.qgis.org/).

Fig. 5.4 shows the predicted distribution of *Larix* spp. and *Fagus* spp. according to the data by EFI. Notably, larch trees are mainly concentrated in Central Europe and the UK, whereas beech forests are distributed across most parts of Europe.

Table 5.2. Total and proportional area of *Larix* spp. and *Fagus* spp. within each country as computed using data from the European Forest Institute (Brus et al., 2012).

Country	*Larix* spp. total area (km^2)	*Larix* spp. proportional area (%)	*Fagus* spp. total area (km^2)	*Fagus* spp. proportional area (%)
Austria	2027	2.4	3748	4.5
Belgium	162	0.5	765	2.5
Bulgaria	9	0.0	7487	6.7
Croatia	0		4415	7.8
Cyprus[55]				
Czech Republic	1009	1.3	1583	2.0
Denmark	278	0.6	1148	2.7
Estonia	8	0.0	0	
Finland	0		0	
France	1239	0.2	13482	2.1
Germany	3021	0.8	16224	4.5
Greece	3	0.0	1714	1.3
Hungary	18	0.0	1055	1.1
Ireland	304	0.4	154	0.2
Italy	2795	0.9	8003	2.6
Latvia	7	0.0	2	0.0
Lithuania	0		2	0.0
Luxembourg	1	0.0	203	7.8
Malta				
Netherlands	187	0.5	131	0.4
Norway	0		10	0.0
Poland	21	0.0	3369	1.1
Portugal	0		0	
Romania	3	0.0	17130	7.2
Slovakia	410	0.8	4091	8.3
Slovenia	119	0.6	4043	19.9
Spain	150	0.0	4085	0.8
Switzerland	717	1.7	638	5.1
Sweden	151	0.0	2108	0.1
United Kingdom	2285	0.9	1011	0.4
Total	14926		96599	

Table 5.2 summarizes the area of each host species considered in this analysis by country. Among the countries analyzed, Germany, Italy, Austria, and the United Kingdom host the largest areas of larch trees, ranging approximately from 2027 km^2 in Austria to 3021 km^2 in Germany. In contrast, countries such as Bulgaria, Croatia, Finland, Greece, Latvia, Lithuania, Luxembourg, Norway,

[55] The EFI dataset does not provide coverage for Cyprus and Malta.

Portugal, and Romania have either very few larch forests (< 10 km^2) or none. In the case of beech trees, Romania has the largest area with approximately 17130 km^2 followed by Germany, France, and Italy with beech areas of 16224, 13482 and 8003 km^2, respectively. Countries such as Estonia, Finland, Latvia, Lithuania, Norway, and Portugal have the smallest beech forest areas or none, according to the EFI data. The total estimated areas for larch and beech across the study area are approximately 15000 and 95600 km^2, respectively.

It should be noted that both larch and beech are extremely susceptible to PhR[56]. However, their disease etiology has significant differences. In larch, the needles and the bark are highly susceptible to PhR infections, i.e., it serves as both a leaf and bark canker host. In contrast, European beech is not a leaf host and requires for stem canker development close proximity of susceptible leaf hosts producing and dispersing high sporangial inoculum (ANSES opinion Collective expert appraisal report, 2018). More specifically, based on the ANSES report (2018), three *Larix* species (*L. kaempferi, L. decidua, L.* × *eurolepis*) are classified at the top of vulnerability and competence. Beech appears as highly vulnerable and with low or insignificant competence, which means that it might not contribute to disease spread but it can be infected if there is a dense understory of sporulating leaf hosts around it. Examples of such highly competent leaf hosts that allow the production and dispersal of sporangia that may infect bark tissues are Common ash (*Fraxinus excelsior*), Douglas fir (*Pseudotsuga menziessi*), Sweet chestnut (*Castanea sativa*), *Rhododendron ponticum*, Holm oak (*Quercus ilex*), etc. as well as other PhR host trees such as larch (ANSES opinion Collective expert appraisal report, 2018; Sansford et al., 2009).

To identify areas where beech mortality due to PhR is plausible, we developed a composite binary raster map representing the distribution of relevant sporulating hosts, namely *P. menziesii*, *F. excelsior*, *C. sativa*, *R. ponticum,* and *Larix* spp. This composite layer was overlayed with the distribution map of beech, clipped to areas with an EI≥26 to isolate zones where favorable climatic conditions, host presence, and inoculum sources coincide.

Spatial data were obtained for three major foliar hosts of PhR, *P. menziesii*, *F. excelsior*, and *C. sativa*, for Europe from the Joint Research Centre (JRC) of the European Commission (de Rigo et al., 2016a, 2016b, 2016c). These maps provide the relative probability of a species' presence (RPP) per 1 km² grid cell (**Fig. 5.5**). The RPP values range from -1 (uncertain, no data) to 1 (very high presence) in each grid cell. According to (Beck et al., 2023) , an RPP threshold of **≥ 0.5** was applied to classify "medium-high" presence. Each resulting raster was converted to a binary format (1 = presence, 0 = absence).

[56]The concept of the susceptibility of a host species to a pest or pathogen consists of two components: vulnerability and competence. Vulnerability refers to a host species' ability to develop symptoms and damage after infection, while competence describes its ability to multiply and transmit the pathogen after infection by allowing sporulation (ANSES opinion Collective expert appraisal report, 2018; Johnson et al., 2013).

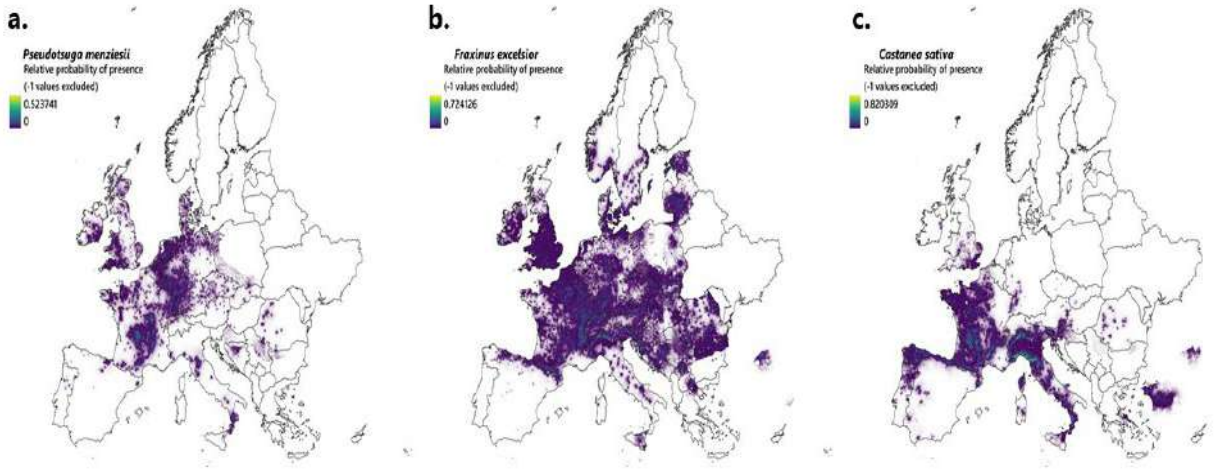

Figure 5.5. Relative probability of presence of **(a.)** Douglas fir (*P. menziessi*), **(b.)** Common ash (*F. excelsior*), and **(c.)** Sweet chestnut (*C. sativa*) in Europe. Values (-1 to 0) that represent uncertain or incomplete data were excluded. The figure was created with QGIS Desktop version 3.40.2 (https://www.qgis.org/).

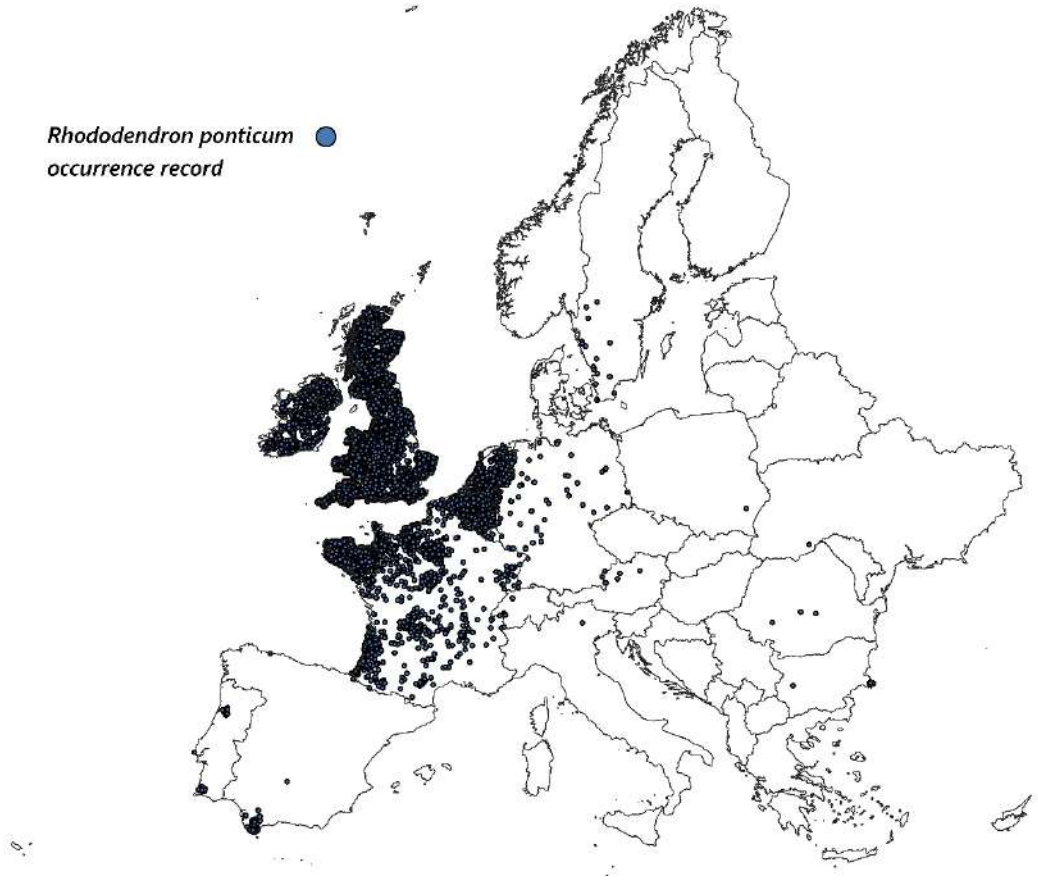

Figure 5.6. *Rhododendron ponticum* occurrence records across Europe. The figure was created with QGIS Desktop version 3.40.2 (https://www.qgis.org/).

Further, we gathered occurrence records[57] for *Rhododendrom ponticum* from the Global Biodiversity Information Facility (GBIF) (**Fig. 5.6**). *R. ponticum* has been identified as a principal foliar host contributing to the production of sporangia that subsequently infect the bark of nearby trees, including beech (DEFRA, 2008). The R code used for the GBIF data acquaintance and cleaning is provided in the **Appendix**. The cleaned presence points were rasterized and buffered to 1 km² resolution to match the other spatial layers. Lastly, the *Larix* spp. data layer from EFI was also converted to a binary layer using a presence threshold of >0, as larch trees and stands can also play a role in PhR transmission to neighbouring beech trees and stands. All resulting binary layers were combined using logical OR operations in QGIS to generate the final composite layer indicating the presence of at least one sporulating host species. This composite layer was then overlayed with the *Fagus* spp. raster (clipped to EI ≥ 26) to delineate areas where beech mortality is ecologically plausible.

5.2.4 Spread modeling

A key factor that heavily influences the potential direct damage costs of PhR is the pathogen's rate of spread. Meentemeyer et al. (2011) simulated the spread of SOD in California for the period 1990-2030, suggesting the typical range of the transmission parameters for short and long-scale dispersal are approximately 0-1 km and 100km, respectively. In their analysis, they used a value of 20.57 m for the scale parameter of short-distance dispersal and 9.5 km for the scale parameter of long-distance dispersal; these values were used to parameterize the dispersal kernel, representing the movement of inoculum over distance (Cunniffe et al., 2016). Hall & Albers (2009) selected 75 km/year[58], 37.5 km/year, and 19 km/year as potential spread rates for PhR under a no-control policy scenario in Oregon. The same study mentions a case where PWD spread from a single point to an area 26 km away within 8 years, corresponding to 3.7 km/year.
We model the affected area at year *t* using a radial range expansion spread model (Robinet et al., 2012; Schneider et al., 2020; Wesseler & Fall, 2010), as follows:

$$IA_t = \begin{cases} (rr \cdot t)^2 \cdot \pi & if IA_t < SA \\ SA & otherwise \end{cases} \quad (2)$$

Where $IA_{i,t}$ is the affected area (km^2) after t years from the beginning of the simulation, rr the radial range expansion rate (km/year), and π the mathematical constant. Further, $IA_{rr,t}$ is constrained by the total susceptible area SA, which represents the area where PhR can be established all year round and cause damage. Consequently, IA_t cannot exceed SA (km^2).
Eq. 2 ensures that IA_t does not exceed SA.
As the radius grows over time, the affected area expands quadratically, as per the geometric relation of the area of a circle. The model assumes that the spread extends at a constant rate over time and that the host trees are uniformly distributed. We solely consider the pathogen's natural dispersal, excluding potential pathways due to anthropogenic activities, such as trade. We chose three spread rates, following PhR maximum distances reported by Peterson et al. (2015) in North Chetco from 2001 to 2011 and in Borax from 2006 to 2011. More specifically, we set rr to 0.249 km/year (lowest reported max. distance), 2.0118 km/year (average value), and 4.261 km/year (highest reported max. distance).

[57] A distribution map with acceptable resolution was not available, so the occurrence record layer was rasterized and extrapolated at 1 km², and then overlayed with the other relevant data layers, as described in the text.
[58] Based on the average spread rate in California.

5.2.5 Determination of impacts – Mortality rates

The impact of PhR on tree mortality has been well documented in the case of SOD in California and Oregon. SOD resulted in 80% mortality of tanoaks in California, killing approximately 3200 ha of forest (Everhart et al., 2014; Rizzo et al., 2005). Furthermore, studies in tanoak forests of California and Oregon report mortality rates of up to 90% for above-ground biomass, while below-ground structures remained unaffected (Cobb et al., 2012, 2020).
Mortality rates vary among PhR's host tree species.
For larch trees, Chastagner et al. (2013) found no significant differences in mortality rates among the NA1, NA2, and EU1 PhR lineages, which ranged from 35% to 40%. Also, mortality rates across larch species (Western, Japanese, and European) due to PhR were reported to vary between 33.3% and 53.3%, confirming the susceptibility of these species. Based on the results by Dun (2021), most larch trees in a site experience complete mortality (>95%) 4 years after PhR infestation with symptoms including shoot and branch dieback. In the Saint-Cadou Forest of France, 27% of mature larch trees were affected by PhR in May 2017, and 42% by September of the same year, showing symptoms of wilting, yellowing/reddening needles, and branch mortality.
Based on the information above, we assume a delay in tree mortality between the initial year of PhR infestation and subsequent tree mortality, which is host tree-specific. Furthermore, we assume this delay to be linear, from the initial year of infestation until maximum mortality is reached[59]:

$$m_t = \begin{cases} m & if\ t \geq d_h \\ m \cdot \dfrac{t}{d_h} & if\ t < d_h \end{cases} \quad (3)$$

Where m_t is the annual percentage loss, m the maximum mortality rate, and d_h is the delay for each host (in years) until maximum mortality is reached.
In the case of *Fagus sylvatica*, the primary beech species in Europe, PhR is known to cause aerial bleeding cankers, especially when the trees are located near infected rhododendron stands (Jung et al., 2005; Sansford et al., 2009). Unfortunately, quantitative information on the mortality rates associated with PhR infection in beech is scarce. However, available qualitative assessments indicate that *F. sylvatica* exhibits "moderate to high" vulnerability to PhR, a level somewhat lower than that reported for larch species, which were classified as having "high" vulnerability (ANSES opinion Collective expert appraisal report, 2018). Similarly, based on wound inoculation trials, *F. sylvatica* was labeled as highly susceptible to PhR (Sansford et al., 2009).
Given these qualitative indications, we assume that *F. sylvatica* is less susceptible when compared to larch, and therefore, we assume a longer delay before reaching maximum mortality. More specifically, we set the delay at 4 years for larch, after Dun (2021), and at 6 years for beech. To ensure comparability across the selected host tree species and considering that our analysis is already limited to high-risk areas, we simulated a bandwidth of maximum mortality rates (10%, 30%, 50%, 70%, and 90%) common to both host species.

5.2.6 Direct economic impact

The direct economic impact of PhR was computed using a partial budgeting approach under a no-control scenario (Soliman et al., 2015; Wesseler & Fall, 2010). The direct economic impact is expressed in terms of the total loss in timber production volume, assuming that the standing stock

[59] An example of time to mortality due to PhR infestation of tanoak trees in California is presented by Cobb et al. (2012).

and timber price remain constant throughout the simulation period. The potential direct damage costs are calculated as:

$$DD_{h,t} = IA_{t,h} \cdot VT_h \cdot m_t \cdot p_h \quad (4)$$

Where,

$DD_{h,t}$: Direct damage costs (€) due to timber loss for each host h and after t years from the beginning of the simulation.

$IA_{t,h}$: Affected host area (km²) after t elapsed years for host h.

VT_h: Average timber volume (m³/km²) for each tree host species h, derived from the EFISCEN Inventory Database. For the present analysis, the values are:

- **Larch**: 23830 m³/km²
- **Beech**: 23047 m³/km².

These values were obtained by averaging timber volumes first at the country level and then across all countries (**Table A5.3**).

m_t: Mortality rate (%). We consider a series of mortality rates (10%, 30%, 50%, 70%, 90%) for both larch and beech trees, so the outcomes are comparable.

p_h: Average timber market price (€/m³)

- **Larch:** Equal to an average price was £50.7/m³, approximately €59.6/m³.[60] This price was derived from the National Statistics on Timber Price Indices by Forest Research using the softwood sawlog price in real terms for Great Britain (2012–2024) (**Table A5.4**).
- **Beech:** Equal to an average price of €74.3/m³. This price was based on roundwood log prices (UNECE/FAO) for Austria (1973–2021), the Czech Republic (2005–2019), Slovenia (2006–2022), and Switzerland (2000–2014). These average prices were €70.3/m³, CZK1626.3/m³ (approximately €63.1/m³)[61], €62.6/m³, and CHF107.3/m³ (approximately €101.2/m³)[62], respectively.

The total direct economic impact was discounted in order to account for the future economic losses to their present value. Thus, $DD_{h,t}$ is expressed in terms of present value PVD_h based on the following equation:

$$PVD_h = \frac{DD_{h,t}}{(1+r)^t} \quad (5)$$

Where PVD_h stands for the damage costs in present value due to PhR infestation. The denominator is the discount factor, where r is equal to 4.49%[63] and t the time step. **Eq. 5** assumes an infinite planning horizon and incorporates the transversality condition, which requires the present value of the state variables to converge to zero as the planning horizon recedes toward infinity. Acting as a boundary condition, the transversality condition ensures that the discounted economic impact of the pest decreases over time. This guarantees the economic feasibility of the analysis and reflects the practical assumption that distant future impacts contribute negligibly.

[60] Based on an average exchange rate of GBP 1 = EUR 1.1755 (for the period 24/01/2015 – 25/01/2025). Source: European Central Bank

[61] Based on an average exchange rate of CZK 1 = EUR 0.03882 (for the period 24/01/2015 – 25/01/2025). Source: European Central Bank

[62] Based on an average exchange rate of CHF 1 = EUR 0.9429 (for the period 24/01/2015 – 25/01/2025). Source: European Central Bank

[63] We use 4.49% as it is the average discount rate for the majority of Member States (Austria, Belgium, Cyprus, Germany, Estonia, Greece, Spain, Finland, France, Croatia, Ireland, Italy, Lithuania, Luxembourg, Latvia, Malta, the Netherlands, Portugal, Slovenia, and Slovakia) over the period 2023-2024. Source: Reference and discount rates (in %) since 01.08.1997, European Commission

The total discounted impact over an infinite time horizon was then used to compute the average annual cost (AAC_h) as follows:

$$AAC_h = r \cdot \sum_{t=1}^{\infty} PVD_h \quad (6)$$

$IA_{t,h}$ was calculated based on **Eq. 2**, assuming that the spread happens uniformly in all directions until the suitable area is fully occupied. A fundamental assumption of the "no-control" scenario is that the impact continues perpetually, reflecting a worst-case scenario where PhR infestation remains uncontrolled. This way, it provides a metric for average annualized costs.

5.3 Results

5.3.1 Area under risk

Table 5.3 presents the area of the considered PhR host species, *Larix* spp. and *Fagus* spp., per country, and the resulting area derived from their overlap with the layer representing the regions where climatic conditions allow for disease expression caused by PhR (EI≥26).
The total European area covered with larch trees is approximately 15000 km^{2,} with approximately 26% (3889 km^2) located within the modelled area under risk, where climate is optimal for disease expression (EI≥26). For beech species – mainly *Fagus sylvatica* in the context of Europe – the total area covered is approximately 96600 km^2, and about 13% (12991 km^2) falls within the EI≥26 regions. However, beech susceptibility to PhR greatly depends on the local presence of foliar hosts capable of allowing sporulation. Therefore, considering the co-occurrence of *Fagus* spp. with at least one of the considered hosts at 1x1 km resolution results in 9211 km^2 of beech trees under risk, or about 9.5% of the total European beech tree area.

Table 5.3. Total area of *Larix spp.* and *Fagus spp.* in Europe and their corresponding areas within climatically suitable zones for *Phytophthora ramorum* disease expression (EI ≥ 26). For *Fagus spp.*, the table provides area estimates considering the co-occurrence of relevant foliar hosts.

Country	*Larix* spp. area within EI≥26 (km^2)	Composite *Fagus* spp.-leaf host area within EI≥26 (km^2)[64]
Austria	652	336
Belgium	77	98
Bulgaria		
Croatia		
Cyprus		
Czech Republic	134	133
Denmark	42	8
Estonia		
Finland		
France	38	44
Germany	384	665
Greece		
Hungary		
Ireland	304	71
Italy	502	499
Latvia		
Lithuania		
Luxembourg		0
Malta		
Netherlands	3	3
Norway		0
Poland	6	18
Portugal		
Romania		
Slovakia	55	207
Slovenia		
Spain		2
Sweden		0
Switzerland	281	188
United Kingdom	1745	304
Total	4223	2577

[64] This column represents the resulting area derived by overlaying the *Fagus* spp. distribution layer with the distribution layers of the considered foliar hosts (*Pseudotsuga menziesii*, *Fraxinus excelsior*, *Castanea sativa*, *Larix spp.*, and *Rhododendron ponticum*) within the EI≥26 zone. The RPP threshold for the first three hosts listed was set to ≥0.5.

For the different countries, the host tree areas at risk after applying the eco-climatic constraints (**Table 5.3**) differ considerably from the total host tree areas (**Table 5.2**) with substantial variations between countries. More specifically, for *Larix* spp., the United Kingdom evidently hosts the largest larch tree area under risk, followed by Austria, Italy, and Germany, with 1745 km^2, 652 km^2, 502 km^2 and 384 km^2, respectively. For *Fagus* spp., while Romania (17130 km^2) and Germany (16224 km^2) host the largest beech area, the accounting for climatic conditions and foliar host presence substantially reduces the susceptible area to 665 km^2 and 0 km^2, respectively. Germany remains the country with the largest beech tree area at risk, followed by Italy (499 km^2), and Austria (336 km^2).

5.3.2 Direct economic impact – *Larix* spp.

Table 5.4 shows an example calculation of the potential direct damage costs in larch trees due to PhR spread until the full occupancy of the total suitable area. In this example, we assume a moderate scenario in terms of spread rate (2.0118 km/year), mortality rate (50%), 59.6 €/m^3 market prices of softwood sawlog, 23830 m^3/km^2, and 4.49% discount rate.

Table 5.4. Example calculation of potential direct damage costs due to PhR in Europe, assuming a spread rate of 2.0118 km/year, 50% yield loss, an average of 0.43% larch tree area on total land, 23830 m³/km^2 timber volume, and a softwood sawlog market price of 59.6 €/m³.

Elapsed years	Affected area (km^2)	Affected larch area (km^2)	Incremental larch area affected (km^2)	m_t (%)	Timber Loss (m^3)	Economic Loss (million €)	Discount Factor	Present Value of economic loss (million €)
0	0	0	0.0	0	0	0	1.000	0
1	356	2	1.5	13	4561	0.2	0.957	0.2
2	1424	6	4.6	25	27367	1.6	0.916	1.4
3	3204	14	7.7	38	68418	4.0	0.877	3.5
4	5696	24	10.7	50	127713	7.6	0.839	6.3
5	8901	38	13.8	50	164202	9.7	0.803	7.8
6	12817	55	16.8	50	200692	11.9	0.768	9.1
7	17445	75	19.9	50	237181	14.1	0.735	10.3
8	22785	98	23.0	50	273671	16.3	0.704	11.4
9	28838	124	26.0	50	310160	18.4	0.673	12.4
10	35602	153	29.1	50	346649	20.6	0.645	30.2[65]
Total								33.0

The results indicate that after 10 years of uncontrolled spread, assuming that there is no prior infestation[66] at year 0, PhR reaches a cumulative affected larch area of 29.1 km^2. The complete occupancy of the larch tree area under risk takes place by year 53 since the beginning of the

[65] Discounted sum from year 10 until infinity in present value.
[66] A substantial area of larch trees, particularly in the UK, is affected by PhR. However, accurately assessing the current extent and status of the infestation is challenging.

simulation[67], using this rather mild spread rate. The total discounted value of timber throughout the simulation period (infinity) is €33.0 million.

Table 5.5. Average annual direct damage costs in € million due to *Phytophthora ramorum* infestation in European larch trees, under different mortality and spread rate scenarios, for an average market price of timber (softwood sawlog) of €59.6/m^3.

Mortality rate (%)	Spread rate (km/year)		
	0.249	**2.0118**	**4.261**
10	0.2	6.6	13.1
30	0.5	19.8	39.2
50	0.8	33.1	65.3
70	1.1	46.3	91.4
90	1.4	59.5	117.5

Table 5.5 presents the average annual direct damage costs on larch trees due to PhR under various mortality and spread rate scenarios. The results suggest that damage costs increase substantially with higher spread and mortality rates. For example, at a mortality rate of 50%, the annual costs range from €0.8 million for a spread rate of 0.249 km/year to €65.3 million for a spread rate of 4.261 km/year. Similarly, at a spread rate of 2.0118 km/year, the costs rise from €6.6 million at 10% mortality to €59.5 million at 90% mortality. The combined effects of higher mortality and faster spread result in notable changes in the outcomes, with the best-case scenario reaching €0.2 million and the worst-case scenario €117.5 million annually.

5.3.3 Direct economic impact – *Fagus* spp.

The results for *Fagus* spp. follow a similar pattern as with larch, although they are notably larger. **Table 5.6** summarizes the potential direct damage costs under a scenario assuming a radial spread rate of 2.0118 km/year, a 50% yield loss, and an average beech timber volume of 23047 m³/km². The economic impact is calculated using a roundwood log market price of €74.31/m³.

[67] Not shown in the table.

Table 5.6. Example calculation of potential direct damage costs due to PhR in Europe, assuming a spread rate of 2.0118 km/year, 50% yield loss, an average of 3.19% beech tree area on total land, 23047 m³/km timber volume, and a roundwood log market price of €74.31 /m³.

Elapsed years	Affected area (km²)	Affected beech area (km²)	Incremental beech area affected (km²)	m_t (%)	Timber Loss (m³)	Economic Loss (million €)	Discount Factor	Present Value of economic loss (million €)
0	0	0	0.0	0	0	0	1.000	0
1	356	11	11.4	13	32723	2.4	0.957	2.3
2	1424	45	34.1	25	196337	14.5	0.916	13.3
3	3204	102	56.8	38	490843	36.4	0.877	31.9
4	5696	182	79.5	50	916240	68.0	0.839	57.1
5	8901	284	102.2	50	1178023	87.5	0.803	70.2
6	12817	409	124.9	50	1439806	106.9	0.768	82.2
7	17445	557	147.7	50	1701589	126.4	0.735	92.9
8	22785	727	170.4	50	1963372	145.8	0.704	102.6
9	28838	920	193.1	50	2225155	165.3	0.673	111.3
10	35602	1136	215.8	50	2486938	184.8	0.645	36.4[68]
Total								61.7

Again, assuming no prior infestation at year 0, the affected beech area grows from an initial 11 km² in year 1 to 1136 km² by year 10. The incremental beech area affected also increases progressively, reaching 215.8 km² in year 10. This leads to a timber loss of approximately 2.4 million m³. The total occupancy of the beech tree area under risk occurs after 16 years since the beginning of the simulation[69]. The economic loss in terms of present value totals €36.4 million from year 10 onwards, with a cumulative total of €62 million over the entire simulation period.

[68] Discounted sum from year 10 until infinity in present value.
[69] Not shown in the table.

Table 5.7. Average annual direct damage costs in € million due to *Phytophthora ramorum* infestation in European beech trees, under different mortality and spread rate scenarios, for an average market price of timber (roundwood logs) of 74.31 €/m^3.

Mortality rate (%)	Spread rate (km/year)		
	0.249	**2.0118**	**4.261**
10	1.3	12.4	14.5
30	3.9	37.1	43.6
50	6.6	61.8	72.7
70	9.2	86.5	101.8
90	11.8	111.2	130.9

Table 5.7 shows the average annual direct damage costs due to *Phytophthora ramorum* damage on beech trees in Europe under different mortality and spread rate scenarios. The calculations assume an average roundwood log market price of €73.41/m³. Again, the results reveal that economic losses increase both with higher mortality rates and faster spread rates. For instance, at a mortality rate of 50%, the average annual cost ranges from approximately €6.6 million for a spread rate of 0.249 km/year to €72.7 million for a spread rate of 4.261 km/year. In the best-case scenario, the annual damage costs are €1.3 million, whereas in the worst-case scenario, they reach up to €130.9 million. The most probable damage costs lie somewhere within that range.

5.4 References

[49] Andrewartha, H. G., & Birch, Charles. (1954). The distribution and abundance of animals. 782. https://books.google.com/books/about/The_Distribution_and_Abundance_of_Animal.html?id=3uzaAAAAMAAJ

[50] ANSES opinion Collective expert appraisal report. (2018). Host species in the context of control of Phytophthora ramorum. https://www.researchgate.net/publication/338478859_Host_species_in_the_context_of_control_of_Phytophthora_ramorum_ANSES_opinion_Collective_expert_appraisal_report_-Scientific_Edition

[51] Beck, P. S. A. ., Caudullo, Giovanni., Forzieri, Giovanni., Girardello, Marco., Houston Durrant, Tracy., Mauri, Achille., Strona, Giovanni., & San-Miguel-Ayanz, J. . (2023). Tree species distribution data and maps for Europe - 2nd edition. Publications Office of the European Union. https://doi.org/10.2760/602977

[52] Brasier, C., & Webber, J. (2010). Sudden larch death. Nature 2010 466:7308, 466(7308), 824–825. https://doi.org/10.1038/466824a

[53] Brus, D. J., Hengeveld, G. M., Walvoort, D. J. J., Goedhart, P. W., Heidema, A. H., Nabuurs, G. J., & Gunia, K. (2012). Statistical mapping of tree species over Europe. European Journal of Forest Research, 131(1), 145–157. https://doi.org/10.1007/S10342-011-0513-5/TABLES/6

[54] CABI, Garbelotto, M., & Frankel, S. J. (2020). Phytophthora ramorum (Sudden Oak Death (SOD)). CABI Compendium. https://doi.org/https://doi.org/10.1079/cabicompendium.40991

[55] Chalupa, V. (1996). Fagus sylvatica L. (European Beech). 138–154. https://doi.org/10.1007/978-3-662-10617-4_8

[56] Chastagner, G., Riley, K., & Elliott, M. (2013). Susceptibility of larch, hemlock, Sitka spruce, and Douglas-fir to Phytophthora ramorum. Proceedings of the Sudden Oak Death Fifth Science Symposium, 243, 77–79. https://research.fs.usda.gov/treesearch/44123

[57] Cobb, R. C., Filipe, J. A. N., Meentemeyer, R. K., Gilligan, C. A., & Rizzo, D. M. (2012). Ecosystem transformation by emerging infectious disease: loss of large tanoak from California forests. Journal of Ecology, 100(3), 712–722. https://doi.org/10.1111/J.1365-2745.2012.01960.X

[58] Cobb, R. C., Haas, S. E., Kruskamp, N., Dillon, W. W., Swiecki, T. J., Rizzo, D. M., Frankel, S. J., & Meentemeyer, R. K. (2020). The magnitude of regional-scale tree mortality caused by the invasive pathogen Phytophthora ramorum. Earth's Future, 8(7), e2020EF001500. https://doi.org/10.1029/2020EF001500

[59] Collins, B. R., Parke, J. L., Lachenbruch, B., & Hansen, E. M. (2009). The effects of Phytophthora ramorum infection on hydraulic conductivity and tylosis formation in tanoak sapwood. Canadian Journal of Forest Research, 39(9), 1766–1776. https://doi.org/10.1139/X09-097/ASSET/IMAGES/LARGE/X09-097F5.JPEG

[60] Cunniffe, N. J., Cobb, R. C., Meentemeyer, R. K., Rizzo, D. M., & Gilligan, C. A. (2016). Modeling when, where, and how to manage a forest epidemic, motivated by sudden oak death in California. Proceedings of the National Academy of Sciences of the United States of America, 113(20), 5640–5645. https://doi.org/10.1073/PNAS.1602153113/SUPPL_FILE/PNAS.1602153113.SM08.AVI

[61] Cushman, J. H., & Meentemeyer, R. K. (2008). Multi-scale patterns of human activity and the incidence of an exotic forest pathogen. Journal of Ecology, 96(4), 766–776. https://doi.org/10.1111/J.1365-2745.2008.01376.X

[62] da Ronch, F., Caudullo, G., Tinner, W., & de Rigo, D. (2016). Larix decidua and other larches in Europe: distribution, habitat, usage and threats. In J. San-Miguel-Ayanz, D. de Rigo, G. Caudullo, T. H. Durrant, & A. Mauri (Eds.), European Atlas of Forest Tree Species . Publication Office of the European Union.

[63] Dart, N. L., Associate, R., & Chastagner, G. A. (2007). Estimated economic losses associated with the destruction of plants due to Phytophthora ramorum quarantine efforts in Washington State. Plant Health Progress. https://doi.org/10.1094/PHP-2007-0508-02-RS

[64] Davidson, J. M., Wickland, A. C., Patterson, H. A., Falk, K. R., & Rizzo, D. M. (2005). Transmission of Phytophthora ramorum in mixed-evergreen forest in California. Phytopathology, 95(5), 587–596. https://doi.org/10.1094/PHYTO-95-0587

[65] De Rigo, D., Caudullo, G., & San Miguel-Ayanz, J. (2016a). Distribution map of Castanea sativa (2006, FISE, C-SMFAv0-3-2). European Commission, Joint Research Centre (JRC) [Dataset]. http://data.europa.eu/89h/4fb09324-9a61-4a90-bdce-48cb0e32b8cf

[66] De Rigo, D., Caudullo, G., & San Miguel-Ayanz, J. (2016b). Distribution map of Fraxinus excelsior (2006, FISE, C-SMFAv0-3-2). European Commission, Joint Research Centre (JRC) [Dataset]. http://data.europa.eu/89h/e6b00fa2-d2c4-431e-a891-0d2dac977605

[67] De Rigo, D., Caudullo, G., & San Miguel-Ayanz, J. (2016c). Distribution map of Pseudotsuga menziesii (2006, FISE, C-SMFAv0-3-2). European Commission, Joint Research Centre (JRC) [Dataset]. http://data.europa.eu/89h/a5907a79-530d-4ad3-b0b6-f1bca46107d4

[68] DEFRA. (2008). Phytophthora ramorum A Practical Guide for Established Parks & Gardens, Amenity Landscape and Woodland Areas. https://planthealthportal.defra.gov.uk/assets/factsheets/pramparks.pdf

[69] Dun, H. (2021). Understanding sudden larch death – from epidemiology to host resistance. PhD Thesis, University of Oxford. https://ora.ox.ac.uk/objects/uuid:20f29a72-771e-4ff4-86e5-0d924e9a1688

[70] EC. (2021, December 14). Commission Implementing Regulation (EU) 2021/2285 of 14 December 2021 amending Implementing Regulation (EU) 2019/2072 as regards the listing of pests, prohibitions and requirements for the introduction into, and movement within, the Union of plants, plant products

and other objects, and repealing Decisions 98/109/EC and 2002/757/EC and Implementing Regulations (EU) 2020/885 and (EU) 2020/1292. Official Journal of the European Union.

[71] EC. (2022, September 19). 2002/757/EC: Commission Decision of 19 September 2002 on provisional emergency phytosanitary measures to prevent the introduction into and the spread within the Community of Phytophthora ramorum Werres, De Cock & Man in 't Veld sp. nov. (notified under document number C(2002) 3380). Official Journal of the European Communities.

[72] ENTRIX. (2008). Economic Analysis for the Impact of Phytophthora ramorum on the Nursery Industry. https://www.oregon.gov/oda/shared/Documents/Publications/PlantHealth/SuddenOakDeathEconomicAnalysisORnurseries.pdf

[73] EPPO. (2024). Phytophthora ramorum. EPPO datasheets on pests recommended for regulation. https://gd.eppo.int/taxon/PHYTRA/datasheet

[74] Eschen, R., Kadzamira, M., Stutz, S., Ogunmodede, A., Djeddour, D., Shaw, R., Pratt, C., Varia, S., Constantine, K., & Williams, F. (2023). An updated assessment of the direct costs of invasive non-native species to the United Kingdom. Biological Invasions, 25(10), 3265–3276. https://doi.org/10.1007/S10530-023-03107-2/TABLES/5

[75] Everhart, S. E., Tabima, J. F., & Grünwald, N. J. (2014). Phytophthora ramorum. Genomics of Plant-Associated Fungi and Oomycetes: Dicot Pathogens, 159–174. https://doi.org/10.1007/978-3-662-44056-8_8/FIGURES/6

[76] Frankel, S. J., & Palmieri, K. M. (2014). Sudden Oak Death, Phytophthora ramorum: a persistent threat to oaks and other tree species. International Oaks No. 25. https://www.internationaloaksociety.org/content/sudden-oak-death-phytophthora-ramorum-persistent-threat-oaks-and-other-tree-species

[77] Grünwald, N. J., Garbelotto, M., Goss, E. M., Heungens, K., & Prospero, S. (2012a). Emergence of the sudden oak death pathogen Phytophthora ramorum. Trends in Microbiology, 20(3), 131–138. https://doi.org/10.1016/j.tim.2011.12.006

[78] Grünwald, N. J., Goss, E. M., Ivors, K., Garbelotto, M., Martin, F. N., Prospero, S., Hansen, E., Bonants, P. J. M., Hamelin, R. C., Chastagner, G., Werres, S., Rizzo, D. M., Abad, G., Beales, P., Bilodeau, G. J., Blomquist, C. L., Brasier, C., Brière, S. C., Chandelier, A., … Widmer, T. L. (2009). Standardizing the nomenclature for clonal lineages of the Sudden Oak Death pathogen, Phytophthora ramorum. Phytopathology, 99(7), 792–795. https://doi.org/10.1094/PHYTO-99-7-0792

[79] Grünwald, N. J., Goss, E. M., & Press, C. M. (2008). Phytophthora ramorum: a pathogen with a remarkably wide host range causing sudden oak death on oaks and ramorum blight on woody ornamentals. Molecular Plant Pathology, 9(6), 729–740. https://doi.org/10.1111/J.1364-3703.2008.00500.X

[80] Hall, K. M., & Albers, H. J. (2009). Economic Analysis for the Impact of Phytophthora ramorum on Oregon Forest Industries. Oregon State University.

[81] Hansen, E. M., Kanaskie, A., Prospero, S., McWilliams, M., Goheen, E. M., Osterbauer, N., Reeser, P., & Sutton, W. (2008). Epidemiology of Phytophthora ramorum in Oregon tanoak forests. Canadian Journal of Forest Research, 38(5), 1133–1143. https://doi.org/10.1139/X07-217/ASSET/IMAGES/X07-217T4H.GIF

[82] Harris, A. R. & Webber, J. F. (2016). Sporulation potential, symptom expression and detection of Phytophthora ramorum on larch needles and other foliar hosts. Plant Pathology, 65, 1441–1451. https://doi.org/10.1111/ppa.12538

[83] Harris, A. R., Brasier, C. M., Scanu, B., & Webber, J. F. (2021). Fitness characteristics of the European lineages of Phytophthora ramorum. Plant Pathology, 70(2), 275–286. https://doi.org/10.1111/PPA.13292

[84] Houston, D. T., de Rigo, D., & Caudullo, G. (2016). Fagus sylvatica in Europe: distribution, habitat, usage and threats. In J. San-Miguel-Ayanz, D. de Rigo, G. Caudullo, T. Houston Durrant, & A. Mauri

(Eds.), European Atlas of Forest Tree Species. Publications Office of the EU. https://forest.jrc.ec.europa.eu/en/european-atlas/atlas-download-page/

[85] Ireland, K. B., Hardy, G. E. S. J., & Kriticos, D. J. (2013). Combining Inferential and Deductive Approaches to estimate the potential geographical range of the invasive plant pathogen, Phytophthora ramorum. PLOS ONE, 8(5), e63508. https://doi.org/10.1371/JOURNAL.PONE.0063508

[86] Ivors, K. L., Hayden, K. J., Bonants, P. J. M., Rizzo, D. M., & Garbelotto, M. (2004). AFLP and phylogenetic analyses of North American and European populations of Phytophthora ramorum. Mycological Research, 108(4), 378–392. https://doi.org/10.1017/S0953756204009827

[87] Johnson, P. T. J., Preston, D. L., Hoverman, J. T., & Richgels, K. L. D. (2013). Biodiversity decreases disease through predictable changes in host community competence. Nature 494, 230–233. https://doi.org/10.1038/nature11883

[88] Jung, T., Hudler, G. W., Jensen-Tracy, S. L., Griffiths, H. M., Fleischmann, F., & Osswald, W. (2005). Involvement of Phytophthora species in the decline of European beech in Europe and the USA. Mycologist, 19(4), 159–166. https://doi.org/10.1017/S0269-915X(05)00405-2

[89] Jung, T., Pérez-Sierra, A., Durán, A., Horta Jung, M., Balci, Y., & Scanu, B. (2018). Canker and decline diseases caused by soil- and airborne Phytophthora species in forests and woodlands. Persoonia, 40, 182–220. https://doi.org/10.3767/persoonia.2018.40.08

[90] Jung, T., Jung, M. H., Webber, J. F., Kageyama, K., Hieno, A., Masuya, H., Uematsu, S., Pérez-Sierra, A., Harris, A. R., Forster, J., Rees, H., Scanu, B., Patra, S., Kudláček, T., Janoušek, J., Corcobado, T., Milenković, I., Nagy, Z., Csorba, I., … Brasier, C. M. (2021). The destructive tree pathogen Phytophthora ramorum originates from the laurosilva forests of East Asia. Journal of Fungi, 7(3), 226. https://doi.org/10.3390/JOF7030226

[91] Jung, T., Scanu, B., Brasier, C. M., Webber, J., Milenković, I., Corcobado, T., Tomšovský, M., Pánek, M., Bakonyi, J., Maia, C., Bačová, A., Raco, M., Rees, H., Pérez-Sierra, A., & Jung, M. H. (2020). A survey in natural forest ecosystems of Vietnam reveals high diversity of both new and described Phytophthora taxa including P. ramorum. Forests 11(1), 93. https://doi.org/10.3390/F11010093

[92] King, K. M., Harris, A. R., & Webber, J. F. (2015). In planta detection used to define the distribution of the European lineages of Phytophthora ramorum on larch (Larix) in the UK. Plant Pathology, 64(5), 1168–1175. https://doi.org/10.1111/PPA.12345

[93] Kliejunas, J. T. (2010). Sudden oak death and Phytophthora ramorum: a summary of the literature. USDA Forest Service, Pacific Southwest Research Station, General Technical Report PSW-GTR-234. https://doi.org/10.2737/PSW-GTR-234

[94] Kovacs, K., Václavík, T., Haight, R. G., Pang, A., Cunniffe, N. J., Gilligan, C. A., & Meentemeyer, R. K. (2011). Predicting the economic costs and property value losses attributed to sudden oak death damage in California (2010–2020). Journal of Environmental Management, 92(4), 1292–1302. https://doi.org/10.1016/J.JENVMAN.2010.12.018

[95] Kriticos, D., Maywald, G., Yonow, T., Zurcher, E., Herrmann, N., & Sutherst, R. (2015). CLIMEX. Version 4. Exploring the Effects of Climate on Plants, Animals and Diseases.

[96] Leuschner, C., Meier, I. C., & Hertel, D. (2006). On the niche breadth of Fagus sylvatica: soil nutrient status in 50 Central European beech stands on a broad range of bedrock types. Annals of Forest Science, 63(4), 355–368. https://doi.org/10.1051/FOREST:2006016

[97] Meentemeyer, R. K., Cunniffe, N. J., Cook, A. R., Filipe, J. A. N., Hunter, R. D., Rizzo, D. M., Gilligan, C. A., Cunniffe, N. J., Cook, A. R., Filipe, J. A. N., Hunter, R. D., Rizzo, D. M., & Gilligan, C. A. (2011). Epidemiological modeling of invasion in heterogeneous landscapes: spread of sudden oak death in California (1990–2030). Ecosphere, 2(2), 1–24. https://doi.org/10.1890/ES10-00192.1

[98] Ministère de l'Agriculture et de la Souveraineté alimentaire. (2017, July). Première observation de Phytophthora ramorum sur Mélèze en France. https://agriculture.gouv.fr/premiere-observation-de-phytophthora-ramorum-sur-meleze-en-france

[99] O'Hanlon, R., Choiseul, J., Brennan, J. M., & Grogan, H. (2018). Assessment of the eradication measures applied to Phytophthora ramorum in Irish Larix kaempferi forests. Forest Pathology, 48(1), e12389. https://doi.org/10.1111/EFP.12389

[100] Peterson, E. K., Hansen, E. M., & Kanaskie, A. (2015). Temporal epidemiology of sudden oak death in Oregon. Phytopathology, 105(7), 937–946. https://doi.org/10.1094/PHYTO-12-14-0348-FI/ASSET/IMAGES/LARGE/PHYTO-12-14-0348-FI_F6-1436787230979.JPEG

[101] Pintos, C., Rial, C., Piñón, P., Salinero, C., & Aguín, O. (2023). Occurrence of Phytophthora ramorum and other Phytophthora species on woody ornamentals in public gardens and parks in Northwestern Spain. Plant Health Progress, 24(1), 37–46. https://doi.org/10.1094/PHP-01-22-0008-RS/ASSET/IMAGES/LARGE/PHP-01-22-0008-RSF3.JPEG

[102] Praciak, A. (2013). The CABI encyclopedia of forest trees. In The CABI encyclopedia of forest trees. CABI. https://doi.org/10.1079/9781780642369.0000

[103] Rizzo, D.M., Garbelotto, M., Davidson, J.M., Slaughter, G. W., & Koike, S. T. (2002). Phytophthora ramorum as the cause of extensive mortality of Quercus spp. and Lithocarpus densiflorus in California. Plant Disease, 86, 205–214. https://doi.org/10.1094/PDIS.2002.86.3.205

[104] Rizzo, D. M., Garbelotto, M., & Hansen, E. M. (2005). Phytophthora ramorum: Integrative research and management of an emerging pathogen in California and Oregon forests. Annual Review of Phytopathology, 43, 309–335. https://doi.org/10.1146/ANNUREV.PHYTO.42.040803.140418/CITE/REFWORKS

[105] Robinet, C., Kehlenbeck, H., Kriticos, D. J., Baker, R. H. A., Battisti, A., Brunel, S., Dupin, M., Eyre, D., Faccoli, M., Ilieva, Z., Kenis, M., Knight, J., Reynaud, P., Yart, A., & van der Werf, W. (2012). A suite of models to support the quantitative assessment of spread in pest risk analysis. PLOS ONE, 7(10), e43366. https://doi.org/10.1371/JOURNAL.PONE.0043366

[106] Sansford, C., Inman, A., Baker, R., Frankel, S., de Gruyter, J., Husson, C., Kehlenbeck, H., Kessel, G., Moralejo, E., Steeghs, M., Webber, J., & Werres, S. (2009). Report on the risk of entry, establishment, spread and socio-economic loss and environmental impact and the appropriate level of management for Phytophthora ramorum for the EU. Deliverable Report 28. EU Sixth Framework Project RAPRA. http://rapra.csl.gov.uk/

[107] Schneider, K., van der Werf, W., Cendoya, M., Mourits, M., Navas-Cortés, J. A., Vicent, A., & Lansink, A. O. (2020). Impact of Xylella fastidiosa subspecies pauca in European olives. Proceedings of the National Academy of Sciences of the United States of America, 117(17), 9250–9259. https://doi.org/10.1073/PNAS.1912206117/-/DCSUPPLEMENTAL

[108] Soliman, T., Mourits, M. C. M., Oude Lansink, A. G. J. M., & van der Werf, W. (2015). Quantitative economic impact assessment of invasive plant pests: What does it require and when is it worth the effort? Crop Protection, 69, 9–17. https://doi.org/10.1016/j.cropro.2014.11.011

[109] Sutton, W., Hansen, E. M., Reeser, P. W., & Kanaskie, A. (2009). Stream monitoring for detection of Phytophthora ramorum in Oregon tanoak forests. Plant Disease, 93(11), 1182–1186. https://doi.org/10.1094/PDIS-93-11-1182

[110] Tjosvold, A., Buermeyer, S. A., Blomquist, K. R., & Tjosvold, S. A. (2005). Nursery Guide for Diseases Caused by Phytophthora ramorum on Ornamentals: Diagnosis and Management. Nursery Guide for Diseases Caused by Phytophthora Ramorum on Ornamentals: Diagnosis and Management. University of California, Division of Agricultural and Natural Resources, Publication 8156. https://doi.org/10.3733/UCANR.8156

[111] Van Poucke, K., Franceschini, S., Webber, J. F., Vercauteren, A., Turner, J. A., McCracken, A. R., Heungens, K., & Brasier, C. M. (2012). Discovery of a fourth evolutionary lineage of Phytophthora ramorum: EU2. Fungal Biology, 116(11), 1178–1191. https://doi.org/10.1016/J.FUNBIO.2012.09.003

[112] Webber, J. F. (2007, March). Status of Phytophthora ramorum and P. kernoviae in Europe. http://www.defra.gov.uk/planth/pramorum.htm

[113] Webber, J. F. & Brasier, C. M. (2018). Ramorum disease of larch. In: Hansen, E. M., Lewis, K. J. & Chastagner, G. A. (eds) Compendium of conifer diseases, second edition. The American Phytopathological Society, St. Paul, USA.
[114] Werres, S., Marwitz, R., Man In'T Veld, W. A., De Cock, A. W. A. M., Bonants, P. J. M., De Weerdt, M., Themann, K., Ilieva, E., & Baayen, R. P. (2001). Phytophthora ramorum sp. nov., a new pathogen on Rhododendron and Viburnum. Mycological Research, 105(10), 1155–1165. https://doi.org/10.1016/S0953-7562(08)61986-3
[115] Wesseler, J., & Fall, E. H. (2010). Potential damage costs of Diabrotica virgifera virgifera infestation in Europe – the 'no control' scenario. Journal of Applied Entomology, 134(5), 385–394. https://doi.org/10.1111/j.1439-0418.2010.01510.x
[116] Woodward, F. I. . (1987). Climate and plant distribution. Cambridge Studies in Ecology, 174 pp.

5.5 Acknowledgments

We thank Marco Pattaca from Wageningen University and Research for helping us obtain the market prices for roundwood logs (beech). We also thank our PurPest project partner, Thomas Jung, for his valuable guidance, constructive suggestions, and support throughout the analysis and preparation of this part of the report.

5.6 Appendix

Table A5.1. Distribution status of *Phytophthora ramorum* in Europe as classified by EPPO (last update: 26-03-2025)

Country	Year of first detection	Status	Link
Austria		Absent, confirmed by survey	Distribution details in Austria
Belgium	2002	Present, restricted distribution	Distribution details in Belgium
Bulgaria			
Croatia	2007	Present, restricted distribution	Distribution details in Croatia
Czech Republic	2003	Absent, pest eradicated	Distribution details in the Czech Republic
Denmark	2003	Present, few occurences	Distribution details in Denmark
Estonia	2010	Absent, confirmed by survey	Distribution details in Estonia
Finland	2004	Transient, under eradication	Distribution details in Finland
France	2002	Present, restricted distribution	Distribution details in France
Germany	2001	Present, few occurrences	Distribution details in Germany
Greece	2010	Absent, pest eradicated	Distribution details in Greece
Hungary			
Ireland	2002	Present, restricted distribution	Distribution details in Ireland
Italy	2004	Absent, pest eradicated	Distribution details in Italy
Latvia		Absent, intercepted only	Distribution details in Latvia
Lithuania	2007	Absent, intercepted only	Distribution details in Lithuania
Luxembourg	?	Present, no details	Distribution details in Luxembourg
Malta			

Netherlands	1993	Present, restricted distribution	Distribution details in the Netherlands
Norway	2003	Present, restricted distribution	Distribution details in Norway
Poland	2002	Present, few occurrences	Distribution details in Poland
Portugal	2006	Absent, confirmed by survey	Distribution details in Portugal
Romania			
Slovakia	2018	Absent, pest eradicated	Distribution details in Slovakia
Slovenia	2003	Present, restricted distribution	Distribution details in Slovenia
Spain	2002	Absent, pest eradicated	Distribution details in Spain
Sweden	2002	Absent, pest eradicated	Distribution details in Sweden
Switzerland	2004	Absent, pest eradicated	Distribution details in Switzerland
United Kingdom	2002	Present, restricted distribution	Distribution details in the United Kingdom

Table A5.2. CLIMEX model parameters for *Phytophthora ramorum* by Ireland et al. (2013) and the ones used in the current study. Parameter values without units are dimensionless indices of plant available soil moisture.

Parameters	Description	Unit	Ireland et al. (2013)	PurPest
DV0	Lower temperature threshold	°C	**0**	**7**
DV1	Lower optimal for growth	°C	**18**	**14**
DV2	Upper optimal for growth	°C	**22**	**17**
DV3	Upper temperature threshold	°C	**30**	**24**
SM0	Lower soil moisture threshold		**0.2**	**0.6**
SM1	Lower optimal soil moisture		**0.7**	**0.8**
SM2	Upper optimal soil moisture		**1.3**	**1.3**
SM3	Upper soil moisture threshold		**2**	**2**
TTCS	Cold stress temperature threshold	°C	**-8**	**-8**
THCS	Cold stress accumulation rate	$week^{-1}$	**-0.02**	**-0.02**
TTHS	Heat stress temperature threshold	°C	**31**	**25**
THHS	Heat stress accumulation rate	$week^{-1}$	**0.03**	**0.005**
SMDS	Soil moisture dry stress threshold		**0.2**	**0.2**
HDS	Dry stress accumulation rate	$week^{-1}$	**-0.005**	**-0.005**
SMWS	Soil moisture wet stress threshold		**2**	**2**
HWS	Wet stress accumulation rate	$week^{-1}$	**0.002**	**0.002**

Data cleaning R code for *Rhododendron ponticum* occurrence records (GBIF)

Occurrence records for *Rhododendron ponticum* were obtained from the Global Biodiversity Information Facility (GBIF) using the "rgbif" R package (version 4.3.3), referencing the GBIF taxon ID 7327990L. To ensure data quality, we implemented a cleaning process using the "CoordinateCleaner" (v3.0.1) and "dplyr" packages. The cleaning steps included the removal of records lacking coordinates or located at (0,0), as well as those flagged as "Fossil", "Living specimen", or "Absent". Additionally, records prior to 2000, those with imprecise coordinate values or high spatial uncertainty, and records likely originating from institutional centroids (e.g., herbaria, zoos, country capitals) were excluded. Finally, marine records were filtered out, retaining only those that plausibly represent terrestrial presence, while records outside Europe were excluded as well. **Fig. 5.6** depicts the visual outcome of the R code below.

```
install.packages("usethis")
usethis::edit_r_environ()

library(rgbif)
library(dplyr)
library(CoordinateCleaner)

species_name <- "Rhododendron ponticum"
taxonkey <- name_backbone(species_name)$usageKey


occ_download(
  pred("taxonKey", taxonkey),
  pred("hasCoordinate", TRUE),
  pred("hasGeospatialIssue", FALSE),
  pred("continent", "EUROPE"),
  format = "SIMPLE_CSV"
)

occ_download_wait('0018239-250310093411724')

Rhodo_pon_data <-
  occ_download_get('0018222-250310093411724') %>%
  occ_download_import() %>%
  setNames(tolower(names(.))) %>%
  filter(occurrencestatus == "PRESENT" | is.na(occurrencestatus)) %>%
  filter(!basisofrecord %in% c("FOSSIL_SPECIMEN","LIVING_SPECIMEN")) %>%
  filter(year >= 2000 | is.na(year)) %>%
  filter(coordinateprecision < 0.01 | is.na(coordinateprecision)) %>%
  filter(coordinateuncertaintyinmeters < 10000 | is.na(coordinateuncertaintyinmeters)) %>%
  filter(!coordinateuncertaintyinmeters %in% c(301,3036,999,9999)) %>%
  filter(!decimallatitude == 0 | !decimallongitude == 0) %>%
  cc_cen(lon="decimallongitude", lat="decimallatitude", buffer=2000, value="clean") %>%
  cc_cap(lon="decimallongitude", lat="decimallatitude", buffer=2000, value="clean") %>%
  cc_inst(lon="decimallongitude", lat="decimallatitude", buffer=2000, value="clean") %>%
  cc_sea(lon="decimallongitude", lat="decimallatitude") %>%
```

```
  distinct(decimallongitude, decimallatitude, specieskey, datasetkey, .keep_all = TRUE) %>%
  glimpse()

write.csv(Rhodo_pon_data, paste0(species_name, "_cleaned.csv"), row.names = FALSE)
```

Table A5.3. Average timber volume (m^3/ha) for *Larix spp.* and *Quercus spp.* across the countries considered. Each value represents the average of host-specific data for the respective country. Empty cells indicate the absence of available data.

Country	Average volume (m^3/ha)	
	Larix spp.	*Fagus spp.*
Austria		
Belgium	183.00	212.95
Bulgaria		191.32
Croatia		
Czech Republic	359.23	331.49
Denmark		218.35
Estonia		
Finland		
France		237.96
Germany	270.40	304.82
Greece		
Hungary		
Ireland	163.03	
Italy	257.63	229
Latvia		
Lithuania		148.27
Luxembourg		259.38
Malta		
Netherlands	196.54	310.72
Norway		
Poland		215.79
Portugal		
Romania		144.83
Slovakia		233.59
Slovenia		
Spain		
Switzerland		
Sweden		
United Kingdom		188.18
Average	238.30	230.47

Table A5.4. Average prices of softwood sawlog from 2012 to 2024 in £/m^3. Source: Forest Research

6 months to	Average prices in nominal terms	Average prices in real (=2021 prices) terms
31-Mar-12	31.87	37.70
30-Sep-12	33.88	39.84
31-Mar-13	35.36	41.05
30-Sep-13	31.51	36.24
31-Mar-14	39.54	45.17
30-Sep-14	40.40	45.85
31-Mar-15	37.29	42.15
30-Sep-15	29.15	32.94
31-Mar-16	35.09	39.28
30-Sep-16	36.13	40.01
31-Mar-17	40.01	43.70
30-Sep-17	43.35	47.19
31-Mar-18	51.73	55.73
30-Sep-18	56.39	60.13
31-Mar-19	65.42	69.01
30-Sep-19	53.01	55.24
31-Mar-20	55.42	57.05
30-Sep-20	49.76	48.40
31-Mar-21	67.70	67.28
30-Sep-21	79.39	79.39
31-Mar-22	76.89	75.21
30-Sep-22	67.25	63.41
31-Mar-23	53.53	48.37
30-Sep-23	55.30	48.37
31-Mar-24	55.98	48.40
30-Sep-24	59.94	50.78
Average	49.28	50.68

6 CONCLUSIONS

The present report evaluates the potential direct economic impact of five key pests in Europe, namely *Halyomorpha halys*, *Helicoverpa armigera*, *Spodoptera frugiperda*, *Bursaphelenchus xylophilus*, and *Phytophthora ramorum*, considering their key host species, including **apple** and **pear** for *H. halys*, **tomato** and **sunflower** for *H. armigera*, **maize** for *S. frugiperda*, major European pine species (***Pinus sylvestris*, *P. pinaster*, *P. nigra***) for *B.s xylophilus*, and beech and larch species (***F. sylvatica*, *F. orientalis*, *L. decidua*, *L. kaempferi***) for *P. ramorum*.

All analyses were conducted under a "no-control" scenario to provide a bandwidth of worst-case cost to understand the damage potential for each target pest. This scenario assumes that no control measures are in place to contain the spread or establishment of these pests, thereby representing the maximum potential economic losses. The resulting cost estimates can serve as a baseline for assessing the economic viability of potential management strategies, which should cost less than the expected damages caused by a pest.

Key results are summarized in the table below and indicate the substantial damage potential associated with each pest-host combination. For instance, *Halyomorpha halys* is projected to cause annual direct economic losses ranging from €154 million to €6.4 billion in apple production and €144 million to €4.6 billion in pear production[70], depending on the spread and yield loss scenarios. Similarly, *Helicoverpa armigera* may cause damages of up to €13 billion annually in tomato production and €5 billion in sunflower seed production. *Spodoptera frugiperda* poses a significant threat to grain maize, with damage costs reaching €901 million per year. Among forest species, *Bursaphelenchus xylophilus* may inflict up to €8.1 billion in damages annually to pine trees and *Phytophthora ramorum* up to €117.5 million and €130.9 million to larch and beech trees, respectively.

Table 6.1. Summary of the resulting average annual potential direct economic costs under best- and worst-case scenarios.

Pest/Pathogen	Host	Average direct economic impact (€ million/year)	
		Best-case scenario	Worst-case scenario
***Halyomorpha halys* (BMSB)**	Apple	154	6428
	Pear	144	4622
***Helicoverpa armigera* (CBW)**	Tomato	173	13038
	Sunflower	338	5060
***Spodoptera frugiperda* (FAW)**	Grain maize	18	901
***Bursaphelenchus xylophilus* (PWN)**	Pine trees	54	8121
***Phytophthora ramorum* (PhR)**	Larch trees	0.2	117.5
	Beech trees	1.3	130.9

[70] Yield losses for pear trees were assumed to be higher than the ones for apple trees based on the distribution of reported damage extent in Italy (Maistrello, 2024).

Additionally, the outcomes of this study emphasize the importance of prevention and early eradication measures, which are expected to be far more cost-effective than managing widespread populations. The results also demonstrate that higher spread rates lead to exponential increases in the infested area, thus amplifying economic damages. Conversely, timely control efforts during the early stages of invasion can significantly limit the spread, reducing both the scale of infestation and the associated direct and/or indirect potential damages.

This analysis focuses solely on direct impacts, excluding potential indirect consequences such as biodiversity loss and reductions in the recreational or aesthetic value of affected landscapes. This likely results in an underestimation of the social costs, particularly for forest species. Additionally, due to the polyphagous nature of most target pests, the analysis had to be limited to a subset of host plants. Host selection was guided primarily by data availability and relevance to the PurPest project, prioritizing those host-pest combinations being tested for volatile organic compounds (VOCs). Consequently, the economic losses induced by the target pests are likely to exceed the estimates provided in this report.

Lastly, farm-level data from FADN are not available at the NUTS3 level, as specified in the DoA, which constitutes an external constraint beyond the PurPest consortium's control. In addition, FADN farm-level data were only used for the analysis of *H. halys* and *H. armigera*, while different data sources were needed for the case of *P. ramorum* and *B. xylophilus*. We present the results at country-level to ensure consistency across all pest–host combinations regardless of the resolution of the different data sources that were used. Beyond data availability, this choice is also methodologically justified. The spatially implicit radial range expansion spread model applied in this study assumes expansion from an initial introduction point across a contiguous susceptible area. Applying this framework at finer spatial scales (e.g., NUTS2) would lead to unrealistically rapid saturation of smaller and fragmented regions, thereby limiting the role of temporal dynamics and substantially undermining the influence of discounting in the estimation of direct economic impacts. In contrast, the use of country-level units allows for economically more meaningful representation of invasion dynamics, consistent with the literature, while also facilitating comparability and interpretation of results across species.

Invasive alien species management has a transboundary dimension, as pest control efforts in one country generate positive externalities for neighboring countries by reducing the risk of cross-border spread (Wesseler & Fall, 2010). Effective management, therefore, requires coordinated and collaborative action at the European level to maximize the collective benefits.

Lastly, the results underscore the urgency of implementing early detection systems, robust monitoring, and rapid-response measures to tackle the issue of invasive alien species. By providing a quantitative economic assessment of the target pests in the European context, this report addresses a critical knowledge gap and lays the groundwork for informed decision-making and future research.